DISS. ETH NO. 27181

TNF SUPERFAMILY MEMBERS AS PAYLOADS FOR ANTIBODY-CYTOKINE ANTICANCER THERAPEUTICS

A thesis submitted to attain the degree of
DOCTOR OF SCIENCES of ETH ZURICH
(Dr. sc. ETH Zurich)

presented by
JACQUELINE CAROLINE MOCK

M.Sc., Interdisciplinary Sciences
ETH Zürich

born on 24.05.1992

citizen of
Appenzell, AI, Switzerland

accepted on the recommendation of

Prof. Dr. Dario Neri
Prof. Dr. Cornelia Halin

2021

Contents

1. Abstract **5**

2. Zusammenfassung **7**

3. Introduction **9**

3.1. Cancer 9
3.2. Antibodies and antibody engineering 15
3.3. Antibody-based therapeutics for cancer therapy 20
3.4. Tumor necrosis factor superfamily of cytokines 34
3.5. Antibody-cytokine fusions with "activity on demand" 48
3.6. Aim of the Thesis 53

4. A universal reporter cell line for bioactivity evaluation of engineered cytokine products **55**

4.1. Introduction 55
4.2. Results 57
4.3. Discussion 62
4.4. Materials and Methods 63

5. Antibody fusion proteins featuring single-chain trimeric CD40L **69**

5.1. Introduction 69
5.2. Results and Discussion 69
5.3. Conclusion and Outlook 71
5.4. Materials and Methods 71

6. Engineering murine GITRL for antibody- mediated delivery to tumor-associated blood vessels **75**

6.1. Introduction 76
6.2. Results 77
6.3. Discussion 83
6.4. Materials and Methods 85

7. An engineered 4-1BBL fusion protein with "activity-on-demand" **93**

7.1. Introduction 94
7.2. Results 95
7.3. Discussion 103
7.4. Materials and Methods 104

8. Conclusion and Outlook 111

9. Acknowledgements 113

Appendix A. Supplementary material "Reporter Cell Line" 117

Appendix B. Supplementary material "Engineering murine GITRL" 131

Appendix C. Supplementary material "An engineered 4-1BBL fusion protein" 139

Appendix D. List of vectors 153

Appendix E. List of primers 159

Appendix F. Bibliography 163

1. Abstract

The recent clinical success of immune checkpoint inhibitors in a subset of patients[1–3] has fueled interest in the discovery of additional immunotherapeutic agents in order to achieve durable clinical benefit in a larger cohort of cancer patients. Costimulatory members of the TNF superfamily (TNFSF) have emerged as promising targets to improve the anti-tumor immune response.[4,5] Agonists for the TNFRSF members 4-1BB (CD137) and glucocorticoid-induced TNF related receptor (GITR, CD357) were shown to reinvigorate the response of exhausted T cells and to promote the formation of memory T cells,[6,7] while CD40 agonists were shown to promote immune infiltration into immunologically "cold" tumors and to enhance T cell priming.[8] This work aimed at the development of antibody-cytokine fusion proteins (immunocytokines) for the targeted delivery of TNFSF ligands such as CD40L, GITRL and 4-1BBL to the tumor. Our research group has specialized in the development of immunocytokines featuring the F8 antibody,[9,10] which binds with high affinity to the alternatively spliced extracellular domain A of fibronectin (EDA).[11] In the adult human body, EDA is selectively expressed in the neovasculature of most tumors, chronically inflamed tissue and is virtually absent from healthy tissues (exception made for the female reproductive tract), making it an ideal target for the delivery of therapeutic agents.[11–13]

To facilitate the development of novel immunoconjugates, two universal reporter cell lines were developed for the quantitative *in vitro* evaluation of cytokine potency. As described in chapter 4, the murine cytotoxic T cell line CTLL-2 and the murine B cell lymphoma cell line A20 were transduced with a reporter construct. In response to the activation of NF-κB, the expression of a secreted luciferase and intracellular mCherry is induced in the transduced cell lines. The two cell lines were chosen since they express a wide variety of immunologically interesting receptors. Since most cytokines trigger the activation of NF-κB, these cell lines could be used to evaluate the bioactivity of a range of cytokines.

The reporter cell lines were used to screen for immunocytokines that selectively regain biological activity upon antigen binding in order to restrict cytokine activity to the tumor tissue ("activity on demand"). All F8-CD40L and F8-GITRL immunocytokines that were developed in this work retained constitutive biological activity even in the absence of the antigen (chapter 5 and chapter 6). In addition, quantitative biodistribution studies of F8-CD40L and F8-GITRL revealed fast clearance of the proteins *in vivo*. The tumor targeting properties of F8-GITRL could be improved by enzymatic deglycosylation and site-directed mutagenesis of the *N*-glycosylation consensus sequence. Despite the improved targeting, no anti-tumor effect was observed for the F8-GITRL featuring aglycosylated GITRL, neither alone nor in combination with a PD-1 inhibitor. By con-

trast, one F8-4-1BBL fusion protein showed "activity on demand" properties and also gave a favorable biodistribution profile. The chosen F8-4-1BBL fusion protein revealed potent anti-tumor activity in several mouse models of cancer such as WEHI-164 fibrosarcoma, CT26 colon carcinoma, MC38 colon carcinoma and an orthotopic mouse model of glioblastoma alone and in combination with PD-1 blockade as described in chapter 7.

In conclusion, this work highlights some of the challenges and opportunities associated with the development of neovasculature-targeted immunocytokines featuring TNFSF ligands as immunostimulatory payload. Both the payload and the molecular format were found to crucially determine the *in vitro* bioactivity and the *in vivo* tumor-targeting properties of the fusion proteins. Therefore, careful *in vitro* screening of different formats of the fusion proteins proved crucial to find the most promising candidates for *in vivo* testing. In addition, the *in vivo* performance of the fusion proteins needed to be critically evaluated. While this work raised questions about the suitability of CD40L and GITRL as immunostimulatory payloads for immunocytokines, it clearly emphasized the potential of targeted 4-1BBL to treat preclinical models of cancer. Further studies are warranted to investigate the translatability of the findings based on murine 4-1BBL as payload towards a fully human protein for clinical development.

2. Zusammenfassung

Mit den jüngsten klinischen Erfolgen von Immun-Checkpoint-Inhibitoren[1–3] wurde das Interesse an der Entwicklung weiterer Immuntherapeutika geweckt, um langfristigen therapeutischen Nutzen für möglichst viele Krebspatienten zu erzielen. Die Aktivierung kostimulatorischer Rezeptoren der TNF Superfamilie (TNFSF) ist eine vielversprechende Strategie, um die krebsgerichtete Immunantwort zu verstärken.[4,5] Es wurde nachgewiesen, dass Agonisten für die TNFSF Rezeptoren 4-1BB (CD137) und Glucocorticoid-induziertes TNFR-verwandtes Protein (GITR, CD357) die Immunantwort von erschöpften T Zellen wiederherstellen und die Bildung von T Gedächtniszellen fördern können.[6,7] CD40-Agonisten hingegen können die Migration von Immunzellen in immunologisch "kalte" Tumoren fördern und die Aktivierung von T Zellen verbessern.[8] Das Ziel dieser Arbeit bestand darin, Antikörper-Zytokin Fusionsproteine (Immunozytokine) zu entwickeln, um TNFSF Liganden wie CD40L, GITRL und 4-1BBL selektiv in Tumoren anzureichern. Unsere Forschungsgruppe ist spezialisiert auf die Entwicklung von Immunozytokinen mit dem F8 Antikörper.[9,10] Der F8 Antikörper bindet mit hoher Affinität an die alternativ gespleisste extrazelluläre Domäne A von Fibronektin (EDA).[11] Im erwachsenen menschlichen Körper ist EDA ausschliesslich in neu gebildeten Blutgefässen von Tumoren und chronisch entzündeten Geweben vorhanden, während EDA in gesunden Geweben (mit Ausnahme des weiblichen Fortpflanzungstraktes) nicht zu finden ist. Aus diesem Grund ist EDA ein idealer Marker für die zielgerichtete Verabreichung von Therapeutika.[11–13]

Um die Entwicklung neuartiger Immunokonjugate zu erleichtern, wurden zwei universelle Reporterzelllinien entwickelt, mit denen die biologische Aktivität von Zytokinen *in vitro* gemessen werden kann. Wie in Kapitel 4 beschrieben, wurden die Mauszelllinien CTLL-2 (zytotoxische T Zellen) und A20 (B-Zell Lymphom) mit einem Reporterkonstrukt transduziert. Diese beiden Zelllinien wurden ausgewählt, weil sie ein breites Spektrum an immunologisch interessaten Rezeptoren auf ihrer Oberfläche tragen. Da die meisten Zytokine die Aktivierung von NF-κB auslösen, können diese Zelllinien dazu benutzt werden, die biologische Aktivität vieler verschiedener Zytokine zu messen.

Die Reporterzelllinien wurden benutzt, um nach Immunozytokinen zu suchen, die nur dann biologisch aktiv werden, wenn der Antikörper an das entsprechende Antigen gebunden hat. Somit kann die Aktivität der Zytokine idealerweise auf das Tumorgewebe beschränkt werden ("activity on demand"). Alle F8-CD40L und F8-GITRL Immunozytokine, die im Lauf dieser Arbeit entwickelt wurden, behielten ihre biologische Aktivität auch in Abwesenheit des Antigens (Kapitel 5 and 6). Ausserdem haben quantitative Biodistributionsstudien von F8-CD40L und F8-GITRL gezeigt, dass die Proteine *in vivo* schnell eliminiert werden. Die Anreicherung von F8-GITRL im Tumor konnte durch

enzymatische Deglykosylierung oder ortsgerichtete Mutagenese der *N*-Glykosylierungs-Erkennungssequenz verbessert werden. Trotz der verbesserten Anreicherung wurde kein therapeutischer Effekt mit F8-GITRL, weder alleine noch in Kombination mit einem PD-1 Inhibitor, erzielt. Ein F8-4-1BBL Fusionsprotein hingegen wies "activity on demand" Eigenschaften und ein vielversprechendes Biodistributionsprofil auf. Dieses F8-4-1BBL Fusionsprotein zeigte ausserdem eine vielversprechende therapeutische Wirkung in verschiedenen Krebs-Mausmodellen wie dem WEHI-164 Fibrosarkom, CT26 Dickdarmkarzinom, MC38 Dickdarmkarzinom und einem orthotopen Maus-Glioblastom-Modell als Monotherapie und in Kombination mit einem PD-1 Inhibitor (Kapitel 7).

Zusammengefasst zeigt diese Arbeit die Herausforderungen und Möglichkeiten im Zusammenhang mit der Entwicklung von neovaskulatur-gerichteten Immunozytokinen mit TNFSF Liganden. Sowohl die immunostimulatorische Fracht als auch das molekulare Format haben sich als entscheidend für die Bioaktivität *in vitro* und die Tumoranreicherung *in vivo* erwiesen. Somit hat sich sorgfältiges Screening *in vitro* als essentiell herausgestellt, um die vielversprechendsten Kandidaten für *in vivo* Studien zu bestimmen. Ausserdem war es auch wichtig, die *in vivo* Eigenschaften kritisch zu bewerten. Während diese Arbeit die Wirksamkeit von CD40L und GITRL als immunostimulatorische Fracht für Immunozytokine in Frage gestellt hat, wurde das Potential von zielgerichtetem 4-1BBL für die Behandlung von vorklinischen Krebsmodellen klar hervorgehoben. Weitere Studien sind nötig um herauszufinden, inwiefern die Erkenntnisse basierend auf dem Maus-4-1BBL für die Entwicklung eines Fusionsproteines für die therapeutische Anwendung im Menschen verwendet werden können.

3. Introduction

3.1. Cancer

Despite tremendous improvements both in prevention and therapy, cancer remains a leading cause of death. According to estimations by the World Health Organization (WHO), almost 10 million people worldwide died of cancer in 2018.[14] In Switzerland, cancer was the leading cause of death for people aged 40 - 85 years in 2016.[15] Over the last 30 years, the incidence has remained stable, while there was a marginal decline in the death rates.[15] In the United States of America the cancer incidence rate declined annually by 1-2% over the past 20 years and a cumulative drop in cancer-related death of 29% between 1991 and 2017 has recently been reported.[16] The most striking declines in cancer incidence were reported for prostate, lung and colorectal cancer in men, while for women mainly the incidence rate of colorectal cancer was declining.[16] For both sexes, the sharpest decline in mortality was observed for lung cancer, while the mortality also decreased steadily for colorectal, breast and prostate cancer.[16] These remarkable reductions are at least to some extent counter-balanced by the increase in incidence of other cancer types such as melanoma, liver and breast cancer.[16] The major drivers of the reduction in incidence and mortality include better hygiene to prevent infection-related cancers, improved early diagnosis allowing more efficient treatment and the approval of novel therapies such as immune checkpoint inhibitors.[14] Nevertheless, the high mortality especially at a late metastatic stage clearly demonstrates the urgent need for improved cancer treatments.

Cancer is a complex disease characterized by uncontrolled celldivision leading to the formation of a neoplastic mass that can eventually disseminate to and invade distant organs. Cancer progression is therefore often divided into different stages. Stage I cancer describes a localized tumor mass that has not yet invaded the basal membrane or adjacent lymph nodes. By contrast, stage II and III cancer show invasion of the nearby tissue and draining lymph nodes. Stage IV, which is the most severe state, refers to the metastatic state of cancer where distant tissues are invaded.[17] At an early stage, when the neoplastic mass is still clearly defined and has not yet invaded the basal membrane, the tumor can in most cases be surgically removed.[18] When the surrounding tissue has been invaded and especially once metastases have formed, the treatment becomes increasingly challenging. This is also reflected by the steep stage-dependent increase in mortality that is observed for most cancer types.[16]

During the oncogenic transformation, the tumor mass acquires a number of characteristics that were described as "hallmarks of cancer" by Hanahan and Weinberg[19](Figure 3.1). Some of the hallmarks describe cell-intrinsic characteristics of malignant cells such as

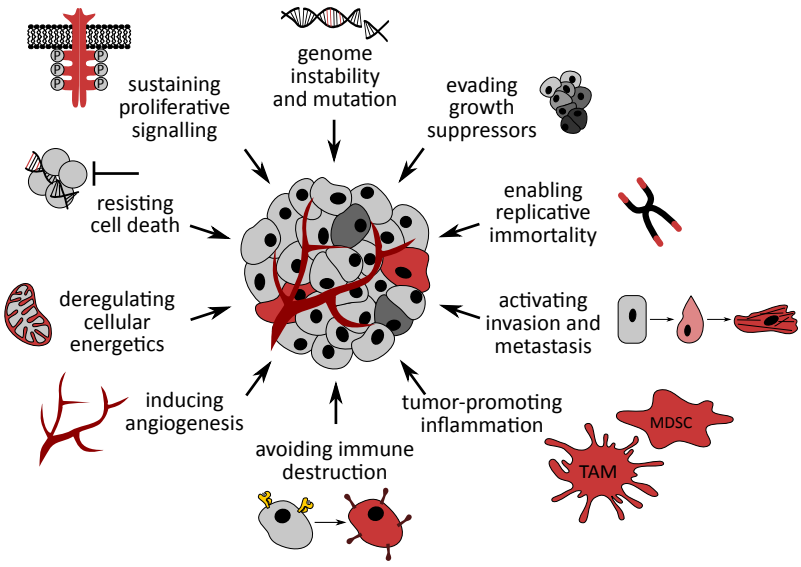

Figure 3.1.: The hallmarks of cancer. Adapted from Hanahan and Weinberg (2011)[19]

genome instability and mutation, resistance to cell death, resistance to growth suppressors, replicative immortality, sustained proliferative signalling, the ability to avoid immune destruction, activation of invasion and metastasis and deregulation of cellular energetics. In addition, an important feature of the tumor mass is the ability to modulate the surrounding tissue to create a favorable microenvironment that is characterized by tumor-promoting inflammation and induction of angiogenesis.[19,20] In the end, each type of cancer is characterized by a unique balance between the different hallmarks.

3.1.1. Genomic instability and mutation

Genomic instability can be considered as the feed-forward mechanism enabling neoplastic transformation. The accumulation of somatic mutations in cancerous cells drives the acquisition of the above-described hallmark features. This is one of the reasons why the cancer incidence raises with age.[18] Cancer types that have a younger median age at incidence such as melanoma and lung cancer are typically associated with the exposure to mutagenic agents such as UV light or cigarette smoke.[18] However, it is important to notice that the mutational burden differs from cancer type to cancer type and also from patient to patient.[21,22]

Somatic mutations in the DNA repair machinery drive the accumulation of further mutations in each round of cell division.[23] The increase in mutational burden from generation to generation can lead to substantial intratumoral heterogeneity, which in turn influences the treatment success especially with modern immunotherapeutic regimes.[24,25] Other mutations in genes encoding proteins involved in the cell cycle regulation enable replicative immortality and growth factor-independent cell division. Replicative immortality of can-

cer cells is often due to the expression of the enzyme telomerase that prevents replicative senescence from telomere shortening upon cell division.[26,27] Besides, typical mutations that are found in human melanomas affect the structure of the B-Raf protein in a way that leads to constitutive signalling through the mitogen-activated protein (MAP)-kinase pathway.[28] Loss-of-function mutations in the DNA-damage sensor TP53, which normally induces apoptosis in response to DNA damage and chromosomal aberration, are also typical for many types of cancer.[29,30]

As a consequence of the genetic instability, a unique set of neoantigens arises in each tumor.[31] Neoantigens can emerge due to mutations in the protein-coding regions or stem from non-coding regions that are incorporated into the mature mRNAs due to mutationally-induced changes in the splicing pattern.[32] Tumor cells present peptide neoantigens to $CD8^+$ T cells in an MHC-I-dependent manner. Upon recognition by an antigen-specific $CD8^+$ T cell, the effector cell induces apoptosis of the tumor cell. Neoantigens presented on MHC-II can be recognized by antigen-specific $CD4^+$ T cells which in turn contribute to the anti-tumor immune response by secreting pro-inflammatory cytokines.[33] Under inflammatory conditions, the proteasome contains different proteases than under normal conditions which influences the peptides that are generated and loaded onto MHC complexes.[34] In established tumors, various mechanisms prevent immune destruction. Some tumors progressively lose immunogenicity in a process called 'immunoediting'[35] while other types of cancer successfully exclude the immune system.[36–38] Many cancers also induce a tumor-promoting inflammation by recruiting immune suppressor cells.[39]

3.1.2. Avoiding immune destruction

The concept of cancer 'immunoediting' was introduced by Schreiber *et al.* in the early 2000s.[35] By then, it was largely established that the immune system could protect the host against tumor development in a process termed 'cancer immunosurveillance'.[40] The major drivers of this process are lymphocytes that produce IFNγ[41,42] and perforin.[43–45] Yet, the selective pressure from this immune response favors clones with reduced immunogenicity allowing the tumor to gradually escape immune destruction.[35] This dynamic process is termed cancer immunoediting and can be divided into three stages termed the '3 E's of cancer immunoediting': Elimination, Equilibrium and Escape (Figure 3.2).[35]

The first stage termed 'Elimination' phase describes the phase where active immunosurveillance prevents cancer growth.[46] The major drivers of the elimination phase are $CD8^+$ T cells and natural killer (NK) cells that can directly kill tumor cells by secreting the cytotoxic proteins perforin and granzyme or by expressing death ligands such as TNF-related apoptosis-inducing ligand (TRAIL) or Fas ligand (FasL, CD95L). NK cells recognize a number of features that are associated with malignant transformation

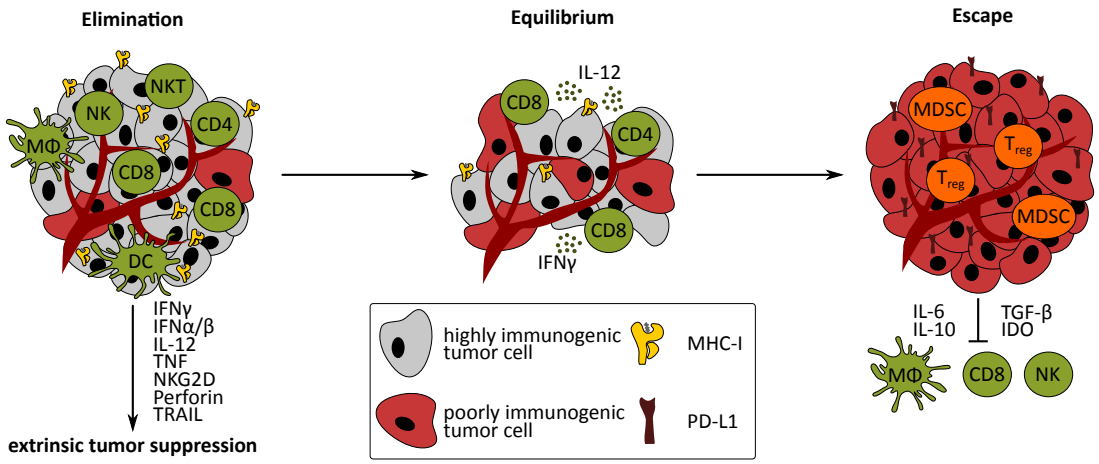

Figure 3.2.: The 3 E's of cancer immunoediting: a highly immunogenic tumor is eliminated by cells of the immune system. This process leads to a selective pressure favoring poorly immunogenic tumor cells that can eventually suppress the immune response and escape. Figure adapted from Dunn *et al.* (2002)[46] , Schreiber *et al.*[47] & Teng *et al.* (2013)[48]

of cells including the downregulation of MHC-I and the upregulation of stress-associated proteins such as NKG2D ligand.[49] $CD8^+$ T cells recognize peptide neoantigens that are presented on MHC-I complexes on tumor cells. $CD8^+$ T cells are activated by dendritic cells (DCs) that present tumor-derived antigens to T cells and provide the necessary costimulatory signals. $CD4^+$ T cells support this process by secreting cytokines that sustain the immune response.[50] The elimination stage could theoretically result in complete tumor eradication.[47] Most of the time, however, it results in progression towards an 'Equilibrium' phase where tumor growth is hindered by the immune system, but at the same time selective pressure favors the emergence of less immunogenic clones.[46] The emergence of less immunogenic clones can be due to the loss of expression of an immunodominant antigen, downregulation of MHC-I or the expression of inhibitory ligands such as PD-L1.[47] For example, in a study of melanoma patients treated with the adoptive transfer of tumor-reactive T cells it was observed that the treatment led to a loss of expression of T-cell antigens.[51]

The equilibrium phase is very similar to a chronic infection. Persistent antigen presence and low-level activation of the immune system drives the involved lymphocytes towards a state of exhaustion.[52] In response to activation, $CD8^+$ T cells not only become cytotoxic, but they also start to upregulate inhibitory receptors such as PD-1, TIM-3 and LAG-3. Signalling through these inhibitory receptors drives the T cells towards a dysfunctional state at which they fail to destroy target cells. This normal physiologic response is important to avoid damage due to an excessive immune response. In the concept of cancer, however, this means that the immune system fails to eliminate the neoplastic mass. This process is supported by the recruitment of regulatory T cells and other immunosup-

pressive cell types such as myeloid-derived suppressor cells to the tumor microenvironment. Hanahan and Weinberg described this process as the hallmark of tumor-promoting inflammation.[19] Finally, the above-described processes lead to the 'Escape' phase which is characterized by outgrowth of the tumor due to the lack of control by the immune system.

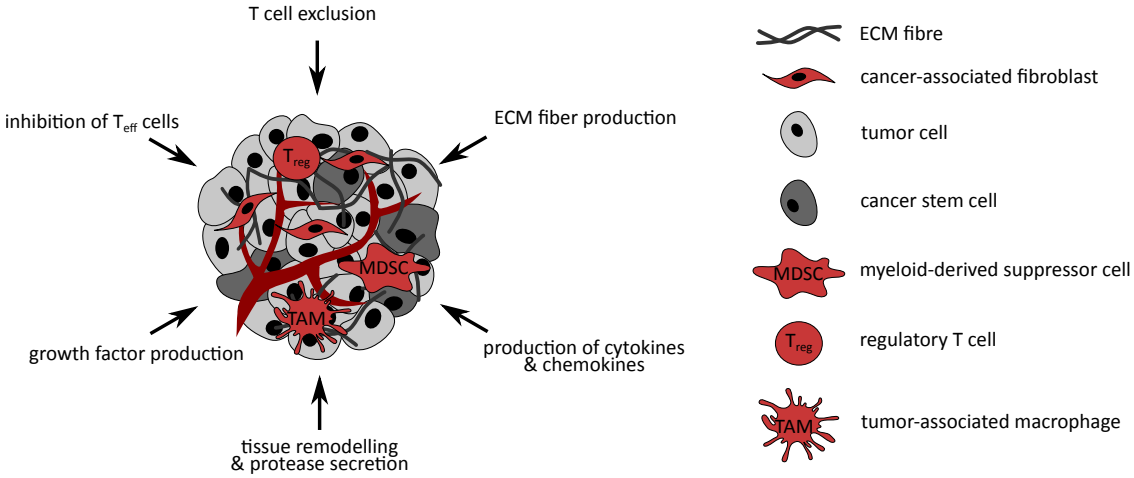

Figure 3.3.: The contribution of the tumor microenvironment to tumor progression

3.1.3. Tumor microenvironment

Progressing tumors crucially depend on the stromal microenvironment for sustained tumor growth and as a protection against immune destruction. Oncogenic signals from cancer cells as well as changes in the environment due to the high nutrient consumption of the tumor modulate the surrounding microenvironment to establish a tumor-promoting niche. A number of stromal cells such as cancer-associated fibroblasts (CAFs) and adipocytes[53–55] have been shown to promote tumor-progression through various mechanisms. In response to signals from cancer cells, CAFs shape the tumor microenvironment by secreting extracellular matrix (ECM) proteins, components of the basement membrane and signalling molecules influencing other surrounding cells.[56] The production of CXCL12 by FAP^+ CAFs further contributes to T cell exclusion,[57] since high concentrations of this chemokine acts as a repellant for T cells.[58] Tumor-associated macrophages (TAMs) are polarized towards a tumor-promoting phenotype by local alterations of the environment, especially hypoxia.[59,60] TAMs support tumor-progression by secreting pro-tumorigenic proteases,[61,62] cytokines and growth factors.[63,64] At a later stage, immune-suppressor cells such as myeloid-derived suppressor cells (MDSCs)[65,66] and regulatory T cells (T_{reg}) are recruited to the tumor. MDSCs are able to disrupt major immune surveillance mechanisms by inhibiting NK cell cytotoxicity,[67] M1 macrophage polarization,[68] T cell activation[69] and antigen presentation by dendritic cells (DCs).[65,66] T_{reg} interfere with immune surveillance especially by inhibiting cytotoxic T cells and DCs in a number of ways.[70] T_{reg} can sequester IL-2 via CD25, their high-affinity IL-2 receptor, thus depriving cytotoxic T cells

of a cytokine they crucially depend on.[71] T_{reg} express the two ectoenzymes CD39 and CD73 which convert ATP into AMP and adenosine. Adenosine in turn suppresses effector T cells.[72,73] The interaction of CTLA-4 on T_{reg} with CD80/86 on DCs prevents T cell activation.[74] In addition, T_{reg} also secrete indoleamine 2,3-dioxygenase (IDO) in a CTLA-4-dependent manner. IDO is an enzyme which converts tryptophan into kynurenine.[75] This process not only deprives T effector cells of the important nutrient tryptophan, but the metabolite kynurenine also promotes apoptosis. Moreover, T_{reg} can secrete a number of anti-inflammatory cytokines such as IL-10 and TGFβ.[76] By secreting perforin and granzyme, T_{reg} can also directly kill effector cells. Thus, the tumor microenvironment is important both to achieve a tumor-promoting inflammation and for immune exclusion. In addition, the tumor microenvironment promotes tissue remodelling including angiogenesis which is important to sustain tumor growth.

3.1.4. Angiogenesis

The rapid, uncontrolled cell division in a tumor mass leads to an increased consumption of oxygen and nutrients. This results in local hypoxia and acidification of the tissue. The induction of angiogenesis as a response to hypoxic conditions is driven by a number of cell types of the tumor microenvironment including TAMs, mesenchymal stem cells and CAFs.[39] On a cellular level, the heterodimeric transcription factors hypoxia-inducible factor (HIFα/β) 1, 2 and 3 control the response to hypoxic conditions.[77] Under normoxic conditions, the HIFα are poly-ubiquitinated by the Von Hippel-Lindau (VHL) E3 ubiquitin ligase complex[78] and therefore rapidly degraded.[79,80] Under hypoxic conditions, however, the prolyl-hydroxylases (PHD) that are normally involved in the degradation of HIF-1α become non-functional.[81,82] As a result, the HIFα subunits can translocate to the nucleus, dimerize with the beta subunit and induce the expression of a number of downstream genes.[78] An important downstream gene encodes the vascular endothelial growth factor (VEGF)[83] which in turn drives the formation of new blood vessels. VEGF stimulates endothelial cells to proliferate and migrate to form new vessels. In addition, VEGF can activate matrix metalloproteinases to facilitate tissue invasion of the newly formed blood vessels. Matrix metalloproteinase-9 was shown to trigger the angiogenic switch by proteolytically activating VEGF-A.[84] While VEGF-A is considered as the rate-limiting factor for blood vessel growth,[85] other factors such as angiopoietins, platelet-derived growth factor B (PDGF-B) and others are also crucial drivers of angiogenesis.[86] Blood vessels formed under these conditions, however, show structural and functional abnormalities including irregular shape of the vessels, lack of organization and the presence of dead ends.[87] The resulting leakiness of the vessels leads to further hypoxia driving more VEGF production.[88]

Since angiogenesis is in general a very rare process in the adult human body, markers of neovasculature can be used as cancer cell-independent tumor markers.[89] One example for these markers are splice isoforms of the extracellular matrix protein fibronectin that contain the extradomains A and B (EDA and EDB) or the A1 domain-containing splice-variant of tenascin C (Figure 3.6). These antigens are virtually absent in the adult human body except for the female reproductive tract,[13,90] chronically inflamed tissues or tumors. Antibodies for all three antigens have been developed and successfully used for tumor-targeting in preclinical and clinical models of cancer,[11,12,91,92] which will be described in later sections.

3.2. Antibodies and antibody engineering

Antibodies are Y-shaped glycoproteins of the immunoglobulin superfamily that consist of two identical heavy chains and two identical light chains that are connected by several disulfide bonds (Figure 3.4). Each chain can be divided into a constant region and a variable region. Each variable region contains three complementarity determining regions (CDR). These are peptide loops that are highly diverse and mediate the binding specificity of the antibody. By contrast, the constant region mediates the effector functions of the antibody through interaction with receptors on different immune cells. The part containing the variable region and the first constant region (C_H1/ C_L) is termed the fragment antigen binding (Fab) region. The part containing the remaining segments of the heavy chain constant region is termed the Fc region. The Fc region is important for interaction with Fc receptors on different cell types. There are two types of light chain termed κ and λ. Each antibody contains only one type of light chain. There are also different classes of heavy chains that mediate different effector functions. Antibodies are produced by B lymphocytes. During B cell development, the gene cluster encoding the antibody is heavily rearranged to create a highly diverse repertoire of antibodies. Fully mature, naïve B cells mainly express the membrane-bound form of the IgD antibody. Upon antigen encounter and activation of the B cell in secondary lymphoid organs, the B cells undergo somatic hypermutation, a process of several rounds of affinity maturation that lead to the emergence of clones that have a higher affinity for the encountered antigen. At this stage, the B cell also undergoes class-switch recombination to encode a specific class of immunoglobulin. The class of immunoglobulin depends on the type of infection and therefore on the signals the cell received upon activation. The activated B cells that emerge from affinity maturation differentiate into antibody-secreting plasma cells and long-lived memory cells. The memory cells can be rapidly activated upon infection with a pathogen that expresses the respective antigens. Therefore, they are important to prevent reinfection with the same disease.[50]

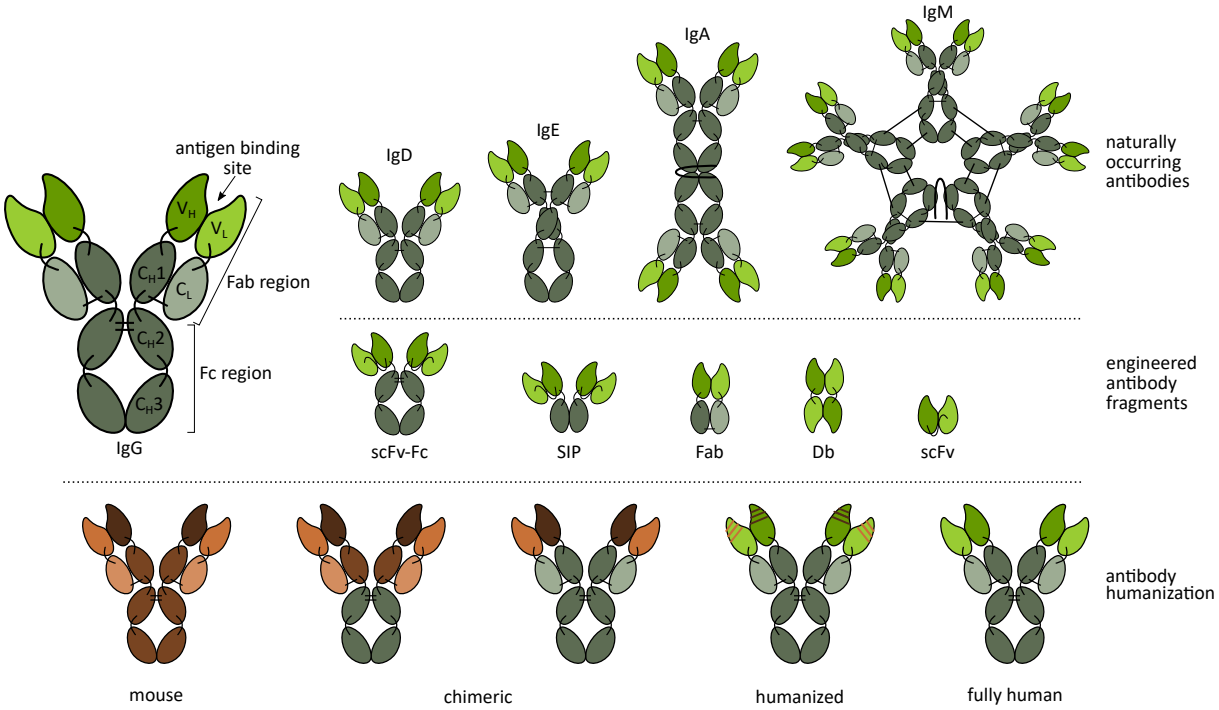

Figure 3.4.: Schematic depiction of different naturally occurring antibody isotypes, engineered antibody fragments and the process of antibody humanization

Circulatory antibodies support the immune response through different mechanisms. Some antibodies neutralize a toxin or a virus by preventing the interaction with the receptor on the target cell through binding to the respective epitope. Antibodies of the IgM and IgG class can activate the complement cascade by binding to C1q resulting in the lysis of the target cell. IgG antibodies can also engage in a number of Fc receptor-dependent processes. They can engage with Fcγ receptors on natural killer cells to induce destruction of a target cell in a process termed antibody-dependent cellular cytotoxicity (ADCC). If they engage with Fcγ receptors on macrophages, they can support phagocytosis of bacteria through receptor-mediated endocytosis in a process called opsonization.[50]

3.2.1. Antibody discovery for biotechnological applications

Due to the high affinity and specificity of the antibody-antigen interaction, antibodies are useful tools for a number of biotechnological and pharmaceutical applications. Polyclonal antibodies can be isolated from the serum of an animal that has been immunized with the antigen of interest.[93] In order to obtain monoclonal antibodies for a specific target, more elaborate *in vitro* selections are performed. The main methods for antibody discovery are the hybridoma technology[94] and phage display.[95] Other display technologies such as ribosome display,[96] bacterial display,[97] yeast display[98] and mammalian display[99] have also been reported.

Hybridoma technology

The goal of the hybridoma technology is to immortalize antibody-producing cells from a rodent, typically a mouse, in order to screen for and produce specific antibodies. In a first step, B cells from an immunized mouse are fused with a murine myeloma cell line. The myeloma cell confers the replicative immortality while the B cell contributes the genetic information encoding the antibody. After selection and single-cell sorting, the cells are screened for the production of antibodies specific for the antigen of interest (Figure 3.5).[94] Disadvantages of this technology include the low efficiency of cell fusion and the relatively low throughput due to the plate-based screening. However, recent developments in the field of microfluidics have contributed to significant improvements in the throughput of the screening.[100]

A further disadvantage of antibodies derived from murine hybridoma libraries is the potential immunogenicity of the antibodies when destined for therapeutic use in humans.[101,102] In order to avoid the development of anti-drug antibodies by the patient, as much of the murine sequence is replaced by human sequences as possible. Different degrees of humanization can be implemented as shown in Figure 3.4. In the most simple form, the Fab region or only the variable domains of the mouse antibody are grafted on a human Fc fragment yielding a so-called chimeric antibody.[103,104] A further reduction of the content of murine antibody sequences can be achieved by grafting only the CDR loops onto a human antibody scaffold.[105,106] Especially in the latter case, extensive engineering is often necessary in order to retain stability and affinity of the resulting antibody.[107]

Phage display

An important method for direct screening of antibody sequences derived from human antibody libraries was pioneered by Sir Gregory Winter[108](Figure 3.5). The variable regions are amplified and inserted into a phagemid vector in order to encode a fusion protein of the variable regions connected by a peptide linker and the pIII protein of the filamentous bacteriophage M13.[108,109] This phagemid vector is then used to create a library of bacteriophages in *Escherichia coli*. The phages are selected against the antigen of interest in several rounds of panning.[108] The selected clones can further be used for the construction of a secondary library for affinity maturation.[110,111] This technology therefore allows for the relatively high throughput screening of human antibody-derived sequences.

3.2.2. Fc engineering

Intact antibodies offer the advantage of full effector functions since the Fc region can interact with cognate receptors. This allows for instance recycling via the neonatal Fc receptor

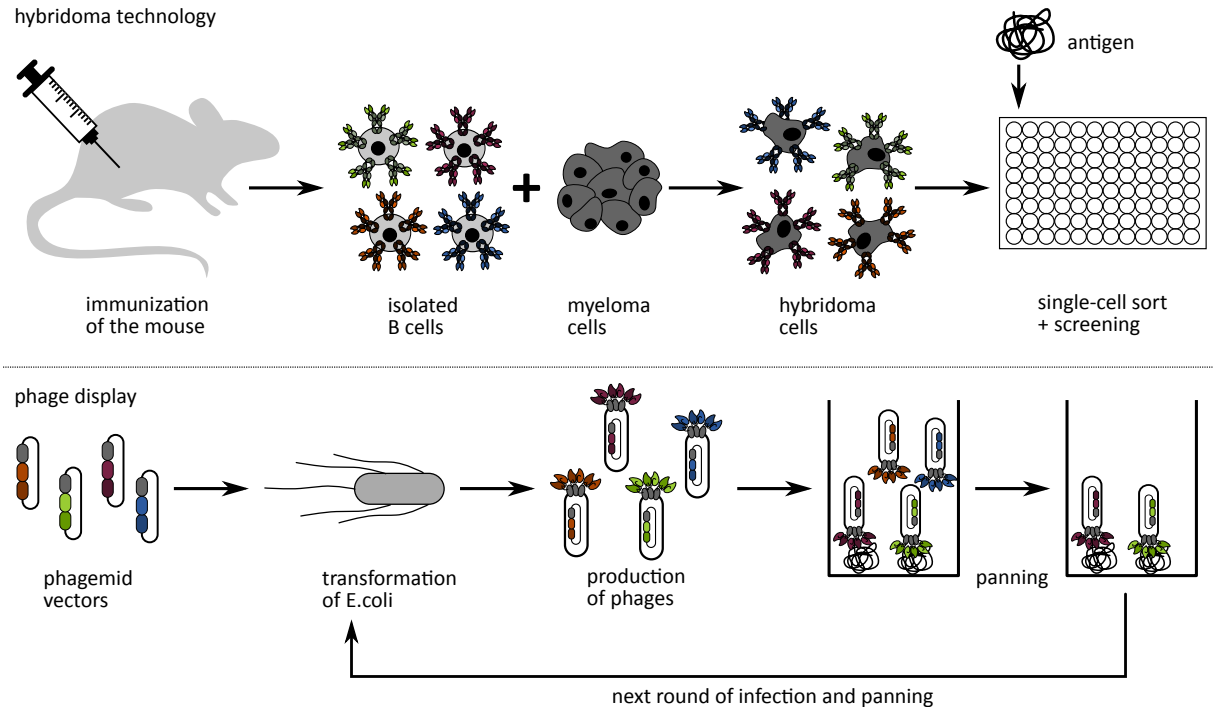

Figure 3.5.: The top panel schematically depicts the hybridoma technology and the lower panel shows the phage display technology

(FcRn) to prolong the *in vivo* half-life.[112,113] Depending on the isotype, the Fc region can interact with other Fc receptors on immune cells and thus promote antibody-dependent cell-mediated cytotoxicity, opsonization or tolerance.[114] Therefore, the choice of antibody isotype is a crucial consideration in the development of antibody-based therapeutics.[114,115]

IgG is the most commonly used isotype for therapeutic antibodies. This class can further be divided into IgG1, IgG2, IgG3 and IgG4 in humans.[116] These four subclasses share around 90% sequence homology.[117] The most significant differences between the subclasses lie in the hinge region and the C_H2 domain.[117,118] The differences thus mainly affect the part of the antibody that interacts with the Fcγ receptors (FcγR). This means that the choice of subclass has a major impact on the effector function of an antibody.[118] Antibodies belonging to the IgG3 subclass have an extended hinge region[119] and more complex disulfide bonds. The *in vivo* half-life of IgG3 is relatively short due to inefficient binding to the FcRn.[120] In addition, this subclass shows greater polymorphism in the population which increases the risk of immunogenicity.[118] For these reasons, the IgG3 subclass is normally not used for therapeutic antibodies. The IgG1 subclass binds strongest to all FcγRs and to C1q. Therefore, it elicits the strongest effector functions. A special feature of the IgG2 subclass are the disulfide bond isomers termed IgG2A, IgG2B and IgG2A/B that can be formed. The isoforms can interconvert into each other both *in vitro* and *in vivo*.[121] The IgG2B subclass is the most compact one and can also relate super-agonistic features to certain antibodies.[122] The IgG4 subclass is even more dynamic. It has a

unique serine residue (S_{228}) in the hinge region that allows for the interchange of disulfide bonds and exchange of Fab arms between different antibodies.[123] Therefore, monovalent bispecific antibodies can form *in vivo*.[123] The Fab arm exchange can be prevented by the introduction of an $S_{228}P$ mutation.[123,124]

There are a number of FcγRs that differ with respect to their binding specificities towards the IgG subclasses and intracellular signalling. IgG1 and IgG3 bind to all human FcγRs. The human FcγRI, FcγRIIa and FcγRIIIa contain an intracellular immunoreceptor tyrosine-based activation motif (ITAM) and are therefore considered as activating receptors. The FcγRI receptor has a high affinity for IgG1 and IgG4 antibodies, but does not bind to IgG2.[125] Its major function is to trigger phagocytosis in dendritic cells and macrophages. The FcγRIIa and FcγRIIIa are low-affinity receptors.[125] They do not bind to free IgG but only to immune complexes.[125] FcγRIIa is a major trigger for phagocytosis while FcγRIIIa is the primary receptor for triggering antibody-dependent cellular cytotoxicity (ADCC). By contrast, the FcγRIIb contains an immunoreceptor tyrosine-based inhibitory motif (ITIM) for signal transduction and therefore functions as inhibitory receptor. FcγRIIb only binds to IgG1 and IgG3, but not to IgG2 and IgG4.[125] Within the human population, there is substantial inter-individual heterogeneity due to genetic polymorphisms of FcγRIIa, FcγRIIIa and FcγRIIIb.[126] These polymorphisms especially influence the binding of IgG2 to FcγRIIa and FcγRIIIa.[125] The binding affinity to FcγRs is further influenced by the glycosylation pattern at the conserved *N*-glycosylation site at N_{297} of the IgG.[125]

A number of so-called Fc silent antibodies have been developed, which contain mutations that preclude binding to Fcγ receptors while retaining the long circulatory half-life upon binding to FcRn. $N_{297}A/S$ mutations preventing the attachment of the glycan yields antibodies with reduced binding to Fcγ receptors.[125] Additional amino acid substitutions to reduce binding of human IgG1 antibodies to FcγRs involve the $L_{234}A/L_{234}A$ double mutation also termed LALA mutation.[127] The interaction with FcγRs can be completely abolished by additionally introducing the $P_{329}G$ mutation which disrupts a conserved proline sandwich motif at the interface of IgGs and FcγRs.[128,129] The same $P_{329}G$ mutation can be combined with an $S_{228}P/L_{235}E$ double mutation to render IgG4 antibodies Fc silent.[128–130] For antibodies of the IgG2 subclass, a combination of seven substitutions namely $V_{234}A$/ $G_{237}A$ / $P_{238}S$/ $H_{268}A$/ $V_{309}L$/ $A_{330}S$/ $P_{331}S$ was reported to eliminate binding to FcγRs and C1q.[131]

3.2.3. Antibody fragments

For pharmacodelivery, intact antibodies are often too large resulting in inefficient extravasation and poor tissue penetration.[132] Therefore, different formats of antibody fragments

have been developed (Figure 3.4). The most simple formats only consist of the variable regions of the heavy and the light chain linked by a short peptide linker. These fragments are termed single-chain Fragment variable (scFv)[133,134] or diabody (Db)[135] depending on whether they dimerize or not. Both retain the affinity of the parent antibody but exhibit significantly faster clearance.[91] A further disadvantage of the scFv format is its monovalency and therefore the lack of binding avidity. The small immune protein (SIP) format is similar to a scFv but contains a C-terminal C_H3 domain.[136] Dimerization via the C_H3 domain renders the antibody fragment bivalent similar to the parent antibody.[136] An scFv can also be linked to the C_H2 and C_H3 subunits of an IgG resulting in a format called scFv-Fc.[137]

3.3. Antibody-based therapeutics for cancer therapy

The most common first-line therapy for cancer consists of surgery combined with systemic chemotherapy and radiotherapy.[18] Many chemotherapeutic agents act on rapidly dividing cells and can therefore also interfere with the physiologic cell division of healthy cells. The systemic administration of cytotoxic agents therefore leads to severe side effects. At the same time the local concentration at the site of disease remains low[138,139] (Figure 3.11a). Similarly, high-energy radiation can severely damage healthy tissue, which is why it should be focused as much as possible on the neoplastic tissue. Targeted delivery of drugs and radionuclides therefore is a promising approach to increase the therapeutic window of therapeutic agents. As targeting moieties small organic molecules,[140–142] antibodies[143] and other engineered binding proteins can be used.[144] While small organic targeting ligands show a good tissue penetration, they are also cleared very rapidly. By contrast, especially full IgG-based antibodies have a relatively long *in vivo* half-life, but extravasate less efficiently and show a poor penetration into solid tumors.[145]

Both surface antigens of cancer cells and stroma-associated antigens can be used as targets for pharmacodelivery. The genetic instability of cancer cells can lead to the upregulation of cell surface markers on cancer cells that are virtually absent in normal adult tissue. Examples of such cell-surface targets include carbonic anhydrase IX (CAIX),[146,147] carcinoembryonic antigen (CEA),[148] prostate-specific membrane antigen (PSMA),[149] the transmembrane glycoprotein A33[150] and many others. However, under the selective pressure of targeted therapeutics to these markers, escape variants that have lost the specific target are favored. More genetically stable targets are associated with the stromal microenvironment of tumors. The most widely used targets of the tumor microenvironment include fibroblast activation protein (FAP)[151] and markers of the tumor neovasculature such as EDA[11] and EDB[91] of oncofetal fibronectin and splice isoforms of tenascin C[92] (Figure 3.6). The tumor targeting properties of the L19 antibody binding to EDB have

been extensively validated in nuclear medicine trials in cancer patients.[152,153]

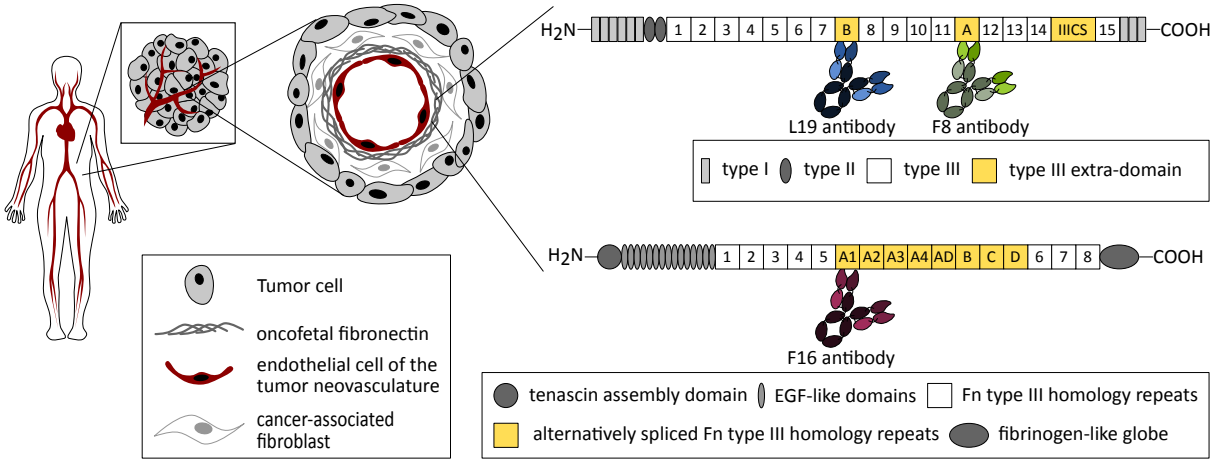

Figure 3.6.: Several antibodies have been developed that target antigens associated with extracellular matrix proteins of the tumor neovasculature. Their different extradomains that can be included by alternative splicing in neovasculature-associated fibronectin. The F8 and L19 antibodies target two of these domains. Also tenascin C contains a number of extradomains that are included by alternative splicing into neovasculature-associated tenascin C. The F16 antibody targets the A1 domain. Figure adapted from Borsi *et al.* (2002),[91] Neri & Bicknell (2005),[154] Brack *et al.*(2006),[92] Villa *et al.* (2008)[11]

3.3.1. Targeted cytotoxics

The targeted delivery of cytotoxic agents is an attempt to achieve a high concentration in the tumor while sparing healthy tissue as much as possible. In 2019 the U.S. Food and Drug Administration (FDA) approved three new antibody-drug conjugates (ADCs) highlighting the importance of this strategy.[155] A list of the currently approved ADCs is provided in Table 3.1. Over the past few decades, the field has made tremendous progress in different aspects including target selection, linker chemistry and cytotoxic payloads.[155] Nevertheless, the therapeutic index is still very narrow due to target-dependent and target-independent mechanisms. On one hand, low-level expression of the antigen in peripheral tissue can lead to significant off-tumor toxicity. On the other hand, the payload can interact with non-target cells in the bloodstream and thus lead to significant off-target toxicity. Initially, internalizing targets were preferentially chosen for the antibody-based delivery of cyototoxics, since most cytotoxic agents act on intracellular targets.[156] Upon antibody binding and target internalization, the drug would be released in the endosome and could act on the target cells.[157] Later it was recognized that these ADCs exhibited substantial toxicity towards non-target cells upon release of the cytotoxic payload during FcRn-mediated recycling. In addition, the poor tissue penetration of full antibodies prevented efficient delivery of the cytotoxic agent.[156] Therefore, for the next generation of ADCs, non-internalizing targets were selected and a major focus was laid on linker

engineering. Linkers were designed that would be cleaved in the tumor microenvironment in order to selectively release the cytotoxic payload at the site of disease.[158,159] Thus, the good tissue penetration property of small molecules could be exploited to also reach bystander cells. This strategy had the further advantage that it was amenable to the use of vascular and stromal targets that are more genetically stable than cell-surface antigens of cancer cells.[156,160,161] The poor tumor penetration of antibodies is often due to perivascular accumulation of the ADC caused by the relatively slow diffusion rate compared to the kinetic association constant. Tumor penetration and therapeutic efficacy was shown to be enhanced when perivascular binding sites were saturated by the administration of "naked" antibody, which led to a more homogeneous distribution of the ADC throughout the tumor.[162] In addition, smaller targeting moieties such as nanobodies were also shown to have a better tumor penetration due to their faster diffusion rate leading to a higher *in vivo* anti-tumor efficacy.[163]

Name	**Tradename**	**Target**	**Payload**	**Indications**
Gemtuzumab ozogamicin	Mylotarg™	CD33	Calicheamicin	AML
Trastuzumab emtansine	Kadcyla™	HER2	DM1	$HER2^+$ MBC
				$HER2^+$ adjuvant
Brentuximab vedotin	Adcentris™	CD30	MMAE	Hodgkin lymphoma
				Anaplastic large cell lymphoma
				Hodgkin disease
Inotuzumab ozogamicin	Besponsa™	CD22	Calicheamicin	B-cell lymphoma
Polatuzumab vedotin	Polivy™	CD79b	MMAE	Refractory DLBCL
Enfortumab vedotin	Padcev™	Nectin-4	MMAE	Refractory urothelial cancer
Trastuzumab deruxtecan	Enhertu™	HER2	Exatecan	Refractory $HER2^+$ MBC
Sacituzumab govitecan	Trodelvy™	Trop-2	SN-38	mTNBC
Belantamab mafodotin	Blenrep™	BCMA	MMAE	Multiple Myeloma

Table 3.1.: List of FDA-approved ADCs (AML: acute myeloid leukemia, MBC: metastatic breast cancer, mTNBC: metastatic triple-negative breast cancer, MMAE: Monomethyl Auristatin E, BCMA: B cell maturation antigen) adapted from Tolcher (2020)[155,164,165]

3.3.2. Targeted radionuclides

Radiotherapy is often used in combination with surgery in order to shrink the tumor before resection (neoadjuvant) or to eradicate tumor cells that are left behind after surgery (adjuvant therapy).[166] The high energy ionizing radiation that is administered damages genetic material and thus prevents cells from further division.[167] Therefore, care needs to be taken to maximize radiation at the site of disease and to avoid damaging normal healthy cells.[166] A number of antibody-based targeted radionuclides have been developed for the treatment of hematological malignancies such as Non-Hodgkin Lymphoma. Most of them target CD20 and are conjugated to ^{90}Y or ^{131}I.[168] One of the most prominent examples is Ibritumomab-Tiuxetan (Zevalin™), a ^{90}Y-conjugated anti-CD20 antibody, which is used

to treat a number of B-cell malignancies.[169] Also, a small immunoprotein targeting a neovasculature-associated splice isoform of tenascin C conjugated to ^{131}I was investigated in clinical trials for recurrent Hodgkin lymphoma.[170] In addition, a variety of antibody-based targeted radionuclides have been investigated for solid tumors. For instance, the PSMA-targeted radioimmunotherapeutic agent ^{177}Lu-J591 yielded promising results in a series of prostate cancer trials.[171]

Targeted radionuclides are not only useful for the delivery of high-dose ionic radiation to neoplastic lesions but also for imaging of these lesions. Further, this allows the assessment of the biodistribution and the dose at the site of disease. For instance, impressive results have been reported using an anti-carbonic anhydrase IX antibody (cG250) labelled with ^{124}I (Redectane™) for imaging of renal cell carcinoma by PET/CT imaging.[172] Successful imaging of lymphoma lesions was also reported with the ^{131}I-labelled EDB-targeting L19 antibody.[173]

3.3.3. Antibody-dependent cellular cytotoxicity as mechanism of action for therapeutic antibodies

Antibodies can mediate direct killing of target cells either via antibody-dependent cellular cytotoxicity (ADCC), complement-mediated cytotoxicity (CDC) or by directly inducing apoptosis.[174] In fact, Rituximab (Rituxan™, MabThera™), the first monoclonal antibody that gained FDA approval, was developed to combat CD20-positive hematological malignancies through ADCC and CDC.[175–177] The binding affinity to the FcγRIIIa and thus the efficiency of ADCC is heavily dependent on the glycosylation profile of the antibody. Antibody variants that bear bisected, defucosylated oligosaccharides bind with higher affinity to FcγRIIIa resulting in more potent ADCC compared to antibodies bearing different glycoforms.[178,179] Attempts to improve the therapeutic efficacy of Rituximab were therefore focused on fine-tuning the glycosylation pattern on the antibody through cell line engineering. It was discovered that genetic engineering of antibody-producing chinese hamster ovary cells to overexpress β1,4-*N*-acetylglucosaminyltransferase III (GnTIII) and α-mannosidase II (Man-II) yielded antibodies bearing bisected, defucosylated oligosaccharides.[180] Thus, a next generation anti-CD20 antibody Obinutuzumab (Gazyva™) was produced in this engineered cell line and gained market approval in 2013.[181] In addition, Obinutuzumab was selected for binding to a slightly different epitope, featuring a different binding geometry than Rituximab to favor ADCC over CDC.[174,182]

The strategy of redirecting complement proteins and NK cells towards malignant cells was also pursued during the development of Daratumumab (Darzalex™)[183] and Elotuzumab (Empliciti™).[184] Daratumumab binds to the type II transmembrane glycoprotein CD38 which is overexpressed on hematological malignancies such as multiple myeloma.[183] Treat-

ment with Daratumumab was shown to significantly increase the progression-free survival in patients suffering from multiple myeloma when administered together with bortezomib and dexamethasone compared to the chemotherapy alone.[185,186] Elotuzumab binds to the signalling lymphocytic activation molecule F7 (SLAMF7, also known as CS1, CD319 or CRACC) and enhances ADCC of SLAMF7-expressing target cells.[184] Elotuzumab also showed promising activity against multiple melanoma in a number of clinical trials.[187,188]

While ADCC-inducing antibodies have shown great success for the treatment of hematological malignancies, limited data is available concerning solid tumors. In general, solid tumors pose an additional challenge for ADCC-inducing therapies since treatment relies on extravasation and tissue penetration, which is generally poor for intact antibodies.[145] Nevertheless, a number of preclinical studies have been published. Notably, it was recently shown in a murine melanoma model that ADCC could be improved by increasing vascular permeability through simultaneous administration of targeted tumor necrosis factor alpha (TNF).[189]

3.3.4. Inhibition of growth factor signalling and angiogenesis

Aberrant growth factor signalling and induction of angiogenesis are two of the hallmark features which can be targeted by antibodies aimed at interfering with the corresponding receptor-ligand interactions. Thus, a number of antibodies have been developed that block growth factors and growth factor receptors such as vascular-endothelial growth factor (VEGF),[190] epidermal growth factor receptor (EGFR)[191] and human epidermal growth factor receptor 2 (HER2, ERBB2).[192]

For example, signalling via the epidermal growth factor receptor (EGFR) is deregulated in a number of cancers such as colorectal cancer and squamous cell carcinoma. Two antibodies against EGFR, Cetuximab (Erbitux™) and Panitumumab (Vectibix™) have been developed. Cetuximab prevents growth factor receptor dimerization and signalling by competitively binding to the extracellular domain of the receptor.[191] In two clinical trials with patients suffering from refractory metastatic colorectal cancer, Cetuximab was shown to increase the median survival time by around 2 months.[193,194] In a further trial it was shown that Cetuximab plus irinotecan, fluorouracil and leucovorin reduced the risk of progression of metastatic colorectal cancer in patients with *KRAS* wild-type tumors.[195] Similarly, a phase III clinical trial revealed that Cetuximab plus FOLFOX4 (oxaliplatin, fluorouracil, leucovorin) increased the overall survival compared to treatment with FOLFOX4 alone in patients with wild-type *KRAS* metastatic colorectal cancer.[196,197]

Human epidermal growth factor receptor 2 (HER2) was shown to be overexpressed in breast cancer and other malignancies.[198] Constitutive signalling through HER2 is believed to drive oncogenesis. Therefore, blocking antibodies were developed and showed

some anti-tumor efficacy.[192,198] Trastuzumab (Herceptin™), an anti-HER2 antibody, was approved by the FDA for the treatment of Her2/neu positive breast cancer. Later, two ADCs, Trastuzumab-DM1 (Kadcyla™)[199,200] and Trastuzumab deruxtecan (Enhertu™)[201] were also developed. Combining Trastuzumab with chemotherapy was shown to prolong the median survival by roughly 5 months to 25 months compared to the treatment with chemotherapy alone.[202] The progression-free survival of patients with HER2-positive advanced breast cancer that had previously been treated with Trastuzumab and taxane was prolonged to 9.6 months when treated with Trastuzumab emtansine as compared to patients treated with lapatinib plus capecitabine for who a progression-free survival of 6.4 months was reported.[203] In a phase II study, a response rate of roughly 60% and a median progression-free survival of 16.4 months was reported for patients with advanced HER2-positive breast cancer treated with Trastuzumab deruxtecan.[201] Thus, the limited efficacy of the naked antibody could be moderately improved by conjugation with a cytotoxic agent.

Since induction of angiogenesis was shown to be a prerequisite for cancer progression especially in solid malignancies, inhibiting angiogenesis was regarded as a promising strategy for cancer treatment. Given that new blood vessels are formed by healthy endothelial cells, it was postulated that by targeting this process, tumor-intrinsic escape mechanisms could be circumvented.[89,204] Thus, a number of antibodies targeting mediators of angiogenesis have been developed. The most famous example is the anti-VEGF antibody Bevacizumab (Avastin™) which was developed in the 90es[190] following impressive pre-clinical results obtained from studies on the anti-tumor effect of VEGF inhibition.[205–208] Importantly, it was shown that VEGF was not only produced by the tumor-associated stroma but also derived from tumor cells.[209] A number of clinical studies were performed with Bevacizumab in combination with other standard-of-care therapeutic regimes and in some cases a moderate increase in survival was observed.[210] As an alternative to antibody-based blockade of VEGF, a recombinant receptor-based VEGF trap has been developed and some anti-tumor activity was observed in pre-clinical studies.[211] So far, Bevacizumab has received more than 10 FDA approvals as a first-line and second-line therapy for six different malignancies mostly in combination with chemotherapy but also immunotherapy.[212,213] Notably, the anti-angiogenic properties of Bevacizumab were found to be useful not only for cancer therapy but also as treatment for blinding eye diseases such as age-related macular degeneration for which it has also gained market authorization.[214]

3.3.5. Immune checkpoint inhibition

The activation of a mature T cell requires at least three signals. The first being recognition of a peptide antigen presented by an antigen-presenting cell in an MHC-dependent

manner. The second signal is a costimulatory signal typically delivered by the interaction of CD28 on the T cell and CD80/86 on the antigen-presenting cell. In addition, proinflammatory cytokines are necessary to deliver the third signal.[50] The cytotoxic T lymphocyte-associated antigen (CTLA-4) can compete with CD28 for binding to CD80/86. CTLA-4 does not deliver co-stimulatory signals to the T cell and therefore inhibits T cell activation. It was found that CTLA-4 is often upregulated on tumor-specific T cells and T_{reg} and that blockade could enhance anti-tumor activity.[215] The precise mechanism of action of CTLA-4 blockade is still under debate. There is evidence, that some anti-CTLA-4 antibodies act through depletion of T_{reg} in murine models of cancer[216] but not in human patients.[217] Nevertheless, the success of CTLA-4 blockade in preclinical mouse models of cancer led the way to the development of the first FDA-approved immune checkpoint inhibitor Ipilimumab (Yervoy™), which was approved in 2011 for the treatment of metastatic melanoma after the demonstration of impressive clinical benefits in a subset of patients.[218]

Following activation, effector T cells upregulate a number of inhibitory receptors such as programmed death 1 (PD-1),[219–221] which binds to its ligands PD-L1[222] and PD-L2.[223] PD-L1 is expressed in many different tissues and importantly, it is upregulated in many types of cancer. The expression of PD-L1 on tumor cells was shown to correlate with poor patient prognosis.[224] The cytoplasmic domain of PD-1 contains an immunoreceptor tyrosine-based inhibitory motif (ITIM).[225] Signalling through PD-1 leads to the phosphorylation of the ITIM domain. Phosphorylation of the ITIM domain is followed by the recruitment of Src-homology 2 (SHP-2) phosphatase, which inhibits signalling through the T cell receptor.[226–228] As a consequence, cell growth, survival and effector functions of the T cell are inhibited leading to a state of anergy of the T cell. Under physiological conditions, this process is thought to be important to prevent overstimulation of the immune system.[229] Therefore, by inhibiting the PD-1/PD-L1 axis, T cell anergy could be prevented and thus the anti-tumor immune response could be enhanced.[230,231] This strategy was pursued and led to the development of a number of PD-1 and PD-L1 blocking antibodies that are approved for clinical use (Table 3.2).

Name	**Tradename**	**Company**	**Target**	**Year**
Ipilimumab	Yervoy™	Bristol-Myers Squibb	CTLA-4	2011
Nivolumab	Opdivo™	Bristol-Myers Squibb	PD-1	2014
Pembrolizumab	Keytruda™	Merck	PD-1	2014
Atezolizumab	Tecentriq™	Roche	PD-L1	2016
Avelumab	Bavencio™	EMD Serono Inc	PD-1	2017
Durvalumab	Imfinzi™	AstraZeneca	PD-L1	2017
Cemiplimab	Libtayo™	Sanofi & Regeneron	PD-1	2018
Sintilimab	Tyvyt™	Innovent Biologics & Eli Lilly	PD-1	2018

Table 3.2.: Immune checkpoint inhibitors that are currently approved for clinical use. Sintilimab is so far only approved in China. Adapted from Cancerresearch.org (07.04.2020)

Since inhibitors of CTLA-4 and PD-1 act on different axes of negative stimulation of effector T cells, combination treatments of Ipilimumab and Nivolumab[232–234] or Pembrolizumab[235,236] were tested in a number of clinical trials and showed some benefits over the Ipilimumab monotherapy alone.[232,233] For example, in one study, 53% of the patients suffering from advanced melanoma that received alternating administrations of Ipilimumab and Nivolumab (4 doses of each treatment scheduled 3 weeks apart) showed a reduction in tumor volume of at least 80%.[232] A similar treatment schedule led to a complete response in 22% of the patients suffering from *BRAF* wild-type advanced melanoma, while no complete responses were observed with an Ipilimumab monotherapy.[233] Both the CTLA-4 and the PD-1/PD-L1 axes are important for immune homeostasis in healthy individuals. Therefore, it is not surprising that blockade of these two checkpoints leads to a number of immune-related adverse effects such as skin rashes, colitis, hepatotoxicities and endocrinopathies.[237,238]

Despite the remarkable clinical success that has been achieved with the currently approved immune checkpoint inhibitors, a large fraction of patients fails to derive a durable clinical benefit from these therapeutics. Therefore, much effort is dedicated to the discovery of improved predictive biomarkers in order to better stratify the patients.[239,240] In addition, a lot of research activities are aimed at the development of agents towards alternative targets. Both inhibitors blocking other negative immune regulators such as LAG-3[241] or TIM-3[242] and agonists to positive costimulators including OX40,[243] 4-1BB (CD137),[6] GITR[7] and CD40[244] are in development.

3.3.6. Targeted cytokines

Cytokines are small immunomodulatory proteins that are mainly secreted by leukocytes, but also by endothelial cells, fibroblasts and stromal cells. They are important for the maintenance of immune homeostasis in the healthy body and for triggering an appropriate immune response to infections.[50] The immunostimulatory properties of pro-inflammatory cytokines can be exploited to boost the anticancer immune response and a number of cytokine products have been approved for cancer therapies in the clinic. For example, recombinant interferon-α products (Intron A™, Roferon A™) are used for the treatment of hairy cell leukemia, chronic myelogenous leukemia, lymphoma, renal cell carcinoma, malignant melanoma and Kaposi's sarcoma.[245–248] Systemic interleukin 2 (IL-2, Proleukin™) is approved for the therapy of metastatic renal-cell carcinoma and melanoma.[249–252] In addition, tumor necrosis factor alpha (TNF, Beromun™) is used for the treatment of soft tissue sarcoma and melanoma as an isolated limb perfusion in combination with melphalan.[253] On-target off-tumor toxicity drastically limits the dose that can be administered. The most common dose-limiting toxicities include flu-like symptoms, cytokine-release syndrome and vascular leak syndrome causing hypotension and reduced organ

perfusion.[254] Local administration by intratumoral injection or isolated limb perfusion can reduce the side effects, but these modes of administration are not possible for most indications.[255]

As for targeted radionuclides and targeted cytotoxics, the therapeutic index of cytokine products can be improved by antibody-mediated targeted delivery. A number of antibody-cytokine conjugates (immunocytokines) have been developed and tested both in preclinical and clinical studies (Table 3.3 and Figure 3.7). Impressive anti-tumor effects were achieved by the targeted delivery of IL-2,[256] interleukin 12 (IL-12)[257] and TNF[258] in preclinical studies.

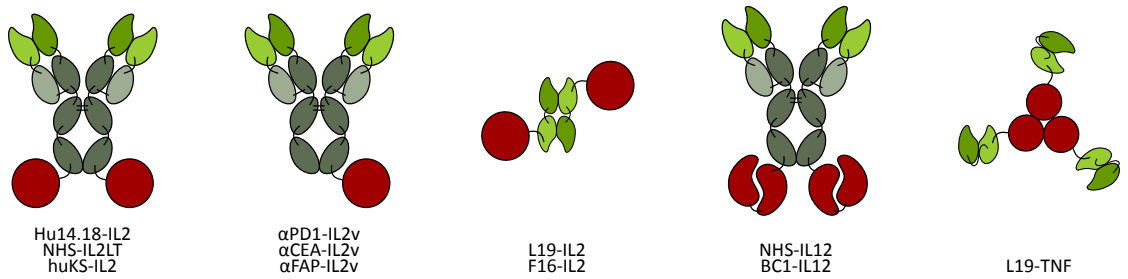

Figure 3.7.: Schematic depiction of some immunocytokines that are currently in clinical trials

One of the main challenges of targeted delivery of cytokines is to achieve high local concentration at the site of disease. Several studies showed that the rate-limiting step for tumor uptake of antibody-constructs was extravasation.[132,259,260] Furthermore, it was shown that accumulation in the tumor is often hindered by peripheral trapping of the immunocytokine due to binding of the cytokine to its receptor in the periphery. A recent study by Ribba *et al.* investigated how IL-2 receptor positive cell populations in the periphery affected the bioavailability of carcinoembryonic antigen (CEA) targeted IL-2.[261] They showed that an increase in dose or a decrease in the time interval between doses led to a higher uptake of the drug in the tumor tissue.[262] While their model fits well with biodistribution data from patients, they fail to clearly demonstrate peripheral trapping in this study. Nevertheless, it is clear that not only the design of the immunocytokine but also the dose and schedule have an important impact on the bioavailability at the site of disease. Both extravasation and peripheral trapping can further be affected by protein glycosylation. For instance, hepatocytes can trap non-sialylated proteins by binding to the asialoglycoprotein receptor leading to rapid hepatobiliary clearance of the respective proteins.[263] Moreover, macrophages and dendritic cells express a mannose receptor which recognizes terminal mannose or *N*-acetylglucosamine.[264] Previous studies by members of our group showed that the tumor-targeting proteins of different immunocytokines could be improved upon enzymatic deglycosylation or via site-directed mutagenesis of the *N*-glycosylation consensus sequence.[265,266] In addition, they could show that the culture

conditions and mode of transfection had an important impact on the structure of the glycan and thus on the tumor-targeting properties.[266]

Immunocytokines featuring IL-2 as payload

One of the first immunocytokines that was reported in literature was IL-2 fused to the anti-ganglioside GD2 antibody ch14.18.[267] It was shown that this immunocytokine enhanced the ability of T cells to kill antigen-positive tumor cells *in vitro*[267] and yielded favorable tumor-targeting properties and anti-tumor activity *in vivo*.[268–270] Initial studies showed that the anti-tumor activity of ch14.18-IL2 was dependent on $CD8^+$ T cells but not necessarily NK cells.[268,270] Later it was demonstrated that ch14.18-IL2 was also able to potentiate ADCC by increasing the adhesion and activating immune synapse formation (AIS) between NK cells and tumor cells.[271] The humanized version Hu14.18-IL2 has entered several phase I and II clinical trials for melanoma and neuroblastoma.[272–275] Roughly 52% of the patients treated with Hu14.18-IL2 developed anti-idiotypic antibodies,[276] which might at least in part explain the limited clinical efficacy that was observed in a number of trials.[272–275] IL-2 bearing immunocytokines with antibodies targeting components of the extracellular matrix such as EDA,[277] EDB[278] and the A1 domain of tenascin C[279] have also been developed. Treatment with L19-IL2 (Darleukin™) was shown to significantly increase the infiltration of NK and T cells into the neoplastic lesion in mice.[278] Thus, when using a cellular target, IL-2 bearing immunocytokines can directly boost tumor cell killing by enhancing ADCC. By contrast, when targeted to the extracellular matrix, IL-2 helps to increase the immune infiltration into solid tumors. The immunocytokine L19-IL2 entered several clinical trials for metastatic renal cell carcinoma, metastatic melanoma and B cell lymphoma.[280–283] It is currently investigated in a phase III clinical trial in combination with L19-TNF. A disadvantage of using IL-2 as a payload is that it not only activates cytotoxic T cells but also T_{reg}.[284] Activation of T_{reg} could be decreased by preventing the binding of IL-2 to the high-affinity IL-2 receptor subunit CD25 (IL2R α-chain).[285] An IL-2 variant (IL2v) whose binding to CD25 is abolished due to the introduction of three amino acid mutations was reported as payload for PD1-, FAP- and CEA-targeted immunocytokines.[261] As an alternative, an antibody (NARA1) has been reported which binds to IL-2 in a way that precludes simultaneous binding to CD25.[284,286]

Immunocytokines featuring IL-12 as payload

The heterodimeric cytokine interleukin 12 (IL-12) is composed of the p35 and p40 subunits which are linked by a disulfide bond.[287] IL-12 induces the release of IFNγ and stimulates the proliferation of NK cells and T cells.[287] The lymphoproliferative properties of IL-12 are currently being tested in a number of clinical trials where recombinant human IL-12

is administered subcutaneously as treatment of the Hematopoietic Syndrome of Acute Radiation Syndrome.[288] In preclinical models, systemic administration of recombinant IL-12 showed anti-tumor and antimetastatic activity against different tumors.[289,290] However, in human patients, dose-limiting toxicities became apparent at doses of 1.0 µg/kg which was too low to achieve anti-tumor activity.[291] Antibody-based delivery of IL-12 to EDB-containing fibronectin in the tumor neovasculature was shown to yield superior anti-tumor and antimetastatic activity compared to untargeted IL-12 while reducing the toxicity.[292] The biodistribution properties of this fusion protein could be improved by using the L19 antibody in a tandem-diabody format[257] instead of an scFv and by optimizing the linker connecting the IL-12 moiety to the tandem-diabody.[293] One of the first immunocytokines reported in literature with IL-12 as a payload linked to a full-length IgG antibody was the huBC1-IL12.[294] The huBC1 antibody targets a cryptic sequence of the human EDB-containing fibronectin which is a marker of the tumor neovasculature.[295–297] A pilot phase I study of BC1-IL12 in patients with malignant melanoma and renal cell carcinoma led to stable disease in 6 out of 11 patients with a maximal tolerated dose of up to 15 µg/kg weekly.[298] The NHS-IL12 immunocytokine which consists of two IL-12 moieties fused to a histone-targeting antibody was shown to have superior anti-tumor activity and a more favorable toxicity profile than systemic recombinant IL-12 in different preclinical models.[299] In a first clinical trial on patients with metastatic solid tumors, 5 out of 59 patients achieved stable disease and increases in frequencies of activated NK and T cells cells were observed in biopsies of patients.[300] In addition, the treatment led to an increase in T-cell receptor diversity of the tumor-infiltrating lymphocytes.[300] Following a successful first-in-human trial, this immunocytokine is currently tested in a number of clinical trials.[300]

Immunocytokines featuring TNF as payload

A third cytokine which is studied in numerous clinical trials is tumor necrosis factor alpha (TNF). TNF acts on endothelial cells to increase vascular permeability and blood clotting. In addition, it can directly induce apoptosis in certain target cells and attract immune effector cells.[50] The systemic administration of TNF is limited by severe adverse effects such as shock, disseminated intravascular coagluation and organ failure.[301] Immunocytokines featuring TNF as a payload were shown to be able to lead to tumor eradication in immunocompetent mice bearing TNF-sensitive tumors through a combination of direct killing of the tumor cells and activation of tumor-infiltrating leukocytes.[302] Rapid hemorrhagic necrosis was observed upon targeted delivery of TNF in preclinical mouse models.[258,302,303] L19-TNF was shown to be potently active in two mouse models of glioblastoma, warranting the initiation of a phase I/II clinical trial in patients suffering from recurrent glioblastoma.[304] However, in many cases no complete tumor eradication

was achieved due to the survival of a rim of tumor cells in the periphery of the tumor.[189] In addition, off-tumor activity of TNF significantly limits the dose that can be administered in preclinical mouse models. Recently, it was shown that these side effects could be alleviated by the transient inhibition of RIPK1 using the small molecule inhibitor GSK963.[305] There is both pre-clinical and clinical evidence of the potent synergism of antibody-mediated targeted delivery of IL-2 and TNF.[283,303,306] For instance, a recent phase II clinical trial in patients with stage IIIC and IVM1a metastatic melanoma reported complete responses in 30% of melanoma lesions upon intralesional injection of a combination of L19-IL2 and L19-TNF.[283] For this reason, a dual cytokine-antibody fusion (IL2-F8-TNF^{mut}) was developed by De Luca *et al.* for which the potency of the cytokines was matched by the introduction of a single point mutation in the TNF gene. This IL2-F8-TNF^{mut} fusion protein was able to eradicate tumors in tumor models that did not respond to the single antibody-cytokine fusion proteins.[307] An analogous construct was reported targeting the tumor-associated antigen carbonic anhydrase IX.[308]

Other immunocytokines

In addition to the above described immunocytokines, a number of other cytokines are investigated as payloads. For example, our group has systematically explored the targeted delivery of members of the TNF superfamily to the tumor neovasculature. When a single unit of the different TNF superfamily members was fused to the F8 antibody in a scFv format, low tumor accumulation and substantial peripheral trapping was observed.[309] Some anti-tumor activity was reported for certain TNF superfamily members in a single-chain trimer format fused to a FAP-targeting antibody fragment.[310] Recently, Roche started a clinical trial with an anti-FAP IgG antibody of which one Fab arm was replaced by single-chain trimeric 4-1BB ligand.[311] Interleukin 15 (IL-15) shares certain functions with IL-2 since both signal through the same β and γ receptor subunits. Since IL-15 does not bind to the high affinity subunit of the IL-2 receptor it is thought to more selectively activate effector T cells and NK cells. Currently, one trispecific antibody-cytokine product consisting of a CD16 and a CD33 binding domain as well as an IL-15 moiety is tested in clinical trials against for high risk hematological malignancies (GTB-3550, NCT03214666).[312,313] The anti-CD16 moiety is thought to activate NK cells and to deliver the IL-15 signal to these cells, while the CD33 targets myeloid cells.[312,313] It was shown by the group of Dafne Müller that the *in vitro* agonist properties and *in vivo* anti-tumor activity of IL-15 fusion proteins could be enhanced by fusing an extended IL-15Rα sushi domain to IL-15, especially when fused to a tumor-targeting moiety.[314] This group also developed trispecific immunocytokines where IL-15 and a cytokine of the TNF superfamily are fused to a FAP-targeting antibody fragment.[315,316]

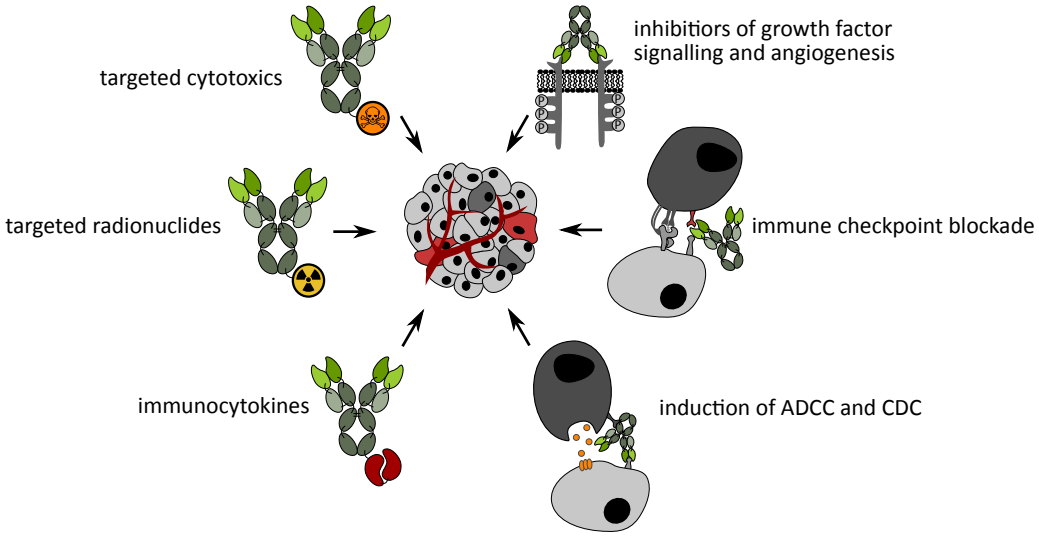

Figure 3.8.: Mechanism of action of antibody-based products used for cancer therapy

Name	Target	Format	Phase	Indication	Identifier	Ref
DI-Leu16-IL2	CD20	IgG	I/II	B-cell NHL	NCT00720135	317
			I/II	B-cell NHL	NCT02151903	318
			I/II	B-cell NHL	NCT01874288	319–321
Hu14.18-IL2/	GD2-ganglioside	IgG	I	Neuroblastoma	NCT03209869	272,273
EMD273063/			II	Recurrent Neuroblastoma	NCT01334515	275
APN301			II	Neuroblastoma	NCT00082758	
			I/II	Melanoma	NCT03958383	
			II	Melanoma	NCT00590824	274
RO7284755/	PD-1	IgG	I	Solid tumors	NCT04303858	322
αPD1-IL2v						
RO6874281/	FAP	IgG	I	Met. Melanoma	NCT03875079	
αFAP-IL2v			II	Adv. Head and Neck, Oesophageal and Cervical Cancers	NCT03386721	323
			I	Solid Tumors	NCT02627274	324
RO6895882/	CEA	IgG	I	Neoplasms	NCT02004106	261,323
αCEA-IL2v			I	Solid Tumors	NCT02350673	
L19-IL2/	EDB	Db	I	Solid Tumors	NCT02086721	325
Darleukin™			I/II	Adv. Solid Tumors	NCT01058538	282
			I	Pancreatic Cancer	NCT01198522	
			I/II	Met. Melanoma	NCT02076646	
			I/II	Diffuse Large B-cell Lymphoma	NCT02957019	
			II	Met. Melanoma	NCT01055522	281

F16-IL2/	TnC	Db	I/II	Breast Cancer	NCT01131364	[326]
Teleukin™			I/II	Solid Tumors	NCT01134250	[327,328]
			I	Acute Myeloid Leukemia	NCT02957032	[329]
			I	Acute Myeloid Leukemia Relapse	NCT03207191	
			II	Met. Merkel Cell Carcinoma	NCT02054884	
EMD521873/	DNA/Histone	IgG	I	Non Small Cell Lung Cancer	NCT00879866	[330]
NHS-IL2LT	complex		I	NHL	NCT01032681	[331]
M9241/	DNA/Histone	IgG	I/II	Adv. Pancreatic Cancer	NCT04327986	[300]
BJ001	integrin		I	Adv./Met. solid tumors	NCT04294576	[332]
NHS-IL12	complex		I	Genitourinary Malignancies	NCT04235777	
			I/II	Kaposi Sarcoma	NCT04303117	
			II	Adv. Bowel/ Colorectal cancer	NCT04491955	
			I/II	Adv. HPV-associated malignancies	NCT04287868	
EMD273066/	EpCAM	IgG	I	Ovarian, Prostate, Colorectal and NSCL Cancer	NCT00132522	[333,334]
Tucotuzumab						
celmoleukin			I	Bladder, Kidney and Lung Cancer	NCT00016237	
			II	Ovarian Cancer	NCT00408967	[335]
BC1-IL12/	D7	IgG	I	Renal Cell Carcinoma and Malignant Melanoma	NCT00625768	[298,336]
AS1409						
IL12-L19L19	EDB	Db	I	Adv. cancer	NCT04287868	
L19-TNFα/	EDB	scFv	I/II	Colorectal Cancer	NCT01253837	
Fibromun™			I	Adv. Solid Tumors	NCT02076620	[337]
			I	Melanoma	NCT01213732	
			I	Soft Tissue Sarcoma	NCT04032964	
			II	Unresectable/Met. Soft Tissue Sarcoma	NCT03420014	[338]
			I/II	Glioma of Brain	NCT03779230	[304]
			I/II	Glioblastoma	NCT04573192	
			I/II	Glioblastoma	NCT04443010	
αFAP-4-1BBL	FAP	IgG	I	B-cell NHL	NCT04077723	[311]
Daromun™	EDB	combo	III	Melanoma	NCT03567889	[283]
			II	Non-melanoma skin cancer	NCT04362722	

Table 3.3.: List of immunocytokines in clinical trials (NHL: Non-Hodgkin Lymphoma, Met.: metastatic, Adv.: advanced, Db: Diabody, scFv: single-chain Fragment variable, TnC: Tenascin C, FAP: fibroblast activation protein), adapted from Murer & Neri 2019[9] and clinicaltrials.gov (accessed 08.04.2020, updated 01.11.2020)

3.4. Tumor necrosis factor superfamily of cytokines

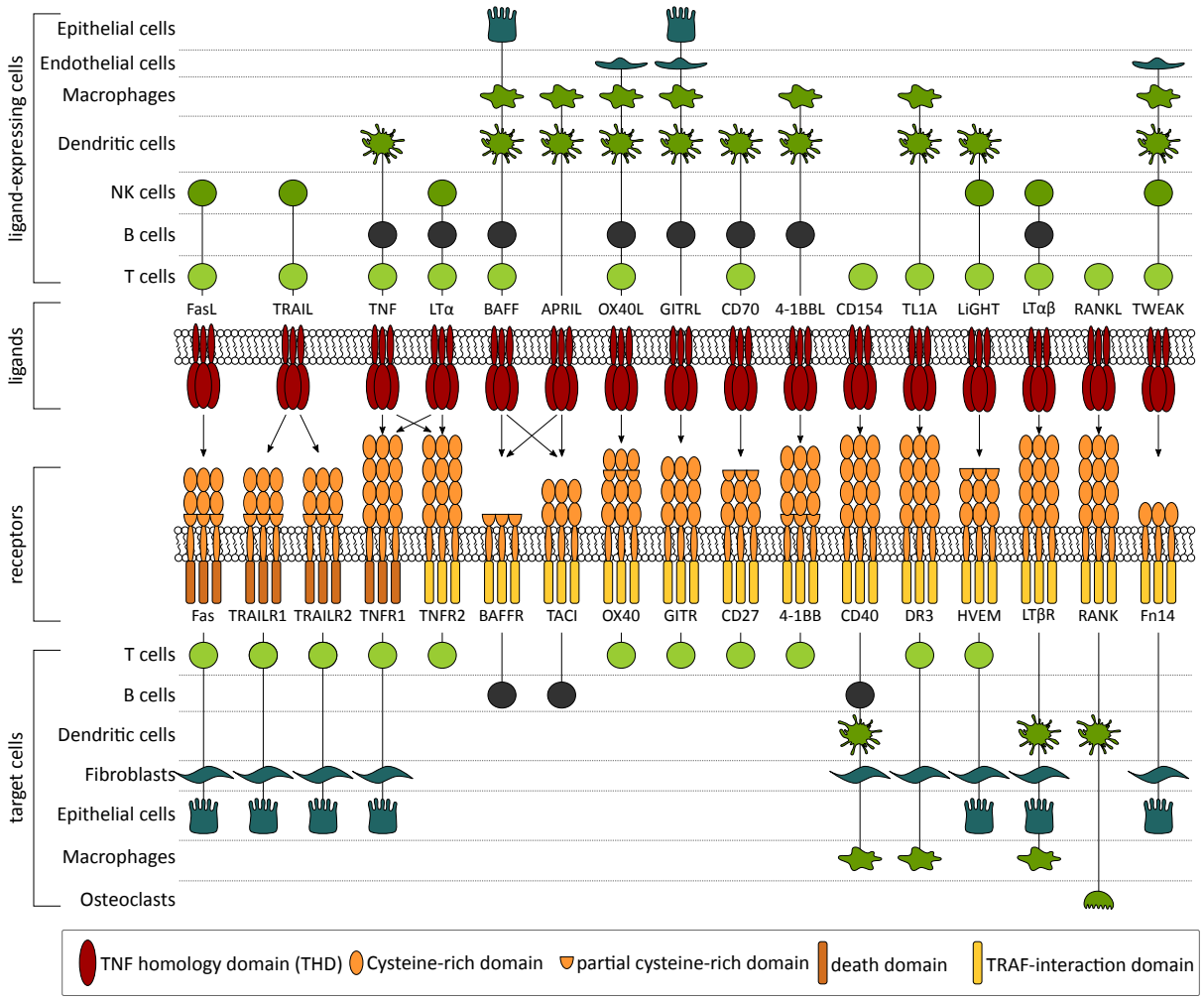

Figure 3.9.: A selection of receptors and ligands of the TNF superfamily. Adapted from Croft & Siegel (2017)[339]

The tumor necrosis factor (TNF) superfamily of cytokines is a large protein family that mediates many important interactions involved in the development of the immune system and inflammatory responses (Figure 3.9).[50] In most cases, both the receptor and the ligand are transmembrane proteins. Some ligands such as TNF, LiGHT and CD154 (CD40L) can be shed proteolytically.[340] Likewise, some receptors also exist in a soluble form acting as scavengers for the ligand.[341] The structure of both the receptors and the ligands is highly conserved. Most ligands are type II transmembrane proteins.[340] The extracellular domain contains a so-called TNF homology domain (THD) which mediates ligand multimerization and interaction with the receptors.[340] Most ligands form non-covalent homotrimers on the cell surface.[340] Ligands typically show a "jelly roll" structure composed of a number of β-strands. The receptors are mostly type I transmembrane proteins.[340] The extracellular domain contains several cysteine-rich domains that are pseudo-repeats containing 6 cysteines that engage in 3 disulfide bonds.[340] As can be seen in Figure 3.9

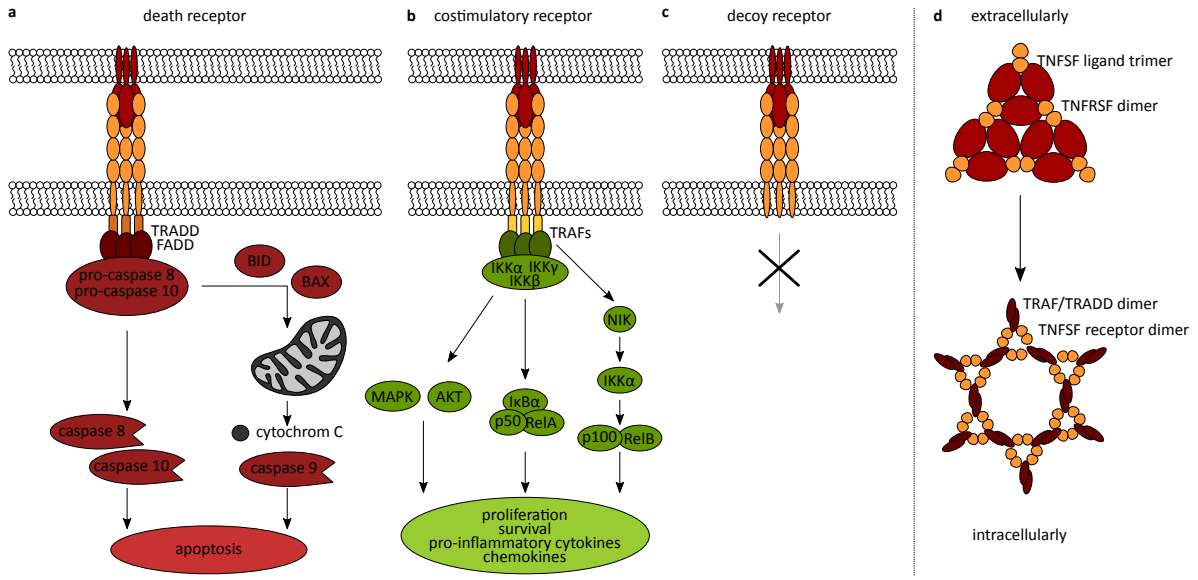

Figure 3.10.: The different types of TNFSF receptors **a)** Signalling via a death receptor (TRAILR, Fas, TNFR) triggers the intrinsic and extrinsic apoptosis pathway. **b)** A costimulatory receptor activates the MAP pathway as well as the canonical and non-canonical NF-κB pathway leading to proliferation, survival and production of pro-inflammatory cytokines. **c)** A decoy receptor does not interact with downstream signalling components and therefore does not transduce any signal. **d)** On the extracellular side, a receptor dimer interacts with a ligand trimer forming oligomeric signalling clusters. On the intracellular side, a receptor dimer associates with a TRAF or TRADD dimer and to form large hexagonal lattices. Adapted from Croft *et al.* (2013),[342] Vanamee and Faustman (2018)[343] and Karathanasis *et al.* (2020)[344]

some ligands interact with more than one receptor and likewise, some receptors bind to more than one ligand.[340]

Signalling is triggered by the ligand-mediated clustering of the receptors on the surface of the target cell. Most ligands with the exception of murine GITRL[345] and murine 4-1BBL[346] that form dimers and LT$\alpha\beta$ that forms a heterotrimer,[347] assemble into homotrimers. The receptor binds to the interface between two ligand monomers thus ensuring that only intact trimeric ligands can trigger signalling.[343] There are two main signal transduction pathways that are triggered by members of the TNF superfamily (Figure 3.10). Some receptors such as Fas, TRAIL receptor and TNF receptor contain an intracellular death domain that interacts with Fas-associated death domain (FADD), TNFR1-associated death domain (TRADD) or other death-domain binding partners to induce apoptosis of the target cell.[343] By contrast, most other receptors interact intracellularly with TNFR associated factors (TRAFs) to activate the MAPK pathway or the transcription factor NF-κB thus promoting cell survival, proliferation and the production of pro-inflammatory cytokines.[348] In addition, there are some decoy receptors that lack a cytosolic signalling domain.[343] The exact monomeric or oligomeric state of most receptors of the TNF superfamily on the surface of healthy cells is still under debate.[340] A recent

study revealed that TNFR1 assembles into monomeric and dimeric receptor units in the absence of the ligand TNF.[344] Upon ligand binding, the receptor units then assemble into trimers and higher-order oligomers, especially 9-mers.[344] Intracellular proteins such as TRAFs and TRADD that interact with the different receptors of the TNF superfamily have been shown to form large hexagonal clusters upon receptor activation. Notably, these clusters are a prerequisite for efficient signal transduction. Thus, the oligomerization of the receptors on the surface by the ligand is a prerequisite for the recruitment of intracellular interaction partners and the assembly of the hexagonal signalling lattice[343] (Figure 3.10 d).

Both the pro-apoptotic and the costimulatory receptors are interesting targets for cancer immunotherapy. Three costimulatory receptors, CD40, GITR and 4-1BB are described in more detail in the following sections.

3.4.1. CD40 (TNFRSF5)

CD40 is a receptor of the TNF superfamily, which is mainly expressed on antigen-presenting cells (APCs) and endothelial cells. Signalling through CD40 is involved in the licensing of dendritic cells (DCs)[349] and regulates processes involved in the activation of B cells such as antibody isotype switching, prevention of B cell apoptosis during the development of memory B cells, germinal center formation and cytokine production.[350,351] Engagement of CD40 expressed on endothelial cells with its ligand is implicated in the activation of the vascular endothelium and the upregulation of adhesion molecules thus facilitating the extravasation of leukocytes.[352] The ligand of CD40 (CD40L, CD154) is expressed primarily on activated T lymphocytes, but also on basophils, mast cells and eosinophils.[353,354]

The extracellular part of both murine and human CD40L is stabilized by a single intra-subunit disulfide bond and contains one occupied *N*-glycosylation consensus sequence.[354,355] Both murine and human CD40L can be proteolytically shed resulting in a soluble protein, which retains the biological activity of the membrane-bound protein.[356] In solution, human and murine CD40L associate as non-covalent trimers resulting in a pyramid-shaped molecule similar to other ligands of the TNF superfamily.[355] Murine CD40L was shown to be able to bind to and activate both murine and human CD40.[354]

CD40 agonists in clinical development

Currently, 10 agonistic CD40 antibodies in the IgG1 and IgG2 format are tested in clinical trials (Table 3.4). Some anti-CD40 antibodies act by enhancing direct killing of $CD40^+$ tumor cells, while others act via stimulation of APCs thus enhancing T cell priming and

immune infiltration into solid tumors. In most cases, dose-limiting toxicities and side effects arise due to peripheral activation of $CD40^+$ cells resulting in a cytokine-release syndrome. In many cases, also a transient loss of $CD19^+$ B cells is reported indicative of CD40-directed cytotoxicity. While this can be desirable in B cell malignancies, this can potentially limit the therapeutic activity against $CD40^-$ types of cancer.

The fully human IgG2 antibody Selicrelumab (CP-870893) was one of the first agonistic CD40-specific antibodies to enter clinical trials. Preclinical studies in $SCID^{beige}$ mice demonstrated that Selicrelumab prevented the growth of $CD40^+$ but not $CD40^-$ tumors in the absence of donor PMBCs. Adoptive transfer of human dendritic cells and T cells potentiated the Selicrelumab-mediated anti-tumor effect against $CD40^+$ tumors and restored the anti-tumor response against $CD40^-$ tumors indicating that the antibody acts both via direct killing of target cells and via its immunomodulatory functions.[357] In a first phase I clinical trial a maximum tolerated dose (MTD) of 0.2 mg/kg was determined.[358] The most common adverse event was reported to be a cytokine release syndrome (grade 1 to 2) leading to fever, chills and headache.[358] In addition, the treatment led to a transient depletion of $CD19^+$ B cells and an upregulation of markers related to lymphocyte activation.[359] Similar results were obtained in combination with gemcitabine in a second trial in patients with advanced pancreatic ductal adenocarcinoma[360] and in combination with carboplatin and paclitaxel in patients with advanced solid tumors.[361] Recently, the results of a phase Ib study of intravenously administered Selicrelumab at doses of up to 64 mg/dose in combination with intravenously administered Atezolizumab were reported. While the treatment was relatively well tolerated, the response rate of the combination treatment did not exceed historical data of treatments with Atezolizumab alone.[362] The most promising results were obtained in a study with patients suffering from metastatic melanoma. In this study, an objective response rate of 27.3% was obtained including two patients (9.1%) achieving a complete response when treated with 0.2 mg/kg Selicrelumab combined with 10 mg/kg of the anti-CTLA-4 antibody Tremelimumab.[363]

While Selicrelumab acts both by depleting $CD40^+$ cancer cells and through its immunostimulatory function, other antibodies such as Chi Lob 7/4, Lucatuzumab, Dacetuzumab and SEA-CD40 were developed primarily to enhance the eradication of $CD40^+$ hematological malignancies. A phase I study of the IgG1 antibody Chi Lob 7/4 revealed a maximum tolerated dose of up to 200 mg/dose leading to disease stabilization and activation of NK cells and monocytes in some patients. In this case, drug-related increases in liver enzymes were reported as dose-limiting toxicity.[359] Similarly, the IgG1 antibody Lucatuzumab was well tolerated with a MTD of 3 - 4.5 mg/kg. Even though at a dose of 3 mg/kg a receptor occupancy of 80 - 90% was reported,[364–366] Lucatuzumab showed only limited therapeutic efficacy as a monotherapy in patients with chronic lymphocytic leukemia,[364] multiple myeloma[365] and advanced lymphoma.[367]

Dacetuzumab was demonstrated to activate multiple pro-apoptotic pathways leading to the cell death of $CD40^+$ Non-Hodgkin's Lymphoma (NHL) cells *in vitro*.[368] Studies from xenograft models of NHL showed that in combination with chemotherapy, Dacetuzumab potentiated the anti-tumor effect of Rituximab.[368] However, a phase 2b clinical trial in patients with diffuse large B-cell lymphoma failed to demonstrate a benefit of Dacetuzumab plus Rituximab, ifosfamide, carboplatin and etoposide over the treatment without Dacetuzumab.[369] Similarly, Dacetuzumab monotherapy failed to elicit any objective responses in patients suffering from multiple myeloma[370] and chronic lymphocytic leukemia.[371] By contrast, Dacetuzumab monotherapy led to an objective response rate of more than 10% in patients suffering from refractory or recurrent NHL and was well tolerated at doses up to 8 mg/kg/week.[372] In addition, complete responses were reported for six out of 30 patients suffering from refractory diffuse large B cell lymphoma treated with Dacetuzumab in combination with Rituximab and gemcitabine.[373] SEA-CD40 is a glycoengineered, non-fucosylated variant of Dacetuzumab with higher affinity for FcγRIIIa and therefore enhanced antibody-dependent cellular cytotoxicity.[374] A phase I clinical trial in patients with solid tumors revealed limited anti-tumor efficacy as a monotherapy accompanied with infusion-related dose-limiting toxicities in 10% of the patients.[375] A dose-dependent increase in cytokine and chemokine expression indicative of enhanced immune cell trafficking and increased activity of $CD4^+$ and $CD8^+$ cells was observed.[376] In November 2019, enrollment of another cohort was started to evaluate the efficacy of SEA-CD40 in combination with Pembrolizumab or nab-Paclitaxel combined with gemcitabine in patients suffering from pancreatic ductal adenocarcinoma.[377]

APX005M is a humanized IgG1 antibody which mimics CD40L by potently activating antigen-presenting cells *in vitro*.[378] During a phase I clinical trial evaluating the safety and efficacy of APX005M in combination with Nivolumab and standard chemotherapy (gemcitabine + nab-paclitaxel) in patients suffering from metastatic pancreatic ductal adenocarcinoma (PDAC), 54% of the patients discontinued the treatment due to adverse events.[379] Among the remaining patients, 58% showed a partial response, warranting continuation to a phase II clinical trial at a dose of 0.3 mg/kg.[379] The dose of 0.3 mg/kg was also found to be safe in combination with Nivolumab in patients suffering from metastatic melanoma or non-small cell lung cancer.[380] Analysis of biopsies revealed increased tumor infiltration by T cells and increased levels of IFN-γ-inducible chemokines.[380]

Several strategies to reduce the toxicity of CD40 agonistic treatments have been reported in clinical trials. For instance, it was reported that premedication with Cetirizine and Montelukast reduced the frequency of infusion-related reactions upon treatment with the CD40 agonistic antibody JNJ-64457107.[381] Based on evidence that intratumoral administration of CD40 agonists could reduce toxicity[382] and prime antigen-presenting cells at the site of disease similar to the *in situ* development of a vaccine, the CD40 agonistic antibody

Mitazalimab (ADC-1013) was specifically developed for intratumoral administration.[383] Evidence of promising anti-tumor activity was obtained from preclinical models of cancer both in NSG mice receiving donor DCs and T cells and in human CD40 transgenic mice.[383] A phase I clinical trial revealed that intralesional administration into liver metastases was associated with increased toxicity compared to the administration into lesions in other organs and most patients still experienced a transient decline in $CD19^+$ B cells, while clinical responses were modest.[384] Similarly, a clinical trial was initiated to evaluate the safety and efficacy of intratumoral APX005M in combination with systemic Pembrolizumab in treatment-naive patients suffering from metastatic melanoma.[385]

In addition, the development of CDX-1140, a CD40-specific IgG2 antibody with balanced agonistic properties was reported.[386] It was shown to bind to CD40 outside the CD40L binding site and its *in vitro* biological activity could be enhanced by the addition of recombinant CD40L.[386] The inability of CDX-1140 to activate APCs in the absence of CD40L could help to reduce systemic toxicities.[386] Promising anti-tumor activity in preclinical xenograft models of cancer warranted the initiation of a number of clinical trials.[386] It was well tolerated at doses up to 0.72 mg/kg in a monotherapy without changes in liver function test.[387] Cytokine responses could be increased when combining CDX-1140 with the recombinant human FLT3 ligand CDX-301.[387]

So far, two targeted CD40 agonists, ABBV-428 and SL172154, have entered clinical trials. ABBV-428 is bispecific antibody binding to mesothelin and CD40. Its CD40 agonistic activity was shown to be mesothelin-dependent.[388] ABBV-428 was well tolerated but did not lead to any objective response in a phase I clinical trial.[389] SL-172154 which is a fusion protein featuring signal regulatory protein α (SIRPα) fused to an antibody Fc domain and human CD40 ligand. CD47 is frequently upregulated on cancer cells[390,391] and represents a "don't eat me" signal by binding to SIRPα on macrophages.[392] There is evidence that antibody-mediated redirection of phagocytic cells to CD47 can enhance T cell priming towards $CD47^+$ cancer cells.[393] SL-172154 mimics this by redirecting $CD40^+$ phagocytes using SIRPα which is the ligand for CD47. Preclinical evaluations of SL-172154 showed promising anti-tumor efficacy with reduced toxicity compared to agonistic CD40 antibodies.[394]

Further CD40 agonists in preclinical development

The relatively high toxicity of agonistic CD40 antibodies upon systemic administration highlights the need for targeted CD40 agonists ideally with conditional activity. Preclinical development of CD40 agonists include fusion proteins featuring the soluble part of CD40L. For instance, researchers at Apogenix developed so-called hexavalent receptor agonists (HERA) which comprise single-chain trimers of a TNF superfamily ligand such

as CD40L fused to an antibody Fc portion. Due to the Fc-mediated dimerization of the protein, this results in a hexameric CD40L fusion protein with potent agonistic activity *in vitro*.[399] Recently, fusion proteins featuring HERA-CD40L linked to an antibody moiety targeting cancer-associated antigens such as CEA and PD-L1 were reported.[400] In addition, a dual fusion protein (Duokine) featuring a second TNF superfamily ligand such as 4-1BBL fused to CD40L was recently reported to reduce the metastatic burden in a mouse model of cancer in combination with a T cell redirecting bispecific antibody.[401] In addition to CD40-specific antibodies and CD40L, other binding moieties specific for CD40 have been developed. For instance, a fibroblast-activation protein (FAP)-targeted CD40-specific DARPin® which exhibited antigen-dependent activity and led to potent anti-tumor immune responses in mouse models of cancer without apparent toxicity was recently described.[402] In addition, a fusion protein comprising amino acids Trp140-Ser149 of CD40L inserted into a permissive loop of the *Salmonella typhi* OmpC protein was reported.[403] The peptide Trp140-Ser149 of CD40L ($CD154_p$) was chosen based on mutagenesis analysis showing that this comprises the main interaction domain with CD40.[404] The OmpC-$CD154_p$ fusion protein showed some biological activity *in vitro* on Raji cells,[405] but no reports of *in vivo* studies are available.

Name	Indication	Combination	Phase	Identifier	Ref
2141 V-11	Solid Tumors	n/a	I	NCT04059588	
	Glioma	DD2C7-IT	I	NCT04547777	
ABBV-428	Adv solid Tumors	Nivolumab	I	NCT02955251	[389]
APX005M	Solid Tumors	n/a	I	NCT02482168	[379]
	Melanoma	Pembrolizumab	I/II	NCT02706353	[385]
	Lung, Melanoma	n/a	I/II	NCT03123783	[380]
	Esophageal	various	II	NCT03165994	
	Met Pancreatic	Nivolumab, nPl, Gem	I/II	NCT03214250	
	Glioma, Medulloblastoma	n/a	I	NCT03389802	
	Solid Tumors	Cabiralizumab, Nivolumab	I	NCT03502330	
	Met Melanoma	NEO-PV-01, Nivolumab, Ipilimumab	I	NCT03597282	
	Soft Tissue Sarcoma	Doxorubicin	II	NCT03719430	[395]
	Adv Rectal Adenocarcinoma	mFOLFOX, Radiation	II	NCT04130854	
	Met Melanoma	n/a	II	NCT04337931	
CDX-1140	Solid Tumors	CDX-301, Pembrolizumab, Chemotherapy	I	NCT03329950	[387]
	Melanoma	various	I/II	NCT04364230	
	Lung Cancer	CDX-301, SBRT	I/II	NCT04491084	
	Malignant Epithelial Neoplasms	ACT, Pembrolizumab	I	NCT04520711	
Chi Lob 7/4	Lymphoma	n/a	I	NCT01561911	[359]
Dacetuzumab	Multiple Myeloma	n/a	I	NCT00079716	[370]
	NHL	n/a	I	NCT00103779	[372]
	Leukemia	n/a	I/II	NCT00283101	[371]
	Lymphoma	n/a	II	NCT00435916	[396]
	Multiple Myeloma	lenalidomide, dexamethasone	I	NCT00525447	[397]
	Lymphoma	Rituximab, etoposide, carboplatin, ifosfamide	II	NCT00529503	[369]
	NHL	Rituximab	I	NCT00556699	
	Lymphoma	Rituximab, Gem	I	NCT00655837	[373]
	Multiple Myeloma	bortezomib	I	NCT00664898	
JNJ-64457107	Adv Solid Neoplasms	n/a	I	NCT02829099	[381]
Lucatuzumab	CLL	n/a	I	NCT00108108	[364]
	Multiple Myeloma	n/a	I	NCT00231166	[365]
	Lymphoma	n/a	I/II	NCT00670592	[367]
	Follicular Lymphoma	n/a	I	NCT01275209	
Mitazalimab	Neoplasms	n/a	I	NCT02379741	[384]
SEA-CD40	Neoplasms	Pembrolizumab, Gem, nP	I	NCT02376699	[375,377]
Selicrelumab	Neoplasms	Paclitaxel + Carboplatin	I	NCT00607048	[361]
	Pancreatic Neoplasm	Chemotherapy	I	NCT00711191	[360]
	Adv. Melanoma	Tremelimumab	I	NCT01103635	[363]
	Adv. Solid Tumors	n/a	I	NCT02225002	[359]
	Adv. Solid Tumors	Emactuzumab	Ib	NCT02760797	[398]
	Solid Tumors	Atezolizumab	I	NCT02304393	[362]
	Pancreatic Cancer	nP, Gem	I	NCT02588443	
	Adv. Met. Solid Tumors	Vanucizumab, Bevacizumab	I	NCT02665416	
	B-Cell NHL	Atezolizumab	I	NCT03892525	
SL-172154	Ovarian Cancer	n/a	I	NCT04406623	
	Squamous Cell Carcinoma	n/a	I	NCT04502888	

Table 3.4.: List of CD40 agonistic proteins in clinical trials (NHL: Non-Hodgkin Lymphoma, CLL: Chronic Lymphocytic Leukemia, SBRT: stereotactic body radiation therapy, Gem: Gemcitabine, nP: Nab-Paclitaxel, Adv: advanced, Met: metastatic) adapted from clinicaltrials.gov (accessed 17.09.2020)

3.4.2. GITR (CD357, TNFRSF18)

GITR is a T cell costimulatory receptor of the TNF superfamily which is upregulated on activated effector T cells and on NK cells. In addition, GITR is constitutively expressed at high levels by T_{reg}. Signalling via GITR induces the expression of antiapoptotic proteins such as Bcl-XL and thus enhances the survival of effector T cells and protects them from activation-induced cell death.[406] There is also evidence that GITR signalling lowers the threshold of CD28 costimulation for the activation of effector T cells.[407] GITR agonism induces the expansion of T_{reg}, but inhibits the suppressive function of T_{reg}[408] and renders effector T cells resistant to suppression by T_{reg}.[409]

The structure of the human GITRL differs substantially from the majority of ligands of the TNF superfamily.[410] It is characterized by a relatively short TNF homology domain (119 aa vs 150 aa) and a relatively small trimerization interface lacking the tightly packed aromatic and hydrophobic residues found in most trimerization interfaces of ligands of the TNF superfamily.[410] The small trimerization interface results in relatively weak non-covalent interactions between the individual subunits and therefore a low tendency to trimerize in solution.[410] However, forced trimerization of the ligand has been shown to tremendously increase the receptor binding affinity and the costimulatory activity.[410] The C-terminal arm of murine GITRL was shown to engage in a unique domain-swapping interaction leading to ligand dimerization instead of trimerization.[345,411] Notably, ligand trimerization could be achieved by deleting the three C-terminal amino acids of GITRL.[411] It is not yet well understood, how dimeric murine GITRL interacts with the receptor and elicits signal transduction.[345]

GITR agonists in clinical development

A list of GITR agonists that are tested in clinical trials is provided in Table 3.5. TRX518 was the first GITR agonist to enter clinical trials. It is a fully humanized, aglycosylated IgG1 antibody whose epitope partially overlaps with the GITRL binding site.[417] Preclinical *in vitro* studies showed that it efficiently costimulated suboptimally stimulated lymphocytes without having any superagonist properties making it a safe candidate for clinical development.[417] A first-in-human clinical trial showed that it was very well tolerated (up to 8 mg/kg as a single dose) but with limited efficacy since only 4/28 patients showed a best response of stable disease.[418] A recent clinical trial with the GITR agonistic antibody BMS-986156 showed no single-agent anti-tumor activity and the responses obtained in combination with Nivolumab did not differ from historical data obtained from Nivolumab treatment alone.[412] MK4166 is another humanized IgG1 antibody which was shown to be particularly effective at modulating regulatory T cells *in vitro*.[421] In a phase I clinical study promising results were obtained in combination with Pembrolizumab in

Name	Format	Indication	Combination	Phase	Identifier	Ref
ASP1951	Ab	Adv Solid Tumors	Pembrolizumab	I	NCT03799003	
BMS-986156	IgG1	Adv Malignant Solid Neoplasm	Ipilimumab, Nivolumab, SBRT	I/II	NCT04021043	[412]
GWN323	IgG	Solid Tumors, Lymphomas	Spartalizumab	I	NCT02740270	
INCAGN1876	IgG1	Adv/ Met Cancer	n/a	I/II	NCT02697591	[413]
		Adv/ Met Cancer	Epacadostat, Pembrolizumab	I/II	NCT03277352	
		Adv/ Met Cancer	Nivolumab, Ipilimumab	I/II	NCT03126110	
		Glioblastoma	INCMGA00012, SRS, Brain surgery	II	NCT04225039	
		Head/Neck cancer	INCMGA00012, DPV-001	I	NCT04470024	
MK1248	IgG4	Adv Solid Tumor	Pembrolizumab	I	NCT02553499	[414,415]
MK4166	IgG1	Glioblastoma	Nivolumab, IDO1 inhibitor INCB024360, Ipilimumab	I	NCT03707457	[416]
REGN6569	Ab	Head/Neck Squamous Cell Carcinoma	Cemiplimab	I	NCT04465487	
TRX518	IgG1	Melanoma, other solid tumors	n/a	I	NCT01239134	[417,418]
MEDI1873	Fc	Adv Solid Tumors	n/a	I	NCT02583165	[419]
OMP-336B11	Fc	Locally Adv/ Met Cancer	n/a	I	NCT03295942	[420]

Table 3.5.: List of GITR agonistic proteins currently in clinical trials (SRS: stereotactic radio-surgery, SBRT: stereotactic body radiation therapy, Ab: antibody, Fc: Fc-fusion protein of the ligand, Adv: advanced, Met: metastatic) adapted from clinicaltrials.gov (accessed 22.05.2020, updated 01.11.2020)

melanoma patients, including an overall response rate of 69% (n=13, 4 CR, 5 PR) in immune checkpoint inhibitor naïve patients.[416] MK1248 has the same CDR regions as MK1466, but is in the IgG4 format and has significantly reduced Fc effector functions.[421] No objective responses were observed in a phase I clinical trial upon single-agent treatment with MK1248, whereas 1 complete response and 2 partial responses were achieved in combination with Pembrolizumab.[415] INCAGN01876 is a humanized IgG1 antibody with an optimized binding profile towards human GITR allowing efficient costimulation of suboptimaly stimulated effector T cells.[413] Data from the first-in-human clinical trial are not yet available. ASP1951 is a tetravalent GITR agonistic antibody that was originally developed by researchers at Potenza therapeutics which was later acquired by Astellas Pharma. Only limited information about preclinical studies and the format are publicly available. In addition to the agonistic antibodies, two GITRL-Fc fusion proteins have been tested in clinical trials. OMB-336B11 is an Fc fusion proteins featuring single-chain

trimeric GITRL moieties as a payload. OMB-336B11 showed promising *in vitro* bioactivity properties including stimulation of patient-derived T and NK cells.[420] However, the phase I clinical trial was terminated by the sponsor in September 2019.[422] MEDI1873 is a fusion protein consisting of the GITRL extracellular domain, fused to a trimerization domain and an Fc portion.[423] In a phase I clinical trial, a best overall response of stable disease was observed in 42.5% of the patients and the treatment had an overall acceptable safety profile.[419] However, also MED1873 was discontinued after the acquisition of MedImmune by AstraZeneca.[424]

Further GITR agonists in preclinical development

Most preclinical studies on GITR agonists are based on the GITR-specific rat IgG2b antibody DTA-1 which has demonstrated potent anti-tumor activity in a number of preclinical models of cancer.[7] In addition to agonistic antibodies, a number of fusion proteins featuring GITRL have been reported. One of the first reports describing the development of an Fc-fusion protein featuring GITRL as payload described a single unit of GITRL fused to the Fc portion of an IgG1 antibody. It showed similar anti-tumor activity as the agonistic antibody DTA-1 in preclinical models of cancer when the treatment was started at early timepoints and was frequently dosed.[425] Researchers at Apogenix developed a fusion protein featuring single-chain trimeric GITRL fused to an IgG1-derived Fc domain. This hexavalent GITR agonistic protein (HERA-GITRL) showed superior costimulatory activity *in vitro* in comparison to the clinical grade agonistic antibody TRX518. However, this HERA-GITRL fusion protein only yielded limited *in vivo* anti-tumor activity in preclinical models of cancer.[426] An immunocytokine featuring both IL-15 and GITRL has also been reported which prevented the formation of lung metastases in a mouse model of cancer.[316]

3.4.3. 4-1BB (CD137, TNFRSF9)

4-1BB is another T cell costimulatory receptor of the TNF superfamily with several properties that make it an interesting target for cancer immunotherapy.[6,427] First, signalling through 4-1BB enhances effector function and survival[428] of cell types that are important for tumor eradication such as $CD8^+$ T cells[429] and natural killer (NK) cells.[430] In particular, it protects T cells from activation-induced cell death by triggering the upregulation of the anti-apoptotic Bcl-2 family members Bcl-xL and Bfl-1.[431] Engagement of 4-1BB by monoclonal antibodies has been shown to prevent and revert anergy in cytotoxic T cells.[432] 4-1BB-mediated activation of the p28-MAPK signal transduction pathway was shown to increase mitochondrial biogenesis.[433] This metabolic reprogramming further enhances the longevity of the T cells and provides the metabolic capacity to acquire a

memory phenotype.[433] 4-1BB is constitutively expressed on resting dendritic cells (DC)[434] and was shown to be important for their survival and their ability to activate T cells.[435] Second, the expression of 4-1BB is restricted to activated T cells.[429] Thus stimulation through 4-1BB can be delivered selectively to antigen-specific T cells.[436] This is especially interesting in the context of tumor therapies since the hypoxic environment of solid tumors was demonstrated to further enhance 4-1BB expression on tumor-infiltrating T cells.[437] Third, hypoxia also drives the expression of 4-1BB on endothelial cells of the tumor blood vessels.[438,439] Agonistic antibodies to 4-1BB on endothelial cells were shown to improve tumor infiltration by $CD8^+$ T cells via the upregulation of adhesion molecules such as ICAM-1, VCAM-1 and E-selectin on the endothelium.[438] Engagement of 4-1BB on endothelial cells in tumor blood vessels also increased the production of CCL21 which in turn facilitates the recruitment of monocyte-derived dendritic cells.[440] However, hypoxia was also shown to drive alternative splicing of the 4-1BB mRNA leading to the secretion of soluble 4-1BB which can act as scavenger for the ligand.[441] A further caveat lies in the fact 4-1BB that is also expressed by regulatory T cells (T_{reg}), especially in the tumor.[442] The role of 4-1BB agonism on T_{reg} is currently under debate. There are some reports that show that antibody-mediated depletion of T_{reg} is responsible for the observed anti-tumor effect.[443] In addition, co-stimulation via 4-1BB was shown to enhance the ability of T_{reg} to suppress colitis.[444] By contrast, there is also evidence that 4-1BB agonism decreases the suppressive potential of T_{reg} *in vitro*.[442] Nevertheless, impressive results have been achieved using 4-1BB agonists in preclinical models of cancer and a number of 4-1BB agonists are currently tested in clinical trials.[445,446]

The structures of both human and murine 4-1BB and 4-1BBL show unique features that are not found in the majority of the TNF superfamily. The human 4-1BBL forms a canonical bell shaped structure as is the case for most ligands of the TNF superfamily.[447] The receptor, however, is special in that it forms a covalent dimer through an inter-subunit disulfide bond.[447] By contrast, the murine 4-1BBL does not form a trimer but a disulfide-linked dimer.[346] It was further shown to interact in a 2:2 stoichiometry with its receptor in a way that each receptor monomer only interacts with one ligand moiety.[346] A role for galectin-9 in bridging adjacent receptor-ligand complexes to promote the clustering necessary for signal transduction has been suggested,[448] but the detailed mechanisms of activation are still under debate.

4-1BB agonists in clinical development

A list of 4-1BB agonistic proteins that are currently tested in clinical trials can be found in Table 3.6. Urelumab (BMS-663513) was the first 4-1BB agonist to enter clinical trials in 2005. It is a fully humanized IgG4 agonistic antibody that was developed by researchers at Bristol-Myers Squibb.[6] Based on promising results of the initial phase I study both in

terms of disease stabilization and immune activation related biomarkers, a phase II study was initiated.[449] However, due to a high incidence of hepatic toxicity during the phase II study the trial was prematurely stopped in 2009. After it was shown that a lower dose was sufficient to achieve comparable results in preclinical studies without leading to substantial toxicity, Urelumab re-entered clinical trials in 2012 and is currently being tested in a number of clinical studies alone and in combination with immune checkpoint inhibitors.[6] In 2011, a second 4-1BB agonistic antibody in the IgG2 format termed Utomilumab (PF-05082566) entered clinical trials alone and in combination with Rituximab. An overall best response of disease stabilization in 22% of the patients together with good tolerability warranted the initiation of a number of further clinical trials of this agent.[450] Since then, at least four more 4-1BB agonistic IgG antibodies have entered clinical trials (Table 3.6). LVGN6051 was developed as part of a study on the influence of both agonistic activity and Fcγ receptor affinity on the therapeutic potential and toxicity of 4-1BB agonists.[451] The authors reasoned that in the tumor microenvironment the tumor-specific T cells are activated in an antigen-dependent manner leading to the upregulation of 4-1BB, which lowers the threshold for costimulation. By contrast, the high abundance of FcγRIIb in the liver would efficiently crosslink 4-1BB agonistic antibodies and therefore deliver potent costimulatory signals to weakly activated T cells leading to hepatotoxicity. Therefore, careful selection of agonistic strength and FcγR dependence is necessary in order to engineer 4-1BB agonists with favorable toxicity profiles and good anti-tumor activities. LVGN6051 was therefore selected for relatively weak agonistic activity and dependence on FcγRIIb-dependent cross-linking and showed comparable anti-tumor efficacy as Urelumab, but less hepatotoxicity in preclinical models of cancer.[451] This finding is consistent with a study by researchers from AbbVie who showed that a higher-affinity of the antibody for 4-1BB did not increase the anti-tumor activity but potentially increased the toxicity in preclinical models.[452] As an alternative to FcγR-mediated cross-linking, clustering of bispecific 4-1BB agonists on tumor-associated antigens is explored as a strategy for next-generation 4-1BB agonists. Currently, several bispecific antibodies and a bispecific antibody-anticalin fusion protein are explored in clinical trials (Table 3.6).[453] DuoBody®-PD-L1×4-1BB (also termed GEN1046),[454] INBRX-105 (also termed ES101) and MCLA-145[455] are all bispecific antibodies targeting PD-L1, which is frequently upregulated on tumor cells, and 4-1BB.[453,456] Therefore, these three bispecific antibodies also block the immunosuppressive PD-1/PD-L1 axis.[456] In addition, NM21-1480, a trispecific antibody which simultaneously engages with 4-1BB, PD-L1 and human serum albumin (HSA), recently entered clinical trials.[457] PRS-343 consists of a HER2-specific IgG antibody fused to a 4-1BB-specific anticalin™. Also in this case, 4-1BB agonistic activities were shown to be dependent on the presence of HER2.[458] No dose limiting toxicities were reported for a phase I clinical trial during which doses of up to 18 mg/kg were administered.[459] Among the 33 patients that were treated at active dose levels, 3% complete responses and 9% partial responses were

observed.[459] RO7227166 features a single-chain trimeric 4-1BBL moiety replacing one arm of a FAP-specific Fc-silenced IgG1 antibody. In preclinical models, it showed promising anti-tumor activity in combination with antigen-targeted bispecific antibodies.[311] A phase I clinical trial revealed that doses of up to 2000 mg per patient were well tolerated and objective responses were reported for 2 out of 62 patients (3.6%). In combination with Atezolizumab objective responses were seen in 18.4% of the patients.[460] In addition to these protein-based 4-1BB agonists, a number of cell-based therapies such as CAR-Ts, dendritic cell vaccines, red blood cells and oncolytic viruses incorporating domains of 4-1BB(L) are currently studied in clinical trials.

Name	**Format**	**Indication**	**Combination**	**Phase**	**Identifier**	**Ref**
ADG106	IgG4	Solid Tumors, NHL	n/a	I	NCT03707093	461
		Solid Tumors, NHL	n/a	I	NCT03802955	462
AGEN2373	IgG1	Advanced Cancer	n/a	I	NCT04121676	463
ATOR-1017	IgG4	Solid Tumor, Neoplasms	n/a	I	NCT04144842	464,465
Urelumab	IgG4	Melanoma	n/a	II	NCT00612664	
		Melanoma	Nivolumab, ACT	I	NCT02652455	
		Urothelial Carcinoma, Bladder Cancer	Nivolumab	II	NCT02845323	
Utomilumab	IgG2	Advanced cancer	Rituximab	I	NCT01307267	466,467
		Advanced Solid Tumors	Pembrolizumab	I	NCT02179918	468
		Neoplasms	PF-04518600	I	NCT02315066	469
		Diffuse Large B-Cell Lymphoma	Avelumab, Rituximab, Azacitidine, Bendamustine, Gemcitabine, Oxaliplatin	III	NCT02951156	
		HPV-16$^+$ Oropharyngeal Cancer	ISA101b	II	NCT03258008	
		Breast Cancer	Trastuzumab, Trastuzumab Emtansine	I	NCT03364348	
		Breast Cancer	Vinorelbine, Trastuzumab, Avelumab	II	NCT03414658	
GEN1046	bispecific	Solid Tumors	n/a	I/II	NCT03917381	454
LVGN6051	IgG	Cancer	n/a	I	NCT04130542	451
INBRX-105	bispecific	Solid Tumor, Neoplasms	n/a	I	NCT04009460	
		Metastatic Solid Tumors	n/a	I	NCT03809624	
MCLA-145	bispecific	Advanced Cancer	n/a	I	NCT03922204	455,456
NM21-1480	trispecific	Advanced Solid Tumor	n/a	I/II	NCT04442126	457
PRS-343	anticalin	HER2$^+$ Solid Tumor	n/a	I	NCT03330561	458,459
		HER2$^+$ Solid Tumor	Atezolizumab	I	NCT03650348	
RO7227166	IC	NHL	Obinutuzumab, RO7082859	I	NCT04077723	311,460

Table 3.6.: List of 4-1BB agonistic proteins currently in clinical trials (NHL: Non-Hodgkin Lymphoma, IC: immunocytokine, ACT: adoptive cell therapy) adapted from clinicaltrials.gov (accessed 01.11.2020)

Further 4-1BB agonists in preclinical development

The partial success of Urelumab in clinical trials sparked immense research interest in the development of enhanced 4-1BB agonists for cancer therapies. For instance, tumor-targeted bispecific 4-1BB agonistic antibodies have been described that include a trimerization domain in order to increase the agonistic activity of the α4-1BB moiety.[470,471] Similar constructs were described targeting carcinoembryonic antigen (CEA) and EGFR. The EGFR targeted variant showed promising anti-tumor activity and a favorable safety profile in preclinical models of cancer.[470] Other formats of bispecific moieties engaging a tumor-specific antigen and 4-1BB include bispecific bicyclic peptides (Bicycles™),[472,473] DARPins™,[474] DART™proteins[475] and bispecific aptamers.[476] Most of these bispecific formats have the advantage that 4-1BB agonism relies on antigen-dependent clustering thus restricting the effect to the tumor microenvironment. Other recent developments include single-chain trimeric fusions of 4-1BBL linked both to a tumor-targeting antibody and an IL-15 moiety. This trispecific proteins showed some anti-tumor activity against the formation of lung metastases in mouse models of cancer.[316] The costimulatory function of 4-1BBL was also exploited in order to potentiate a bispecific antibody aimed at redirecting $CD3^+$ T cells towards $CD33^+$ acute myeloid leukemia (AML). The incorporation of a 4-1BBL moiety into the CD3/CD33 bispecific antibody enhanced the proliferation and effector functions of T cells compared to the original CD3/CD33 bispecific antibody as shown in an *in vitro* tumor cell killing assay. This trend was especially pronounced at low effector:target ratios and against $CD33^{low}$ tumor cells.[477]

3.5. Antibody-cytokine fusions with "activity on demand"

Even though the therapeutic windows of cytokine products could be tremendously improved by the targeted delivery in the form of immunocytokines, many patients still experience severe side effects such as flu-like symptoms, nausea and hypotension especially shortly after the intravenous administration.[9,10,281] At this point in time, the concentration of the active cytokine in the blood and the periphery of the body is highest (Figure 3.11b).[281] This and the observation that these symptoms usually vanish after some time when the concentration in the blood falls below a critical threshold,[478] point towards the fact that most toxicity is due to peripheral activation of the cytokine receptors.[254] Binding to cognate cytokine receptors in the periphery not only induces on-target off-tumor toxicity but it can also diminish the amount of immunocytokine that can accumulate in the tumor due to peripheral trapping of the cytokine.[262,479] Therefore, it would be desirable to engineer variants that are inactive until they reach the tumor where they

regain activity (Figure 3.11c).

3.5.1. Activation through conformational changes

There is evidence that the toxicity associated with intravenously administered IL-2 products is due to over-activation of IL2Rβγ-expressing natural killer cells.[480] Some claim that NK are relatively abundant in the blood stream[481] and are therefore at the first site of contact where they can efficiently sequester a significant proportion of the administered IL-2, even though pharmacokinetic analyses of immunocytokines featuring IL-2 as a payload provide no evidence of IL-2 receptor-mediated trapping by blood cells.[281,282] Under normal physiologic conditions, most NK cells express only the intermediate affinity IL-2 receptor containing only the β and γ subunits.[482] To avoid NK-mediated toxicity, IL-2 variants were engineered that selectively activate only the high affinity IL-2 receptor containing all three subunits (α, β and γ).[483] However, since the high-affinity IL-2 receptor is expressed at high levels on regulatory T cells and is only upregulated on activated effector T cells, other strategies aim at engineering IL-2 variants which selectively bind to the βγ receptor in order to avoid activation of regulatory T cells.[484] A different strategy was described by Stephen Gillies who showed that by fusing the IL-2 moiety to the C-terminus of the light chain of an antibody in the IgG format rather than to the heavy chain via carefully chosen linkers resulted in an IL-2 fusion protein which did not bind to the IL-2Rβγ unless the antibody bound to its target. This on-target restoration of the full biological activity is assumed to be due to conformational changes in the hinge region of the IgG upon binding to the antigen. In addition to showing some selective activity, this construct demonstrated favorable *in vivo* properties such as long circulatory half-life, increased uptake upon subcutaneous administration and efficient antibody effector functions.[485]

3.5.2. Attenuation of cytokine potency

The targeted delivery of cytokine products to tumors often results in a high local concentration of the cytokine at the tumor several hours after administration, while the concentration of the cytokine in the blood stream remains relatively low at all time points. Engineered cytokine variants with reduced affinities for their receptors and which are not potent enough to activate cognate receptors at the concentration at which they can be found in the blood, but that potently activate the cytokine receptor after accumulating in the tumor have been reported.[486–489] This concept was first demonstrated for attenuated IFNα variants targeted to $CD38^+$ multiple myeloma (Attenukine™)[487] or $CD20^+$ lymphoma tumors (AcTaferon).[488] The anti-tumor activity of IFNα relies both on direct

cytotoxicity and via the activation of a number of immune cells. Side effects associated with the administration of IFNα include nausea, flu-like symptoms, vasculopathic complications and neurological symptoms. The systemic toxicity is thought to be mainly due to the ubiquitous expression of IFNα receptors on various cells in the body. In both cases, promising anti-tumor activity without systemic toxicity was observed.[487,488] This strategy was also applied in order to selectively deliver IFNα to Clec9A$^+$ dendritic cells and potent anti-tumor activity was reported in mouse models of melanoma, breast cancer and lymphoma without detectable toxicity.[490] Recently, this strategy was also applied to TNF (AcTafactor) and IFNγ (AcTaferon-II) targeted to CD13 which is a marker of endothelial cells.[489] While CD13-targeted AcTafactor and CD8-targeted AcTaferon-II only showed limited single-agent anti-tumor activity, the combination of the two resulted in a strongly synergistic anti-tumor effect.[489]Thus, targeted delivery of attenuated cytokines can be applied both to delivering engineered cytokines to the tumor microenvironment and to a specific subset of immune effector cells depending on the choice of the antibody.

3.5.3. Targeted reassembly of cytokine subunits

Similar to the strategy described above, cytokine activity can be selectively restored at the site of the tumor by sequential administration of individual subunits of heterodimeric cytokines or by the administration of cytokines that are inactive in solution but regain activity upon antibody-mediated clustering. Since members of the TNF superfamily rely on receptor clustering for efficient signalling, the administration of soluble ligands targeted to the tumor is a possibility to selectively reconstitute activity at the site of disease.[491] This strategy was demonstrated *in vitro* for a number of TNF superfamily ligands such as human OX40L and human 4-1BBL fused to antibodies targeting EGFR.[492] Limited data for *in vivo* single-agent anti-tumor activity for such constructs is available, while triple fusion proteins featuring IL-15 fused to ligands of the TNF superfamily and tumor-targeting antibodies showed some activity in preventing the formation of lung metastases in mouse models of melanoma.[316] The targeted reconstitution of sequentially administered subunits of a heterodimeric cytokine was reported for IL-12. Both the p35 and the p40 subunits were fused to an F8 antibody fragment targeting EDA-positive fibronectin of the tumor neovasculature. Unfortunately, this approach was hampered by the observation that the p35 subunit alone exhibited substantial biological activity and was able to activate CD4$^+$, CD8$^+$ T cells and natural killer cells.[493]

3.5.4. Activation through proteolysis

In order to enable the tissue remodelling which is necessary for the progression of solid malignancies, a number of proteases, especially matrix metalloproteinases (MMPs) 2, 7 and 9, are upregulated in the tumor microenvironment.[494] The expression level increases as the cancer becomes more malignant.[494] Therefore, MMPs are often used as biomarkers for the diagnosis and to monitor disease progression.[495] The substrate specificity of these MMPs could be exploited in order to selectively remove an inhibitory moiety at the site of disease. Researchers at CytomX Therapeutics have developed a number of antibody prodrugs (Probodies™) whose epitopes are proteolytically unmasked in tumors.[496,497] Some of these Probodies™ have recently entered clinical trials.[498] Similarly, TNF prodrugs have been developed that consist of a tumor-targeting antibody fragment and a TNF subunit which is linked to a receptor-derived inhibitory moiety via a protease-cleavable linker. These prodrugs could be potently activated *in vitro* by MMP-2 and urokinase-type plasminogen activator (uPA) mediated proteolytic cleavage of the linker between the ligand and the inhibitory moiety upon target binding.[499–501] Analogous constructs were developed featuring FasL (CD95L). Upon the antibody-mediated binding to the target cell, the protease-cleavable linker becomes accessible for membrane-associated proteases which then release the inhibitory moiety. The unmasked death ligand subsequently induces apoptosis of the target cell.[502] This masked FasL construct showed promising anti-tumor activity in a mouse model of cancer.[502] Recently, an IL2-Fc fusion protein was reported where one chain of the Fc moiety was linked to an engineered IL-2 variant (SumIL2), whereas the other chain of the Fc moiety was fused to IL2Rβ via an MMP-sensitive linker.[503] In the absence of proteases, the fusion protein showed a roughly 10-fold reduction in biological activity *in vitro*. In a preclinical model of cancer it showed promising anti-tumor activity and reduced toxicity compared to the IL-2 fusion without the blocking receptor subunit.[503]

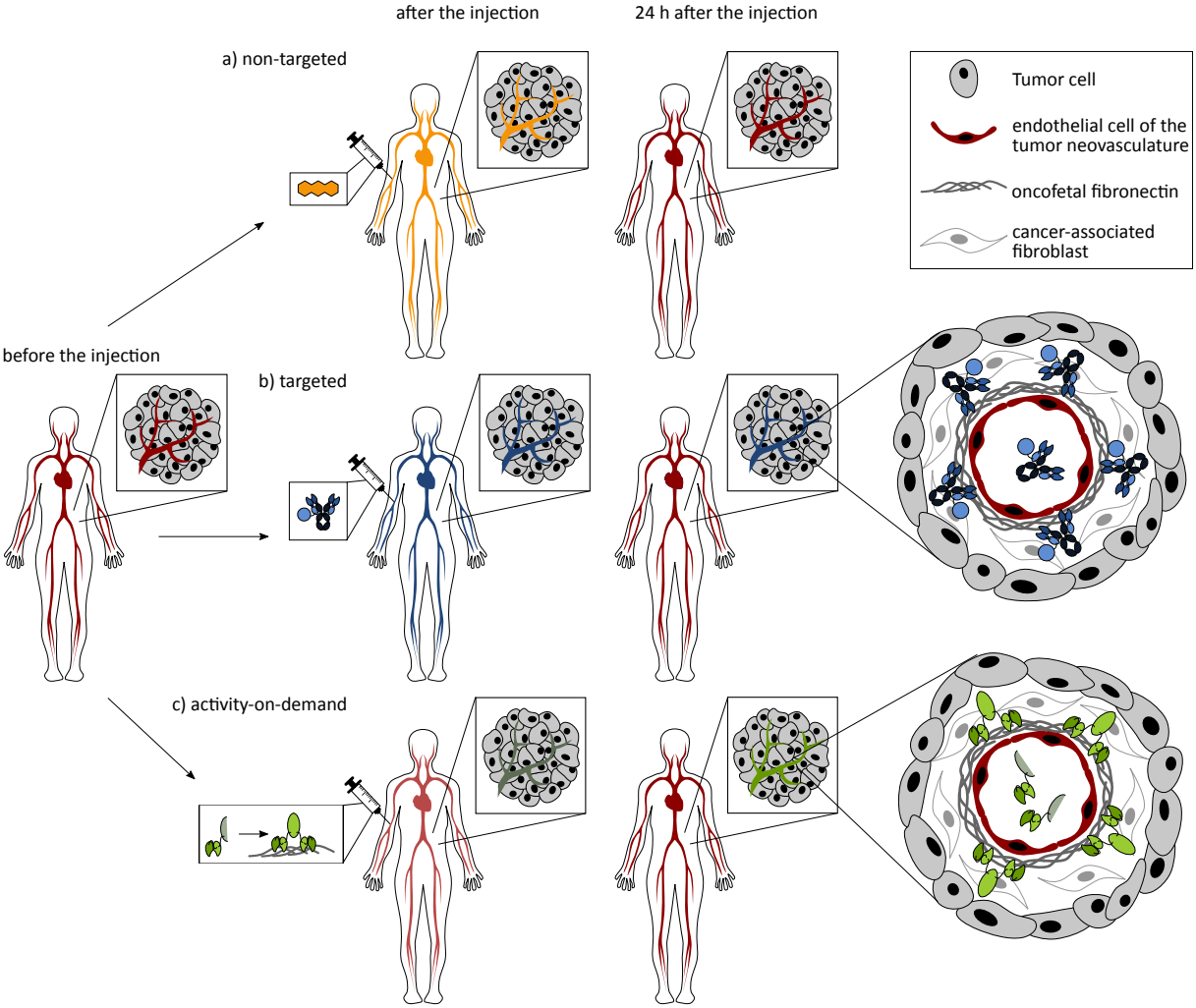

Figure 3.11.: Schematic depiction of the different drug delivery strategies. a) A non-targeted drug is distributed more or less equally in the body and in most cases no preferential accumulation in the tumor is achieved. b) The targeted delivery of a drug leads to the preferential accumulation of the drug at the site of the tumor after injection. On-target off-tumor toxicity can be observed especially at early timepoints after intravenous administration when the concentration of the drug in the periphery is relatively high prior to accumulation in the tumor. c) Activity-on-demand drugs, by contrast, remain in an inactive state until the drug is activated in the tumor. This strategy helps to reduce off-tumor toxicity. The targeted strategies depicted here are based on the example of vascular targeting with antibodies binding to oncofetal fibronectin on the tumor neovasculature. Adapted from Neri & Bicknell (2005)[154]

3.6. Aim of the Thesis

Recently, members of the TNF superfamily (TNFSF) have emerged as important targets for cancer immunotherapy, especially to potentiate the treatment with immune checkpoint inhibitors or chemotherapy.[4,5] There is evidence that targeted or localized delivery of TNFSF agonists to the tumor can increase their therapeutic potential.[382,437,504] In addition, the requirement of receptor multimerization for productive signalling[343,505] makes ligands of the TNF superfamily amenable for antigen-dependent reconstitution of biological activity ("activity on demand") via targeted delivery of monomeric or dimeric payloads. Restricting the biological activity of immunostimulatory payloads to the tumor is an important strategy to reduce the off-tumor toxicity observed in first-generation immunocytokines.[506] Our research group has specialized in the targeted delivery of immunostimulatory payload to the tumor neovasculature[9,10] using the F8 antibody which targets the alternatively spliced extra-domain A (EDA) of fibronectin, a tumor-associated antigen.[11–13]

The principal aim of this work was to develop novel neovasculature-targeted immunocytokines featuring ligands of the TNF superfamily as immunostimulatory payload. A study by Hemmerle *et al.* revealed some of the challenges associated with delivering ligands of the TNF superfamily to the tumor neovasculature.[507] In this work, alternative formats and new payloads are investigated for their potential to improve tumor-targeting and therapeutic efficacy. Three members of the TNF superfamily were chosen as payloads for neovasculature-targeted immunocytokines. CD40L was chosen due to its potential to stimulate APCs, to enhance T cell priming and to increase immune infiltration into immunologically "cold" tumors.[8] GITRL and 4-1BBL were chosen due to their T cell costimulatory activity.[6,7]

In order to obtain a robust method to screen for biologically active variants *in vitro*, a universal bioactivity assay was developed. The assay was based on the fact that most cytokines trigger the activation of NF-κB.[508] Therefore, an NF-κB-responsive reporter construct driving the expression of a secreted luciferase and intracellular mCherry was transduced into a B and a T cell line that express a variety of immunologically interesting receptors. These reporter cell lines could also be used to screen for protein variants with antigen-dependent biological activity by performing the bioactivity assay in the presence and absence of immobilized antigen.

The workflow for the development of immunocytokines featuring ligands of the TNF superfamily as payloads involved the cloning and expression of a variety of molecular formats which were screened for their *in vitro* properties. The fusion proteins showing the most favorable *in vitro* properties were chosen for quantitative biodistribution studies in tumor-bearing mice. Variants which showed promising tumor-targeting properties were

finally tested for their therapeutic activity in murine models of cancer. In order to assess phenotypic changes induced by the therapy, matched draining lymph nodes and tumor infiltrating lymphocytes were collected and analyzed by flow cytometry.

4. A universal reporter cell line for bioactivity evaluation of engineered cytokine products

This chapter corresponds to the publication ''A universal reporter cell line for bioactivity evaluation of engineered cytokine products" by J. Mock, C. Pellegrino & D. Neri published in Scientific Reports 10, 3234 (2020), reproduced with permission (Creative Commons Attribution 4.0 International License).

Abstract

Engineered cytokine products represent a growing class of therapeutic proteins which need to be tested for biological activity at various stages of pharmaceutical development. In most cases, dedicated biological assays are established for different products, in a process that can be time-consuming and cumbersome. Here we describe the development and implementation of a universal cell-based reporter system for various classes of immunomodulatory proteins. The novel system capitalizes on the fact that the signaling of various types of pro-inflammatory agents (e.g., cytokines, chemokines, Toll-like receptor agonists) may involve transcriptional activation by NF-κB. Using viral transduction, we generated stably-transformed cell lines of B or T lymphocyte origin and compared the new reporter cell lines with conventional bioassays. The experimental findings with various interleukins and with members of the TNF superfamily revealed that the newly-developed "universal" bioassay method yielded bioactivity data which were comparable to the ones obtained with dedicated conventional methods. The engineered cell lines with reporters for NF-κB were tested with several antibody-cytokine fusions and may be generally useful for the characterization of novel immunomodulatory products. The newly developed methodology also revealed a mechanism for cytokine potentiation, based on the antibody-mediated clustering of TNF superfamily members on tumor-associated extracellular matrix components.

4.1. Introduction

The clinical success of immune check-point inhibitors for the treatment of various forms of cancer[1–3] has sparked research activities for the discovery and development of novel immunostimulatory products. Various types of engineered cytokine products (e.g., antibody-cytokine fusion proteins[10,506,509] and polymer-cytokine conjugates,[510,511] chemokines[512]

and Toll-like receptor agonists[513]) have been considered for cancer therapy applications.

The development of novel immunostimulatory products requires the implementation of reliable quantitative methods for the determination of biological activity. Such methods are important both at the research stage and during industrial production, since a demonstration of consistent biological activity throughout the development process is a prerequisite for quality assurance and for enabling comparisons of experimental results.

At present, dedicated assays are established for individual products but most methodologies are not readily applicable to different types of biopharmaceuticals.[514] For example, interleukin-2 (IL-2) activity is typically measured by the ability to induce proliferation of the CTLL-2 cell line of T cell origin,[515] while interleukin-12 (IL-12) activity tests measure the production of interferon-γ by NK-92 cells of NK cell origin.[516,517] The activity of tumor necrosis factor (TNF) and of TNF-based biopharmaceuticals is often measured by the killing of transformed fibroblast cell lines,[518] while other members of the TNF superfamily are studied in terms of their ability to stimulate the production of pro-inflammatory cytokines by splenocytes[470,519] or the proliferation of splenic subsets.[520,521]

The development of dedicated methods for individual products is often cumbersome and may require the generation of stably transfected cell lines.[492] Moreover, the optimization of technical parameters, such as cell growth conditions and dose-response relationships, may be time-consuming. Our laboratory has worked on the development and characterization of more than 100 different antibody-cytokine and antibody-chemokine fusion proteins[9,10] and has learned to value the importance of robust, reliable and broadly applicable methodologies for the study of engineered cytokine products.

Here we report on the development of two general reporter cell lines, which are derived from T and B lymphocytes and which are broadly applicable for the quantification of biological activity of immunostimulatory agents. We used viral transduction methodologies with a reporter for NF-κB activity because of the central role played by NF-κB signaling in many different inflammatory processes.[508]

The term NF-κB refers to a variety of homo- and heterodimers that are formed between members of the NF-κB family of proteins. The members of the NF-κB family of proteins all share a related REL homology domain (RHD), which confers both DNA binding and dimerization. Activated NF-κB dimers localize to the nucleus where they bind to the NF-κB response element that has the loose consensus sequence 5'-GGRNN(WYYCC)-3' (where R: purine, N: any base, W: adenine or thymine and Y: pyrimidine)[522–524] and thus activates the transcription of a variety of target genes (via interaction with basal transcription factors and cofactors). In the absence of signaling, the NF-κB proteins are present in the cell as pre-formed complexes that can be rapidly activated upon signaling.[523,524] The signaling complexes can either be activated by degradation of an inhibitory protein or by

the removal of an inhibitory protein domain by upstream signaling components.[525]

Even though class I cytokines typically signal via JAK/STAT activation,[526] there is evidence that most of them directly or indirectly also trigger the activation of NF-κB.[527–530] By contrast, members of the TNF superfamily of proteins signal via the recruitment of TNF Receptor Associated Factors (TRAFs) that activate NF-κB both via the classical and the non-canonical pathway.[5,531,532]

The newly developed cell lines (termed CTLL-2_NF-κB and A20_NF-κB) were used to implement a general bioassay, which was compared to established procedures for the characterization of various types of engineered cytokine products. Moreover, the new methodologies allowed the discovery of a novel strategy for cytokine potentiation, based on the antibody-mediated clustering of multimeric immunostimulatory payloads (e.g., members of the TNF superfamily) on tumor-associated extracellular matrix components.

4.2. Results

Figure 4.1 describes the strategy followed for the generation of a universal reporter system for cytokine activity. The signaling of many different pro-inflammatory mediators (e.g., chemokines, Toll-like receptor agonists, members of the TNF superfamily and various other cytokines) involves the activation of NF-κB, in addition to other signaling pathways (Figure 4.1 a).[522,529,533,534] We constructed a vector for virus-mediated stable cell transduction, which incorporated an NF-κB response element upstream of a secreted luciferase (NanoLuc) and mCherry reporter genes (Figure A.1 and Figure A.2). The two reporter proteins are separated by a T2A peptide. The luciferase is secreted due to the presence of an IL-6 secretion signal while the mCherry is retained in the cytoplasm. A second-generation lentivirus was used for transduction experiments. The lentivirus was produced by the simultaneous transfection of HEK293T cells with the envelope plasmid pCAG-VSVG, the packaging plasmid psPAX2 and pJM046 (harboring the reporter construct) (Figure A.1 and Figure A.2). The transduction strategy was used to stably integrate the NF-κB reporter into CTLL-2 and A20 cell lines, of T-cell and B-cell origin (respectively) (Figure 4.1).

We investigated the possibility of using the newly developed transduction method as a universal reporter for cytokine activity by performing a comparison with established dedicated test systems. For this experiment, antibody-cytokine fusions that have previously been developed in our lab were used.[257,258,278] We used fusions of the L19 antibody targeting the extradomain B of fibronectin[535] linked to human IL2 and murine IL12, as well as fusions of the F8 antibody targeting the extradomain A of fibronectin[11] linked to murine tumor necrosis factor (TNF) (Figure 4.2). Interleukin-2 (IL2) activity was measured both

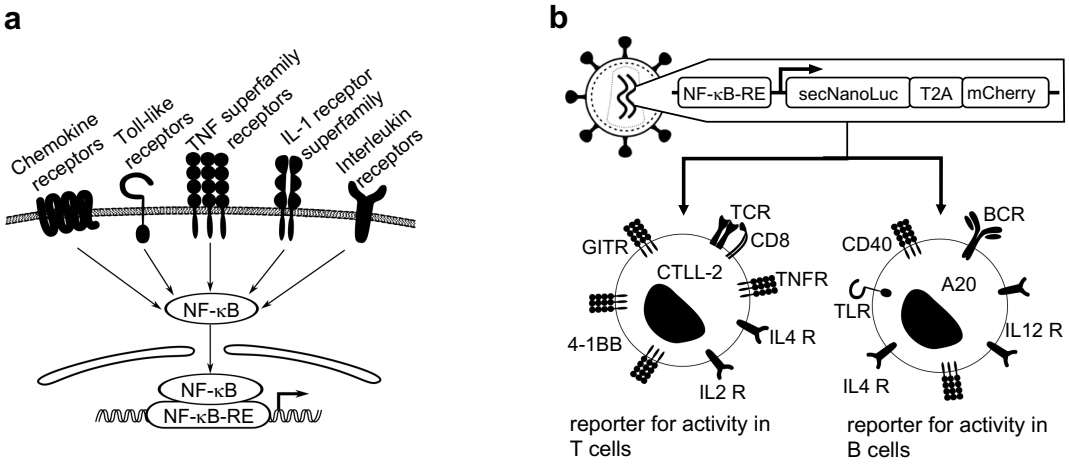

Figure 4.1.: General strategy for the design of the reporter cell line: (a) signal through most of the immunologically relevant receptors results in the activation of NF-κB[522,529,533,534] **(b)** the reporter construct encoding a secreted luciferase (NanoLuc) and mCherry separated by a T2A sequence downstream of an NF-κB response element (NF-κB-RE) was used for the viral transduction of cell lines of T and B cell origin (TCR: T cell receptor, TNFR: TNF receptor, IL4 R: IL-4 receptor, IL2 R: IL-2 receptor, BCR: B cell receptor, IL12 R: IL-12 receptor, TLR: Toll like receptor)

in terms of proliferation of non-transduced CTLL-2 cells and in terms of NF-κB reporter activity in transduced cells. An EC_{50} value in the 10 pM range was observed for both methodologies (Figure 4.2 a & Table A.1). The activity of interleukin-12 (IL12) is often measured in terms of interferon-γ production by NK-92 cells of Natural Killer cell origin.[517] In this case, the EC_{50} values obtained using the NK-92 cell-based system were roughly ten times lower than those obtained by monitoring NF-κB reporter activity (Figure 4.2 b and Table A.1). The performance of the new methodology for the measurement of TNF activity was compared to the results of a conventional cell killing assay, using a transformed fibroblast cell line which is particularly sensitive to the action of TNF. EC_{50} values in the pM range were observed for the killing assay, whereas the EC_{50} values obtained with the universal assay were in the 100 pM range (Figure 4.2 c and Table A.1).

We then used the of NF-κB reporter assay for the characterization of three novel fusion proteins, featuring the F8 antibody (specific to the alternatively-spliced EDA domain of fibronectin, a tumor-associated antigen)[11] fused to three different members of the TNF superfamily (Figure 4.3). 4-1BB and GITR (glucocorticoid-induced TNFR-related gene) are expressed on activated CD8+ T-cells. Activation of each of these two receptors has been shown to prolong longevity of the activated T cells and transition towards a memory phenotype.[6,536] By contrast, CD40 is expressed on antigen-presenting cells.[351] The interaction between CD40 and its ligand, CD154, is important for the licensing of antigen-presenting cells.[349] A variety of agonists to these three members of the TNF superfamily are being developed and tested both at a preclinical stage and in clinical trials as agents

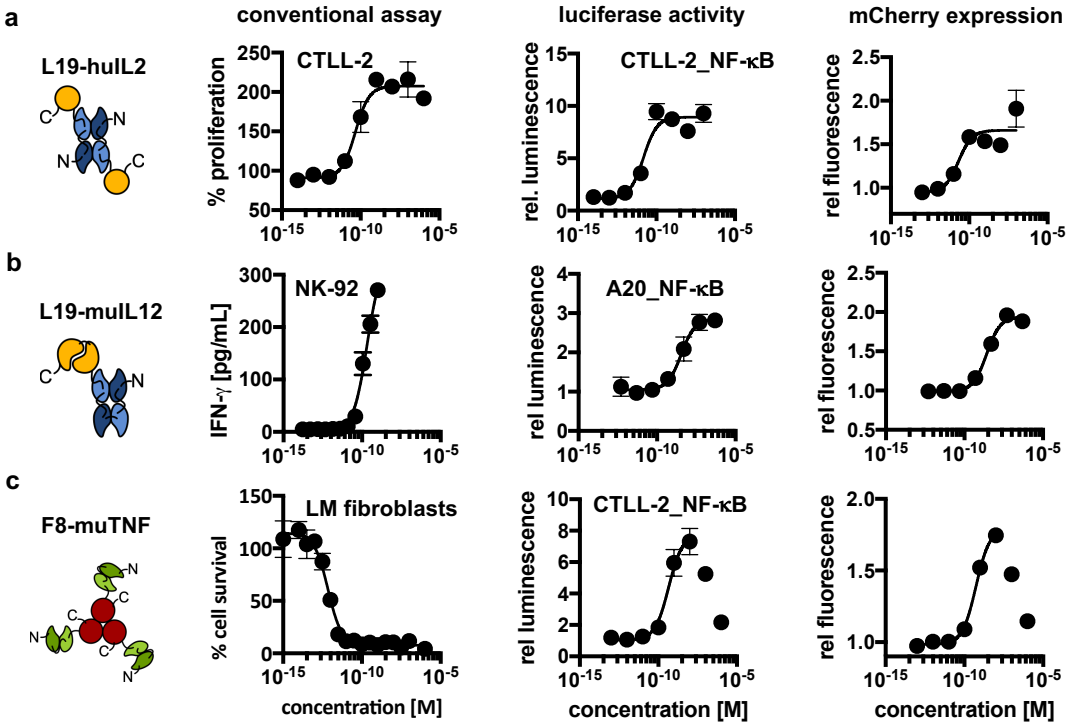

Figure 4.2.: Comparison of the expression of luciferase and mCherry by the newly generated reporter cell lines with the response obtained with the same proteins in the conventional assay. The immunocytokines that were used for this assay are schematically depicted (the antibody moiety is depicted as empty symbols and the cytokine moieties as hatched areas) **(a)** the proliferation of CTLL-2 and the response of the CTLL-2 reporter cell line triggered by L19-IL2 **(b)** the production of interferon-γ by NK-92 cells and the response of the A20 reporter cell line triggered by L19-IL12 **(c)** the cytotoxicity of F8-TNF for L-M fibroblasts compared to the response of the CTLL-2 reporter cell line to F8-TNF. In the cases where a strong hook effect was observed, only the sigmoidal part was used for curve fitting as indicated by the solid line.

for the immunotherapy of cancer.[537] Our lab has had a long-standing interest in the characterization of the tumor-homing properties[507] and anti-cancer activity of antibody fusion proteins with members of the TNF superfamily.[258,538] F8-41BBL, F8-GITRL and F8-CD154 featured the TNF superfamily member as single-chain polypeptide in order to stabilize the homotrimeric structure[492] while the antibodies were used as recombinant diabody moieties.[539] A concentration-dependent NF-κB reporter activity could be measured for all three antibody-cytokine fusions, monitoring both luciferase activity and mCherry expression (Figure 4.3). The EC_{50} values obtained for 4-1BBL and GITRL constructs were in the nanomolar range whereas the values obtained for the CD154 construct were in the 100 pM range (Table A.2).

Antibody-cytokine fusions are increasingly being used for the therapy of cancer[9,506,509] and of chronic inflammatory conditions[540,541] with the aim to concentrate cytokine activity at the site of disease and help spare normal organs. We used derivatives of the F8 antibody to assess whether a localized concentration of cytokine activity in close prox-

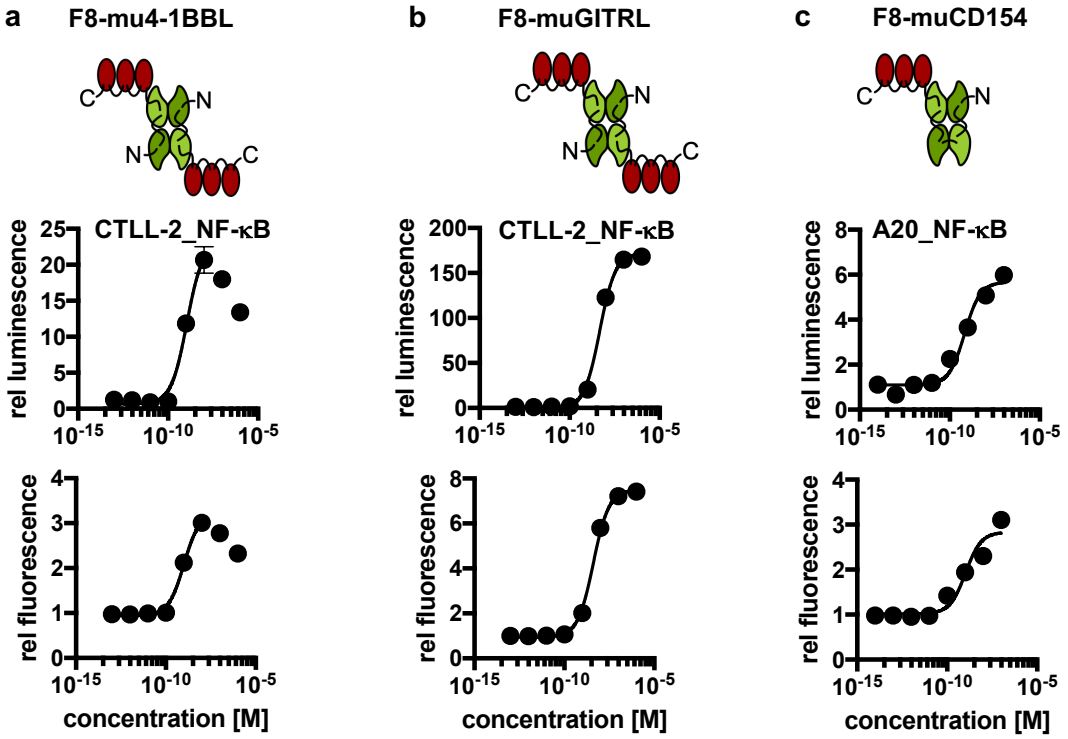

Figure 4.3.: Activity tests of novel antibody-cytokine conjugates using the newly developed reporter cell lines (a) activity tests of the single chain trimeric 4-1BBL fused to the F8 antibody in the diabody format using the CTLL-2 reporter cell line **(b)** activity of single chain trimeric GITRL fused to the F8 antibody in the diabody format using the CTLL-2 reporter cell line **(c)** activity of single-chain trimeric CD154 fused to the F8 antibody in the single-chain diabody format using the A20 reporter cell line. In the cases where a strong hook effect was observed, only the sigmoidal part was used for curve fitting as indicated by the solid line.

imity to target cells of interest may lead to a potentiation of biological activity. The alternatively-spliced extra-domain A (EDA) of fibronectin (i.e., the target antigen of the F8 antibody) is typically found as an abundant component of the modified extracellular matrix associated with newly-formed tumor blood vessels,[12] but is otherwise undetectable in most normal adult tissues, exception made for the female reproductive system.[13] We mimicked the localized deposition of EDA(+)-fibronectin by coating plastic wells with 11-A-12 recombinant fibronectin fragments, containing the EDA domain[11] (Figure 4.4 a). The system was used to compare the biological activity of F8-41BBL, F8-GITRL and F8-CD154 fusion proteins, featuring the F8 antibody either in diabody format linked to a single-chain trimer of the cytokine or as single-chain Fv fragment linked to a single unit of the cytokine (Figure 4.4 b - d). In the case of the F8 antibody in a diabody format linked to a single-chain trimeric 4-1BBL, only a small increase in stimulatory activity was observed when the agonist was clustered on EDA. However, in the case of the single-chain Fv fragment linked to a single 4-1BBL unit, no activity was observed in the absence of clustering. Activity could in this case be restored by clustering the agonist on EDA coated

wells (Figure 4.4 b). By contrast, both F8-GITRL constructs were constitutively active (Figure 4.4 c). In the case of the F8 antibody in a diabody format linked to the single-chain trimer of GITRL, no activity enhancement was observed by clustering on EDA. The EC_{50} of the construct consisting of the F8 antibody in an scFv format linked to a single unit of GITRL, a roughly 5-fold reduction in the EC_{50} was observed when the experiment was performed in the presence of EDA. Some modest increase in activity in the presence of EDA was also observed in the case of the single-chain trimeric CD154 linked to F8 in a single-chain diabody format (Figure 4.4 d).

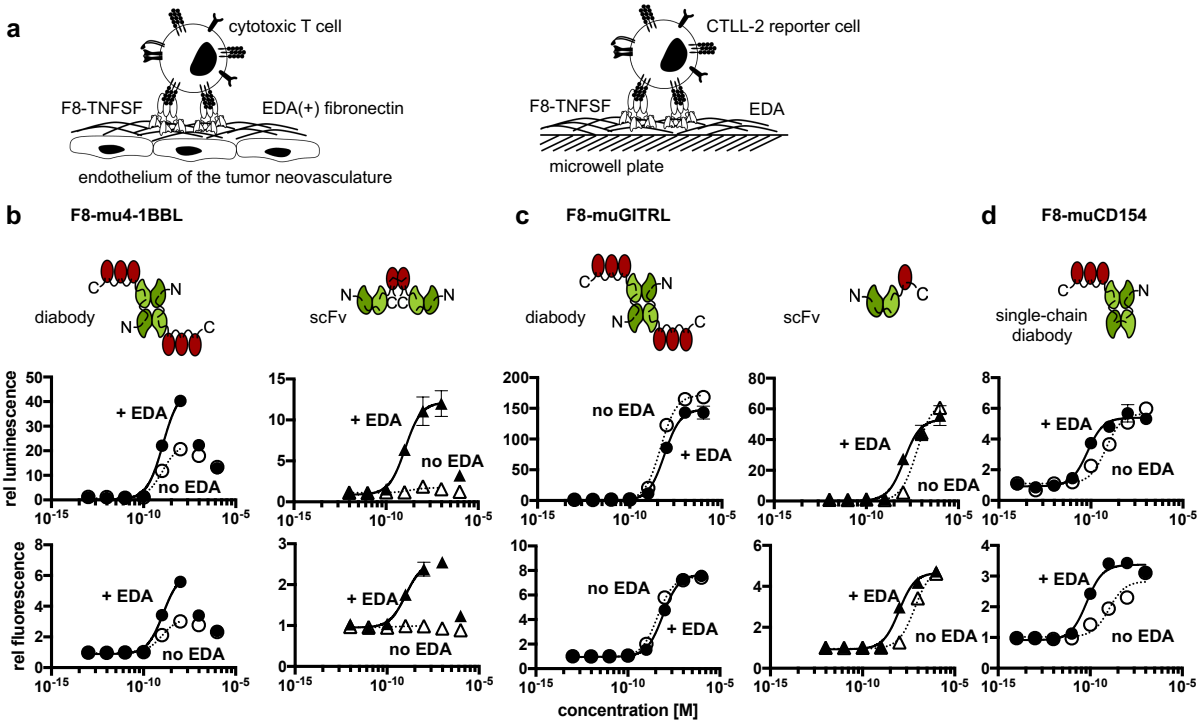

Figure 4.4.: Clustering of cytokines of the TNF superfamily fused to fragments of the F8 antibody on EDA (a) *In vivo* the F8 antibody binds to the extradomain A (EDA) of fibronectin that is present in the tumor-associated neovasculature. This is thought to lead to clustering of the cytokine fused to the F8 antibody and therefore to enhance activation of target cells such as cytotoxic T cells. To mimic this situation *in vitro*, microwell plates were coated with the extradomain A of fibronectin. The activity of the immunocytokine when clustered on EDA and without clustering was compared for different formats. **(b)** activity of 4-1BBL in the single-chain trimeric format fused to the F8 antibody in the diabody format and in the monomeric format fused to the single-chain Fragment variable of F8 (scFv) **(c)** activity of GITRL in the single-chain trimeric format fused to the F8 antibody in the diabody format and in the monomeric format fused to the single-chain Fragment variable of F8 **(d)** activity of CD154 in the single-chain trimeric format fused to the F8 antibody in the single chain diabody format (circles: F8 in diabody format, triangles: F8 in scFv format, filled symbols: plate coated with EDA, empty symbols, dashed line: no EDA)

4.3. Discussion

In this work, we presented the development of two reporter cell lines that can be used to measure the biological activity of a variety of cytokines. The new methodology capitalizes on the fact that many cytokine-triggered signaling events converge at the level of NF-κB activation.

An excellent agreement could be found between bioactivity measurements of IL-2 performed with the conventional cell-based cytokine activity assay and the newly developed method (Figure 4.2 a). A discrepancy between the conventional cell-based cytokine assay and the new method could be seen for two fusion proteins with murine payloads (L19-IL12 and F8-TNF), for which the new methodology indicated a reduction in potency (Figure 4.2 b & c). It is possible that NF-κB signaling may not fully capture the molecular events triggered by murine IL-12 and murine TNF, but the new methodology could still enable a comparative evaluation of multiple pro-inflammatory payloads and cytokine variants (e.g., wildtype and mutated versions).

The observation that the activity of murine 4-1BBL can be potentiated by clustering of antibody fusions on specific tumor-associated extracellular matrix components is surprising and potentially useful for pharmaceutical applications. Murine 4-1BBL is not able to form stable homotrimers, but rather forms low-activity homodimeric structures.[346,448] It is possible that the high-density binding of F8 fusions on EDA-containing fibronectin promotes the formation of supermolecular assemblies, which gain signaling activity in a concentration-dependent manner (Figure 4.4). This approach mimics on the extracellular matrix what happens on murine cells where surface display of multiple copies of dimeric ligands turns an inactive homodimer into an active multimeric assembly.[346,448] Some potentiation upon antigen binding had previously been reported for certain murine TNF fusions[542] and for other members of the TNF superfamily.[543,544] In principle, it would be attractive to engineer antibody-cytokine fusions which gain activity at the site of disease (e.g., upon antigen binding) while sparing normal tissues, as this approach could lead to biopharmaceuticals with improved therapeutic index. Our group has recently described a conceptually similar strategy, based on the assembly of heterodimeric split cytokine fusions (e.g., interleukin-12 superfamily members).[493] Other strategies for the conditional potentiation of antibody-cytokine include the allosteric regulation of cytokine activity[485] or the attenuation of cytokine potency ("attenukine").[545] Strategies aimed at potentiating the activity of antibody therapeutics based on conditional oligomerization include the development of hexameric IgG antibodies to augment complement-mediated cytotoxicity.[546,547]

Not all TNF superfamily members seem to need antigen-dependent clustering in order to gain activity (Figure 4.2 c & Figure 4.4 c). This is also reflected by the fact that some

ligands of the TNF superfamily including TNF and CD154 are enzymatically shed in vivo and act as soluble ligands.[548,549] Although GITRL is so far not known to be present as soluble ligand[411] our data indicates that the recombinant soluble ligand shows similar behavior (Figure 4.4 c).

In this article we have mainly focused on recombinant and engineered cytokine products. While many interleukins mainly signal through JAK/STAT activation,[526] NF-κB-driven transcriptional events are also induced, in line with previous reports on this matter.[527–530] NF-κB reporters should be broadly applicable also to other classes of pro-inflammatory products. Both Toll-like receptors and members of the interleukin-1 receptor superfamily activate NF-κB through the recruitment of MyD88 as part of their signal transduction.[533] In addition, there is also evidence that NF-κB can be activated by chemokine signaling.[534]

The CTLL-2 and A20 cell lines express on their surface a large variety of receptors of immunological importance and should be therefore applicable for many different bioactivity assays. If a researcher is interested in the use of a different cell line, the viral transduction system described in Figure 4.1 should enable the rapid preparation of the corresponding reporter system. The intracellular expression of mCherry was found to be useful for sorting of positively transduced cells by flow cytometry, while the secreted luciferase provided a facile readout of the reporter activity.

In summary, we have generated new universal reporter systems for the facile measurement of biological activity of various types of pro-inflammatory mediators and engineered cytokine products. We anticipate that the newly-developed cell lines and vector may find a broad applicability in biological, pharmaceutical and immunological research.

4.4. Materials and Methods

Cell lines The murine cytotoxic T cell line CTLL-2 (ATCC®TIB-214™), the murine B lymphocyte cell line A20 (ATCC®TIB-208™) and the murine fibroblast cell line L-M (ATCC®CCL-1.2™) and were obtained from ATCC, expanded and stored as cryopreserved aliquots in liquid nitrogen. The CTLL-2 cells were grown in RPMI-1640 (Gibco, #21875034) supplemented with 10% FBS (Gibco, #10270106), 1 X antibiotic-antimycoticum (Gibco, #15240062), 2mM ultraglutamine (Lonza, #BE17-605E/U1), 25 mM HEPES (Gibco, #15630080), 50 µM β-mercaptoethanol (Sigma Aldrich) and 60 U/mL human IL-2 (Proleukin, Roche Diagnostics). The A20 cells were grown in RPMI-1640 (Gibco, #21875034) supplemented with 10% FBS (Gibco, #10270106), 1 X antibiotic-antimycoticum (Gibco, #15240062) and 50 µM β-mercaptoethanol (Sigma Aldrich). The L-M fibroblasts were grown in DMEM (Gibco, high glucose, pyruvate, #41966-029) supplemented with 10% FBS (Gibco, #10270106) and 1 X antibiotic-antimycoticum (Gibco,

#15240062). The cells were passaged at the recommended ratios and never kept in culture for more than one month. The NK-92 cells were obtained from DSMZ (ACC 488) and grown in in MEM Alpha medium (Gibco, #22571-020) supplemented with 5 ng/mL recombinant human interleukin 2 (Gibco, #PHC0027), 2 mM L-glutamine (Lonza, #17-605E), 12.5% Fetal Bovine Serum (Gibco, #10099-141) and 12.5% Horse serum (Sigma Aldrich, #H1270).

Cloning of the reporter construct The plasmid pNL3.2.NF-κB-RE[NlucP/NF-κB-RE/Hygro] (#N1111) encoding the NanoLuc luciferase under the control of the NF-κB response element was obtained from Promega AG. The IL-6 secretion signal was inserted into the plasmid by polymerase chain reaction (PCR) and subsequent blunt-end ligation. The cassette was then transferred into a lentiviral transfer vector by Gibson Isothermal assembly. The lentiviral vector was based on the EF1-T2A vector which was kindly provided by Dr. Renier Myburgh and Prof. Dr. Markus Manz. A detailed representation of the vector pJM046 and the DNA sequence can be found in Figure A.1 and Figure A.2.

Protein production Various antibody-cytokine fusions were produced and tested in this work. The cloning and construction of L19-IL2,[278] F8-TNF[258] and L19-IL12[257] is described elsewhere. Soluble single-chain trimers of 4-1BBL, glucocorticoid-induced tumor necrosis factor receptor ligand (GITRL) and CD154 were designed by linking the extracellular domain with suitable glycine-serine linkers. Genetic sequences encoding the TNF-homology domain of murine 4-1BBL (amino acids 139 – 309), of the extracellular domain of murine GITRL (amino acids 46 – 170) and of the soluble part of murine CD154 (amino acids 112 – 260) as single-chain trimers were ordered from Eurofins Genomics. These sequences were then introduced into vectors encoding the F8 in a diabody format by Gibson Isothermal Assembly. To clone the single-chain variable Fragment (scFv) linked to the TNFSF monomer, the genetic sequence encoding the diabody was replaced by the sequence encoding the scFv and two domains of 4-1BBL and GITRL respectively were removed by PCR followed by blunt-end ligation. The protein sequences are provided in Supplementary Figure A.3. Proteins were produced by transient transfection of CHO-S cells and purified by protein A affinity chromatography as described previously 35-37. Quality control of the purified products included SDS-PAGE, size exclusion chromatography and, where applicable, mass spectrometry Figure A.4 and Figure A.5.

Virus production and stable transduction For the virus production, 5 million HEK293T cells were seeded at a density of 300,000 cells/mL on the day prior to transfection. They were then transiently co-transfected with the reporter plasmid pJM046 as well as the packaging plasmid psPAX2 (Addgene, #12260; http://n2t.net/addgene:12260;RRID:Ad

dgene_12260) and the envelope plasmid pCAG-VSVG (Addgene, #35616; http://n2t.net/addgene:35616;RRID:Addgene_35616) using the jetPRIME reagent (Polyplus transfection). The packaging and the envelope plasmid were kindly provided by the group of Prof. Dr. Patrick Salmon. The medium was replaced on the day after the transfection and the virus was harvested on the following day. The virus was aliquoted and snap-frozen in an ethanol dry ice mixture. An aliquot was thawed and used for the transduction of 500,000 target cells. For the transduction 500,000 cells in 1 mL of medium were seeded in a 24 well plate and 1 mL of virus was added. Polybrene (Santa Cruz Biotechnology, #134220) was added to a final concentration of 8 µg/mL. The cells were then centrifuged for 90 min at 1000 x g, 32°C. Afterwards, the cells were incubated at 37°C, 5% CO_2. The medium was exchanged daily for the following three days. The cells were then expanded, activated and mCherry-positive cells were sorted by FACS (BD FACS AriaIII).

CTLL-2 proliferation assay In order to starve the CTLL-2 cells from IL-2, the cells were washed twice with prewarmed HBSS (Gibco, #14175095) and then grown in the absence of IL-2 for 24 h in RPMI-1640 (Gibco, # 21875034) medium supplemented with 10% FBS (Gibco, #10270106), 1 X antibiotic-antimycoticum (Gibco, #15240062), 2 mM ultraglutamine (Lonza, # BE17-605E/U1), 25 mM HEPES (Gibco, # 15630080) and 50 µM β-mercaptoethanol (Sigma Aldrich). The starved CTLL-2 cells were seeded in a 96-well plate (20'000 cells/well) and medium supplemented with varying concentrations of IL-2 was added. The total volume per well was 200 µL which corresponds to a concentration of 100,000 cells/mL. All dilutions were done in triplicates. After 48 h incubation at 37°C, 5% CO_2 CellTiter 96 Aqueous One Solution (Promega, #G3582) was added to measure cell proliferation. Absorbance at 490 nm and 620 nm was measured after 1.5 h. The relative proliferation was calculated using the formula: relative proliferation = ($OD_{490\text{-}620}{}^{\text{treated}}$-$OD_{490\text{-}620}{}^{\text{medium}}$)/ ($OD_{490\text{-}620}{}^{\text{untreated}}$-$OD_{490\text{-}620}{}^{\text{medium}}$) x 100%. The data was fitted using the [Agonist] vs. response (three parameters) fit of the GraphPad Prism 7.0 a software to estimate the EC_{50}.

IL-12 assay The method was adapted from previous publications.[517,550] Briefly, NK92 cells were seeded at a density of 100,000 cells per well in a 96-well plate and 100 µL of medium containing varying concentrations of L19-IL12 was added. The total volume per well was 200 µL which corresponds to a cell density of 500,000 cells/mL. After 24 h of incubation at 37°C, 5% CO_2, the concentration of IFN-γ in the cell culture supernatant was determined by ELISA (Invitrogen, #EHIFNG2). An IFN-γ standard was included in the ELISA and linear curve fitting using the GraphPad Prism 7.0 a software was used to derive the IFN-γ concentration in the samples from the absorbance at 450 nm (A450) (Supplementary Figure A.7. The data was fitted using the [Agonist] vs. response (three

parameters) fit of the GraphPad Prism 7.0 a software to estimate the EC_{50}.

TNF assay L-M fibroblasts were seeded at a density of 20,000 cells/well in a 96-well plate and incubated for 24 h at 37°C, 5% CO_2. The medium was replaced by 100 µL fresh medium containing 2 µg/mL actinomycin D (BioChemica, #A1489,0005) and varying concentrations of F8-TNF. The cells were seeded at a concentration of 100,000 cells/mL. One day after seeding, the cell density should correspond to approximately 200,000 cells/mL, in a total of 200 µL, but this concentration was not measured immediately prior to the assay. The cells were incubated at 37°C, 5% CO_2 for another 24 h before 20 µL of CellTiter 96 Aqueous One Solution (Promega, #G3582) was added and absorbance at 490 nm and 620 nm was measured. The % cell survival was calculated using the formula: relative proliferation = ($OD_{490\text{-}620}{}^{\text{treated}}$-$OD_{490\text{-}620}{}^{\text{medium}}$)/ ($OD_{490\text{-}620}{}^{\text{untreated}}$-$OD_{490\text{-}620}{}^{\text{medium}}$) x 100%. The data was fitted using the [Agonist] vs. response (three parameters) fit of the GraphPad Prism 7.0 a software to estimate the EC_{50}.

NF-κB response assay CTLL-2 reporter cells were starved for 6 - 9 h as described above prior to use in order to reduce the background signal. If necessary, 100 µL 100 nM 11-A-12 fibronectin in phosphate buffered saline (PBS) was added to each well to be coated with EDA and the plate was incubated at 37°C for 90 min. Cells were seeded in 96-well plates (50,000 cells/well) and growth medium containing varying concentrations of the cytokine to be tested was added. The cells were incubated at 37°C, 5% CO_2 for several hours. To assess luciferase production, 20 µL of the supernatant was transferred to an opaque 96-well plate (Perkin-Elmer, Optiplate-96, white, #6005290) and 80 µL 1 µg/mL Coelenterazine (Carl Roth AG, #4094.3) in phosphate buffered saline (PBS) was added. Luminescence at 466 nm was measured immediately. mCherry expression was measured by flow cytometry (CytoFLEX, Beckman Coulter) and the data was analyzed using FlowJo (v.10, Tree Star). The cells were resuspended in growth medium and transferred to a 96-well U bottom plate (Greiner BioOne, Cellstar, #650180) and harvested by centrifugation. The medium was discarded and the cells were washed with FACS buffer (0.5% BSA, 2 mM EDTA, PBS) and resuspended in FACS buffer. The relative luminescence and the relative fluorescence were calculated by dividing the obtained results by the results obtained when no inducer was added.

Acknowledgements

Financial support by the ETH Zürich, the Swiss National Science Foundation (grant number 310030B_163479/1), the European Research Council (ERC) under the European Union's Horizon 2020 research and innovation program (grant agreement 670603),

and the Federal Commission for Technology and Innovation (KTI, grant number 12803.1 VOUCH-LS) is gratefully acknowledged. In addition, the ETH Zurich Flow Cytometry Core Facility is acknowledged for their help with the sorting of the transduced cell lines. We also thank scientists at Philogen for help with the development of some cytokine assays. Further, we thank Emanuele Puca for providing the samples of L19-IL2 and L19-IL12 that were used for this study. Moreover, we would like to thank Dr. Renier Myburgh and Prof. Dr. Markus Manz for kindly providing the lentiviral vectors.

Author contributions

D.N. and J.M. designed and planned the study. J.M. carried out most of the experimental work and prepared the figures. C.P. was involved in the design of the reporter construct and the virus production. D.N. and J.M. wrote the manuscript.

Competing interests

Dario Neri is a cofounder and shareholder of Philogen SpA (Siena, Italy), the company that owns the F8 and the L19 antibodies. No potential conflicts of interest were disclosed by the other authors.

Data availability statement

The datasets generated during and/or analyzed during the current study are available from the corresponding author on reasonable request.

5. Antibody fusion proteins featuring single-chain trimeric CD40L

5.1. Introduction

Contrary to so-called "hot" tumors in which case the escape of immune surveillance is driven by progressive exhaustion of tumor-reactive T cells and the upregulation of immunosuppressive ligands as described in subsection 3.1.2, so-called "cold" tumors are characterized by insufficient T cell priming and immune exclusion starting early during tumorigenesis.[551] The CD40-CD154 axis has emerged as a major target to convert cold tumors into hot tumors.[8] CD40 is expressed on antigen-presenting cells (APCs) and interaction with its ligand CD154 is important for the licensing of APCs.[349] Licensing of dendritic cells (DCs) drives the expression of pro-inflammatory cytokines such as interleukin-12 and the upregulation of antigen-presenting molecules, costimulatory molecules and adhesion molecules, which in turn enables T cell priming by DCs.[349] Evidence from preclinical murine models of cold tumors such as pancreatic ductal adenocarcinoma (PDA) showed that CD40 agonism drives the infiltration of activated macrophages into the tumor microenvironment.[552] These activated macrophages contributed to the tumor eradication and depletion of the tumor stroma.[552] Another study showed that CD40 agonism resulted in a clonal expansion of T cells in the tumor and a potent anti-tumor response was observed in combination with chemotherapy.[553] However, the systemic administration of CD40 agonists is accompanied by substantial toxicity such as cytokine release syndrome[358] and hepatotoxicity.[359] The observation that intratumoral administration of agonistic anti-CD40 antibodies abrogated systemic toxicity and resulted in durable anti-tumor immunity,[382] fuelled interest in the development of tumor-targeted CD40 agonists. In this chapter, the development of fusion proteins featuring the F8 antibody which targets the extradomain A of fibronectin, a tumor-associated antigen,[11] linked to CD154 is described. Since forced trimerization of ligands of the TNF superfamily was reported to enhance the agonistic activity,[492] CD154 was fused in a single-chain trimeric format to the F8 antibody in two diabody formats.

5.2. Results and Discussion

The two fusion proteins are schematically depicted in Figure 5.1a. Format **1** comprises the F8 antibody in a single-chain diabody format (scDb), while format **2** includes the F8 in a dimeric diabody format (dDb) linked to single-chain trimeric CD40L. Both fusion

proteins were produced at yields ranging from 4.8 to 7 mg/L in CHO-S cells and yielded clean size exclusion profiles (Figure 5.1a). Under non-reducing conditions the two variants migrated at a single band corresponding to the molecular weight of the protein on SDS PAGE. By contrast, the SDS PAGE profile was smeared when performed using a reducing sample buffer (Figure 5.1a). The two protein variants retained binding to the antigen EDA as measured by Enzyme-linked Immunosorbent Assay (ELISA) on plates coated with recombinant 11-A-12 fibronectin fragments (Figure 5.1b). Likewise, the proteins were biologically active as evidenced by the concentration-dependent release of TNF-α by murine splenocytes after incubation with the recombinant protein for 48 h (Figure 5.1c).

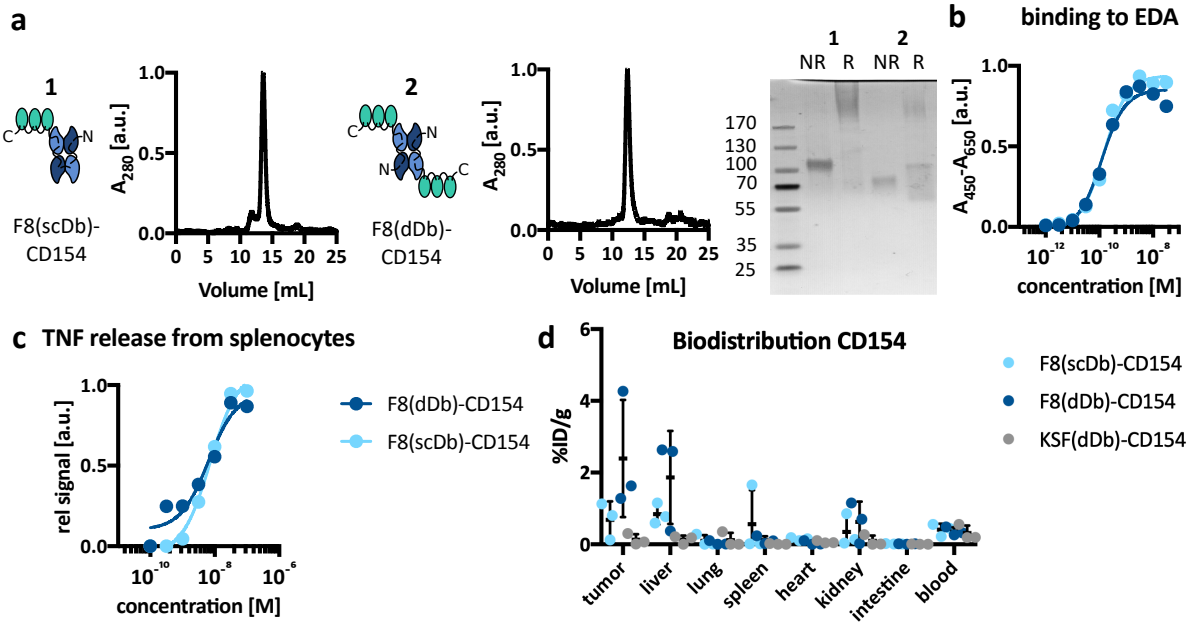

Figure 5.1.: Engineering F8-CD40L fusion proteins **(a)** schematic representations, size exclusion profiles and SDS PAGE of F8 in a single-chain diabody (scDb) or dimeric diabody (dDb) format fused to the soluble extracellular domain of murine CD40L in a single-chain trimeric format **(b)** binding of F8-CD40L to EDA as measured by ELISA **(c)** TNF release by mouse splenocytes in response to stimulation with the CD40L fusion proteins was measured by ELISA **(d)** the quantitative biodistribution of the two F8-CD40L fusion proteins as well as the KSF fusion was measured 24 h after administration of the radioiodinated compound (individual measurements, mean ± SD, n = 3)

A quantitative biodistribution study revealed substantial trapping of the proteins in the liver. In addition, the tumor uptake was very low in all except for one mouse (Figure 5.1d). A higher tumor uptake accompanied by substantial accumulation in the liver, spleen, kidney and intestine was previously reported for an F8-CD40L fusion protein featuring the F8 antibody in a single chain Fragment variable format linked to a single CD40L subunit.[507] Since the fast clearance and the accumulation in the liver could be due to glycan-mediated trapping,[265,266] site-specific mutagenesis was applied in order to produce aglycosylated F8-CD154 variants. Unfortunately, the N239Q mutant could not

be expressed. In addition, enzymatic deglycosylation yielded a poorly soluble protein indicating that the *N*-linked glycan is important for folding and solubility.

5.3. Conclusion and Outlook

This project was abandoned due to the poor biodistribution profile and the failure to express the aglycosylated N239Q variant. Other mutations to remove the *N*-glycosylation consensus sequence could be tested. However, the poor solubility of the enzymatically deglycosylated protein indicates that the glycan is essential for the protein stability in solution. Further studies could be warranted to elucidate the exact mechanism of the trapping in the liver. Peripheral trapping via CD40 on liver Kupfer cells and other immune cells could for instance be prevented by prior administration of unlabelled CD40L or CD40-blocking antibodies similar the work done by Hemmerle and Neri for fusion proteins featuring IFN-γ.[479] In addition, other CD40 binding moieties such as anticalins™, DARPin® or fynomers could be fused to the F8 antibody. The observation that a short peptide might be sufficient for CD40 activation when included in a suitable scaffold[405] could guide the development of next-generation CD40 agonists. In addition, peripheral trapping by CD40 in the liver could be prevented by fusing a masking peptide to CD40L via a protease cleavable linker similar to the prodrug approach described in subsection 3.5.4.

5.4. Materials and Methods

Cloning The genetic sequence encoding the soluble part of the extracellular domain of murine CD40L (amino acids 112 – 260) as a single-chain trimer separated by linkers encoding "GGGS" was obtained from Eurofins genomics. The gene fragment was introduced into a vector encoding F8 in a single-chain diabody or dimeric diabody format via Gibson Isothermal assembly (NewEnglandBiolabs, NEBuilder® HiFi DNA Assembly Master Mix, #E2621S). N293Q mutations were introduced by site-directed mutagenesis according to the MISO protocol.[554] Brief, primers were designed with the desired point mutations in the center flanked upstream by an overhang of 14 bp and a downstream by primer binding sequence with a melting point of around 60°C (calculated using tmcalculator.neb.com, Phusion® High-Fidelity PCR Master Mix, 200 nM primer concentration). The fragments between two adjacent point mutations were amplified by PCR. Adjoining fragments were assembled by PCR and introduced into the backbone by Gibson Isothermal Assembly. Quality control of the plasmids was performed by Sanger Sequencing by Microsynth AG.

Protein expression and characterization Proteins were produced by transient transfection of CHO-S cells (Lonza) and purified by protein A affinity chromatography as described previously.[257,258,278] Quality control of the purified proteins included SDS-PAGE and size exclusion chromatography. Size exclusion chromatography was performed using an Äkta Pure FPLC system (GE Healthcare) with a Superdex S200 10/300 increase column at a flow rate of 0.75 mL/min (GE Healthcare) in PBS.

Binding measurement by ELISA Maxisorp Multiwell plates were coated with 100 µL of a 100 nM dilution of recombinantly produced 11-A-12 EDA fragment overnight at 4 °C. On the next day, the plate was washed three times with 200 µL phosphate buffered saline (PBS) and blocked by incubation with 200 µL of a 2% solution of non-fat dried milk in PBS for 1 h at room temperature. After another three washing steps with 200 µL of PBS varying concentrations of the F8-CD40L fusion proteins were added to each well. After incubating it for 1 h at room temperature, the plate was washed three times with 200 µL PBS each and 100 µL of a biotinylated anti-CD40L antibody (Biolegend, #106503) was added to each well at a 1:1000 dilution in 2% milk in PBS. The plate was incubated for 1 h at room temperature and washed three times with 200 µL PBS. For detection, 100 µL of a 1:1000 dilution of HRP coupled streptavidin (Biolegend, #405210) in 2% milk in PBS was added to each well and the plate was incubated for 1 h at room temperature. The plate wash washed three times with PBS containing 0.5% Tween-20 followed by three washing steps with PBS. To each well, 100 µL of TMB substrate was added and quenched after 2 - 3 min by adding 50 µL of 1 M sulfuric acid. Absorbance at 450 nm and 650 nm was measured. The absorbance values were normalized and the K_D was estimated using the [Agonist] vs. response (three parameters) fit of the GraphPad Prism 7.0 a software.

Splenocyte bioactivity assay Spleens were obtained from mice that were euthanized in the course of *in vivo* studies by other members of the group. For splenocyte isolation the spleen was cut into small pieces using surgical scissors and passed through a 40 µm cell strainer. Cells were harvested by centrifugation and red blood cells were removed using a red blood cell lysis buffer (Roche). Splenocytes were resuspended in RPMI-1640 to a final density of $5{\cdot}10^6$ cells/mL and 500'000 cells were seeded in each well of a 96 well plate. The F8-CD40L protein was diluted in RPMI-1640 and 100 µL were added to each well. The plate was incubated at 37°C, 5% CO_2 for 48 h. TNF release into the supernatant was measured using a Mouse TNF-α ELISA MAX™ kit (Biolegend, #430901) according to the manufacturer's recommendation.

Quantitative biodistribution Eight weeks old female 129/Sv mice were obtained from Janvier. After one week of acclimatization at the facility, the mice were shaved for iden-

tification. The mice were kept in individually ventilated cages in groups of 5 mice per cage in a specific pathogen free facility. They received food and water ad libitum and the cages were changed once per week by trained caretakers. F9 teratocarcinoma cells were obtained from ATCC, expanded and stored as cryopreserved aliquots. The cells were grown in DMEM (Gibco, high glucose, pyruvate, #41966-029) supplemented with 10% FBS (Gibco, #10270106) and 1 X antibiotic-antimycoticum (Gibco, #15240062) in flasks coated with 0.1% gelatin (Type B from Bovine Skin, Sigma Aldrich, #G1393). Tumors were implanted into the right flank by subcutaneous injection of $15{\cdot}10^6$ cells per mouse resuspended in 150 µL of Hank's Balanced Salt Solution (HBSS, no calcium, no magnesium, no phenol red, Gibco, #14175053). The body weight and the tumor size were measured daily. The tumor volume was calculated using the formula [volume = length x width x width x 0.5]. After 10 days of tumor growth, the mice were grouped into groups of three mice and 10 µg of radioiodinated protein was injected into the lateral tail vein. The mice were sacrificed 24 h after the administration of the radiolabeled protein and the weight and dose in the different organs was measured to calculate the percentage injected dose per gram of tissue (%ID/g).

Acknowledgements

Dr. Barbara Ziffels is gratefully acknowledged for her help with the biodistribution study.

Supplementary Material

F8(scDb)-(CD40L)$_3$: $F8_{VH}$-linker-$F8_{VL}$-linker- $F8_{VH}$-linker-$F8_{VL}$-linker-CD40L-linker-CD40L-linker-CD40L (Format **1**)

EVQLLESGGGLVQPGGSLRLSCAASGFTFSLFTMSWVRQAPGKGLEWVSAISGSGGSTYYADSVKGRFTISRDNSK
NTLYLQMNSLRAEDTAVYYCAKSTHLYLFDYWGQGTLVTVSS-GGSGG- EIVLTQSPGTLSLSPGERATLSCRASQS
VSMPFLAWYQQKPGQAPRLLIYGASSRATGIPDRFSGSGSGTDFTLTISRLEPEDFAVYYCQQMRGRPPTFGQGT
KVEIK-GGGGSGGGGSGGGGS-EVQLLESGGGLVQPGGSLRLSCAASGFTFSLFTMSWVRQAPGKGLEWVSAISGS
GGSTYYADSVKGRFTISRDNSKNTLYLQMNSLRAEDTAVYYCAKSTHLYLFDYWGQGTLVTVSS-GGSGG- EIVLT
QSPGTLSLSPGERATLSCRASQSVSMPFLAWYQQKPGQAPRLLIYGASSRATGIPDRFSGSGSGTDFTLTISRLEPED
FAVYYCQQMRGRPPTFGQGTKVEIK-SSSSGSSSSGSSSSG-QRGDEDPQIAAHVVSEANSNAASVLQWAKKGYYTM
KSNLVMLENGKQLTVKREGLYYVYTQVTFCSNREPSSQRPFIVGLWLKPSSGSERILLKAANTHSSSQLCEQQSVHL
GGVFELQAGASVFVNVTEASQVIHRVGFSSFGLLKL-GGGS-QRGDEDPQIAAHVVSEANSNAASVLQWAKKGYYT
MKSNLVMLENGKQLTVKREGLYYVYTQVTFCSNREPSSQRPFIVGLWLKPSSGSERILLKAANTHSSSQLCEQQSV
HLGGVFELQAGASVFVNVTEASQVIHRVGFSSFGLLKL-GGGS-QRGDEDPQIAAHVVSEANSNAASVLQWAKKGY
YTMKSNLVMLENGKQLTVKREGLYYVYTQVTFCSNREPSSQRPFIVGLWLKPSSGSERILLKAANTHSSSQLCEQQ
SVHLGGVFELQAGASVFVNVTEASQVIHRVGFSSFGLLKL

F8(dDb)-(CD40L)$_3$: $F8_{VH}$-linker-$F8_{VL}$-linker-CD40L-linker-CD40L-linker-CD40L (Format **2**)

EVQLLESGGGLVQPGGSLRLSCAASGFTFSLFTMSWVRQAPGKGLEWVSAISGSGGSTYYADSVKGRFTISRDNSK
NTLYLQMNSLRAEDTAVYYCAKSTHLYLFDYWGQGTLVTVSS-GGSGG- EIVLTQSPGTLSLSPGERATLSCRASQS
VSMPFLAWYQQKPGQAPRLLIYGASSRATGIPDRFSGSGSGTDFTLTISRLEPEDFAVYYCQQMRGRPPTFGQGT
KVEIK-SSSSGSSSSGSSSSG-QRGDEDPQIAAHVVSEANSNAASVLQWAKKGYYTMKSNLVMLENGKQLTVKREGL
YYVYTQVTFCSNREPSSQRPFIVGLWLKPSSGSERILLKAANTHSSSQLCEQQSVHLGGVFELQAGASVFVNVTEAS
QVIHRVGFSSFGLLKL-GGGS-QRGDEDPQIAAHVVSEANSNAASVLQWAKKGYYTMKSNLVMLENGKQLTVKRE
GLYYVYTQVTFCSNREPSSQRPFIVGLWLKPSSGSERILLKAANTHSSSQLCEQQSVHLGGVFELQAGASVFVNVTE
ASQVIHRVGFSSFGLLKL-GGGS-QRGDEDPQIAAHVVSEANSNAASVLQWAKKGYYTMKSNLVMLENGKQLTVKR
EGLYYVYTQVTFCSNREPSSQRPFIVGLWLKPSSGSERILLKAANTHSSSQLCEQQSVHLGGVFELQAGASVFVNVT
EASQVIHRVGFSSFGLLKL

Figure 5.2.: Sequences of the F8-CD40L fusion proteins developed in this study

6. Engineering murine GITRL for antibody-mediated delivery to tumor-associated blood vessels

This chapter corresponds to the publication "Engineering murine GITRL for antibody-mediated delivery to tumor-associated blood vessels" by J. Mock, I. Astiazaran-Rascon, M. Stringhini, M. Catalano & D. Neri, manuscript submitted.

Highlights

- Different formats of fusion proteins featuring glucocorticoid-induced TNFR-related protein ligand (GITRL) fused to a tumor-targeting antibody were produced.
- The tumor uptake of the fusion proteins could be increased by enzymatic deglycosylation of the fusion protein or by site-directed mutagenesis of the *N*-glycosylation consensus sequences.
- The fusion protein developed in this study failed to show any anti-tumor activity either alone or in combination with PD-1 inhibition.

Abstract

Preclinical evidence has suggested that the glucocorticoid-Induced TNFR-related protein (GITR) may be a valuable target for the development of anticancer therapeutics, but clinical studies with GITR ligand (GITRL) have been disappointing. Here, we report the development of a fusion protein featuring GITRL fused to the F8 antibody which targets the alternatively-spliced EDA domain of fibronectin, a tumor-associated antigen often found around the tumor neovasculature. Five different formats for F8-GITRL fusion proteins were cloned and characterized, but quantitative biodistribution studies failed to evidence a preferential accumulation at the tumor site. The *in vivo* tumor targeting properties of F8-GITRL could be substantially improved by enzymatic deglycosylation or site-directed mutagenesis of the *N*-glycosylation consensus sequence. However, therapy studies in a murine model of cancer with the glycoengineered F8-GITRL N74S and N157T variant failed to elicit a durable anti-tumor response, both in monotherapy and in combination with PD-1 blockade.

6.1. Introduction

The recent clinical success of immune checkpoint inhibitors in a subset of patients[555–557] has fueled interest in the development of additional immunostimulatory products for the treatment of cancer.[2,3] Attractive targets include T cell costimulatory receptors such as glucocorticoid-induced TNFR-related protein (GITR).[7] GITR is of particular interest since there is evidence that it not only delivers additional costimulatory signals to activated effector T cells and enhances the survival of this subset,[406] but that it also reduces the suppressive function of regulatory T cells.[408] In addition, it was shown to render effector T cells more resistant to suppression by regulatory T cells.[409] It was recently shown that the delivery of agonistic signals to GITR combined with PD-1 inhibition would revert CD8+ T cell dysfunction and enhance the memory function of this subset.[536] While most GITR agonists in preclinical and clinical development are antibodies, the delivery of recombinant soluble GITR ligand (GITRL) is also an option.[7]

One advantage of recombinant soluble ligands is that they are amenable to multimerization by linking several subunits via short oligopeptide linkers and by genetically fusing these single-chain multimers to antibodies or antibody fragments.[426,492] Importantly, clustering of receptors of the TNF superfamily is a prerequisite for signaling through this class of receptors.[343,505] Researchers at Apogenix have developed a fusion protein of a single-chain trimeric GITRL and an Fc portion yielding a hexavalent GITR agonist which showed superior *in vitro* agonistic activity compared to a clinical-grade agonistic antibody and showed some anti-tumor activity in preclinical models of cancer.[426] In spite of these promising preclinical results, a recent clinical trial featuring the use of an Fc fusion of human GITRL failed to show objective responses, even at very high (750 mg) doses.[419]

In addition to non-targeted GITR agonists, efforts are being made to develop tumor-targeted GITRL fusion proteins,[316,492] since there is evidence that the local delivery of GITR agonists can improve the therapeutic activity of GITR agonists.[504] Our group has worked for the last two decades on the antibody-based delivery of cytokine payloads to tumors and has characterized more than 100 fusion proteins until now,[9] but had never worked before with GITRL payloads. The F8 antibody, specific to the alternatively-spliced EDA domain of fibronectin,[11] is an attractive vehicle for pharmacodelivery applications. EDA is virtually absent from the adult human body (exception made for the female reproductive tract[13]) but represents an abundant component of the extracellular matrix of tumor-associated blood vessels.[12,13,90]

The targeted delivery of antibody-cytokine fusions, especially those featuring ligands of the TNF superfamily, to tumors has been demonstrated to be challenging in a number of cases.[507] Interaction of the cytokine moiety with cognate receptors outside the tumor can prevent accumulation of the antibody-cytokine fusion in the tumor.[479] While activation of

the cytokine receptors in the periphery can lead to off-tumor toxicity, some anti-tumor activity might still be achieved.[558] In addition, many therapeutic proteins feature *N*-linked glycans which can be recognized by various glycoprotein receptors leading to degradation of the protein. For instance, terminal mannose or *N*-acetylglucosamine can be recognized by the mannose receptor expressed on macrophages and dendritic cells.[264] In addition, non-sialylated proteins with terminally exposed galactose moieties are recognized by hepatocytes expressing the asialoglycoprotein receptor.[263] Culture conditions[559,560] during protein expression as well as the transfection method[266] have a significant impact on the structure of the glycan making it difficult to obtain uniform glycosylation patterns across batches. Engineered aglycosylated protein variants that lack the consensus sequence for *N*-linked glycosylation offer a possibility to circumvent the problem of glycosylation-dependent protein degradation.

Here, we report the development of an antibody-cytokine fusion featuring GITRL as a payload linked to the F8 antibody. Initial studies with the fusion protein featuring wild-type GITRL showed rapid degradation and lack of tumor accumulation *in vivo* which could be prevented by enzymatic deglycosylation of the protein. Therefore, fusion proteins featuring aglycosylated GITRL were developed by site-specific mutagenesis of *N*-linked glycosylation consensus sequence in the GITRL moiety. Similar to the enzymatically deglycosylated protein, the fusion protein featuring aglycosylated GITRL exhibited superior tumor-targeting properties compared to the fusion proteins featuring wild-type GITRL. Unfortunately, despite the improved targeting properties, no therapeutic anti-tumor activity could be observed.

6.2. Results

Five fusion proteins featuring wild-type murine GITRL linked to the F8 antibody were cloned and expressed. The different formats are schematically depicted in Figure 6.1a. GITRL was fused to the F8 antibody both as a monomer and as a single-chain trimer, since forced trimerization was previously reported to increase the bioactivity of fusion proteins featuring members of the TNF superfamily.[492] The protein sequences are listed in Figure B.1. The fusion proteins featuring wild-type GITRL as a payload were produced at yields ranging from 13 – 22 mg/L (Table B.2). All variants yielded homogenous size exclusion chromatography profiles (Figure 6.1b) and bound both to recombinant EDA [as measured by surface plasmon resonance] (Figure 6.1c) and to the GITR-expressing murine cell line CTLL-2 [as measured by flow cytometry] (Figure 6.1d). In addition, measurements of the biological activity using an NF-κB reporter cell line showed that all formats triggered signal transduction in target cells (Figure 6.1e). Forced trimerization of the GITRL seemed to enhance the binding affinity and increased the biological activity

in most cases (Table B.3). Due to its favorable *in vitro* properties format **1** was chosen for *in vivo* evaluation.

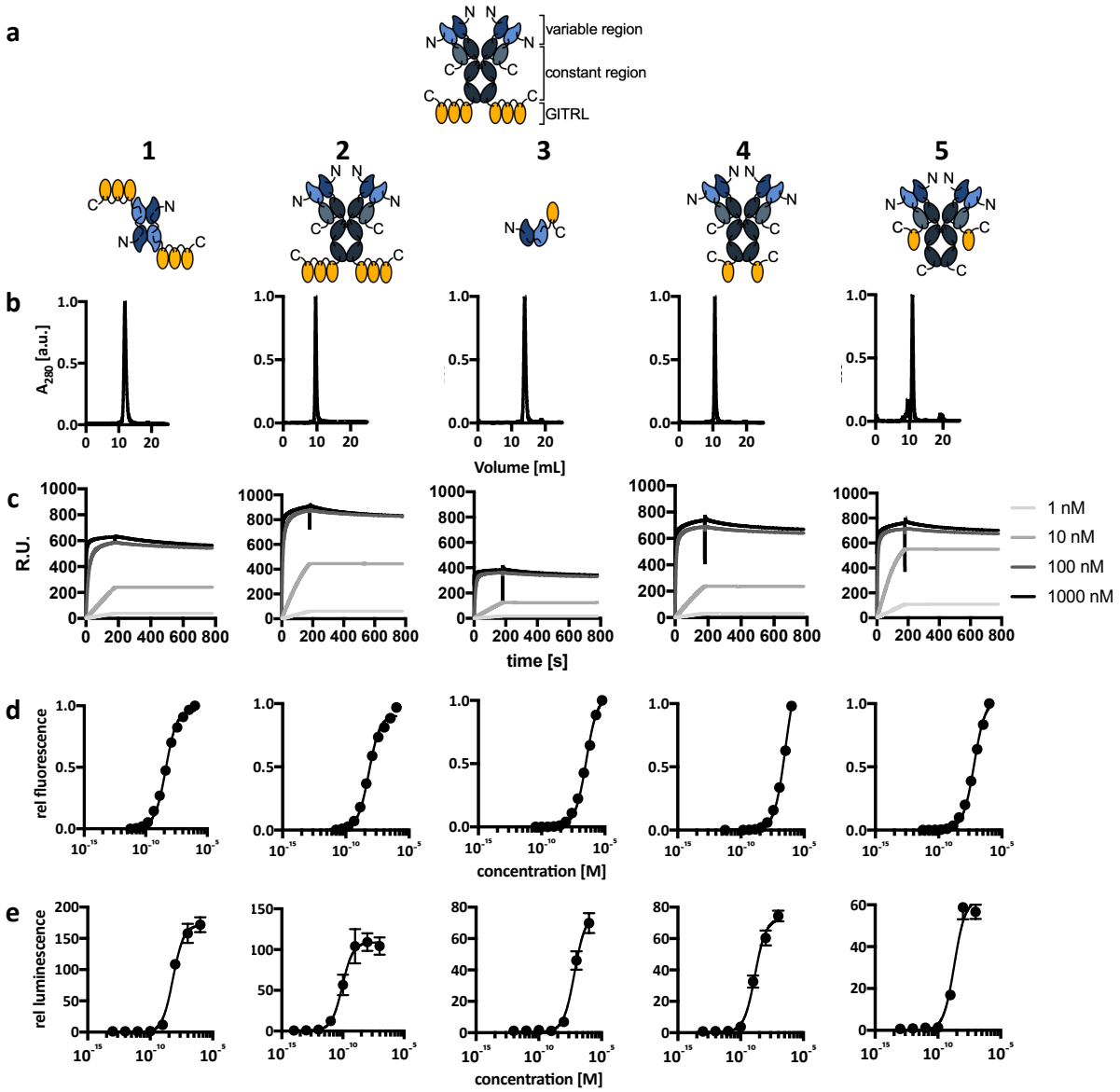

Figure 6.1.: Screening of F8 antibody-cytokine fusion proteins featuring wild-type GITRL as immunomodulatory payload **(a)** Different formats of the F8 antibody such as diabody (format **1**), full IgG (formats **2** and **4**) or single-chain Fragment variable (scFv, format **3**) were fused to GITRL either as a single-chain trimer (formats **1** and **2**) or a monomer (formats **3**, **4** and **5**) **(b)** the size exclusion profile for each variant was measured using a Superdex S200 10/300 increase column **(c)** binding to recombinant EDA was measured by surface plasmon resonance **(d)** binding to GITRL was measured by flow cytometry on CTLL-2 cells **(e)** the *in vitro* bioactivity was measured using a CTLL-2 reporter cell line that secretes luciferase in response to NF-κB activation via GITR agonism. Data represents mean ± SD.

A quantitative biodistribution of format **1** revealed that the protein was rapidly cleared from the circulation without preferential tumor accumulation 24 h after the injection of the radio-iodinated protein (Figure 6.2). The tumor-targeting could be improved by en-

zymatic deglycosylation of the protein indicating that trapping of the antibody-cytokine fusion via the *N*-linked glycan lead to rapid degradation of the protein *in vivo*. In addition, after enzymatic deglycosylation also a higher %ID/g of 3% was measured in blood as compared to the native form for which only 0.1% ID/g were measured 24 h after administration of the protein. However, the dose at the tumor site varied considerably from mouse to mouse with one mouse reaching 5.6 %ID/g in the tumor and the other two reaching only 1-2 %ID/g of tumor.

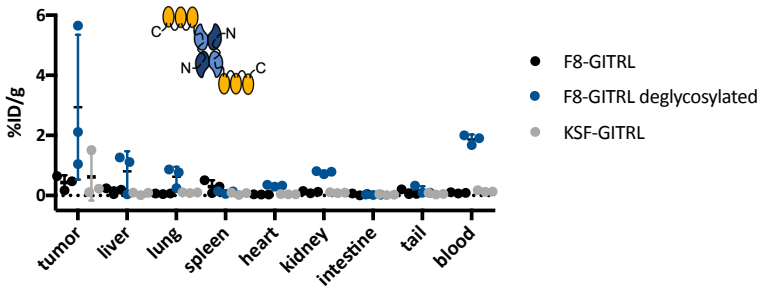

Figure 6.2.: Quantitative Biodistribution of F8-GITRL in format **1**: The mice were sacrificed 24 h after intravenous administration of radiolabelled protein preparations and the radioactivity in the different organs was measured and expressed as percent injected dose per gram (%ID/g). The F8-GITRL protein was administered both in the native form and after enzymatic deglycosylation. As a negative control, a fusion protein featuring the KSF antibody which binds to hen egg lysozyme was used.[90] Data represents individual mice and mean ± SD (n = 3).

In order to circumvent the need for enzymatic deglycosylation of F8-GITRL for *in vivo* applications, attempts were made to engineer aglycosylated variants. Therefore, the asparagine residues in the consensus sequence for *N*-linked glycosylation were sequentially removed by site-directed mutagenesis. At least in the absence of the glycan at position N74 of GITRL, the position N157 was occupied by a glycan and vice versa. Different combinations of double mutants were tested of which only the N74S and N157T could be expressed and was free of *N*-linked glycans (Figure 6.3a). However, the expression yield dropped from 13 mg/L for the fusion protein in format **1** featuring wild-type GITRL to 1.5 mg/L for the aglycosylated variant (Table B.2). More formats of antibody-cytokine fusions featuring the aglycosylated GITRL_N74S_N157T mutant ($GITRL^{mut}$) were developed and tested *in vitro* (Figure 6.3b, Figure B.4, Figure B.5). While format $\mathbf{1^{mut}}$ yielded equivalent results in terms of purity to the variants featuring wild-type GITRL, format $\mathbf{2^{mut}}$ was highly prone to aggregation and degradation (Figure B.3) and therefore not used for further studies. Format $\mathbf{6^{mut}}$exhibited substantial batch to batch variability in terms of protein quality. While some batches were of high quality, other batches contained substantial amounts of heavily degraded protein. In all cases, a significant decrease in expression yield was observed compared to the variant featuring wild-type GITRL (Table B.2). By contrast, both the fusion protein in format **1** featuring wild-type

glycosylated GITRL and the one featuring aglycosylated GITRL retained the biological activity after incubation in mouse serum for up to 48 h at 37°C (Figure B.6).

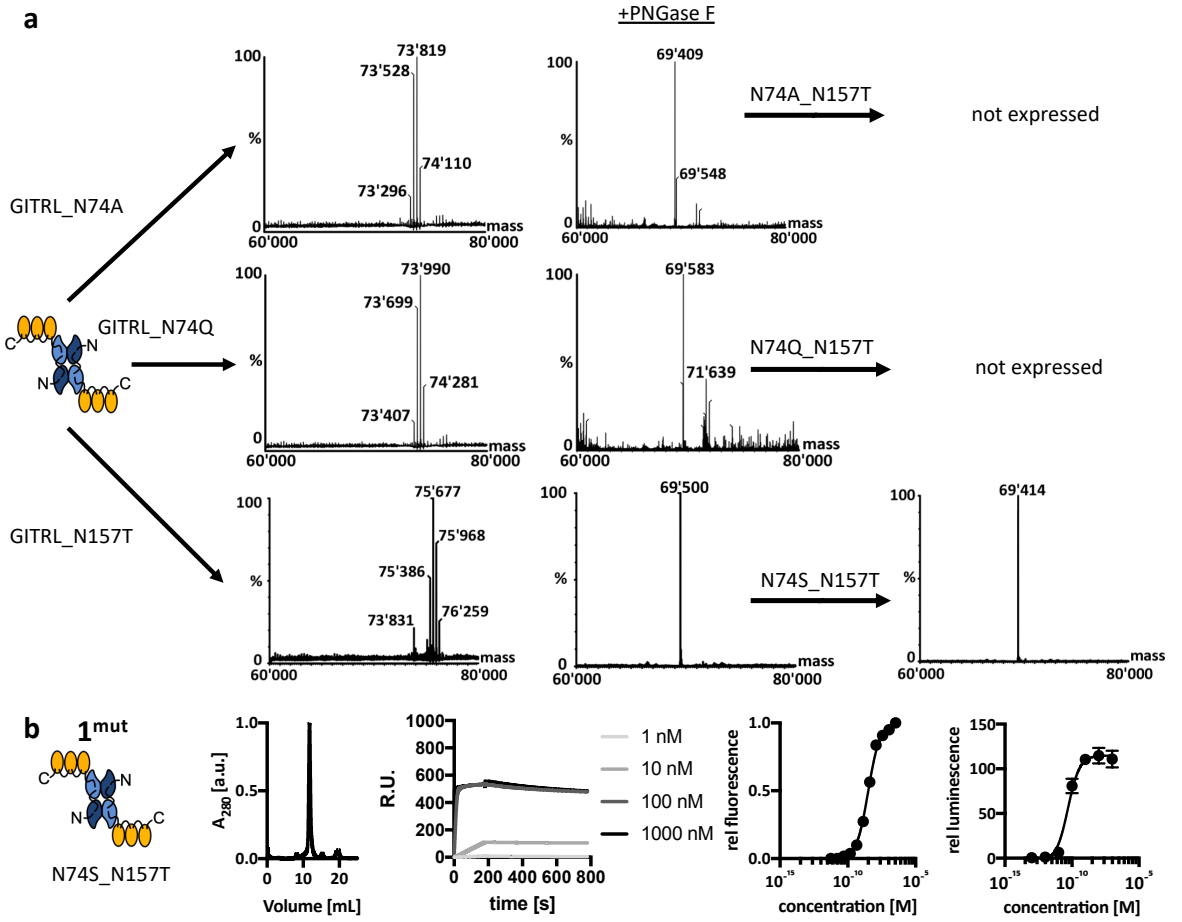

Figure 6.3.: Development of aglycosylated variants of F8-GITRL **(a)** the asparagine residues N74 and N157 of GITRL were sequentially mutated and the resulting proteins were tested for the absence of *N*-linked glycans by mass spectrometry. Remaining *N*-linked glycans were removed by enzymatic deglycosylation with PNGase F. The single-site mutants retained a glycan while the double mutant N74S, N157T was the only non-glycosylated variant that could be expressed. **(b)** Characterization of the F8-GITRL fusion protein in format $\mathbf{1^{mut}}$ featuring aglycosylated GITRL_N74S_N157T

Quantitative biodistribution studies with format $\mathbf{1^{mut}}$ featuring aglycosylated GITRL _N74S_N157T as payload showed that the fusion protein exhibited favorable tumor-targeting properties similar to what was observed after enzymatic deglycosylation of the fusion protein featuring wild-type GITRL (Figure 6.4a). As in the study in which enzymatically deglycosylated GITRL was used, a relatively high mouse to mouse variability in tumor uptake was observed. Selective accumulation of F8-GITRL featuring aglycosylated GITRL in the tumor was observed in F9 teratocarcinoma- and CT26 colon carcinoma-bearing mice 24 h after the injection of FITC-labelled protein (Figure 6.4b). Therefore, format $\mathbf{1^{mut}}$ featuring aglycosylated GITRL was selected for a therapy experiment in CT26 colon carcinoma-bearing mice.

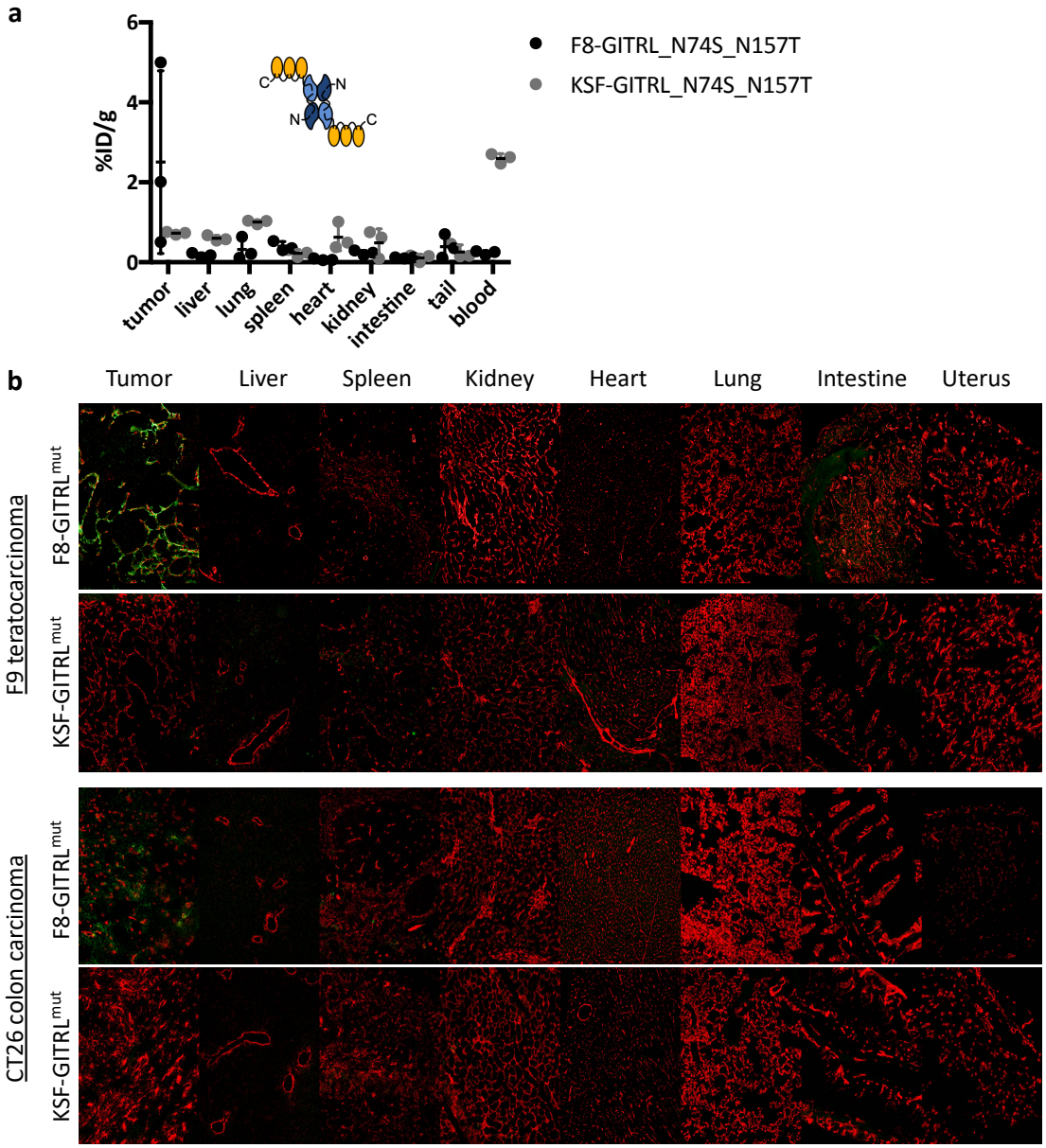

Figure 6.4.: *In vivo* biodistribution of the F8 fusion protein in format $\mathbf{1^{mut}}$ featuring aglycosylated GITRL_N74S_N157T (GITRL^{mut}) **(a)** Mice were sacrificed 24 h after the intravenous administration of radiolabelled proteins and the radioactivity of the different organs was measured and expressed as % injected dose per gram of tissue (%ID/g). GITRL_N74S_N157T (GITRL^{mut}) fused to the KSF antibody was used as negative control. The data represents individual measurements and mean ± SD (n = 3). **(b)** Mice were sacrificed 24 h after intravenous administration of FITC-labelled protein preparations. The FITC-labelled proteins were detected *ex vivo* on cryosections (green: αFITC, red: αCD31)

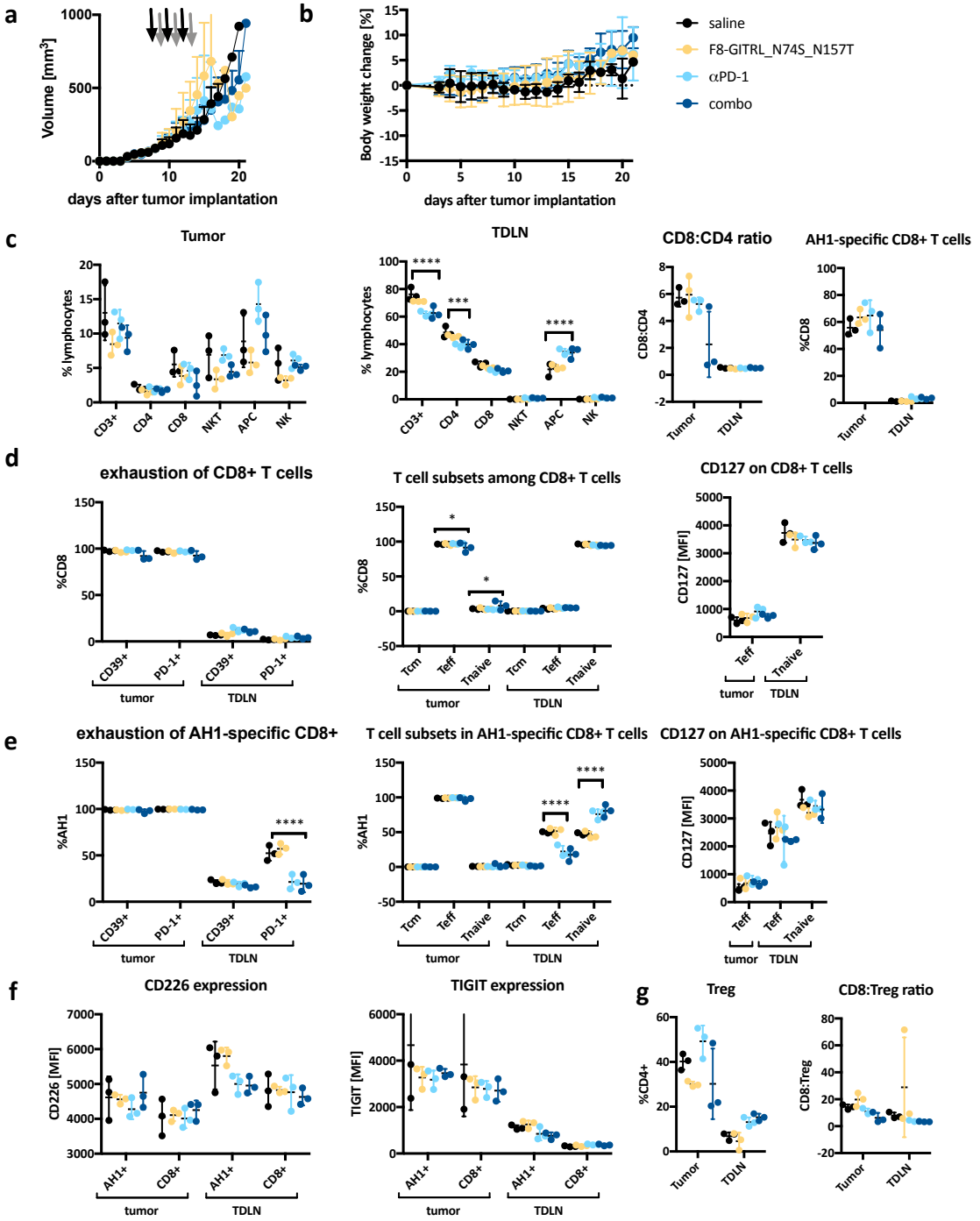

Figure 6.5.: Therapy studies and immune infiltrate analysis in CT26 colon carcinoma-bearing mice **(a)** CT26 tumor-bearing mice received three cycles of injections of either twice saline, F8-GITRL_N74S_N157T followed by saline, αPD-1 followed by saline or αPD-1 followed by F8-GITRL_N74S_N157T. The black arrows indicate the first injection of each cycle whereas the grey arrows indicate the second injection of each cycle. The tumor volume is depicted as average + SD for each group (n= 5). **(b)** The average body weight change after tumor cell implantation is depicted as mean ± SD. **(c)** The composition of tumor-infiltrating lymphocytes and the tumor-draining lymph nodes (TDLN) **(d)** the phenotype of CD8+ T cells in the tumor and TDLN **(e)** the phenotype of CD8+ T cells specific for the tumor-rejection antigen AH1 in the tumor and TDLN **(f)** expression of CD226 and TIGIT on CD8+ T cells in the tumor and TLDN **(g)** regulatory T cells in the tumor and TDLN as analyzed by flow cytometry. Data represents individual

Figure 6.5.: (continued) measurements and mean ± SD (n = 3). Statistical analysis was performed by a regular two-way ANOVA with Tukey's post-test in Graph Pad prism 7 ($p < 0.0001$: ****, $p < 0.001$: ***, $p < 0.01$: **, $p < 0.05$: *, $p > 0.05$: not significant)

The *in vivo* anti-tumor activity of F8-GITRL in format $\mathbf{1^{mut}}$ featuring aglycosylated GITRL_N74S_N157T was evaluated in CT26 colon carcinoma-bearing mice alone and in combination with a PD-1 inhibitor. The treatment schedule is shown in Table B.4. The different treatments did not show any effect on the growth rate of the tumors when compared to the group treated with saline only (Figure 6.5a). In general, the treatment was well tolerated as indicated by the absence of weight loss during the therapy (Figure 6.5b). Analysis of the tumor-infiltrating lymphocytes indicated an increase in antigen-presenting cells both in the tumor and the tumor-draining lymph nodes in the group treated with PD-1 inhibitor alone and in combination with F8-GITRL compared to the group treated with F8-GITRL only (Figure 6.5c). In addition, we observed an increase in the proportion of effector T cells in the tumor-draining lymph nodes amongst the CD8+ T cells specific for the tumor-rejection antigen AH1.[561] The increase was higher in the groups treated with saline and F8-GITRL only (Figure 6.5d). In all treatment groups, the tumor-infiltrating CD8+ T cells were strongly positive for the exhaustion markers PD-1 and CD39 and expressed the negative costimulatory receptor TIGIT (Figure 6.5e,f). In addition, there was a non-significant tendency towards a higher proportion of regulatory T cells in the tumor-draining lymph nodes upon treatment with a PD-1 inhibitor (Figure 6.5g). In conclusion, the treatment failed to reinvigorate the anti-tumor immune response.

6.3. Discussion

The clinical success of immune checkpoint inhibitors in a subset of patients highlighted the need for additional immunomodulatory treatments in order to reach therapeutic success in a wider population of cancer patients. In the recent years, GITR has emerged as a promising target to deliver costimulatory signals to effector T cells and to rescue this subset from suppression by regulatory T cells.[7] Several lines of evidence showed potent synergistic anti-tumor activity of GITR agonists in combination with PD-1 inhibitors.[562,563] A number of GITR agonists are currently investigated in clinical trials.

In this study, we developed a fusion protein consisting of murine GITRL and the F8 antibody targeting the EDA-positive splice isoform of fibronectin which is a marker of the tumor neovasculature.[11,12] We demonstrated that the *in vivo* stability and tumor-targeting properties of the F8-GITRL fusion protein featuring wild-type murine GITRL as a payload were hampered by glycan-mediated clearance of the protein. Although glycan-mediated clearance could to some extent be prevented by enzymatic deglycosylation and

site-specific mutagenesis of the *N*-glycosylation consensus sequence, a substantial mouse-to-mouse variability in tumor uptake was observed. In addition, the yield of fusion proteins featuring aglycosylated GITRL was significantly lower than for the constructs featuring wild-type GITRL. Given the importance of *N*-linked glycosylation for folding and quality control of secreted proteins,[564] the lower yield could indicate a reduction in protein folding efficiency during the production in CHO cells. In addition, the removal of the *N*-linked glycan could unmask cleavage sites for serum proteases or render the protein more prone to denaturation. However, both the wild-type and the aglycosylated mutant of GITRL fused to F8 in the diabody format retained the *in vitro* biological activity when incubated in mouse serum for up to 48 h, indicating that the absence of a glycan did not significantly impair the stability of the fully folded protein. While this is a rather indirect readout for the stability of the protein, we speculated that upon degradation or unfolding, the protein would lose its bioactivity. In addition, a protein which does not retain *in vitro* bioactivity under the given conditions is also not expected to have any therapeutic activity *in vivo*.

Treatment with F8-GITRL, alone or in combination with a PD-1 inhibitor, failed to mediate an anti-tumor immune response in CT26 colon carcinoma-bearing mice. The presence of CD8+ T cells specific for the retroviral tumor rejection antigen AH1 among the tumor infiltrating lymphocytes was confirmed by flow cytometry (Figure 6.5c). Previous reports had shown that AH1-specific CD8+ T cells constitute the major drivers of the anti-tumor immune response against CT26 colon carcinoma.[302,561,565] In line with previous reports, tumor infiltrating CD8+T cells were positive for the exhaustion markers[566] such as CD39 and PD-1 (Figure 6.5d,e). Previous studies had shown that the combination of GITR agonistic antibodies and PD-1 inhibitors could revert the dysfunctional state of tumor-specific CD8+ T cells by inducing the downregulation of TIGIT and the upregulation of the costimulatory receptor CD226 in murine models of cancer.[562] We did not observe any modulation of the expression of TIGIT or CD226 on tumor-infiltrating CD8+T cells. We also did not observe any modulation in the number of regulatory T cells or the ratio of effector T cells to regulatory T cells which was suggested as a biomarker for anti-GITR activity in other reports.[563]

The biological role of GITR as a target for anti-cancer intervention is questionable, also in light of the findings of our work. A number of preclinical studies has previously reported a promising anti-tumor activity of GITR agonists.[7,567] However, a Phase I clinical trial with a GITRL-Fc fusion (MEDI1873[423]) failed to demonstrate objective responses, in spite of the fact that a very broad dose range was tested (i.e., between 1.5 mg and 750 mg per injection).[419] Similarly, a lack of clinical benefit was reported for a number of GITR agonistic antibodies such as TRX518,[563] AMG228,[568] BMS-986156[412] and MK-1248.[414]

In summary, we could identify a molecular format and suitable glycoengineering strategies, that allowed the creation of a novel fusion protein (F8-GITRL) with promising

tumor-homing properties, as revealed by quantitative biodistribution analysis and by *ex vivo* immunofluorescence studies in tumor-bearing mice. However, the lack of anticancer activity of the fusion protein *in vivo* casts doubts about the potential of GITRL as a payload for tumor therapy strategies.

Abbreviations APC, Allophycocyanin; BV421, Brilliant violet 421; CD, cluster of differentiation; CH, constant region of the heavy chain; CL, constant region of the light chain; dDb, dimeric Diabody; EDA, alternatively spliced extradomain A of fibronectin; Fc, fragment crystallizable; FITC, Fluorescein Isothiocyanate; FSC, forward scattering; GITR(L), Glucocorticoid Induced TNFR-related protein (Ligand); HC, heavy chain; i.v., intravenous; IgG, immunoglobulin G; LC, light chain; LC-MS, Liquid chromatography-mass spectrometry; MHC, major histocompatibility complex; NF-kB, nuclear factor kappa B; NK cell, natural killer cell; PBS, phosphate buffered saline; PD-1, programmed cell death protein 1; PE, Phycoerythrin; scFv, single-chain Fragment variable; SDS PAGE, Sodium dodecyl sulfate polyacrylamide gel electrophoresis; SEC, Size exclusion chromatography; SSC, side scattering; TDLN, tumor-draining lymph node; Teff, effector T cell; Tnaive, naive T cell; Treg, regulatory T cell; VH, variable region of the heavy chain; VL, variable region of the light chain;

6.4. Materials and Methods

Cell lines The murine cytotoxic T cell line CTLL-2 (ATCC® TIB-214), the murine F9 teratocarcinoma cell line (ATCC® CRL-1720) and the murine CT26 colon carcinoma cell line (ATCC® CRL-2638) were obtained from ATCC, expanded and stored as cryopreserved aliquots in liquid nitrogen. The CTLL-2 cells were grown in RPMI-1640 (Gibco, #21875034) supplemented with 10% FBS (Gibco, #10270106), 1 X antibiotic-antimycoticum (Gibco, #15240062), 2 mM ultraglutamine (Lonza, #BE17-605E/U1), 25 mM HEPES (Gibco, #15630080), 50 µM β-mercaptoethanol (Sigma Aldrich) and 60 U/mL human IL-2 (Proleukin, Roche Diagnostics). The F9 teratocarcinoma cells were grown in DMEM (Gibco, high glucose, pyruvate, #41966-029) supplemented with 10% FBS (Gibco, #10270106) and 1 X antibiotic-antimycoticum (Gibco, #15240062) in flasks coated with 0.1% gelatin (Type B from Bovine Skin, Sigma Aldrich, #G1393). The CT26 colon carcinoma were grown in RPMI 1640 (Gibco, #21875034) supplemented with 10% FBS (Gibco, #10270106) and 1 X antibiotic-antimycoticum (Gibco, #15240062). The cells were passaged at the recommended ratios and never kept in culture for more than one month.

Mouse studies Eight weeks old female 129/Sv and Balb/c mice were obtained from Janvier. The mice were kept in individually ventilated cages in groups of 5 mice per cage in a specific pathogen free facility. They received food and water ad libitum and the cages were changed once per week by trained caretakers. After at least one week of acclimatization, 7 – $10{\cdot}10^6$ F9 cells (129/Sv) or $3{\cdot}10^6$ CT26 cells (Balb/c) were subcutaneously implanted into the right flank. The tumor size was monitored daily by caliper measurements and the volume was calculated using the formula [length x width x width x 0.5]. The animals were euthanized when the tumor diameter exceeded 15 mm or when the tumor started to ulcerate. The animal experiments were carried out under the project license ZH04/2018 granted by the Veterinäramt des Kantons Zürich, Switzerland, in compliance with the Swiss Animal Protection Act (TSchG) and the Swiss Animal Protection Ordinance (TSchV).

Cloning For PCR amplification of genetic sequences, the Phusion® High-Fidelity PCR Master Mix (NewEnglandBiolabs, #M0532S) was used with a primer concentration of 200 nM. Genetic sequences encoding a single-chain trimer of the extracellular domain of murine GITRL (amino acids 46 – 170) linked by a short polypeptide linker (GGGSGGG) were obtained from Eurofins Genomics and introduced into a vector encoding the F8 or KSF antibody in the diabody format by Gibson Isothermal Assembly (NewEnglandBiolabs, NEBuilder® HiFi DNA Assembly Master Mix, #E2621S). IgG fusions were cloned by fusing the sequence encoding GITRL to the genetic sequence encoding a chain of the IgG by PCR and introduced into the vector by restriction cloning. The genetic sequence encoding the diabody was replaced by the genetic sequence encoding the single-chain Fragment variable (scFv) by Gibson Isothermal Assembly and two domains of GITRL were removed by PCR followed by blunt-end ligation. Site-directed mutagenesis of the glycosylation consensus sequences were performed by Multichange Isothermal Mutagenesis (MISO) as described by Mitchell *et al.*[554] Brief, primers were designed including the desired point mutations, an upstream overhang of 14 bp and a downstream primer binding sequence with a melting point of around 60°C (calculated using tmcalculator.neb.com, Phusion® High-Fidelity PCR Master Mix, 200 nM primer concentration). The fragments between two adjacent point mutations were amplified by PCR. Adjoining fragments were assembled by PCR and introduced into the backbone by Gibson Isothermal Assembly. Quality control of the plasmids was performed by Sanger Sequencing by Microsynth AG. The sequences of the proteins are provided in Figure B.1.

Protein production Proteins were produced by transient transfection of CHO-S cells and purified by protein A affinity chromatography as described previously.[257,258,278] Brief, CHO-S cells were resuspended at a density of 4 mio cells/mL in ProCHO 4 medium

(Lonza, #LZ-BE12-029Q) supplemented with 8 mM ultraglutamine (Lonza, #BE17-605E/U1), 1 X HT supplement (Gibco, # 41065012) and 1 X antibiotic-antimycoticum (Gibco, #15240062). DNA was added at a final concentration of 0.675 µg/mio cells and polyethylenimine (Polysciences, #23966-1) was added to a final concentration of 0.01 mg/mL. The cells were incubated in a shaking incubator at 31°C for 6 days before the supernatant was harvested and the proteins were purified by protein A affinity chromatography. The supernatant was filtered and applied to a protein A column at a speed of 2 mL/min at 4°C. The protein was washed by 100 – 200 mL of wash buffer A (100 mM NaCl, 0.5 mM EDTA, 0.1% Tween in PBS) and wash buffer B (500mM NaCl, 0.5 mM EDTA in PBS). The proteins were eluted in 10 mL of either 0.1 M glycine at pH 3 or 0.1 M Triethylamine, depending on the isoelectric point of the protein. The purified proteins were dialyzed overnight against 3 L phosphate buffered saline (PBS). Quality control of the purified products included SDS-PAGE (Figure B.2), liquid chromatography- mass spectrometry (LC-MS) and size exclusion chromatography (SEC). Size exclusion chromatography was performed using an Äkta Pure FPLC system (GE Healthcare) with a Superdex S200 10/300 increase column at a flow rate of 0.75 mL/min (GE Healthcare) in PBS.

Binding measurements by Surface Plasmon Resonance To evaluate the binding kinetics of the F8 moiety to EDA, a CM5 sensor chip (GE Healthcare) was coated with 500 resonance units of an EDA-containing recombinant fragment of fibronectin. The measurements were carried out with a Biacore S200 (GE Healthcare) setting the contact time to 3 min followed by a dissociation for 10 min and a regeneration of the chip using 10 mM HCl at a flow rate to 20 µL/min.

Binding measurements by Flow Cytometry In order to assess the binding of the GITR moiety to cells expressing GITR, CTLL-2 cells were incubated with varying concentrations of the fusion proteins for 1 h. The bound protein was detected by addition of an excess of AlexaFluor488-labelled protein A (Thermofisher, #P11047) and subsequent measurement of the fluorescence using a Cytoflex Flow Cytometer. The mean fluorescence was normalized by subtracting the lowest measurement and dividing by the highest measurement. The resulting binding curve was fitted using the [Agonist] vs. response (three parameters) fit of the GraphPad Prism 7.0 a software to estimate the apparent K_D.

NF-κB response assay The development of the CTLL-2 reporter cell line was described previously.[569] Briefly, CTLL-2 reporter cells were washed with prewarmed HBSS (Gibco, #14175095) and grown for 6 - 9 h in growth medium without IL-2 prior to use in order

to reduce the background signal. Cells were seeded in 96-well plates (50,000 cells/well) and growth medium containing varying concentrations of the antibody-GITRL conjugate was added. The cells were incubated at 37°C, 5% CO_2 overnight. To assess luciferase production, 20 µL of the supernatant was transferred to an opaque 96-well plate (Perkin-Elmer, Optiplate-96, white, #6005290) and 80 µL 1 µg/mL Coelenterazine (Carl Roth AG, #4094.3) in phosphate buffered saline (PBS) was added. Luminescence at 466 nm was measured immediately. The relative luminescence was calculated by dividing the obtained results by the results obtained when no inducer was added. The resulting curve was fitted using the [Agonist] vs. response (three parameters) fit of the GraphPad Prism 7.0 a software to estimate the EC_{50}.

Serum stability assay In order to assess the *in vitro* stability of the proteins in mouse serum, the fusion proteins were diluted in mouse serum (Invitrogen) to 200 nM and incubated at 37°C for up to 48 h. After the incubation in mouse serum, a 10-fold dilution series was prepared and the above-described bioactivity assay was performed. The EC_{50} was estimated using the [Agonist] vs. response (three parameters) fit of the GraphPad Prism 7.0 a software.

Quantitative biodistribution Quantitative biodistribution experiments were carried out as described previously.[11] Brief, F9 teratocarcinoma cells were cultivated and implanted into 129/Sv mice as described above. The fusion proteins were radioactively labelled with ^{125}I using Chloramine-T. When the tumors reached a volume of 100 – 300 mm^3 the mice were randomly assigned into groups of 3 mice and 10 – 15 µg of radioiodinated protein was injected into the lateral tail vein. The mice were sacrificed 24 h after the injection of the radiolabelled protein. The radioactivity of the excised organs was measured (Packard Cobra II Gamma Counter) and expressed as percentage of the injected dose per gram of tissue (%ID/g ± SD, n = 3). Enzymatic deglycosylation was performed overnight at 37°C using 3 U/µg protein PNGase F (NewEnglandBiolabs, #P0705S). As a negative control, equivalent antibody-cytokine fusions were used featuring the KSF antibody targeting hen egg lysozyme[90](Figure B.3).

***Ex vivo* detection of fluorescently labelled proteins** Proteins were fluorescently labelled in a 0.1 M sodium carbonate buffer at pH 9.1 in the presence of excess Fluorescein Isothiocyanate overnight at 4°C. Uncojugated FITC was separated from the labelled proteins using PD-10 spin columns (Sigma Aldrich, PD Spintrap™ G25, #GE28-9180-04) according to the manufacturer's recommendations. Approximately 100 µg of fluorescently labelled protein in PBS was injected into the lateral tail vein of tumor-bearing mice. The mice were sacrificed 24 h after the injection, the organs were embedded in NEG-50

cryoembedding medium (ThermoFisher, Richard-Allan-Scientific, #6502) and frozen. Of all samples, 8 µm cryosections were prepared and fixed in ice-cold acetone. The fixed slices were incubated with goat-anti-mouse CD31 (R&D system, #AF3628, 1:200) and rabbit-anti-FITC (Biorad, #4510-7804) followed by donkey-anti-goat-AF594 (Invitrogen, #A11058) and donkey-anti-rabbit-AF488 (Invitrogen, #A21206). Images were acquired using a Zeiss Axioscope 2 mot plus with an Axiocam 503 camera at a 20 X magnification in the RGB mode. The images were processed using the software ImageJ v1.52k.

Therapy studies CT26 colon carcinoma cells were cultivated and implanted into Balb/c mice as described above. The tumor volume and the weight of the mice was monitored daily. When the tumor volume reached a value of 80 – 100 mm^3 the mice were randomly assigned into groups of 5 animals in order to obtain uniform average tumor volumes for each group. Mice from each group were randomly distributed over the different cages. The mice received three cycles of intravenous injections of 200 µL of therapeutic agent. The experiment was performed under blinding conditions meaning that a second person prepared and labeled the therapeutic doses with a code which was only revealed to the researcher performing the animal experiments after the termination of the study. The control group received injections of phosphate buffered saline (PBS, Gibco, #1010023) only, one group received 200 µg of F8-GITRL followed by saline, one group received 200 µg of PD-1 inhibitor (BioXCell, clone 29F.1A12) followed by saline and the combination treatment group received 200 µg of PD-1 inhibitor followed by 200 µg of F8-GITRL (Table B.4).

Flow cytometry analysis of tumor infiltrating lymphocytes CT26 tumor-bearing mice were treated as described above for the therapy (Table B.4). The mice were sacrificed 24 h after the last therapeutic cycle and the tumor and draining lymph nodes were excised. The lymph nodes were mechanically disrupted on a 70 µm cell strainer. The tumors were cut into small pieces using a pair of surgical scissors and afterwards incubated in 5 mL of a digestion mix (RPMI-1640, 1 mg/mL collagenase II, 100 µg/mL DNaseI) in a shaking incubator at 37°C for 30 min. After the digestion of the extracellular matrix the tumor cells were passed through a cell strainer. The cells were harvested by centrifugation and red blood cells were removed using a red blood cell lysis buffer (Roche). Samples for intracellular staining were stained with zombie red for 15 min at room temperature. Surface staining was performed for 30 min on ice. For surface staining the following antibodies were used: αCD3-APC/Cy7 (Biolegend, #100222), αCD4-APC (Biolegend, #100412), αCD8-FITC (Biolegend, #100706), αCD8-APC/Cy7 (Biolegend, #100714), αNK1.1-PE (Biolegend, #108708), αCD62L-BV421 (Biolegend, #104436), αCD44-APC/Cy7 (Biolegend, #103028), αMHCII(IA/IE)-BV421 (Biolegend, #107631), αPD-1-BV421 (Biole-

gend, #109121), αCD39-APC (Biolegend, #143809), αCD127-APC (Biolegend, #135011), αCD226 (Biolegend, #128809), αTIGIT (Biolegend, #142111) and αGITR (Biolegend, #120205). The staining panel is depicted in Table B.5. The cells were washed twice in FACS buffer (0.5% BSA, 2 mM EDA, PBS). Samples that were stained for cell surface staining only were incubated for 5 min on ice in 7-AAD (Biolegend, #420404). Samples that were stained for intracellular markers were fixed and permeabilized using the eBioscience™ FoxP3/Transcription Factor Staining Buffer Set (Thermofisher, #00-5523-00) according to the manufacturer's instructions. The samples were analyzed using a Beckmann Coulter Cytoflex and later processed using FlowJo v10.7.1. Statistical analysis was done using a regular two-way ANOVA followed by a Tukey's multiple comparison test in GraphPad Prism v7. The gating strategy is shown in Figure B.7.

Acknowledgements

Financial support by the ETH Zürich, the Swiss National Science Foundation (grant number 310030_182003/1), the European Research Council (ERC) under the European Union's Horizon 2020 research and innovation program (grant agreement 670603), and the Federal Commission for Technology and Innovation (KTI, grant number 12803.1 VOUCH-LS) is gratefully acknowledged. The authors gratefully acknowledge Fiona Ammann and Sabrina Müller for their technical assistance.

Author contributions

Jacqueline Mock: Conceptualization, Methodology, Project administration, Investigation, Writing – Original Draft. **Itzel Astiazaran Rascon**: Investigation. **Marco Stringhini**: Investigation, Methodology. **Marco Catalano**: Investigation. **Dario Neri**: Supervision, Funding acquisition, Writing – Original Draft, Resources, Conceptualization.

Competing interests

Dario Neri is a cofounder and shareholder of Philogen SpA (Siena, Italy), the company that owns the F8 and the L19 antibodies. No potential conflicts of interest were disclosed by the other authors.

Data availability statement

The datasets generated during and/or analyzed during the current study are available from the corresponding author on reasonable request. The sequences of the fusion proteins are available via GenBank (Accession numbers MW115896-MW115905).

7. An engineered 4-1BBL fusion protein with "activity-on-demand"

This chapter is based on the publication ”An engineered 4-1BBL fusion protein with "activity-on-demand" ” by J. Mock, M. Stringhini, A. Villa, M. Weller, T. Weiss & D. Neri *Proceedings of the National Academy of Sciences of the United States of America (PNAS)*, 2020 Dec 15;117(50):31780-31788. doi: 10.1073/pnas.2013615117. Epub 2020 Nov 25. PMID: 33239441, reproduced with permission (https://www.pnas.org/page/about/rights-permissions)

Abstract

Engineered cytokines are gaining importance for cancer therapy, but these products are often limited by toxicity, especially at early time points after intravenous administration. 4-1BB is a member of the tumor necrosis factor receptor superfamily, which has been considered as a target for therapeutic strategies with agonistic antibodies or using its cognate cytokine ligand, 4-1BBL. Here we describe the engineering of an antibody fusion protein (termed F8-4-1BBL), which does not exhibit cytokine activity in solution, but regains biological activity upon antigen binding. F8-4-1BBL bound specifically to its cognate antigen, the alternatively-spliced EDA domain of fibronectin, and selectively localized to tumors *in vivo*, as evidenced by quantitative biodistribution experiments. The product promoted a potent anti-tumor activity in various mouse models of cancer, without apparent toxicity at the doses used. F8-4-1BBL represents a prototype for antibody-cytokine fusion proteins, which conditionally display “activity-on-demand” properties at the site of disease upon antigen binding and reduce toxicity to normal tissues.

Significance Statement Antibody-cytokine fusion proteins have been successfully applied for the treatment of preclinical models of cancer and yielded promising results in early clinical trials. The antibody moiety redirects the immunostimulatory payload to the tumor in order to boost the anti-tumor immune response. However, especially at early timepoints after administration, the relatively high concentration of the antibody-cytokine conjugate in blood can lead to severe side effects due to peripheral activation of cytokine receptors. Therefore, protein engineering approaches are necessary in order to develop antibody-cytokine conjugates that selectively regain their immunostimulatory activity upon antigen binding in the tumor. In this work, we have developed an antibody-cytokine conjugate that meets these criteria and which showed anti-tumor activity in preclinical models of cancer.

7.1. Introduction

Cytokines are immunomodulatory proteins, which have been considered for pharmaceutical applications for the treatment of cancer patients[9,570,571] and other types of disease.[9] There is a growing interest in the use of engineered cytokine products as anti-cancer drugs, capable of boosting the action of T cells and natural killer (NK) cells against tumors,[571,572] alone or in combination with immune checkpoint inhibitors.[3,318,571,573]

Recombinant cytokine products on the market include IL2 (Proleukin®),[249,574] IL11(Neumega®),[575,576] TNF (Beromun®),[577] IFNα (Roferon A®, Intron A®),[247,578] IFNβ (Avonex®, Rebif®, Betaseron®),[579,580] IFNγ (Actimmune®),[581] G-CSF (Neupogen®),[582] GM-CSF (Leukine®).[583,584] The recommended dose is typically very low (often at less than one milligram per day),[585–587] as cytokines may exert biological activity in the subnanomolar concentration range.[254] In order to develop cytokine products with improved therapeutic index, various strategies have been proposed. Protein PEGylation or Fc fusions may lead to prolonged circulation time in the bloodstream, allowing the administration of low doses of active payload.[588,589] In some implementation, cleavable PEG polymers may be considered, yielding prodrugs which regain activity at later time points.[590] Alternatively, tumor-homing antibody fusions have been developed, since the preferential concentration of cytokine payloads at the tumor site has been shown in preclinical models to potentiate therapeutic activity, helping spare normal tissues.[292,591–596] Various antibody-cytokine fusions are currently being investigated in clinical trials for the treatment of cancer and of chronic inflammatory conditions [for reviews, see [9,596–599]].

Antibody-cytokine fusions display biological activity immediately after injection to patients, which may lead to unwanted toxicity and prevent escalation to therapeutically active dose regimens.[249,586,600] In the case of pro-inflammatory payloads (e.g., interleukin-2, interleukin-12, tumor necrosis factor alpha), common side effects include hypotension,

nausea and vomiting, as well as flu-like symptoms.[254,281,282,300,337] These side-effects typically disappear when the cytokine concentration drops below a critical threshold, thus providing a rationale for slow-infusion administration procedures.[478] It would be highly desirable to generate antibody-cytokine fusion proteins with excellent tumor targeting properties and with "activity-on-demand" (i.e., with a biological activity which is conditionally gained upon antigen binding at the site of disease, helping spare normal tissues).

Here, we describe a fusion protein, consisting of the F8 antibody (specific to the alternatively-spliced EDA domain of fibronectin[11,12]) and of murine 4-1BBL, which did not exhibit cytokine activity in solution but could regain potent biological activity upon antigen binding. The antigen (EDA+ fibronectin) is conserved from mouse to man,[601] is virtually undetectable in normal adult tissues (exception made for placenta, endometrium and some vessels in the ovaries), but is expressed in the majority of human malignancies.[11–13,602] 4-1BBL is a member of the tumor necrosis factor superfamily.[603] It is expressed on antigen-presenting cells[604,605] and binds to its receptor 4-1BB which is upregulated on activated cytotoxic T cells,[429] activated dendritic cells,[429] activated NK and NKT cells[430] and on regulatory T cells.[606] Signaling through 4-1BB on cytotoxic T cells protects them from activation-induced cell death and skews the cell towards a more memory-like phenotype.[6,433]

We engineered nine formats of the F8-4-1BBL fusion protein and one of them exhibited a superior performance in quantitative biodistribution studies and conditional gain of cytokine activity upon antigen binding. The antigen-dependent reconstitution of the biological activity of the immunostimulatory payload represents an example for an antibody fusion protein with "activity on demand". The fusion protein was potently active against different types of cancer, without apparent toxicity at the doses used. The EDA domain of fibronectin is a particularly attractive antigen for cancer therapy, in view of its high selectivity, stability and abundant expression in most tumor types.[11–13,602]

7.2. Results

Human 4-1BBL is a homotrimeric protein (Figure 7.1 a),[447] while its murine counterpart forms stable homodimers.[346,448] Stable trimeric structures can be engineered by connecting 4-1BBL monomeric domains with suitable polypeptide linkers.[492] Recombinant antibodies can be expressed as full IgG or as fragments, forming single-chain Fv (scFv)[133,134] or diabody[135]structures (Figure 7.1 b and Figure C.1).[9,10,541] Nine different fusion proteins containing F8 antibody and murine 4-1BBL moieties were expressed in mammalian cells, in order to identify products with promising features for subsequent *in vivo* investigations. Mutational scans had revealed that the disulfide bond linking two 4-1BBL monomers

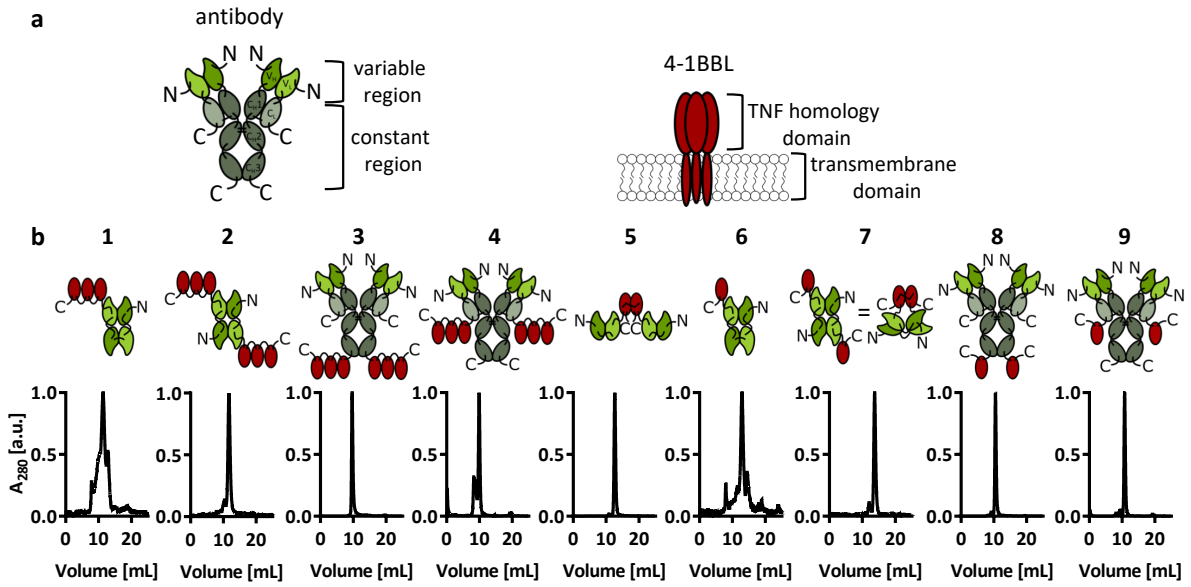

Figure 7.1.: The nine F8-4-1BBL fusion proteins that were designed and tested in this study **(a)** schematic depiction of an antibody in the IgG format and of the human 4-1BBL. The human 4-1BBL is a transmembrane protein which forms a non-covalent homotrimer[447] **(b)** the fusion proteins featuring murine 4-1BBL are schematically depicted and size exclusion chromatograms are provided.

is crucial for protein stability (Figure C.2). The observation that the TNF homology domain (THD) within 4-1BBL was sufficient for full *in vitro* activity (Figure C.3) guided the design of the modules to be included in the fusion proteins. Six out of nine products exhibited favorable size exclusion and SDS-PAGE profiles (Figure 7.1 b and Figure C.4). We selected formats **2**, **3**, **5**, **7** and **8** for further investigations, since those proteins gave the best yields and did not show signs of aggregation even after repeated freeze-thaw cycles.

Figure 7.2 presents a comparative analysis of *in vitro* properties of F8-4-1BBL in various formats. The 4-1BBL and F8 moieties were able to recognize the cognate targets in the **2**, **3**, **5**, **7** and **8** formats. Indeed, all proteins bound with high affinity to murine CTLL-2 cells, which are strongly positive for murine 4-1BB (i.e., the 4-1BBL receptor) (Figure 7.2a) and to recombinant EDA domain of fibronectin (Figure 7.2b). A functional assay with an NF-κB reporter cell line[569] revealed that all fusion proteins preferentially activated downstream signaling events in the presence of the cognate EDA fibronectin antigen, immobilized on a solid support and thus mimicking the tumor environment (Figure 7.2c). Formats **5** [consisting of two disulfide-linked 4-1BBL monomeric units fused to scFv(F8)] and **8** [in which monomeric units of 4-1BBL were fused at the C-terminal ends of the heavy chains of IgG(F8)] exhibited the best discrimination between low biological activity in solution and high cytokine activity in the presence of antigen. For this reason, formats **5** and **8** were selected for an *in vivo* characterization of their tumor targeting

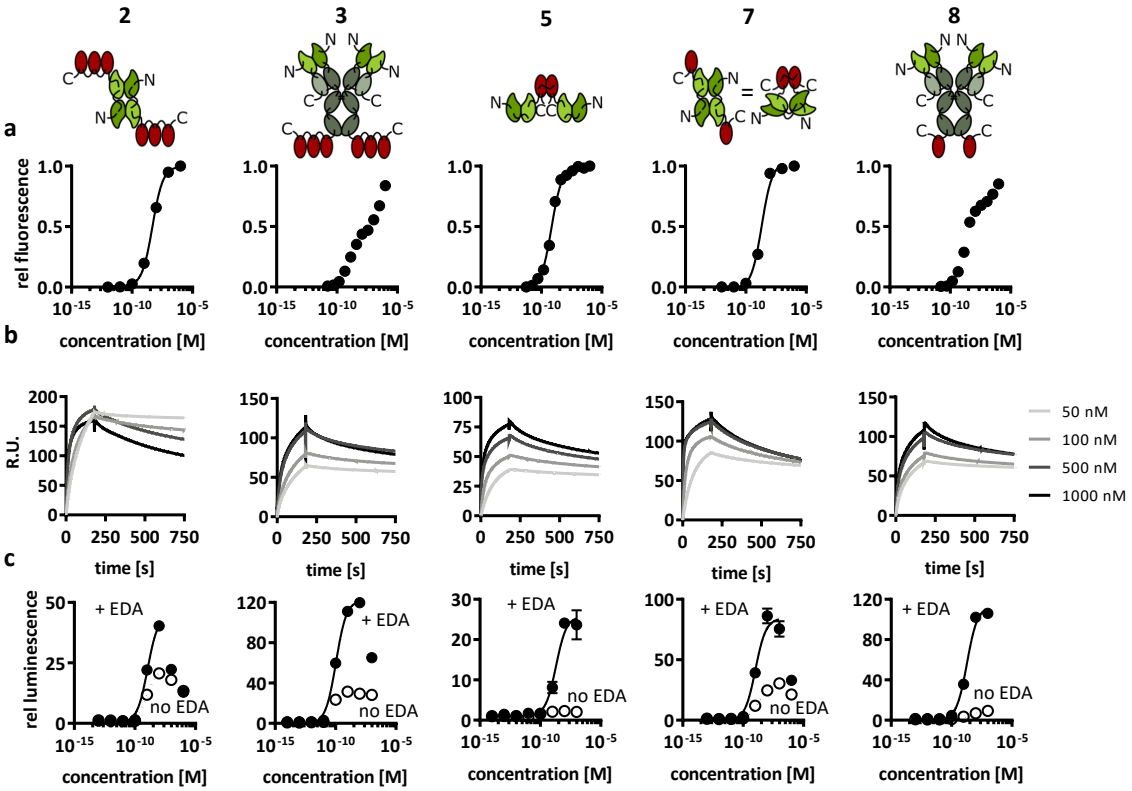

Figure 7.2.: *In vitro* characterization of five F8-4-1BBL formats **(a)** binding to 4-1BB was measured by flow cytometry with the murine cytotoxic T cell line CTLL-2 which expresses 4-1BB **(b)** binding of the F8 moiety to the EDA-positive ectodomain of fibronectin was measured by surface plasmon resonance on chips coated with recombinant EDA **(c)** biological activity was tested using an NF-κB reporter cell line that secretes luciferase upon activation of the NF-κB pathway by signaling through 4-1BB. The assay was performed both with and without EDA immobilized on solid support (n = 3). Curve fitting was done using the [agonist] vs response (three parameters) fit of GraphPad Prism v7.0. Data represent mean ± SD.

properties. Format **2** was also included in the comparison, since diabody-based antibody cytokine fusion proteins have previously been used for clinical development programs.[9,10]

Protein preparations were radio-iodinated and injected into immunocompetent 129/Sv mice, bearing subcutaneously-grafted murine F9 teratocarcinomas, which express EDA fibronectin around tumor blood vessels.[11] Mice were sacrificed 24 hours after intravenous administration and biodistribution results were expressed as percent of injected dose per gram of tissue (%ID/g) (Figure 7.3a and Figure C.5). Format **2** exhibited only a modest tumor uptake (1.0% ID/g) and poor selectivity. Format **8** showed, as expected, a longer circulatory half-life, as evidenced by the high %ID/g in blood after 24 h, but the tumor uptake and selectivity were not significantly higher compared to KSF-4-1BBL (a fusion protein based on the KSF antibody, specific to hen egg lysozyme and serving as negative control[90]). By contrast, format **5** exhibited a preferential accumulation in the tumor (2.8

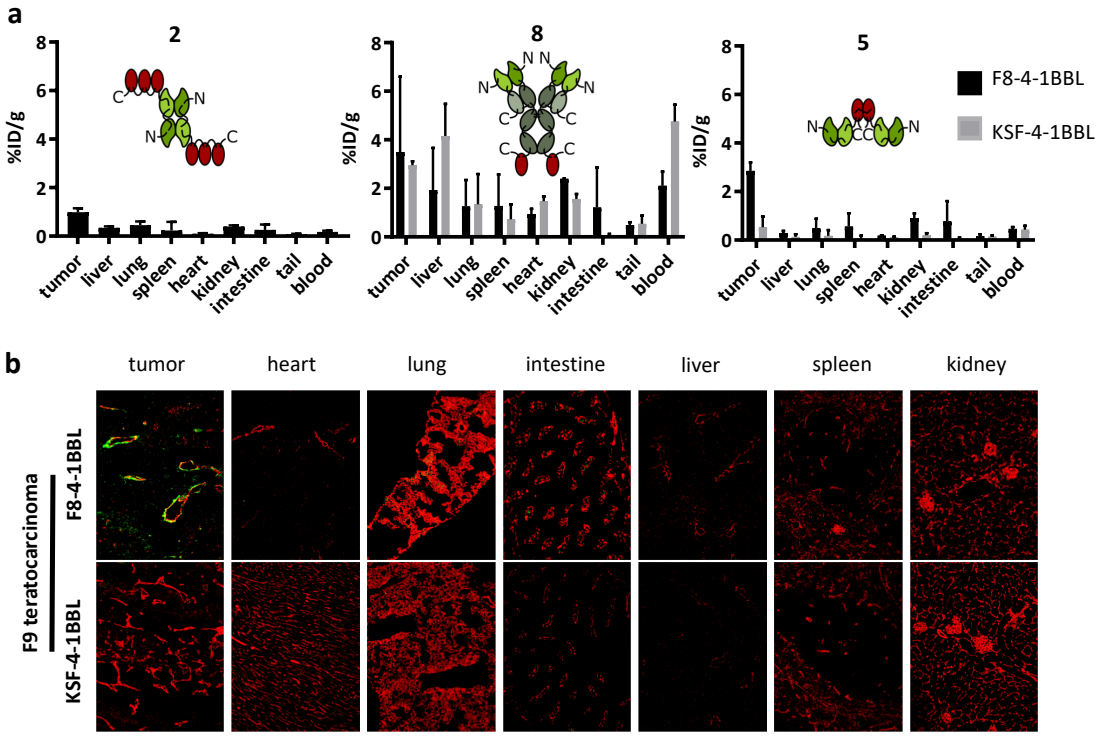

Figure 7.3.: *In vivo* biodistribution studies of three F8-4-1BBL formats **(a)** The mice were sacrificed 24 h after the injection of the radio-iodinated proteins and the radioactivity of excised organs was measured and expressed as percent injected dose per gram of tissue (%ID/g ± SD, n = 3). The KSF antibody targeting hen egg lysozyme was used as untargeted control.[90] **(b)** The mice were sacrificed 24 h after the injection of FITC-labelled F8-4-1-BBL or KSF-4-1-BBL in format 5. The proteins were detected *ex vivo* on cryosections (green: αFITC, red: αCD31).

% ID/g) and a good tumor-to-normal organ selectivity. EDA targeting was essential for tumor homing, as revealed by the comparison of the biodistribution results with the negative control KSF-4-1BBL fusion protein (Figure 7.3a and Figure C.5). In order to confirm selective tumor uptake with a different methodology, format **5** was injected into tumor-bearing mice. An *ex vivo* immunofluorescence analysis revealed a preferential accumulation of format **5** around tumor blood vessels, while no staining was detectable in normal organs or when the KSF fusion protein was used (Figure 7.3b and Figure C.6). In line with previous reports on this matter,[11–13,602] the EDA-domain of fibronectin is an ideal target for pharmacodelivery applications in mouse and in man, as the antigen is undetectable in normal adult tissues, but is strongly expressed in the stroma and around the blood vessels in many different tumor types (Figure C.7).

Therapy studies were performed using format **5** of F8-4-1-BBL, both in a preventive setting starting at a tumor volume of 40 mm^3 and in a therapeutic setting starting at a tumor volume of 75 – 100 mm^3. In a preventive setting in WEHI-164 fibrosarcoma, three out of five mice rejected the tumor using F8-4-1-BBL as single agent, while four out of five mice showed a complete response when treated with PD-1 blockade, alone

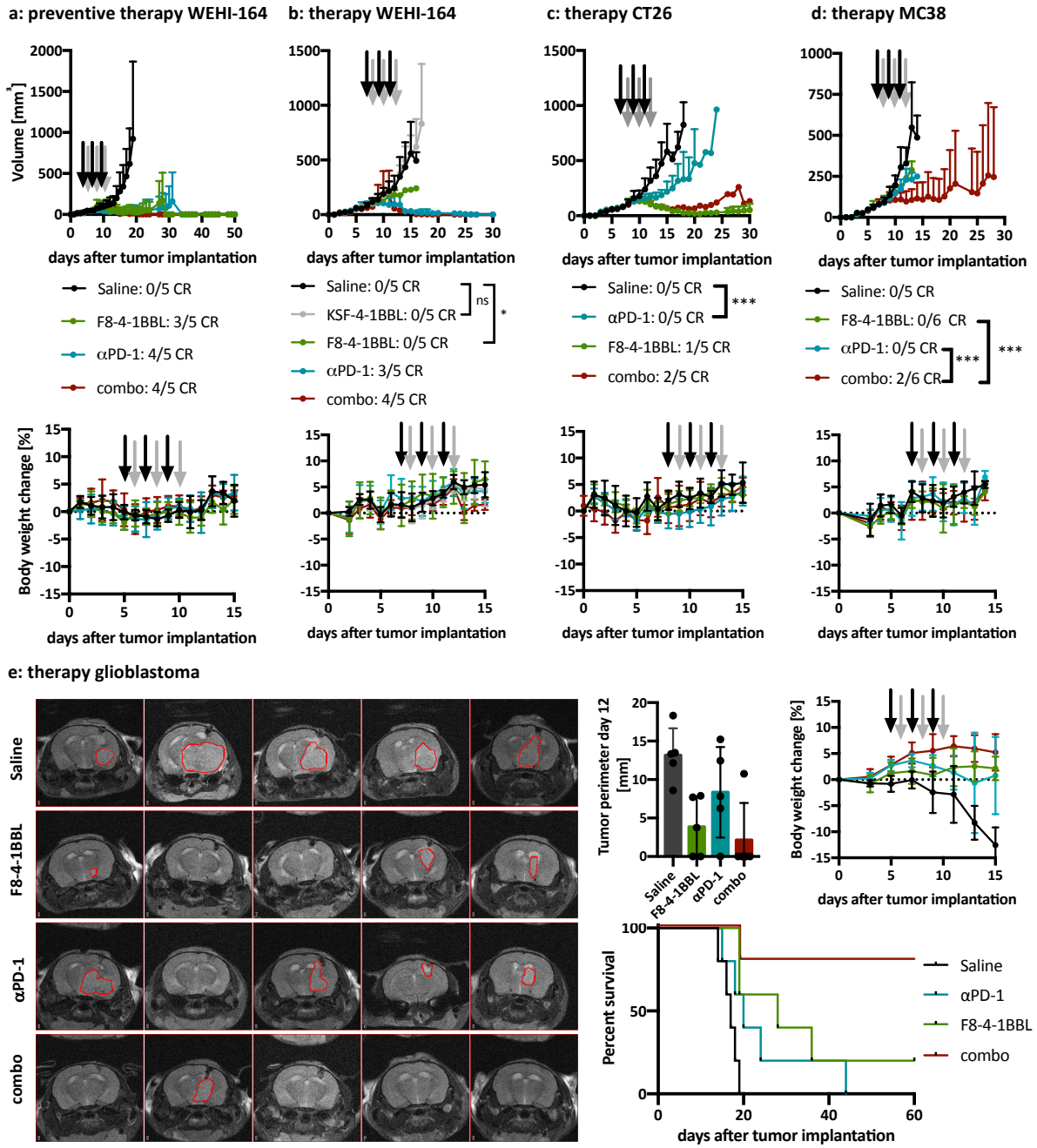

Figure 7.4.: Therapy studies with F8-4-1BBL in format 5 **(a)** The preventive therapy in WEHI-164 fibrosarcoma-bearing mice was started on day 5 when the tumors reached a volume of 40 mm^3. The tumor sizes are shown as mean + SD (n = 5). The body weight data is represented as mean body weight change ± SD for each group. **(b)** The therapy in WEHI-164 fibrosarcoma-bearing mice was started on day 7 when the tumor volume was > 80mm^3. The tumor sizes are shown as mean + SD (n = 5). The statistical results of a regular two-way ANOVA followed by a Tukey's multiple comparison test using GraphPad Prism v8.4.1 on day 13 are shown (ns: not significant, * p = 0.0427). The body weight data is represented as mean body weight change ± SD for each group. **(c)** In CT26-colon carcinoma-bearing mice the therapy was started on day 7 when the tumor volume exceeded 80 mm^3. The tumor sizes are shown as mean + SD (n = 5). The result of a regular two-way ANOVA followed by a Tukey's multiple comparison test using GraphPad Prism v8.4.1 is shown for day 13 (*** p = 0.0004). **(d)** In MC38 colon carcinoma-bearing mice the therapy was started on day 7 when the tumor volume exceeded 75 mm^3.

Figure 7.4.: (continued) The tumor sizes are shown as mean + SD (n = 5 - 6). The result of a regular two-way ANOVA followed by a Tukey's multiple comparison test using GraphPad Prism v8.4.1 is shown for day 12 (*** $p < 0.001$). The body weight data is represented as mean body weight change ± SD for each group. **(e)** GL-261 were implanted orthotopicaly in C57BL/6 mice. Subsequently, mice were treated intravenously with saline, F8-4-1BBL, αPD-1 or the combination starting on day 5. Tumor size was assessed at day 12 after tumor implantation. MRI of five mice per group are shown on the left with tumors outlined in red and the quantification of tumor perimeters in 5 mice per group on the right. The survival data are presented as Kaplan-Meier plots. The body weight data is represented as mean body weight change ± SD for each group. (black arrows: injections of the single-agents, grey arrows: injection of F8-4-1BBL in the combination treatment, CR: complete response)

or in combination with F8-4-1-BBL (Figure 7.4a). The cured mice rejected subsequent challenges with WEHI-164 fibrosarcoma cells. In some cured mice, a challenge with CT26 colon carcinoma cells was also rejected, similar to what we had previously reported for other F8-based immunocytokine therapeutics[258,302](Figure C.8). When the therapy was repeated in mice bearing larger WEHI-164 fibrosarcoma tumors, a significant [$p = 0.0427$, regular two-way ANOVA, Tukey's multiple comparison test, day 13] tumor growth retardation was observed in mice treated with F8-4-1BBL (Figure 7.4b). There was no difference in tumor growth between mice receiving injections of saline and the KSF fusion proteins, underlining the importance of the antigen-dependent activation of 4-1BBL (Figure 7.4b). Similar experiments performed in immunocompetent mice bearing CT26 tumors showed a tumor regression in 4/5 mice treated with F8-4-1BBL. One mouse was cured, while tumors eventually regrew in the other mice. Therapy was potent also when F8-4-1BBL was combined with PD-1 blockade (Figure 7.4c). When MC38 colon carcinoma-bearing mice were treated with F8-4-1BBL or PD-1 blockade as single agents, a moderate tumor growth retardation compared to mice treated with saline was observed [$p < 0.0001$, regular two-way ANOVA, Tukey's multiple comparison test, day 12]. By contrast, the combination treatment was potently active and led to durable complete remissions in 2/6 mice (Figure 7.4d). All treatments in all experiments were well tolerated, as indicated by the absence of body weight loss (Figure 7.4).

To further investigate the therapeutic activity of F8-4-1BBL, alone or in combination with PD-1 blockade, we studied an orthotopic model of glioblastoma in immunocompetent mice. Treatment was started 5 days after intracerebral implantation of GL-261 tumor cells. Mice were imaged at day 12 by magnetic resonance imaging (MRI) and were monitored in terms of body weight and behavior. Mice were sacrificed when they developed neurologic symptoms. In keeping with previous reports, none of the mice from the saline treatment group survived more than 20 days. By contrast, F8-4-1BBL exhibited a potent anticancer activity, which was potentiated by PD-1 blockade. Eighty percent of the mice

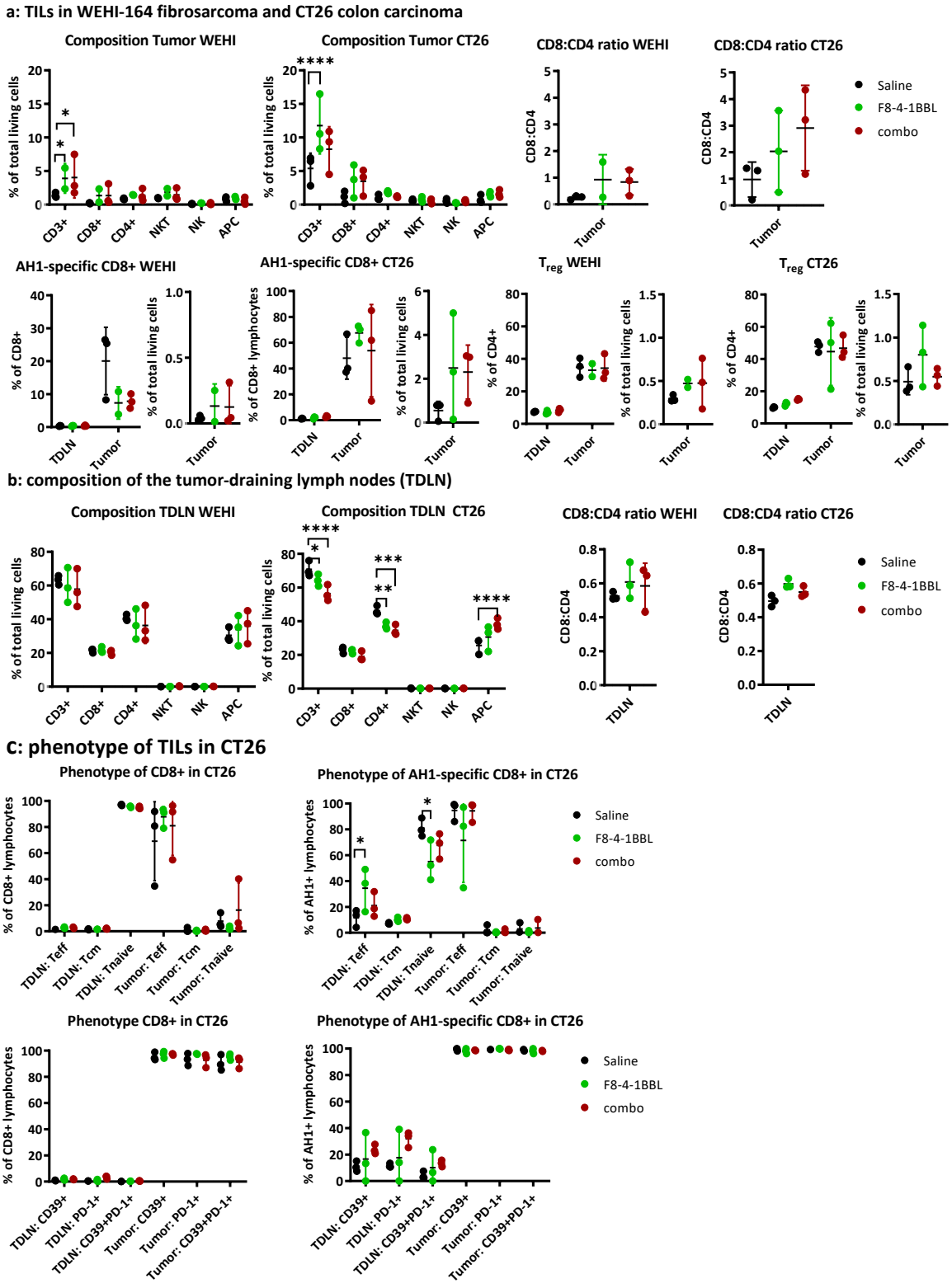

Figure 7.5.: Analysis of tumor-infiltrating leukocytes (TIL) and tumor-draining lymph nodes (TDLN) **(a)** Composition of the tumor-infiltrating immune cells, including the CD8:CD4 ratio, the proportion of AH1-specific CD8+ T cells and regulatory CD4+ T cells in WEHI-164 and CT26 tumors treated with saline, F8-4-1BBL and the combo therapy (αPD-1 and F8-4-1BBL). Proportion of AH1-specific CD8+ T cells and regulatory CD4+ T cell are shown also for matching TDLNs. **(b)** Composition of the TDLNs in WEHI-164 and CT26 tumor-bearing mice, including the CD8:CD4 ratio

Figure 7.5.: (continued)**(c)** Phenotype of the CD8+ T cells and AH1-specific CD8+ T cells in CD26 tumor-bearing mice from different treatment groups. The phenotype was assessed based on the expression of CD62L, CD44 and the exhaustion markers CD39 and PD-1. The data represents individual values, means and standard deviations. Statistical evaluations were performed using a regular two-way ANOVA followed by a Tukey's multiple comparison test using GraphPad Prism v8.4.1 [* $p < 0.05$, ** $p < 0.01$, *** $p < 0.001$, **** $p < 0.0001$] (TIL: tumor-infiltrating leukocyte, NKT: natural killer T cell, NK: natural killer cell, APC: antigen-presenting cell, Treg: regulatory T cell, TDLN: tumor-draining lymph node, Teff: effector T cell [CD44+CD62L-], Tcm: central memory T cell [CD44+CD62L+], Tnaive: naïve T cell [CD44-CD62L+])

in the combination treatment group were rendered tumor-free, as evidenced both by MRI analysis and by survival data (Figure 7.4e).

In order to analyze the tumor infiltrating leukocytes, mice were sacrificed 48 h after the second cycle of injections. Tumors and tumor-draining lymph nodes were excised, homogenized and stained for analysis by flow cytometry. CT26 tumors were found to be highly infiltrated by lymphocytes, in keeping with previous reports,[607–609] while WEHI-164 lesions were rather immunologically "cold" (Figure 7.5a). The proportion of CD8+ T cells, specific to AH1 (a retroviral antigen, which plays a dominant role for the rejection of tumors implanted in BALB/c mice[302,561]) was higher in CT26 tumors (Figure 7.5a). Treatment with F8-4-1BBL led to a significant increase in intratumoral CD3+ T cell density in both models, but the proportion of CD4+ or CD8+ T cells did not vary substantially. No difference was observed in terms of regulatory T cell (Treg) density (Figure 7.5a). In keeping with what was previously reported for other studies,[610] the proportion of AH1-specific CD8+ T cells did not vary substantially as a result of pharmacological treatment (Figure 7.5a). Treatment with F8-4-1BBL led to a decrease in CD3+ and CD4+ T cells in the tumor-draining lymph nodes with a concomitant increase of antigen-presenting cells in CT26 tumor-bearing mice (but not in WEHI-164) (Figure 7.5b). An increase in the proportion of effector T cells (CD44+CD62L-) was observed among the AH1-specific CD8+ T cells in the tumor-draining lymph nodes (Figure 7.5c). Virtually all tumor-infiltrating CD8+ T cells were positive for the exhaustion markers PD-1 and CD39 (Figure 7.5c).[611,612] The gating strategy used in the study can be found in Figure C.9. Collectively, the markers used in this study did not detect a phenotypic change in tumor-infiltrating T cells, but an increase in effector T cells was observed for the AH1-specific CD8+ T cell population in tumor-draining lymph nodes as a result of F8-4-1BBL treatment.

7.3. Discussion

We have described the development of an antibody-cytokine fusion protein targeted to the tumor neovasculature, featuring an engineered murine homodimeric 4-1BBL moiety as immunostimulatory payload. Some formats were completely inactive in solution while others retained a low biological activity in the absence of antigen. The low constitutive biological activity of the formats featuring two single-chain trimeric ligands could be due to a residual receptor clustering triggered by hexameric 4-1BBL. The size exclusion profile of format **7** revealed the presence of a minor fraction of aggregated protein, which could potentially trigger some downstream signaling. However, since it was not possible to remove the aggregated fraction, this hypothesis could not be experimentally proven. Subtle variations in the molecular format were observed to not only lead to a different performance *in vitro* but also affected the biodistribution properties *in vivo*. Both preferential localization in the tumor and antigen-dependent gain in activity are prerequisites for restricting the activity of the fusion protein to the site of disease. The selected format **5** was inactive in solution but regained activity upon clustering on the antigen. Favorable tumor-targeting results and potent tumor growth inhibition were observed *in vivo*, making F8-4-1BBL a promising prototype for the development of next-generation immunocytokines with antigen-dependent activation properties.

4-1BB, the receptor for 4-1BBL has been recognized as important target for the immunotherapy of cancer, as this member of the TNF receptor superfamily delivers costimulatory signals to activated cytotoxic T cells.[427] The first 4-1BB agonistic antibody, Urelumab, showed promising anti-cancer activity in preclinical models, but unfortunately revealed substantial hepatotoxicity in clinical trials.[613] The hepatic toxicity was mainly due to the activation of liver Kupffer cells and monocytes, leading to a massive infiltration by T cells.[613,614] Efforts are being made to develop 4-1BB agonists with more favorable toxicity profiles that retain potent costimulatory capacities.[451,452,470,471] In addition to the optimization of anti-4-1BB immunoglobulins,[451,452] various formats of targeted 4-1BB agonists are being investigated. Bispecific antibodies capable of simultaneous recognition of 4-1BB and of tumor-associated antigens (e.g., EGFR or CEA) have been developed and tested in preclinical models of cancer, with encouraging results.[470,471] Novel formats of targeted 4-1BB agonists have recently been considered for clinical development. A FAP-targeted immunocytokine with trimeric single-chain 4-1BBL has recently started phase I clinical testing in cancer patients.[311] A fusion protein of Trastuzumab with a 4-1BB-specific anticalin™ has been described,[458] which had shown antigen-dependent modulation of 4-1BB agonistic activity *in vitro* and which has recently started clinical trials.[458]

The search for antibody-cytokine products with "activity-on-demand" has been recognized as an important research goal, in order to generate products with improved activity and

safety profiles.[485,506] One possible strategy features the use of cytokine-binding polypeptides, acting as proteolytically-cleavable inhibitory moieties.[499] Fusing cytokines at the C-terminal end of the IgG light chain may restrict conformational changes in the hinge region and slightly modulate cytokine activity upon antibody binding to the cognate antigen.[485] The attenuation of cytokine potency by targeted mutagenesis has been considered as a strategy to increase the dose of antibody-cytokine fusion proteins[489] or to conditionally activate tumor cells which express both a tumor-associated antigen and a cytokine receptor (e.g., IFNα receptor) on their surface.[487,488] In addition, the targeted reconstitution of antibodies fused with "split-cytokine" moieties (i.e., subunits of heterodimeric cytokines that can reassemble at the tumor site) has been reported. Until now, the performance of that approach has been limited by the fact that the cytokine subunits used in the study (e.g., the p35 chain of IL12) retained biological activity.[493]

Most ligands of the TNF superfamily including human 4-1BBL form homotrimers instead of homodimers as is the case for murine 4-1BBL.[340] However, the activation of receptors of the TNF superfamily requires higher-order multimerization. The approach described in this article may be generally applicable to members of the TNF superfamily,[492] if we were able to generate stable homodimers as payloads for antibody fusion. Alternative approaches may involve bispecific antibodies,[453,615] the modular use of small protein domains[458,616] or of chemically-modified bicyclic peptides.[617] Members of the TNF receptor superfamily are particularly suited for cooperative activation strategies in view of their homotrimeric structure and clustering-driven activation properties.[343,505,531] The development of immunotherapeutics with "activity-on-demand" for monomeric cytokines may be more challenging, as one cannot rely on protein assembly for the reconstitution of biological activity.

7.4. Materials and Methods

Cell lines The murine cytotoxic T cell line CTLL-2 (ATCC® TIB-214), the murine F9 teratocarcinoma cell line (ATCC® CRL-1720), the murine WEHI-164 fibrosarcoma cell line (ATCC® CRL-1751) and the murine CT26 colon carcinoma cell line (ATCC® CRL-2638) were obtained from ATCC. The MC38 colon carcinoma cell line was a kind gift from Prof. Onur Boyman (Department of Immunology, University Hospital Zurich, Zurich, Switzerland). The cells were expanded and stored as cryopreserved aliquots in liquid nitrogen. The CTLL-2 cells were grown in RPMI 1640 (Gibco, #21875034) supplemented with 10% FBS (Gibco, #10270106), 1 X antibiotic-antimycoticum (Gibco, #15240062), 2 mM ultraglutamine (Lonza, #BE17-605E/U1), 25 mM HEPES (Gibco, #15630080), 50 µM β-mercaptoethanol (Sigma Aldrich) and 60 U/mL human IL-2 (Proleukin, Roche Diagnostics). The F9 teratocarcinoma cells were grown in DMEM (Gibco, high glu-

cose, pyruvate, #41966-029) supplemented with 10% FBS (Gibco, #10270106) and 1 X antibiotic-antimycoticum (Gibco, #15240062) in flasks coated with 0.1% gelatin (Type B from Bovine Skin, Sigma Aldrich, #G1393). The WEHI-164 fibrosarcoma and the CT26 colon carcinoma were grown in RPMI 1640 (Gibco, #21875034) supplemented with 10% FBS (Gibco, #10270106) and 1 X antibiotic-antimycoticum (Gibco, #15240062). The MC38 colon carcinoma cells were grown in Advanced DMEM (Gibco, #12491915) supplemented with 10% FBS (Gibco, #10270106), 1 X antibiotic-antimycoticum (Gibco, #15240062) and 2 mM ultraglutamine (Lonza, #BE17-605E/U1). GL-261 cells were obtained from the National Cancer Institute (Frederick, Maryland, USA) and cultured as previously described.[618,619] The cells were passaged at the recommended ratios and never kept in culture for more than one month.

Mice Eight weeks old female C57BL/6, Balb/c and 129/Sv mice were obtained from Janvier. After at least one week of acclimatization, 10^7 F9 cells, $2.5{\cdot}10^6$ WEHI-164 cells, $4{\cdot}10^6$ CT26 or 10^6 MC38 cells were subcutaneously implanted into the right flank. The tumor size was monitored daily by caliper measurements and the volume was calculated using the formula [length x width x width x 0.5]. For mouse studies mouse models of glioblastoma, eight weeks old female C57BL/6 mice were purchased from Charles River Laboratories (Sulzfeld, Germany). Intracranial tumor cell implantation has been previously described.[618] The animal experiments were carried out under the project license ZH04/2018 (subcutaneous tumor models) and ZH73/2018 (glioblastoma) granted by the Veterinäramt des Kantons Zürich, Switzerland, in compliance with the Swiss Animal Protection Act (TSchG) and the Swiss Animal Protection Ordinance (TSchV).

Cloning A soluble single-chain trimer of murine 4-1BBL was designed by linking the TNF homology domain (amino acids 139 – 309) with a single glycine as a linker. The genetic sequence was ordered from Eurofins Genomics. The sequence was introduced into a vector encoding the F8 in a diabody format by Gibson Isothermal Assembly. To clone the single-chain variable Fragment (scFv) linked to the 4-1BBL monomer, the genetic sequence encoding the diabody was replaced by the sequence encoding the scFv and two domains of 4-1BBL were removed by PCR followed by blunt-end ligation. Additional base pairs of 4-1BBL were added to the 4-1BBL sequence by PCR followed by blunt-end ligation. The IgG fusion proteins were cloned by fusing the 4-1BBL sequence to the sequence of the antibody in the IgG format by PCR before introducing it into an appropriate vector by restriction cloning. The protein sequences are provided in Figure C.1.

Protein production Proteins were produced by transient transfection of CHO-S cells and purified by protein A affinity chromatography as described previously.[257,258,278] Qual-

ity control of the purified products included SDS-PAGE and size exclusion chromatography using an Äkta Pure FPLC system (GE Healthcare) with a Superdex S200 10/300 increase column at a flow rate of 0.75 mL/min (GE Healthcare) (Figure 7.1 & Figure C.2).

Binding measurements by Surface Plasmon Resonance To evaluate the binding kinetics of the F8 antibody fragment to EDA, a CM5 sensor chip (GE Healthcare) was coated with approximately 500 resonance units of an EDA-containing recombinant fragment of fibronectin. The measurements were carried out with a Biacore S200 (GE Healthcare). The contact time was set to 3 min at a flow rate of 20 µL/min followed by a dissociation for 10 min and a regeneration of the chip using 10 mM HCl.

Binding measurements by Flow Cytometry In order to measure the binding of the 4-1BBL moiety to cells expressing 4-1BB, CTLL-2 cells were incubated with varying concentrations of the fusion proteins for 1 h. The bound protein was detected by addition of an excess of AlexaFluor488-labelled protein A (Thermofisher, #P11047) and subsequent measurement of the fluorescence using a Cytoflex Flow Cytometer. The mean fluorescence was normalized and the resulting binding curve was fitted using the the [Agonist] vs. response (three parameters) fit of the GraphPad Prism 7.0 a software to estimate the functional K_D.

NF-κB response assay The development of the CTLL-2 reporter cell line is described elsewhere.[569] CTLL-2_NF-κB reporter cells were starved by washing the cells twice with prewarmed HBSS (Gibco, #14175095) followed by growth in the absence of IL-2 for 6 - 9 h in RPMI 1640 (Gibco, #21875034) medium supplemented with 10% FBS (Gibco, #10270106), 1 X antibiotic-antimycoticum (Gibco, #15240062), 2 mM Ultraglutamine (Lonza, #BE17-605E/U1), 25 mM HEPES (Gibco, #15630080) and 50 µM β-mercaptoethanol (Sigma Aldrich) in order to reduce the background signal. To coat the wells with antigen, 100 µL 100 nM 11-A-12 fibronectin in phosphate buffered saline (PBS) was added to each well and the plate was incubated at 37°C for 90 min. Cells were seeded in 96-well plates (50,000 cells/well) and growth medium containing varying concentrations of the antibody-cytokine conjugate was added. The cells were incubated at 37°C, 5% CO_2 for several hours. To assess luciferase production, 20 µL of the supernatant was transferred to an opaque 96-well plate (Perkin-Elmer, Optiplate-96, white, #6005290) and 80 µL 1 µg/mL Coelenterazine (Carl Roth AG, #4094.3) in phosphate buffered saline (PBS) was added. Luminescence at 466 nm was measured immediately. The relative luminescence was calculated by dividing the obtained results by the results obtained when no inducer was added. The data was fitted using the [Agonist] vs. response (three parameters) fit of the GraphPad Prism 7.0 a software to estimate the EC_{50}.

Quantitative biodistribution studies Quantitative biodistribution experiments were carried out as described previously.[11] Briefly, 8 weeks old female 129/Sv mice were injected subcutaneously in the right flank with 10^7 F9 teratocarcinoma cells. The tumor size was measured daily with a caliper and the volume was calculated using the formula [volume = length x width x width x 0.5]. When the tumors reached a volume of 100 – 300 mm^3, 10 µg of radio-iodinated protein was injected into the lateral tail vein. The mice were sacrificed 24 h after the injection and the organs were excised and weighed. The radioactivity of the different organs was measured (Packard Cobra II Gamma Counter) and expressed as percentage of injected dose per gram of tissue (%ID/g ± SD, n = 3).

***Ex vivo* detection of fluorescently labelled immunocytokines** For fluorescent labelling, the proteins were resuspended in a 0.1 M sodium carbonate buffer at pH 9.1 and an excess of Fluorescein Isothiocyanate (FITC) was added. The reaction was carried out overnight at 4°C. The labelled proteins were separated from unconjugated FITC by PD-10. Approximately 100 µg of fluorescently-labelled protein was injected into the lateral tail-vein of tumor-bearing mice. The mice were sacrificed 24 h after the injection. The organs were excised and embedded in NEG-50 cryoembedding medium (ThermoFisher, Richard-Allan-Scientific, #6502) prior to freezing. For staining, 8 µm cryosections were fixed in acetone and incubated with goat-anti-mouse CD31 (R&D system, #AF3628, 1:200) and rabbit-anti-FITC (Biorad, #4510-7804) followed by donkey-anti-goat-AF594 (Invitrogen, #A11058) and donkey-anti-rabbit-AF488 (Invitrogen, #A21206). Images were acquired using a Zeiss Axioscope 2 mot plus with an Axiocam 503 camera at a 200 X magnification in the RGB mode. The images were processed using the software ImageJ v1.52k setting the thresholds for the red channel to 14-80 and the green channel to 15 - 100.

Therapy studies in subcutaneous tumor models After the subcutaneous implantation of the tumor cells into the right flank of 8 weeks old female mice, the tumor size was monitored by caliper measurements on a daily basis [volume = length x width x width x 0.5]. In the preventive setting, the therapy was started when the tumor reached a volume of 40 mm^3 and for the therapeutic setting, the therapy was started when the tumors reached a volume of 75 – 100 mm^3. The mice were grouped in order to obtain groups of similar average tumor size (n = 5-6). The mice either received 100 µL Saline (PBS, Gibco, #1010023), 500 µg F8(scFv)-4-1BBL, 200 µg αPD-1 (BioXCell, clone 29F.1A12) or a combination of the checkpoint inhibitor and the immunocytokine. For the combination treatment, the checkpoint inhibitor was administered one day prior to the immunocytokine. The therapeutic agents were administrated every second day in a total of three cycles intravenously into the lateral tail vein. The animals were sacrificed if the tumor

diameter exceeded 15 mm or when the tumor started to ulcerate. Some cured mice were rechallenged by the subcutaneous injection of WEHI 164 or CT26 tumor cells after being tumor-free for at least 4 weeks. Statistical evaluations were done using a standard two-way ANOVA followed by the Tukey's multiple comparison test with GraphPad Prism v8.4.1.

Magnetic resonance imaging Coronal T2-weighted MRI images at day 12 after tumor implantation were acquired using Paravision 6.0 (Bruker BioSpin) on a 4.7 T small animal magnetic resonance imager (Pharmascan; Bruker Biospin, Ettlingen, Germany). Mean ± SD of the tumor perimeter in mm at the maximum circumference were determined using the Medical Image Processing, Analysis, and Visualization (MIPAV) software (https://mipav.cit.nih.gov/). Kaplan Meier survival analysis was performed to assess survival differences among the treatment groups and p values were calculated with Gehan-Breslow-Wilcoxon test. Significance was tested at *$p < 0.05$ and **$p < 0.01$.

Analysis of tumor-infiltrating lymphocytes by flow cytometry The mice were sacrificed 48 h after the second therapy cycle. The tumor-draining lymph nodes as well as the tumor were excised. A single-cell suspension of the tumor was obtained by digesting it in RPMI 1640 supplemented with 1 mg/mL collagenase II and 100 µg/mL DNase I for 30 min at 37°C. After the digestion, the suspension was passed through a 70 µm cell strainer. If necessary, the red blood cells were removed using a red blood cell lysis buffer (Roche). The lymph nodes were smashed on a 70 µm cell strainer and washed with PBS. For cell surface staining, cells were incubated with a mix of suitable antibodies: αCD3-APC/Cy7 (Biolegend, #100222), αCD4-APC (Biolegend, #100412), αCD8-FITC (Biolegend, #100706), αNK1.1-PE (Biolegend, #108708), αCD62L-BV421 (Biolegend, #104436), αCD44-APC/Cy7 (Biolegend, #103028), αMHCII(IA/IE)-BV421 (Biolegend, #107631), αPD-1-BV421 (Biolegend, #109121) and αCD39-APC (Biolegend, #143809). After staining of the cell surface markers, the cells were stained with 7-AAD (Biolegend) for live/dead discrimination. For intracellular staining, the cells were first stained with Zombie Red (SigmaAldrich) and then the cell surface stain was performed. The cells were fixed and permeabilized using the eBioscienceTM FoxP3/Transcription Factor Staining Buffer Set (Thermofisher, #00-5523-00) according to the manufacturer's instructions. The fluorescence was measured using a Cytoflex Flow Cytometer and the data was evaluated using the FlowJo software. The gating strategy is depicted in Figure C.9. Statistical evaluations were done using a regular two-way ANOVA followed by a Tukey's multiple comparison test or a regular one-way ANOVA followed by a Sidak's multiple comparison test in GraphPad Prism v8.4.1.

Acknowledgements

Financial support from the ETH Zürich, the Swiss National Science Foundation (grant number 310030_182003/1) and the European Research Council (ERC) under the European Union's Horizon 2020 research and innovation program (grant agreement 670603) is gratefully acknowledged. The authors gratefully acknowledge the support of the Scientific Center for Optical and Electron Microscopy (ScopeM) of the ETH Zurich. In addition, Sabrina Müller and Fiona Amman are gratefully acknowledged for their technical assistance especially for the protein production. The authors would also like to thank Lisa Nadal for her help with some immunofluorescence stainings.

Author contributions

D.N. and J.M. designed and planned the study. J.M. performed most of the experiments. M.S. helped with the biodistribution studies with radiolabelled proteins, designed the infiltrate analysis and helped to perform the experiment. A.V. coordinated immunohistochemical studies. T.W. and M.W. organized and performed the studies in glioblastoma. J.M. prepared the figures. D.N. and J.M. wrote the manuscript.

Competing interests

Dario Neri is a cofounder and shareholder of Philogen SpA (Siena, Italy), the company that owns the F8 and the L19 antibodies. No potential conflicts of interest were disclosed by the other authors.

Data availability statement

All data is included in the manuscript and supporting information. The DNA sequences encoding the fusion proteins developed in this studies are available via GenBank (accession numbers: MW086510, MW086511, MW086512, MW086513, MW086514, MW086515, MW086516, MW086517, MW086518, MW086519, MW086520)

8. Conclusion and Outlook

The development of immunocytokines with tumor-restricted biological activity has been recognized as important research goal for the development of next-generation cytokine products with improved safety profiles.[485,506] The requirement for higher-order receptor clustering by ligands of the TNF superfamily for productive signalling,[343,505] opens the possibility to develop targeted agonists which exhibit antigen-dependent biological activity. For instance, antibody fusion proteins featuring monomeric or dimeric agonists could be developed which are inactive in solution but regain potent biological activity upon antigen-binding through the antibody moiety.[402,458,620] Several members of the TNF superfamily have been identified as promising targets for cancer immunotherapy, especially in combination with immune checkpoint inhibitors.[4,5]

In this work, neovasculature-targeted fusion proteins featuring three members of the TNF superfamily were designed, produced and tested *in vitro* as well as *in vivo*. In order to facilitate the evaluation of the *in vitro* bioactivity, a universal reporter cell assay was developed as described in chapter 4. The cell lines developed for this assay could be used for the *in vitro* bioactivity evaluation of various cytokines that are important for cancer immunotherapy without the need to establish dedicated assays for each cytokine.[569] In addition, the bioactivity assay could be used to screen for protein variants with antigen-dependent biological activity.[569]

The F8-CD40L fusion proteins described in chapter 5 showed promising *in vitro* characteristics, but failed to accumulate in the tumor in a preclinical model of cancer. Since attempts to engineer the fusion protein for better tumor-targeting characteristics were not successful, the project was not further pursued. Similarly, a fusion protein featuring wild-type GITRL failed to accumulate in the tumor due to glycosylation-dependent clearance of the protein as described in chapter 6. In this case, engineering of an aglycosylated variant was successful and a fusion protein with improved tumor-targeting properties could be produced. However, the aglycosylated protein failed to elicit an anti-tumor immune response both alone and in combination with PD-1 blockade. By contrast, a fusion protein featuring 4-1BBL as a payload showed both promising tumor-targeting properties and potent anti-tumor activity in several mouse models of cancer as described in chapter 7. In addition, the selected F8-4-1BBL fusion protein conditionally regained *in vitro* bioactivity in the presence of immobilized antigen ("activity on demand").

While this work cumulated in the development of a prototype of an immunocytokine with "activity on demand", it also raised a number of questions. The most important question related to chapter 5 is why the F8-CD40L fusion proteins failed to accumulate selectively in the tumor. This question is particularly interesting also in light of the

findings of Hemmerle *et al.* who demonstrated strikingly different biodistribution profiles of molecularly similar fusion proteins featuring ligands of the TNF superfamily.[507] The answer to this question will guide the development of the next generation of targeted CD40 agonists. If CD40-mediated peripheral trapping prevented the accumulation of F8-CD40L, a prodrug approach as described in section 3.5.4 could be valuable for the development of safer and more efficacious CD40 agonists. By contrast, if the main trapping mechanism is related to protein *N*-glycosylation, non-ligand based CD40 agonists such as bispecific antibodies could be used. An additional advantage of engineered binders is that they are amenable to fine-tuning of the binding affinity and epitope selection, which could be essential for the development of novel agonists with "activity on demand" properties. The findings from the project focused on targeting GITRL to the tumor neovasculature essentially raise questions about the potential of GITRL for cancer immunotherapy. While it is possible that the engineered F8-GITRL fusion protein developed in this study failed to accumulate at a sufficiently high dose in the tumor to elicit an anti-tumor response, the results of recent clinical trials raise reasonable doubts about the benefit of GITR agonists in a clinical setting.[412,414,419,423,563,568]

The impressive results obtained with F8-4-1BBL in several mouse models of cancer (chapter 7) including a hard-to-treat orthotopic model of glioblastoma[304,618,619] and the promising results obtained from clinical trials with other 4-1BB agonists[459] provide a rationale for further development of F8-4-1BBL towards clinical use. The greatest challenge in the development of F8-4-1BBL fusion proteins for clinical development will lie in the design of a dimeric fusion protein which mirrors the "activity on demand" properties of the murine fusion protein described in this study. In addition, as is evidenced by the high doses administered of other 4-1BB agonists such as PRS-343[459] and RO7227166,[460] high yields of the fusion protein will be necessary to overcome economical hurdles in product development. For instance, PRS-343 was tested in a xenograft model in human PBMC-reconstituted mice and lead to tumor regressions at a dose of 5 mg/kg.[458] By contrast, objective responses were observed in a phase I clinical trial at doses of 8 mg/kg and more.[459] Similarly, RO7227166 was administered at doses of 3 mg/kg in combination with bispecific antibodies to human stem cell engrafted mice bearing human xenograft tumors,[311] while patients received doses of up to 2000 mg.[460] If a similar dose factor from mouse to man can be assumed when extrapolating from a syngeneic murine setting to a fully human setting, doses of more than 25 mg/kg might be required of F8-4-1BBL. Therefore, careful studies on the minimal necessary dose will be essential in addition to exploring different molecular formats that can yield the required quantities of therapeutic agent within an economically reasonable setting.

9. Acknowledgements

Research is never a one-man-show and I was privileged to be surrounded by outstanding scientists and wonderful people that supported me in my work. Help and support from other people came in many different flavours. While advice based on previous experience is the most straightforward input to solve a problem, discussions and critical questions are essential to move forward and improve a project. In addition, a great environment during work and free time are important to maintain the motivation to drive successful research.

I am infinitely grateful to **Prof. Dr. Dario Neri** for being a wonderful PhD supervisor. By "playing the devil's advocate" he taught me to critically reflect my work and to challenge my understanding of proteins, immunotherapy and cancer. I could benefit tremendously from his impressive knowledge and vast experience in the field. Also the other members of my PhD committee, **Prof. Dr. Cornelia Halin, Prof. Dr. Jonathan Hall** and **Prof. Dr. Peter Kast** greatly supported me both with innovative ideas and interesting questions and I am very grateful to them for investing time in the annual meetings on my project. In addition, I thank Prof. Dr. Cornelia Halin for acting as my co-examiner.

Many day-to-day problems could be solved efficiently thanks to my great colleagues in the lab, who were always ready to give me advice and help if needed. I am especially grateful to **Marco Stringhini** for the many chats, valuable advice and helpful discussions. I am still amazed by how many problems got solved through spontaneous discussions with colleagues. For instance, many technical problems were solved thanks to brief chats with **Dr. Emanuele Puca**, who was always ready to give valuable advice. Similarly, one of the many discussions with **Dr. Christian Pellegrino** during work in the cell culture sparked the development of the universal bioassay leading to my first publication.

Especially in the beginning of my PhD, I received a lot of precious help from the more experienced members of the lab, especially **Dr. Barbara Ziffels**, who supported me tremendously during my first *in vivo* studies and also **Dr. Patrizia Murer**, **Dr. Davor Bajic** and **Dr. Jonathan Kiefer**. Throughout my PhD, other former members of the group such as **Dr. Samuele Cazzamalli** and **Dr. Roberto De Luca** never failed to provide valuable advice. Thanks to many fruitful collaborations with them and their PhD students such as **Sheila Dakhel**, **Riccardo Corbellari**, **Jacopo Millul** and **Baptiste Gouyou**, I was able to gain insight into additional interesting projects.

In addition to the many collaborations with researchers at Philochem AG, I was privileged to be able to collaborate with **Dr. Tobias Weiss** to study the effect of F8-4-1BBL on

glioblastoma. I am immensely grateful that this experiment was possible within a very short period of time despite his extremely busy schedule and huge workload.

A great value of our group is the interdisciplinarity of the team. I could benefit tremendously from discussions with chemists such as **Dr. Marco Catalano**, who not only inspired me to think in numbers, magnitudes and chemical interactions, but with whom I also lead many discussions about philosophy and life. Also **Dr. Gabriele Bassi** sparked many interesting discussions thanks to his insightful questions.

I have always had a passion for teaching and I was very lucky to have been able to accompany three outstanding students during part of their educational journey. My former master student **Itzel Astiazaran Rascon** proved to be an extremely interested student who showed an admirable level of perseverance to make her project work. In addition, I was priviledged to be the supervisor of two lovely apprentices, **Fiona Ammann** and **Sabrina Müller**. I could learn a lot from all three of them and I am immensely grateful for all their precious help for my projects.

In addition, I would like to thank **Pia Steinbak** for all her administrative support and **Dr. Jörg Scheuermann** for all his help and day-to-day management of the laboratory.

Our group has an outstanding culture of friendliness and helpfulness. The positive atmosphere of mutual respect and collegiality makes everyone feel at home immediately, drives the motivation to work hard and thus tremendously contributes to research success. I am very grateful for all the friendly smiles and kind words I got from all the above-mentioned people and also my other colleagues including **Abdullah El-Sayed**, **Diana Tintor**, **Lisa Nadal**, **Laura Volta**, **Louise Plais**, **Dr. Michael Mortensen**, **Michelle Keller**, **Dr. Nicholas Favalli**, **Dr. Philipp Probst**, **Sebastian Oehler**, **Tiziano Ongaro** and **Dr. Yuichi Onda**.

I believe that the path towards a successful PhD is paved long before the first day of the doctorate. Thanks to my fantastic master's thesis supervisor **Dr. Tsvetan Kardashliev** I was extremely well prepared to start my own independent research. I continue to benefit from the many helpful advice I got from him and from everything I learned during my master's thesis.

I also received wonderful support from many people outside the laboratory. Most importantly, I would like to thank my wonderful partner **Andreas Zingg** for all his patience and kind support. Being a fantastic scientist, he never failed to offer me valuable advice or to spark an interesting discussion. Moreover, with his kindness and patience, he always motivated me to persevere. I greatly appreciate how we share our passion not only for science, but also for travelling, hiking and photography.

I am very grateful to my friends for all their support during high school and university and for the many unforgettable moments we spent together. Thanks to my best friends

from university, **Salome Püntener** and **Florin Isenrich**, I not only managed to pass university exams but I also had a lot of fun. Likewise, I am also very grateful to my wonderful friends from high school **Jlonca Gosztonyi**, **Mengda Shi**, **Christina Leistner**, **Carola Gloor**, **Michelle Notter** and **Fabienne Seiler**. We all chose very different paths after high school and it is always interesting to gain insight into a different field including music, arts and architecture.

Last but not least I am infinitely grateful to my family for all their support. Despite their non-scientific background they always showed interest in my work and tried to understand what problems I am dealing with. I appreciate very much how they are always there for me, cheer me up or provide a million reasons to laugh.

A. Supplementary material "Reporter Cell Line"

This section contains the supplementary data accompanying the publication ''A universal reporter cell line for bioactivity evaluation of engineered cytokine products" by J. Mock, C. Pellegrino & D. Neri published in Scientific Reports 10, 3234 (2020), reproduced with permission (Creative Commons Attribution 4.0 International License).

Supplementary Materials and Methods

SDS PAGE The proteins were diluted to 0.1 mg/mL and 4 µL Lämmli buffer (0.25 M Tris-HCl pH 6.8, 40% glycerol, 8% sodium dodecyl sulfate, 0.02% bromophenol blue) was added to 12 µL of the protein dilution. Reducing Lämmli buffer was prepared fresh by adding 20% β-mercaptoethanol to the non-reducing Lämmli buffer. The samples were incubated at 95°C for 5 min and then directly loaded onto a TruPAGE Precasd 4-12% gel (Sigma Aldrich, #PCG2003 or #PCG2007). The gel was run in TruPAGE TEA-Tricine buffer (Sigma Aldrich, #PCG3001) diluted according to the manufacturer's recommendations at 180 V, 110 mAmp for 1 h. Afterwards, the gel was rinsed with deionized water and stained for 1 h in Coomassie blue (2.4 g/L Brilliant blue, 24% methanol, 8% acetic acid). The gel was then destained in destaining solution (30% methanol, 10% acetic acid) for several hours at room temperature. Finally, the gel was left in deionized water at room temperature overnight to complete the destaining process.

Size exclusion chromatography For size exclusion chromatography, a Superdex 200 10/300 increase column (GE healthcare) was used together with an Äkta Pure FPLC machine (GE healthcare). The size exclusion chromatography was run in PBS at a speed of 0.75 mL/min.

a)

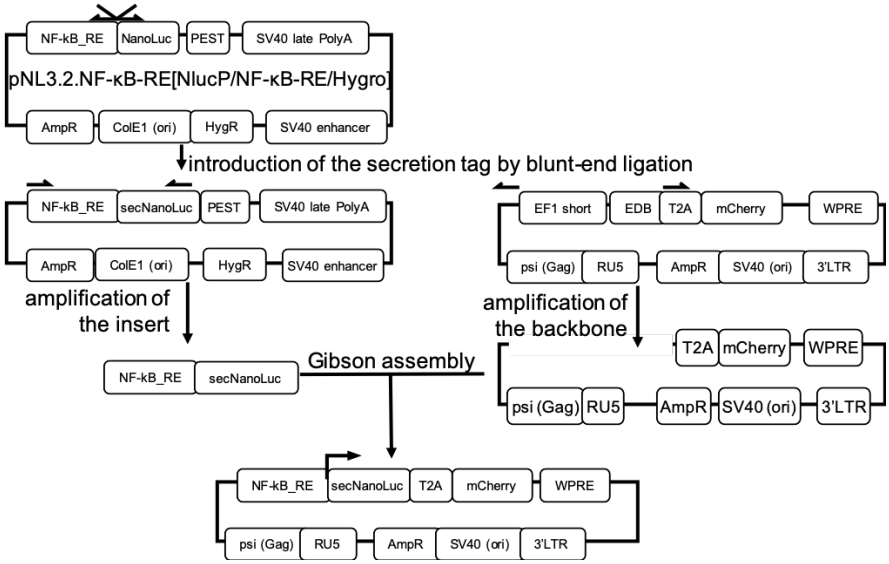

b)

NF-κB_RE-minimalPromoter-hIL6-secretionSignal-Nanoluc-T2A-mCherry

GGGAATTTCCGGGGACTTTCCGGGAATTTCCGGGGACTTTCCGGGAATTTCC-AGATCTGGCCTCG
GCGGCCAAGCTTAGACACT-AGAGGGTATATAATGGAAGCTCGACTTCCAG-CTTGGCAATCCGGT
ACTGTTGGTAAAGCCACC-ATGAACTCCTTCTCCACAAGCGCCTTCGGTCCAGTTGCCTTCTCCCTGGGCCT
GCTCCTGGTGTTGCCTGCTGCCTTCCCTGCCCCA-GTCTTCACACTCGAAGATTTCGTTGGGGACTGGCGAC
AGACAGCCGGCTACAACCTGGACCAAGTCCTTGAACAGGGAGGTGTGTCCAGTTTGTTTCAGAATCTCGGG
GTGTCCGTAACTCCGATCCAAAGGATTGTCCTGAGCGGTGAAAATGGGCTGAAGATCGACATCCATGTCAT
CATCCCGTATGAAGGTCTGAGCGGCGACCAAATGGGCCAGATCGAAAAAATTTTTAAGGTGGTGTACCCTG
TGGATGATCATCACTTTAAGGTGATCCTGCACTATGGCACACTGGTAATCGACGGGGTTACGCCGAACATG
ATCGACTATTTCGGACGGCCGTATGAAGGCATCGCCGTGTTCGACGGCAAAAAGATCACTGTAACAGGGAC
CCTGTGGAACGGCAACAAAATTATCGACGAGCGCCTGATCAACCCCGACGGCTCCCTGCTGTTCCGAGTAA
CCATCAACGGAGTGACCGGCTGGCGGCTGTGCGAACGCATTCTGGCG-GAGGGCAGAGGAAGTCTTCTAAC
ATGCGGTGACGTGGAGGAGAATCCCGGCCCT-ATGGTGAGCAAGGGCGAGGAGGATAACATGGCCATCAT
CAAGGAGTTCATGCGCTTCAAGGTGCACATGGAGGGCTCCGTGAACGGCCACGAGTTCGAGATCGAGGGCG
AGGGCGAGGGCCGCCCCTACGAGGGCACCCAGACCGCCAAGCTGAAGGTGACCAAGGGTGGCCCCCTGCCC
TTCGCCTGGGACATCCTGTCCCCTCAGTTCATGTACGGCTCCAAGGCCTACGTGAAGCACCCCGCCGACATC
CCCGACTACTTGAAGCTGTCCTTCCCCGAGGGCTTCAAGTGGGAGCGCGTGATGAACTTCGAGGACGGCGG
CGTGGTGACCGTGACCCAGGACTCCTCCCTGCAGGACGGCGAGTTCATCTACAAGGTGAAGCTGCGCGGCA
CCAACTTCCCCTCCGACGGCCCCGTAATGCAGAAGAAGACCATGGGCTGGGAGGCCTCCTCCGAGCGGATG
TACCCCGAGGACGGCGCCCTGAAGGGCGAGATCAAGCAGAGGCTGAAGCTGAAGGACGGCGGCCACTACGA
CGCTGAGGTCAAGACCACCTACAAGGCCAAGAAGCCCGTGCAGCTGCCCGGCGCCTACAACGTCAACATCA
AGTTGGACATCACCTCCCACAACGAGGACTACACCATCGTGGAACAGTACGAACGCGCCGAGGGCCGCCAC
TCCACCGGCGGCATGGACGAGCTGTACAAGTAA

Figure A.1.: cloning strategy and sequence of the reporter construct **(a)** outline of the cloning strategy **(b)** sequence of the reporter construct, primer binding sites are underlined

RU5-Psi (Gag)-EF1(short)-NF-κB_RE(response element)-minimal promoter (minP)-IL6 secretion tag-Nanoluc-T2A-mCherry-WPRE-3'LTR-SV40 ori-Ampicillin resistance

GCGCGTTTCGGTGATGACGGTGAAAACCTCTGACACATGCAGCTCCCGGAGACGGTCACAGCTTGTCTGTA
AGCGGATGCCGGGAGCAGACAAGCCCGTCAGGGCGCGTCAGCGGGTGTTGGCGGGTGTCGGGGCTGGCTT
AACTATGCGGCATCAGAGCAGATTGTACTGAGAGTGCACCATATGCGGTGTGAAATACCGCACAGATGCGT
AAGGAGAAAATACCGCATCAGGCGCCATTCGCCATTCAGGCTGCGCAACTGTTGGGAAGGGCGATCGGTGC
GGGCCTCTTCGCTATTACGCCAGCTGGCGAAAGGGGGATGTGCTGCAAGGCGATTAAGTTGGGTAACGCCA
GGGTTTTCCCAGTCACGACGTTGTAAAACGACGGCCAGTGCCAAGCTGACGCGTGTAGTCTTATGCAATAC
TCTTGTAGTCTTGCAACATGGTAACGATGAGTTAGCAACATGCCTTACAAGGAGAGAAAAAGCACCGTGCA
TGCCGATTGGTGGAAGTAAGGTGGTACGATCGTGCCTTATTAGGAAGGCAACAGACGGGTCTGACATGGAT
TGGACGAACCACTGAATTGCCGCATTGCAGAGATATTGTATTTAAGTGCCTAGCTCGATACAATAAACG GG
TCTCTCTGGTTAGACCAGATCTGAGCCTGGGAGCTCTCTGGCTAACTAGGGAACCCACTGCTTAAGCCTCAA
TAAAGCTTGCCTTGAGTGCTTCAAGTAGTGTGTGCCCGTCTGTTGTGTGACTCTGGTAACTAGAGATCCCTC
AGACCCTTTTAGTCAGTGTGGAAAATCTCTAGCA GTGGCGCCCGAACAGGGACCTGAAAGCGAAAGGGAAA
CCAGAGCTCTCTCGACGCAGGACTCGGCTTGCTGAAGCGCGCACGGCAAGAGGCGAGGGGCGGCGACTGGT
GAGTACGCCAAAAATTTTGACTAGCGGAGGCTAGAAGGAGAGAG ATGGGTGCGAGAGCGTCAGTATTAAG
CGGGGGAGAATTAGATCGCGATGGGAAAAAATTCGGTTAAGGCCAGGGGGAAAGAAAAAATATAAATTAAA
ACATATAGTATGGGCAAGCAGGGAGCTAGAACGATTCGCAGTTAATCCTGGCCTGTTAGAAACATCAGAAG
GCTGTAGACAAATACTGGGACAGCTACAACCATCCCTTCAGACAGGATCAGAAGAACTTAGATCATTATATA
ATACAGTAGCAACCCTCTATTGTGTGCATCAAAGGATAGAGATAAAAGACACCAAGGAAGCTTTAGACAAG
ATAGAGGAAGAGCAAAACAAAAGTAAGACCACCGCACAGCAA GCGGCCACTGATCTTCAGACCTGGAGGAG
GAGATATGAGGGACAATTGGAGAAGTGAATTATATAAATATAAAGTAGTAAAAATTGAACCATTAGGAGTA
GCACCCACCAAGGCAAAGAGAAGAGTGGTGCAGAGAGAAAAAAGAGCAGTGGGAATAGGAGCTTTGTTCCT
TGGGTTCTTGGGAGCAGCAGGAAGCACTATGGGCGCAGCGTCAATGACGCTGACGGTACAGGCCAGACAAT
TATTGTCTGGTATAGTGCAGCAGCAGAACAATTTGCTGAGGGCTATTGAGGCGCAACAGCATCTGTTGCAA
CTCACAGTCTGGGGCATCAAGCAGCTCCAGGCAAGAATCCTGGCTGTGGAAAGATACCTAAAGGATCAACA
GCTCCTGGGGATTTGGGGTTGCTCTGGAAAACTCATTTGCACCACTGCTGTGCCTTGGAATGCTAGTTGGA
GTAATAAATCTCTGGAACAGATTTGGAATCACACGACCTGGATGGAGTGGGACAGAGAAATTAACAATTAC
ACAAGCTTAATACACTCCTTAATTGAAGAATCGCAAAACCAGCAAGAAAAGAATGAACAAGAATTATTGGA
ATTAGATAAATGGGCAAGTTTGTGGAATTGGTTTAACATAACAAATTGGCTGTGGTATATAAAATTATTCA
TAATGATAGTAGGAGGCTTGGTAGGTTTAAGAATAGTTTTTGCTGTACTTTCTATAGTGAATAGAGTTAGG
CAGGGATATTCACCATTATCGTTTCAGACCCACCTCCCAACCCCGAGGGGACCCGACAGGCCCGAAGGAATA
GAAGAAGAAGGTGGAGAGAGAGACAGAGACAGATCCATTCGATTAGTGAACGGATCTCGACGGTATCGGTT
AACTTTTAAAAGAAAAGGGGGGATTGGGGGGTACAGTGCAGGGGAAAGAATAGTAGACATAATAGCAACAG
ACATACAAACTAAAGAATTACAAAAACAAATTACAAAATTCAAAATTTTATCGATACTAGT GGATCTGCGA
TC GCAGGTGCCAGAACATTTCTCTGGCCTAACTGGCCGGTACCTGAGCTCGCTAGC GGGAATTTCCGGGGA
CTTTCCGGGAATTTCCGGGGACTTTCCGGGAATTTCC AGATCTGGCCTCGGCGGCCAAGCTTAGACACT AG
AGGGTATATAATGGAAGCTCGACTTCCAG CTTGGCAATCCGGTACTGTTGGTAAAGCCACCATG AACTCCT
TCTCCACAAGCGCCTTCGGTCCAGTTGCCTTCTCCCTGGGCCTGCTCCTGGTGTTGCCTGCTGCCTTCCCTG
CCCCA GTCTTCACACTCGAAGATTTCGTTGGGGACTGGCGACAGACAGCCGGCTACAACCTGGACCAAGTC
CTTGAACAGGGAGGTGTGTCCAGTTTGTTTCAGAATCTCGGGGTGTCCGTAACTCCGATCCAAAGGATTGT
CCTGAGCGGTGAAAATGGGCTGAAGATCGACATCCATGTCATCATCCCGTATGAAGGTCTGAGCGGCGACC
AAATGGGCCAGATCGAAAAAATTTTTAAGGTGGTGTACCCTGTGGATGATCATCACTTTAAGGTGATCCTG
CACTATGGCACACTGGTAATCGACGGGGTTACGCCGAACATGATCGACTATTTCGGACGGCCGTATGAAGG
CATCGCCGTGTTCGACGGCAAAAAGATCACTGTAACAGGGACCCTGTGGAACGGCAACAAAATTATCGACG
AGCGCCTGATCAACCCCGACGGCTCCCTGCTGTTCCGAGTAACCATCAACGGAGTGACCGGCTGGCGGCTG
TGCGAACGCATTCTGGCG GAGGGCAGAGGAAGTCTTCTAACATGCGGTGACGTGGAGGAGAATCCCGGCC
CT

ATGGTGAGCAAGGGCGAGGAGGATAACATGGCCATCATCAAGGAGTTCATGCGCTTCAAGGTGCACATGGA
GGGCTCCGTGAACGGCCACGAGTTCGAGATCGAGGGCGAGGGCGAGGGCCGCCCCTACGAGGGCACCCAGA
CCGCCAAGCTGAAGGTGACCAAGGGTGGCCCCCTGCCCTTCGCCTGGGACATCCTGTCCCCTCAGTTCATGT
ACGGCTCCAAGGCCTACGTGAAGCACCCCGCCGACATCCCCGACTACTTGAAGCTGTCCTTCCCCGAGGGCT
TCAAGTGGGAGCGCGTGATGAACTTCGAGGACGGCGGCGTGGTGACCGTGACCCAGGACTCCTCCCTGCAG
GACGGCGAGTTCATCTACAAGGTGAAGCTGCGCGGCACCAACTTCCCCTCCGACGGCCCCGTAATGCAGAA
GAAGACCATGGGCTGGGAGGCCTCCTCCGAGCGGATGTACCCCGAGGACGGCGCCCTGAAGGGCGAGATCA
AGCAGAGGCTGAAGCTGAAGGACGGCGGCCACTACGACGCTGAGGTCAAGACCACCTACAAGGCCAAGAAG
CCCGTGCAGCTGCCCGGCGCCTACAACGTCAACATCAAGTTGGACATCACCTCCCACAACGAGGACTACACC
ATCGTGGAACAGTACGAACGCGCCGAGGGCCGCCACTCCACCGGCGGCATGGACGAGCTGTACAAGTAA GT
CGAC AATCAACCTCTGGATTACAAAATTTGTGAAAGATTGACTGGTATTCTTAACTATGTTGCTCCTTTTA
CGCTATGTGGATACGCTGCTTTAATGCCTTTGTATCATGCTATTGCTTCCCGTATGGCTTTCATTTTCTCCT
CCTTGTATAAATCCTGGTTGCTGTCTCTTTATGAGGAGTTGTGGCCCGTTGTCAGGCAACGTGGCGTGGTG
TGCACTGTGTTTGCTGACGCAACCCCCACTGGTTGGGGCATTGCCACCACCTGTCAGCTCCTTTCCGGGACT
TTCGCTTTCCCCCTCCCTATTGCCACGGCGGAACTCATCGCCGCCTGCCTTGCCCGCTGCTGGACAGGGGCT
CGGCTGTTGGGCACTGACAATTCCGTGGTGTTGTCGGGGAAATCATCGTCCTTTCCTTGGCTGCTCGCCTG
TGTTGCCACCTGGATTCTGCGCGGGACGTCCTTCTGCTACGTCCCTTCGGCCCTCAATCCAGCGGACCTTCC
TTCCCGCGGCCTGCTGCCGGCTCTGCGGCCTCTTCCGCGTCTTCGCCTTCGCCCTCAGACGAGTCGGATCTC
CCTTTGGGCCGCCTCCCCGCCT GGTACCTTTAAGACCAATGACTTACAAGGCAGCTGTAGATCTTAGCCAC
TTTTTAAAAGAAAAGGGGGGAC TGGAAGGGCTAATTCACTCCCAACGAAAATAAGATCTGCTTTTTGCTTG
TACTGGGTCTCTCTGGTTAGACCAGATCTGAGCCTGGGAGCTCTCTGGCTAACTAGGGAACCCACTGCTTA
AGCCTCAATAAAGCTTGCCTTGAGTGCTTCAAGTAGTGTGTGCCCGTCTGTTGTGTGACTCTGGTAACTAG
AGATCCCTCAGACCCTTTTAGTCAGTGTGGAAAATCTCTAGCA GTAGTAGTTCATGTCATCTTATTATTCA
GTATTTATAACTTGCAAAGAAATGAATATCAGAGAGTGAGAGGAACTTGTTTATTGCAGCTTATAATGGTT
ACAAATAAAGCAATAGCATCACAAATTTCACAAATAAAGCATTTTTTTCACTGCATTCTAGTTGTGGTTTGT
CCAAACTCATCAATGTATCTTATCATGTCTGGCTCTAGCT ATCCCGCCCCTAACTCCGCCCAGTTCCGCCCA
TTCTCCGCCCCATGGCTGACTAATTTTTTTTATTTATGCAGAGGCCGAGGCCGCCTCGGCCTCTGAGCTATT
CCAGAAGTAGTGAGGAGGCTTTTTTGGAGGCCTAGACTTTTGC AGAGACGGCCCAAATTCGTAATCATGGT
CATAGCTGTTTCCTGTGTGAAATTGTTATCCGCTCACAATTCCACACAACATACGAGCCGGAAGCATAAAGT
GTAAAGCCTGGGGTGCCTAATGAGTGAGCTAACTCACATTAATTGCGTTGCGCTCACTGCCCGCTTTCCAGT
CGGGAAACCTGTCGTGCCAGCTGCATTAATGAATCGGCCAACGCGCGGGGAGAGGCGGTTTGCGTATTGGG
CGCTCTTCCGCTTCCTCGCTCACTGACTCGCTGCGCTCGGTCGTTCGGCTGCGGCGAGCGGTATCAGCTCAC
TCAAAGGCGGTAATACGGTTATCCACAGAATCAGGGGATAACGCAGGAAAGAACATGTGAGCAAAAGGCCA
GCAAAAGGCCAGGAACCGTAAAAAGGCCGCGTTGCTGGCGTTTTTCCATAGGCTCCGCCCCCCTGACGAGC
ATCACAAAAATCGACGCTCAAGTCAGAGGTGGCGAAACCCGACAGGACTATAAAGATACCAGGCGTTTCCC
CCTGGAAGCTCCCTCGTGCGCTCTCCTGTTCCGACCCTGCCGCTTACCGGATACCTGTCCGCCTTTCTCCCT
TCGGGAAGCGTGGCGCTTTCTCATAGCTCACGCTGTAGGTATCTCAGTTCGGTGTAGGTCGTTCGCTCCAA
GCTGGGCTGTGTGCACGAACCCCCCGTTCAGCCCGACCGCTGCGCCTTATCCGGTAACTATCGTCTTGAGTC
CAACCCGGTAAGACACGACTTATCGCCACTGGCAGCAGCCACTGGTAACAGGATTAGCAGAGCGAGGTATG
TAGGCGGTGCTACAGAGTTCTTGAAGTGGTGGCCTAACTACGGCTACACTAGAAGGACAGTATTTGGTATC
TGCGCTCTGCTGAAGCCAGTTACCTTCGGAAAAAGAGTTGGTAGCTCTTGATCCGGCAAACAAACCACCGCT
GGTAGCGGTGGTTTTTTTGTTTGCAAGCAGCAGATTACGCGCAGAAAAAAAGGATCTCAAGAAGATCCTTT
GATCTTTTCTACGGGGTCTGACGCTCAGTGGAACGAAAACTCACGTTAAGGGATTTTGGTCATGAGATTAT
CAAAAAGGATCTTCACCTAGATCCTTTTAAATTAAAAATGAAGTTTTAAATCAATCTAAAGTATATATGAGT
AAACTTGGTCTGACAGTTACCA

ATGCTTAATCAGTGAGGCACCTATCTCAGCGATCTGTCTATTTCGTTCATCCATAGTTGCCTGACTCCCCGT
CGTGTAGATAACTACGATACGGGAGGGCTTACCATCTGGCCCCAGTGCTGCAATGATACCGCGAGACCCAC
GCTCACCGGCTCCAGATTTATCAGCAATAAACCAGCCAGCCGGAAGGGCCGAGCGCAGAAGTGGTCCTGCA
ACTTTATCCGCCTCCATCCAGTCTATTAATTGTTGCCGGGAAGCTAGAGTAAGTAGTTCGCCAGTTAATAGT
TTGCGCAACGTTGTTGCCATTGCTACAGGCATCGTGGTGTCACGCTCGTCGTTTGGTATGGCTTCATTCAGC
TCCGGTTCCCAACGATCAAGGCGAGTTACATGATCCCCCATGTTGTGCAAAAAAGCGGTTAGCTCCTTCGGT
CCTCCGATCGTTGTCAGAAGTAAGTTGGCCGCAGTGTTATCACTCATGGTTATGGCAGCACTGCATAATTCT
CTTACTGTCATGCCATCCGTAAGATGCTTTTCTGTGACTGGTGAGTACTCAACCAAGTCATTCTGAGAATAG
TGTATGCGGCGACCGAGTTGCTCTTGCCCGGCGTCAATACGGGATAATACCGCGCCACATAGCAGAACTTT
AAAAGTGCTCATCATTGGAAAACGTTCTTCGGGGCGAAAACTCTCAAGGATCTTACCGCTGTTGAGATCCA
GTTCGATGTAACCCACTCGTGCACCCAACTGATCTTCAGCATCTTTTACTTTCACCAGCGTTTCTGGGTGAG
CAAAAACAGGAAGGCAAAATGCCGCAAAAAAGGGAATAAGGGCGACACGGAAATGTTGAATACTCATACTC
TTCCTTTTTCA ATATTATTGAAGCATTTATCAGGGTTATTGTCTCATGAGCGGATACATATTTGAATGTATT
TAGAAAAATAAACAAATAGGGGTTCCGCGCACATTTCCCCGAAAAGTGCCACCTGACGTCTAAGAAACCATT
ATTATCATGACATTAACCTATAAAAATAGGCGTATCACGAGGCCCTTTCGTCTC

Figure A.2.: sequence of the lentiviral reporter plasmid pJM046; the important regions are highlighted in color

a) F8(dDb)-4-1BBL: $F8_{VH}$-*linker*-$F8_{VL}$-*linker*-4-1BBL-*linker*-4-1BBL-*linker*-4-1BBL

EVQLLESGGGLVQPGGSLRLSCAASGFTFSLFTMSWVRQAPGKGLEWVSAISGSGGSTYYADSVKGRFTISRDNSK
NTLYLQMNSLRAEDTAVYYCAKSTHLYLFDYWGQGTLVTVSS-*GGSGG* -EIVLTQSPGTLSLSPGERATLSCRASQ
SVSMPFLAWYQQKPGQAPRLLIYGASSRATGIPDRFSGSGSGTDFTLTISRLEPEDFAVYYCQQMRGRPPTFGQGT
KVEIK- *SSSSGSSSSGSSSSG* -ATTQQGSPVFAKLLAKNQASLCNTTLNWHSQDGAGSSYLSQGLRYEEDKKELVVD
SPGLYYVFLELKLSPTFTNTGHKVQGWVSLVLQAKPQVDDFDNLALTVELFPCSMENKLVDRSWSQLLLLKAGHR
LSVGLRAYLHGAQDAYRDWELSYPNTTSFGLFLVKPDNPWE- *G* -ATTQQGSPVFAKLLAKNQASLCNTTLNWHS
QDGAGSSYLSQGLRYEEDKKELVVDSPGLYYVFLELKLSPTFTNTGHKVQGWVSLVLQAKPQVDDFDNLALTVEL
FPCSMENKLVDRSWSQLLLLKAGHRLSVGLRAYLHGAQDAYRDWELSYPNTTSFGLFLVKPDNPWE- *G* -ATTQQ
GSPVFAKLLAKNQASLCNTTLNWHSQDGAGSSYLSQGLRYEEDKKELVVDSPGLYYVFLELKLSPTFTNTGHKVQ
GWVSLVLQAKPQVDDFDNLALTVELFPCSMENKLVDRSWSQLLLLKAGHRLSVGLRAYLHGAQDAYRDWELSYP
NTTSFGLFLVKPDNPWE

b) F8(scFv)-4-1BBL: $F8_{VH}$-*linker*-$F8_{VL}$-*linker*-4-1BBL

EVQLLESGGGLVQPGGSLRLSCAASGFTFSLFTMSWVRQAPGKGLEWVSAISGSGGSTYYADSVKGRFTISRDNSK
NTLYLQMNSLRAEDTAVYYCAKSTHLYLFDYWGQGTLVTVSS- *GGGGSGGGGSGGGG* -EIVLTQSPGTLSLSPGE
RATLSCRASQSVSMPFLAWYQQKPGQAPRLLIYGASSRATGIPDRFSGSGSGTDFTLTISRLEPEDFAVYYCQQMR
GRPPTFGQGTKVEIK- *SSSSGSSSSGSSSSG* -ATTQQGSPVFAKLLAKNQASLCNTTLNWHSQDGAGSSYLSQGLRY
EEDKKELVVDSPGLYYVFLELKLSPTFTNTGHKVQGWVSLVLQAKPQVDDFDNLALTVELFPCSMENKLVDRSW
SQLLLLKAGHRLSVGLRAYLHGAQDAYRDWELSYPNTTSFGLFLVKPDNPWE

c) F8(dDb)-GITRL: $F8_{VH}$-*linker*-$F8_{VL}$-*linker*-GITRL-*linker*-GITRL-*linker*-GITRL

EVQLLESGGGLVQPGGSLRLSCAASGFTFSLFTMSWVRQAPGKGLEWVSAISGSGGSTYYADSVKGRFTISRDNSK
NTLYLQMNSLRAEDTAVYYCAKSTHLYLFDYWGQGTLVTVSS- *GGSGG* -EIVLTQSPGTLSLSPGERATLSCRASQ
SVSMPFLAWYQQKPGQAPRLLIYGASSRATGIPDRFSGSGSGTDFTLTISRLEPEDFAVYYCQQMRGRPPTFGQGT
KVEIK- *SSSSGSSSSGSSSSG* -PTAIESCMVKFELSSSKWHMTSPKPHCVNTTSDGKLKILQSGTYLIYGQVIPVDKKY
IKDNAPFVVQIYKKNDVLQTLMNDFQILPIGGVYELHAGDNIYLKFNSKDHIQKNNTYWGIILMPDLP- *GGGSGGG*
-PTAIESCMVKFELSSSKWHMTSPKPHCVNTTSDGKLKILQSGTYLIYGQVIPVDKKYIKDNAPFVVQIYKKNDVLQ
TLMNDFQILPIGGVYELHAGDNIYLKFNSKDHIQKNNTYWGIILMPDLP- *GGGSGGG* -PTAIESCMVKFELSSSKWH
MTSPKPHCVNTTSDGKLKILQSGTYLIYGQVIPVDKKYIKDNAPFVVQIYKKNDVLQTLMNDFQILPIGGVYELHA
GDNIYLKFNSKDHIQKNNTYWGIILMPDLP

d) F8(scFv)-GITRL: $F8_{VH}$-*linker*-$F8_{VL}$-*linker*-GITRL

EVQLLESGGGLVQPGGSLRLSCAASGFTFSLFTMSWVRQAPGKGLEWVSAISGSGGSTYYADSVKGRFTISRDNSK
NTLYLQMNSLRAEDTAVYYCAKSTHLYLFDYWGQGTLVTVSS- *GGGGSGGGGSGGGG* -EIVLTQSPGTLSLSPGE
RATLSCRASQSVSMPFLAWYQQKPGQAPRLLIYGASSRATGIPDRFSGSGSGTDFTLTISRLEPEDFAVYYCQQMR
GRPPTFGQGTKVEIK- *SSSSGSSSSGSSSSG* -PTAIESCMVKFELSSSKWHMTSPKPHCVNTTSDGKLKILQSGTYLI
YGQVIPVDKKYIKDNAPFVVQIYKKNDVLQTLMNDFQILPIGGVYELHAGDNIYLKFNSKDHIQKNNTYWGIILMP
DLP

e) F8(scDb)-CD154: $F8_{VH}$-*linker*-$F8_{VL}$- *linker*- $F8_{VH}$-*linker*-$F8_{VL}$-*linker*-CD154-*linker*-CD154-*linker*-CD154

EVQLLESGGGLVQPGGSLRLSCAASGFTFSLFTMSWVRQAPGKGLEWVSAISGSGGSTYYADSVKGRFTISRDNSK
NTLYLQMNSLRAEDTAVYYCAKSTHLYLFDYWGQGTLVTVSS- *GGSGG* -EIVLTQSPGTLSLSPGERATLSCRASQ
SVSMPFLAWYQQKPGQAPRLLIYGASSRATGIPDRFSGSGSGTDFTLTISRLEPEDFAVYYCQQMRGRPPTFGQGT
KVEIK- *GGGGSGGGGSGGGGS* -EVQLLESGGGLVQPGGSLRLSCAASGFTFSLFTMSWVRQAPGKGLEWVSAISG
SGGSTYYADSVKGRFTISRDNSKNTLYLQMNSLRAEDTAVYYCAKSTHLYLFDYWGQGTLVTVSS- *GGSGG* -EIVL
TQSPGTLSLSPGERATLSCRASQSVSMPFLAWYQQKPGQAPRLLIYGASSRATGIPDRFSGSGSGTDFTLTISRLEPE
DFAVYYCQQMRGRPPTFGQGTKVEIK- *SSSSGSSSSGSSSSG* -QRGDEDPQIAAHVVSEANSNAASVLQWAKKGYY
TMKSNLVMLENGKQLTVKREGLYYVYTQVTFCSNREPSSQRPFIVGLWLKPSSGSERILLKANTHSSSQLCEQQSV
HLGGVFELQAGASVFVNVTEASQVIHRVGFSSFGLLKL- *GGGS* -QRGDEDPQIAAHVVSEANSNAASVLQWAKKG
YYTMKSNLVMLENGKQLTVKREGLYYVYTQVTFCSNREPSSQRPFIVGLWLKPSSGSERILLKANTHSSSQLCEQQ
SVHLGGVFELQAGASVFVNVTEASQVIHRVGFSSFGLLKL- *GGGS* -QRGDEDPQIAAHVVSEANSNAASVLQWAK
KGYYTMKSNLVMLENGKQLTVKREGLYYVYTQVTFCSNREPSSQRPFIVGLWLKPSSGSERILLKANTHSSSQLCE
QQSVHLGGVFELQAGASVFVNVTEASQVIHRVGFSSFGLLKL

Figure A.3.: Sequences of the immunocytokines that were developed in this study, the linker sequences are depicted in italics

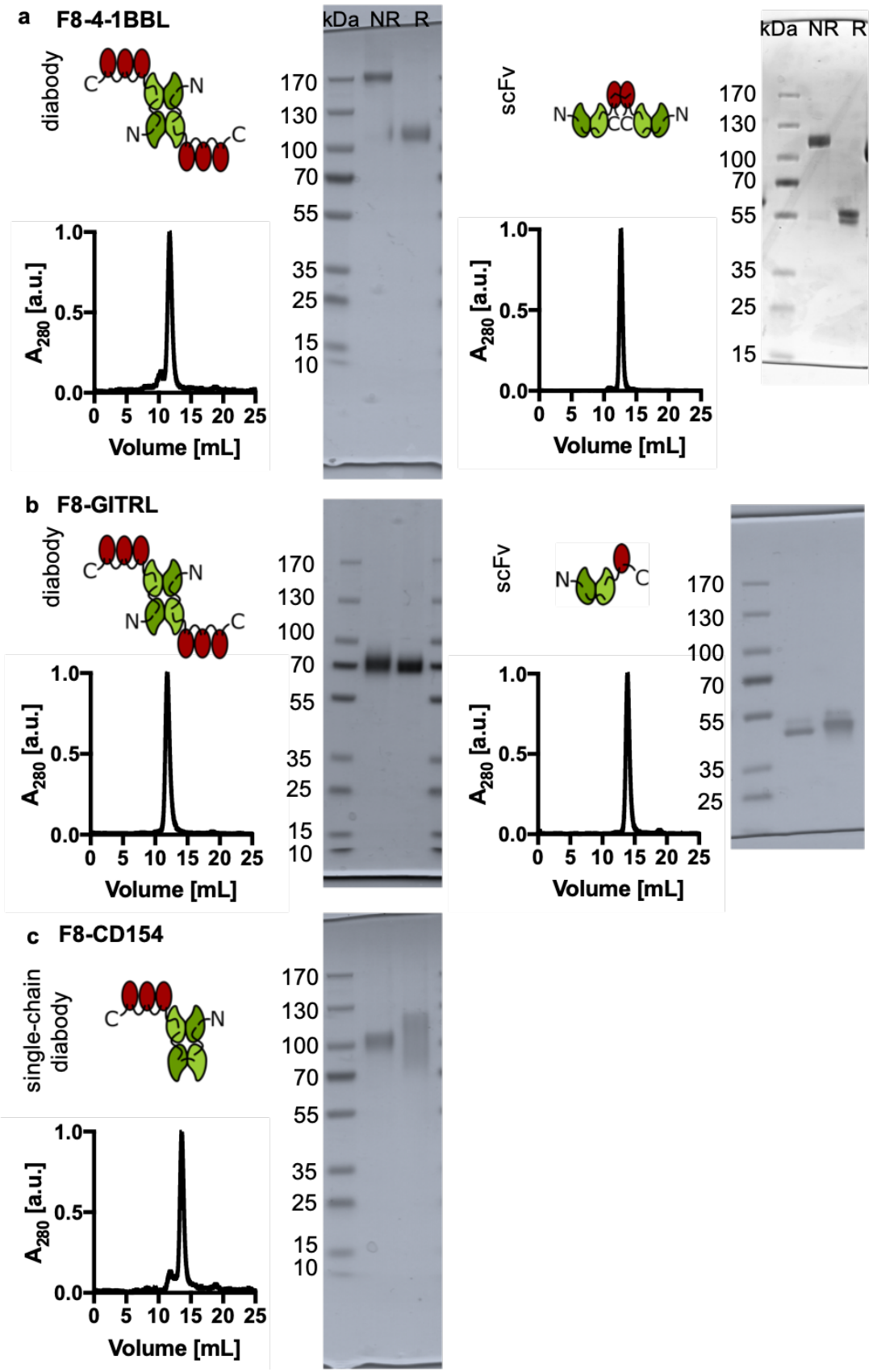

Figure A.4.: The proteins were characterized by SDS PAGE (NR: non-reducing, R: reducing sample buffer) and size exclusion chromatography (Superdex 200 Increase, 10/300 GL, GE Healthcare) after purification.

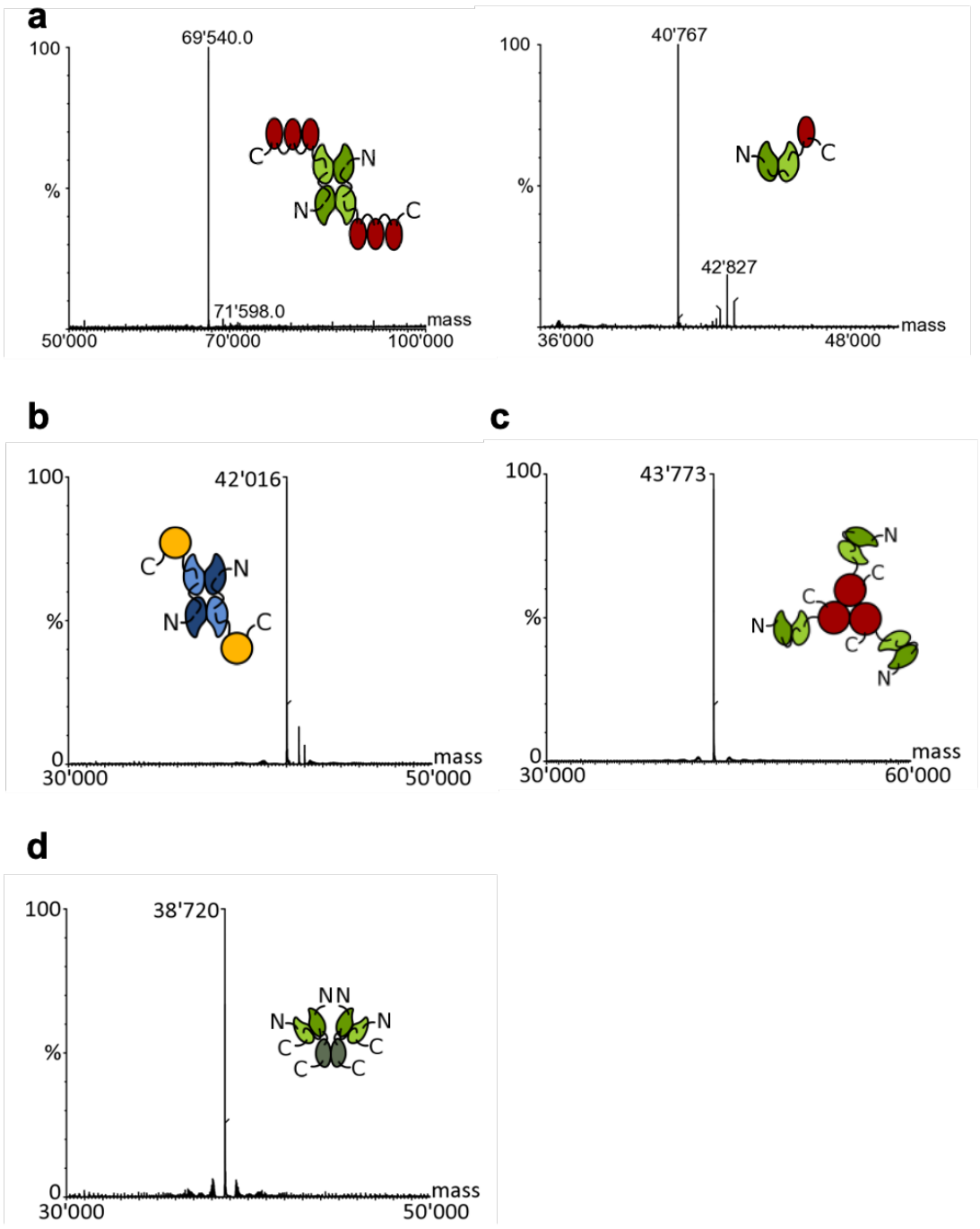

Figure A.5.: Mass spectrometry data for **(a)** the F8-GITRL constructs, **(b)** L19-IL2, **(c)** F8-TNF and **(d)** F8 in the small immune protein (sip) format

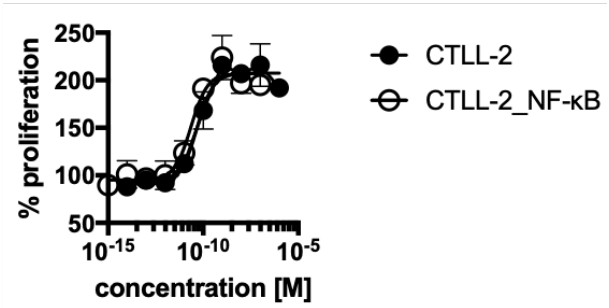

Figure A.6.: Comparison of the conventional CTLL-2 proliferation both with the transduced and the non-transduced cell line using L19-IL2

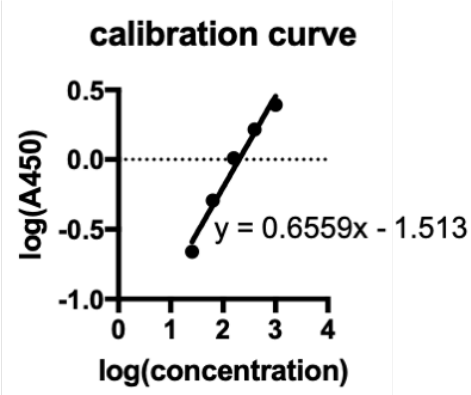

Figure A.7.: Standard curve used to determine the IFN-γ concentration from the A450 measurements. A linear curve fit was applied using the GraphPad Prism 7.0 a software and this curve fit was then used to calculate the IFN-γ concentration from the absorbance measurements.

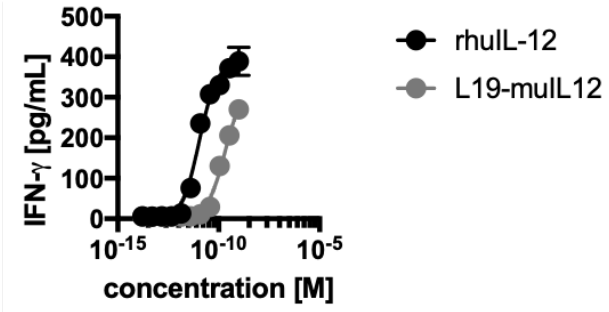

Figure A.8.: The standard activity of IL-12 measuring the IFN-γ release by NK-92 cells was performed both with the L19-IL12 immunocytokine featuring the murine IL-12 and with WHO calibrated recombinant human IL-12. Since IL-12 is not 100% cross-reactive between mouse and human, differences in activity were observed.

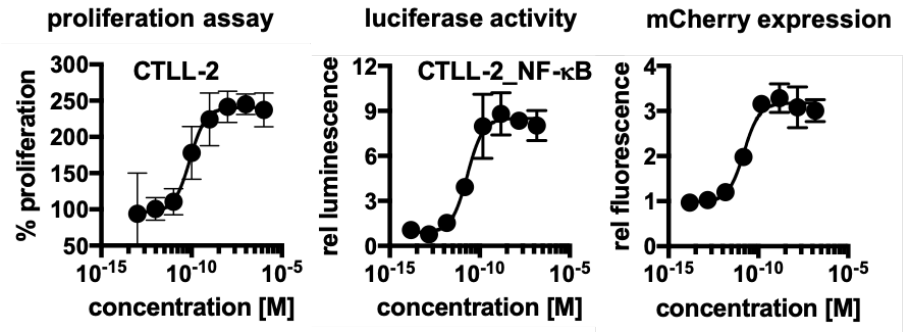

Figure A.9.: The CTLL-2 proliferation assay as well as the NF-κB reporter assays were also performed with recombinant human IL-2 (Proleukin, Roche Diagnostics)

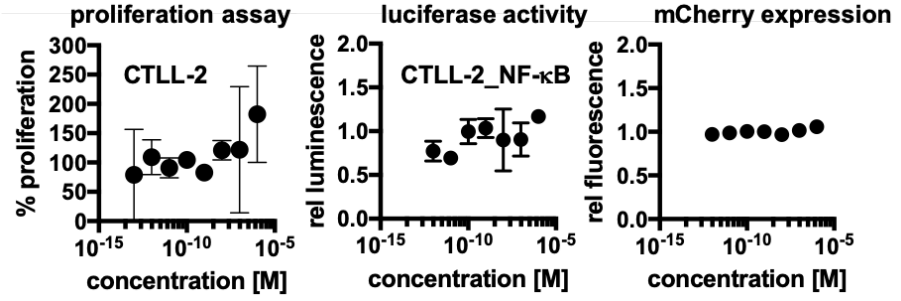

Figure A.10.: The CTLL-2 proliferation assay as well as the NF-κB reporter assays were also performed with "naked" F8 in the small immune protein format as a negative control

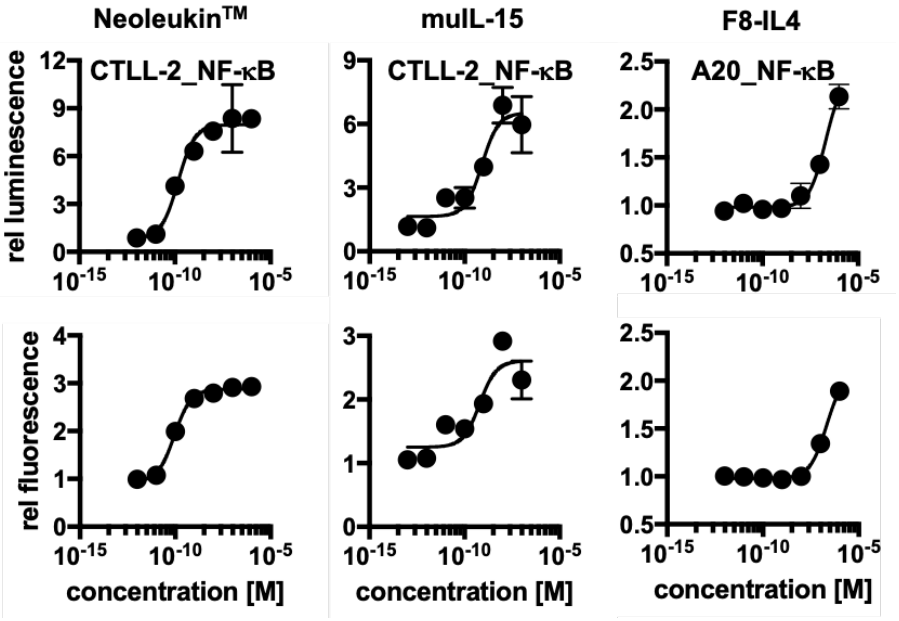

Figure A.11.: The NF-κB reporter assay were also performed with recombinant Neoleukin^{TM}, a fully synthetic cytokine that was first described by Silva et al.,[621] recombinant murine IL-15 (Peprotech, #210-15) and the F8-IL4 fusion protein[622]

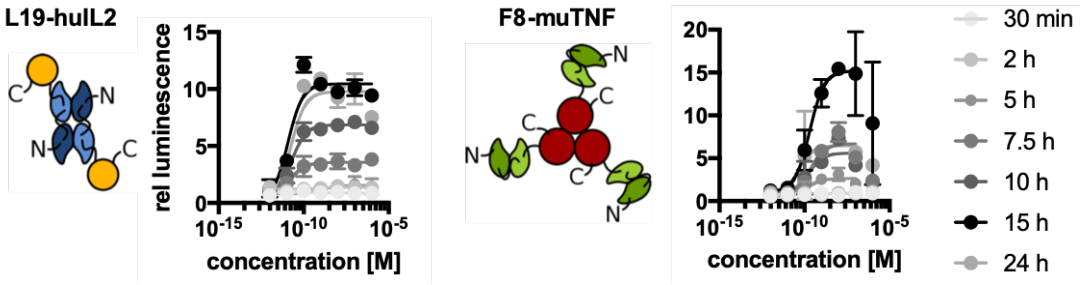

Figure A.12.: The luciferase assay was performed at different time points after addition of the cytokines. In both cases, the signal was strongest after 15 h which corresponds to the time point when the samples were taken for the other measurements.

	conventional assay			luciferase activity			mCherry expression		
	EC_{50}	**95% CI**	**R^2**	**EC_{50}**	**95% CI**	**R^2**	**EC_{50}**	**95% CI**	**R^2**
L19-IL2	47 pM	26 to 83 pM	0.9489	15 pM	8.5 to 26 pM	0.9376	21 pM	6.3 to 74 pM	0.8178
L19-IL12	0.13 nM	0.10 to 0.16 nM	0.99	3.5 nM	1.9 to 6.0 nM	0.95	2.6 nM	2.0 to 3.4 nM	0.99
F8-TNF	0.7 pM	0.6 to 0.9 pM	0.976	450 pM	280 to 730 pM	0.96	540 pM	450 to 650 pM	0.99

Table A.1.: EC_{50} obtained from a sigmoidal curve fit for conventional assay as well as for the readouts with the new cell lines (95% CI: 95% confidence interval)

		+ EDA						no EDA					
		luciferase activity			mCherry expression			luciferase activity			mCherry expression		
4-1BBL	diabody	1.1 nM	0.9 to 1.4 nM	0.99	1.2 nM	0.9 to 1.5 nM	0.99	1.1 nM	0.8 to 1.5 nM	0.98	1.0 nM	0.8 to 1.3 nM	0.99
	scFv	1.1 nM	0.7 to 1.8 nM	0.9713	1.0 nM	0.7 to 1.6 nM	0.9762	n/a	n/a	n/a	n/a	n/a	n/a
GITRL	diabody	7.6 nM	6.2 to 9.3 nM	0.9912	7.9 nM	7.0 to 8.9 nM	1	4.7 nM	3.9 to 5.7 nM	0.9898	4.1 nM	3.6 to 4.6 nM	0.9953
	scFv	11 nM	7.5 to 18 nM	0.9716	9.6 nM	7.5 to 12 nM	0.992	56 nM	43 to 72 nM	0.9864	67 nM	57 to 79 nM	0.9888
CD154	diabody	65 pM	45 to 9.3 pM	0.98	64 pM	49 to 85 pM	0.99	660 pM	0.4 to 1.1 nM	0.97	1.1 nM	0.4 to 2.7 nM	0.93

Table A.2.: EC_{50} values obtained from a sigmoidal curve fit for the different F8-TNFSF fusion proteins (95% CI: 95% confidence interval)

B. Supplementary material "Engineering murine GITRL"

This chapter contains the supplementary data accompanying the publication "Engineering murine GITRL for antibody-mediated delivery to tumor-associated blood vessels"

Format		**GenBank identifier**
1:	F8(dDb)-$(GITRL)_3$	MW115896
$\mathbf{1^{KSF}}$:	KSF(dDb)-$(GITRL)_3$	MW115898
2:	F8(IgG)-$(GITRL)_3$_HC	MW115899
3:	F8(scFv)-GITRL	MW115897
4:	F8(IgG)-GITRL_HC	MW115900
5:	F8(IgG)-GITRL_LC	MW115905
$\mathbf{1^{mut}}$:	F8(dDb)-$(GITRL\_N74S\_N157T)_3$	MW115901
$\mathbf{1^{KSF,mut}}$:	KSF(dDb)-$(GITRL\_N74S\_N157T)_3$	MW115903
$\mathbf{2^{mut}}$:	F8(IgG)-$(GITRL_N74S_N157T)_3$_HC	MW115902
$\mathbf{6^{mut}}$:	F8(IgG)-$(GITRL_N74S_N157T)_3$_LC	MW115904

Table B.1.: GenBank identifiers for the sequences encoding the fusion proteins developed in this study.

F8(dDb)-(GITRL)$_3$: $F8_{VH}$-linker-$F8_{VL}$-linker-GITRL-linker-GITRL-linker-GITRL (Format **1**)

EVQLLESGGGLVQPGGSLRLSCAASGFTFSLFTMSWVRQAPGKGLEWVSAISGSGGSTYYADSVKGRFTISRDNSK
NTLYLQMNSLRAEDTAVYYCAKSTHLYLFDYWGQGTLVTVSS-GGSGG- EIVLTQSPGTLSLSPGERATLSCRASQS
VSMPFLAWYQQKPGQAPRLLIYGASSRATGIPDRFSGSGSGTDFTLTISRLEPEDFAVYYCQQMRGRPPTFGQGT
KVEIK-SSSSGSSSSGSSSSG-PTAIESCMVKFELSSSKWHMTSPKPHCVNTTSDGKLKILQSGTYLIYGQVIPVDKKYI
KDNAPFVVQIYKKNDVLQTLMNDFQILPIGGVYELHAGDNIYLKFNSKDHIQKNNTYWGIILMPDLP-G-PTAIESC
MVKFELSSSKWHMTSPKPHCVNTTSDGKLKILQSGTYLIYGQVIPVDKKYIKDNAPFVVQIYKKNDVLQTLMNDF
QILPIGGVYELHAGDNIYLKFNSKDHIQKNNTYWGIILMPDLP-G-PTAIESCMVKFELSSSKWHMTSPKPHCVNTTS
DGKLKILQSGTYLIYGQVIPVDKKYIKDNAPFVVQIYKKNDVLQTLMNDFQILPIGGVYELHAGDNIYLKFNSKDHI
QKNNTYWGIILMPDLP

F8(IgG)-(GITRL)$_3$_HC: $F8_{VL}$-$F8_{CL}$**$F8_{VH}$-$F8_{CH}$-linker-GITRL-linker-GITRL-linker-GITRL (Format **2**)

EIVLTQSPGTLSLSPGERATLSCRASQSVSMPFLAWYQQKPGQAPRLLIYGASSRATGIPDRFSGSGSGTDFTLTISR
LEPEDFAVYYCQQMRGRPPTFGQGTKVEIKRTVAAPSVFIFPPSDEQLKSGTASVVCLLNNFYPREAKVQWKVDN
ALQSGNSQESVTEQDSKDSTYSLSSTLTLSKADYEKHKVYACEVTHQGLSSPVTKSFNRGEC** EVQLLESGGGLV
QPGGSLRLSCAASGFTFSLFTMSWVRQAPGKGLEWVSAISGSGGSTYYADSVKGRFTISRDNSKNTLYLQMNSLRA
EDTAVYYCAKSTHLYLFDYWGQGTLVTVSSASTKGPSVFPLAPSSKSTSGGTAALGCLVKDYFPEPVTVSWNSGA
LTSGVHTFPAVLQSSGLYSLSSVVTVPSSSLGTQTYICNVNHKPSNTKVDKKVEPKSCDKTHTCPPCPAPELLGGP
SVFLFPPKPKDTLMISRTPEVTCVVVDVSHEDPEVKFNWYVDGVEVHNAKTKPREEQYNSTYRVVSVLTVLHQD
WLNGKEYKCKVSNKALPAPIEKTISKAKGQPREPQVYTLPPSRDELTKNQVSLTCLVKGFYPSDIAVEWESNGQP
ENNYKTTPPVLDSDGSFFLYSKLTVDKSRWQQGNVFSCSVMHEALHNHYTQKSLSLSPGK-SSSSGSSSSGSSSSG-P
TAIESCMVKFELSSSKWHMTSPKPHCVNTTSDGKLKILQSGTYLIYGQVIPVDKKYIKDNAPFVVQIYKKNDVLQT
LMNDFQILPIGGVYELHAGDNIYLKFNSKDHIQKNNTYWGIILMPDLP-G-PTAIESCMVKFELSSSKWHMTSPKPH
CVNTTSDGKLKILQSGTYLIYGQVIPVDKKYIKDNAPFVVQIYKKNDVLQTLMNDFQILPIGGVYELHAGDNIYLKF
NSKDHIQKNNTYWGIILMPDLP-G-PTAIESCMVKFELSSSKWHMTSPKPHCVNTTSDGKLKILQSGTYLIYGQVIPV
DKKYIKDNAPFVVQIYKKNDVLQTLMNDFQILPIGGVYELHAGDNIYLKFNSKDHIQKNNTYWGIILMPDLP

F8(scFv)-GITRL: $F8_{VH}$-linker-$F8_{VL}$-linker-GITRL (Format **3**)

EVQLLESGGGLVQPGGSLRLSCAASGFTFSLFTMSWVRQAPGKGLEWVSAISGSGGSTYYADSVKGRFTISRDNSK
NTLYLQMNSLRAEDTAVYYCAKSTHLYLFDYWGQGTLVTVSS-GGGGSGGGGSGGGG- EIVLTQSPGTLSLSPGE
RATLSCRASQSVSMPFLAWYQQKPGQAPRLLIYGASSRATGIPDRFSGSGSGTDFTLTISRLEPEDFAVYYCQQMR
GRPPTFGQGTKVEIK-SSSSGSSSSGSSSSG-PTAIESCMVKFELSSSKWHMTSPKPHCVNTTSDGKLKILQSGTYLIY
GQVIPVDKKYIKDNAPFVVQIYKKNDVLQTLMNDFQILPIGGVYELHAGDNIYLKFNSKDHIQKNNTYWGIILMPD
LP

F8(IgG)-GITRL_HC: $F8_{VL}$-$F8_{CL}$**$F8_{VH}$-$F8_{CH}$-linker-GITRL (Format **4**)

EIVLTQSPGTLSLSPGERATLSCRASQSVSMPFLAWYQQKPGQAPRLLIYGASSRATGIPDRFSGSGSGTDFTLTISR
LEPEDFAVYYCQQMRGRPPTFGQGTKVEIKRTVAAPSVFIFPPSDEQLKSGTASVVCLLNNFYPREAKVQWKVDN
ALQSGNSQESVTEQDSKDSTYSLSSTLTLSKADYEKHKVYACEVTHQGLSSPVTKSFNRGEC** EVQLLESGGGLV
QPGGSLRLSCAASGFTFSLFTMSWVRQAPGKGLEWVSAISGSGGSTYYADSVKGRFTISRDNSKNTLYLQMNSLRA
EDTAVYYCAKSTHLYLFDYWGQGTLVTVSSASTKGPSVFPLAPSSKSTSGGTAALGCLVKDYFPEPVTVSWNSGA
LTSGVHTFPAVLQSSGLYSLSSVVTVPSSSLGTQTYICNVNHKPSNTKVDKKVEPKSCDKTHTCPPCPAPELLGGPS
VFLFPPKPKDTLMISRTPEVTCVVVDVSHEDPEVKFNWYVDGVEVHNAKTKPREEQYNSTYRVVSVLTVLHQDW
LNGKEYKCKVSNKALPAPIEKTISKAKGQPREPQVYTLPPSRDELTKNQVSLTCLVKGFYPSDIAVEWESNGQPEN
NYKTTPPVLDSDGSFFLYSKLTVDKSRWQQGNVFSCSVMHEALHNHYTQKSLSLSPGK-SSSSGSSSSGSSSSG-PTAI
ESCMVKFELSSSKWHMTSPKPHCVNTTSDGKLKILQSGTYLIYGQVIPVDKKYIKDNAPFVVQIYKKNDVLQTLMN
DFQILPIGGVYELHAGDNIYLKFNSKDHIQKNNTYWGIILMPDLP

F8(IgG)-GITRL_LC: $F8_{VL}$-$F8_{CL}$-linker-GITRL**$F8_{VH}$-$F8_{CH}$ (Format **5**)

EIVLTQSPGTLSLSPGERATLSCRASQSVSMPFLAWYQQKPGQAPRLLIYGASSRATGIPDRFSGSGSGTDFTLTISR
LEPEDFAVYYCQQMRGRPPTFGQGTKVEIKRTVAAPSVFIFPPSDEQLKSGTASVVCLLNNFYPREAKVQWKVDN
ALQSGNSQESVTEQDSKDSTYSLSSTLTLSKADYEKHKVYACEVTHQGLSSPVTKSFNRGEC-SSSSGSSSSGSSSSG-P
TAIESCMVKFELSSSKWHMTSPKPHCV**NTT**SDGKLKILQSGTYLIYGQVIPVDKKYIKDNAPFVVQIYKKNDVLQT
LMNDFQILPIGGVYELHAGDNIYLKFNSKDHIQK**NNT**YWGIILMPDLP** EVQLLESGGGLVQPGGSLRLSCAASGF
TFSLFTMSWVRQAPGKGLEWVSAISGSGGSTYYADSVKGRFTISRDNSKNTLYLQMNSLRAEDTAVYYCAKSTHL
YLFDYWGQGTLVTVSSASTKGPSVFPLAPSSKSTSGGTAALGCLVKDYFPEPVTVSWNSGALTSGVHTFPAVLQSS
GLYSLSSVVTVPSSSLGTQTYICNVNHKPSNTKVDKKVEPKSCDKTHTCPPCPAPELLGGPSVFLFPPKPKDTLMIS
RTPEVTCVVVDVSHEDPEVKFNWYVDGVEVHNAKTKPREEQYNSTYRVVSVLTVLHQDWLNGKEYKCKVSNKA
LPAPIEKTISKAKGQPREPQVYTLPPSRDELTKNQVSLTCLVKGFYPSDIAVEWESNGQPENNYKTTPPVLDSDGS
FFLYSKLTVDKSRWQQGNVFSCSVMHEALHNHYTQKSLSLSPGK

KSF(dDb)-$(GITRL)_3$: KSF_{VH}-linker-KSF_{VL}-linker-GITRL-linker-GITRL-linker-GITRL (Format **1**)

EVQLLESGGGLVQPGGSLRLSCAASGFTFSSYAMSWVRQAPGKGLEWVSAISGSGGSTYYADSVKGRFTISRDNSK
NTLYLQMNSLRAEDTAVYYCAKSPKVSLFDYWGQGTLVTVSS-GGSGG- SELTQDPAVSVALGQTVRITCQGDSL
RSYYASWYQQKPGQAPVLVIYGKNNRPSGIPDRFSGSSSGNTASLTITGAQAEDEADYYCNSSPLNRLAVVFGGG
TKLTVLG-SSSSGSSSSGSSSSG-PTAIESCMVKFELSSSKWHMTSPKPHCV**NTT**SDGKLKILQSGTYLIYGQVIPVDK
KYIKDNAPFVVQIYKKNDVLQTLMNDFQILPIGGVYELHAGDNIYLKFNSKDHIQK**NNT**YWGIILMPDLP-G-PTA
IESCMVKFELSSSKWHMTSPKPHCV**NTT**SDGKLKILQSGTYLIYGQVIPVDKKYIKDNAPFVVQIYKKNDVLQTL
MNDFQILPIGGVYELHAGDNIYLKFNSKDHIQK**NNT**YWGIILMPDLP-G-PTAIESCMVKFELSSSKWHMTSPKPHC
V**NTT**SDGKLKILQSGTYLIYGQVIPVDKKYIKDNAPFVVQIYKKNDVLQTLMNDFQILPIGGVYELHAGDNIYLKFN
SKDHIQK**NNT**YWGIILMPDLP

Figure B.1.: Sequences of the fusion proteins that were developed in this study. The asparagine residues N74 and N157 of GITRL that were mutated to S and T are highlighted in bold. The consensus sequences for N-linked glycosylation are underlined.

Format		Yield WT-GITRL [mg/L]	Yield GITRL_N74S_N157T [mg/L]
1:	F8(dDb)-$(GITRL)_3$	13	1.5
2:	F8(IgG)-$(GITRL)_3$_HC	22	n/a
3:	F8(scFv)-GITRL	19	5
6:	F8(IgG)-$(GITRL)_3$_LC	n/a	4.7

Table B.2.: Expression yields from the purification of the different F8-GITRL fusion proteins featuring wild-type and aglycosylated GITRL as payloads. The proteins were expressed in CHO cells as described in the methods section.

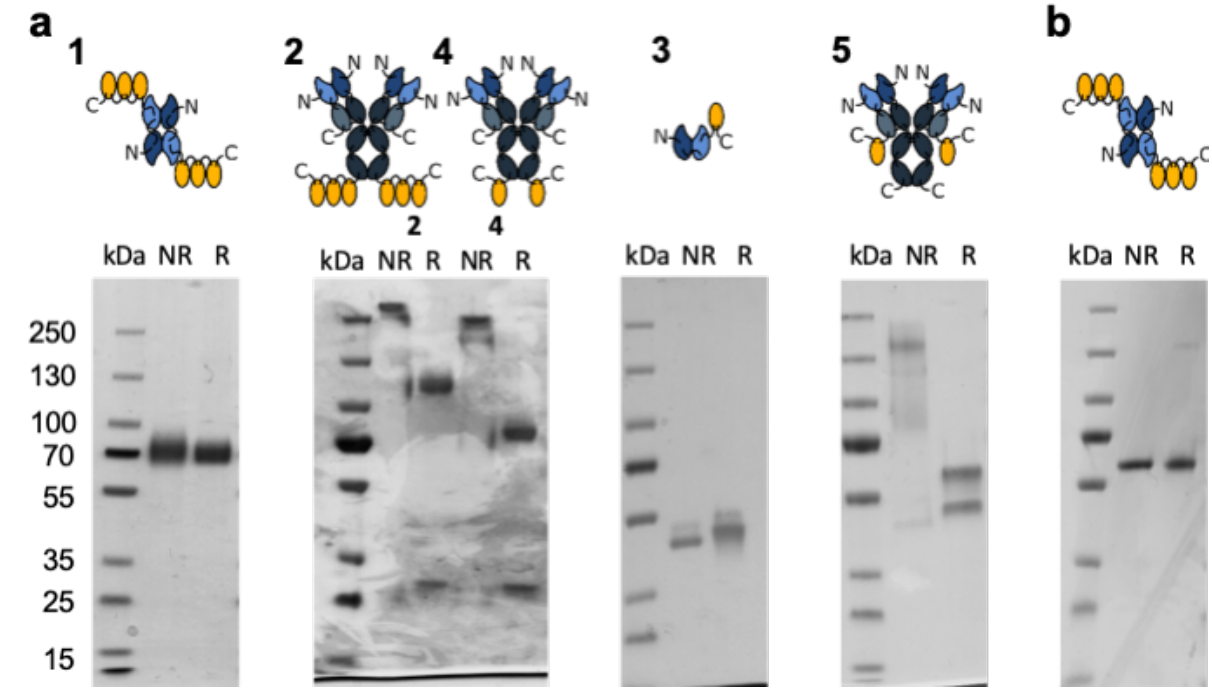

Figure B.2.: SDS PAGE analysis of the F8-GITRL fusion proteins featuring **(a)** wild-type GITRL and **(b)** aglycosylated GITRL (NR: non-reducing sample buffer, R: reducing sample buffer)

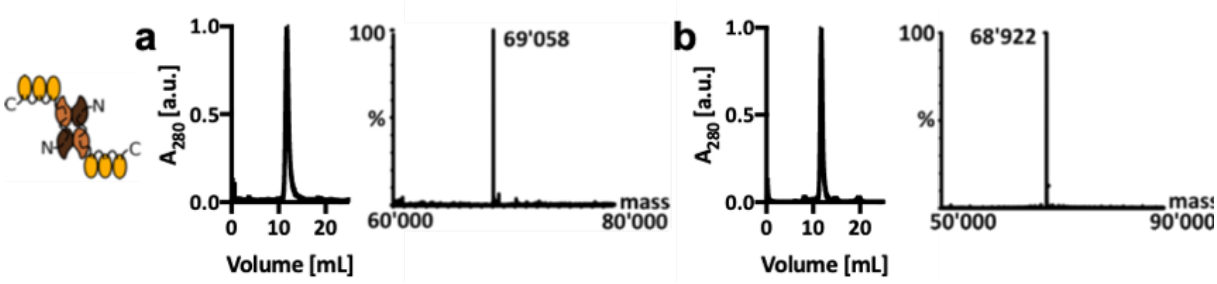

Figure B.3.: Characterization of the KSF-GITRL fusion proteins that were used as negative control in the quantitative biodistribution studies **(a)** Size exclusion chromatogram and LC-MS spectrum of KSF-GITRL in Format 1 featuring wild-type GITRL **(b)** Size exclusion chromatogram and LC-MS spectrum of KSF-GITRL_N74S_N157T in Format $\mathbf{1^{mut}}$ featuring the aglycosylated GITRL mutant

Format		Apparent K_D [M]			EC_{50} [M]		
1:	F8(dDb)-$(GITRL)_3$	$4.4{\cdot}10^{-9}$	±	$4.4{\cdot}10^{-10}$	$4.7{\cdot}10^{-9}$	±	$4.8{\cdot}10^{-10}$
2:	F8(IgG)-$(GITRL)_3$_HC	$6.7{\cdot}10^{-9}$	±	$8.1{\cdot}10^{-10}$	$8.9{\cdot}10^{-11}$	±	$1.9{\cdot}10^{-11}$
3:	F8(scFv)-GITRL	$3.4{\cdot}10^{-7}$	±	$3.1{\cdot}10^{-8}$	$7.0{\cdot}10^{-8}$	±	$9.7{\cdot}10^{-9}$
4:	F8(IgG)-GITRL_HC	$3.3{\cdot}10^{-7}$	±	$2.2{\cdot}10^{-8}$	$5.8{\cdot}10^{-9}$	±	$9.2{\cdot}10^{-10}$
5:	F8(IgG)-GITRL_LC	$6.4{\cdot}10^{-8}$	±	$5.6{\cdot}10^{-9}$	$2.0{\cdot}10^{-9}$	±	$4.2{\cdot}10^{-10}$
$\mathbf{1^{mut}}$:	F8(dDb)-$(GITRL\_N74S\_N157T)_3$	$3.2{\cdot}10^{-9}$	±	$2.5{\cdot}10^{-10}$	$5.0{\cdot}10^{-11}$	±	$8.6{\cdot}10^{-12}$
$\mathbf{6^{mut}}$:	F8(IgG)-$(GITRL_N74S_N157T)_3$_LC	$1.5{\cdot}10^{-9}$	±	$3.6{\cdot}10^{-10}$	$1.5{\cdot}10^{-11}$	±	$2.6{\cdot}10^{-12}$

Table B.3.: Binding affinity and in vitro bioactivity of the F8-GITRL as measured by flow cytometry binding to CTLL-2 cells and using the CTLL-2 NF-κB reporter cell line.

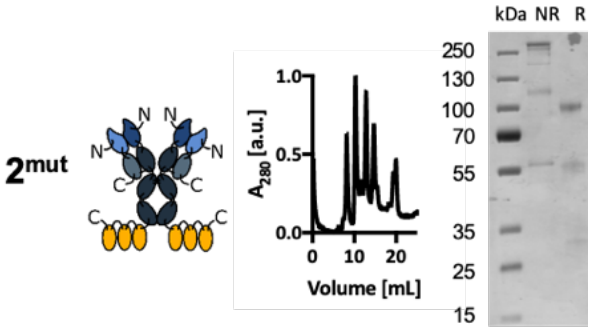

Figure B.4.: The fusion protein consisting of aglycosylated GITRL_N74S_N157T fused to the heavy chain of the F8 antibody (Format $\mathbf{2^{mut}}$) yielded a heavily degraded protein as can be seen on the size exclusion chromatogram and on SDS PAGE (NR: non-reducing sample buffer, R: reducing sample buffer).

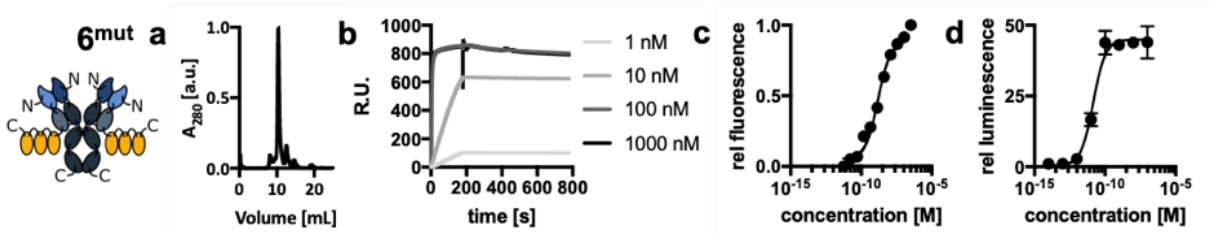

Figure B.5.: Characterization of aglycosylated GITRL_N74S_N157T fused to the light chain of the F8 antibody in the IgG format (Format $\mathbf{6^{mut}}$) **(a)** size exclusion chromatogram **(b)** surface plasmon resonance measurement of the binding to EDA **(c)** flow cytometry measurement of the binding to CTLL-2 **(d)** *in vitro* bioactivity

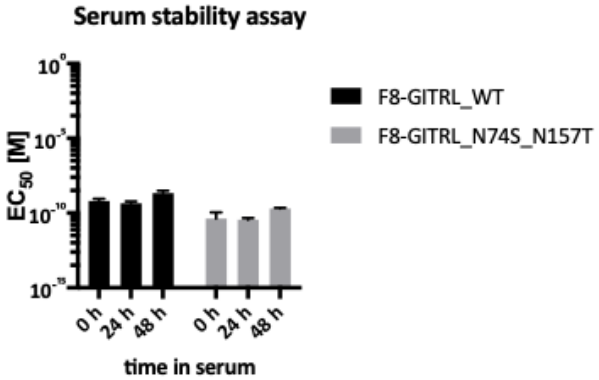

Figure B.6.: *In vitro* serum stability assay, the protein was incubated in mouse serum at 37°C for up to 48 h and the biological activity was measured using the NF-κB reporter cell line.

	Days after tumor implantation					
Group	**8**	**9**	**10**	**11**	**12**	**13**
Saline	PBS	PBS	PBS	PBS	PBS	PBS
F8-GITRL	F8-GITRL	PBS	F8-GITRL	PBS	F8-GITRL	PBS
αPD-1	αPD-1	PBS	αPD-1	PBS	αPD-1	PBS
combo	αPD-1	F8-GITRL	αPD-1	F8-GITRL	αPD-1	F8-GITRL

Table B.4.: Treatment schedule for the therapy and infiltrate analysis of CT26 colon carcinoma-bearing mice using F8-GITRL_N74S_N157T in Format 1^{mut} and a PD-1 inhibitor

	FITC	**APC/Cy7**	**PE**	**APC**	**BV421**	**Live/Dead**
Stain 1	CD8	CD3	NK1.1	CD4	IA/IE	7-AAD
Stain 2	CD8	CD44	AH1 CD127	CD62L	7-AAD	
Stain 3	CD8	-	AH1	CD39	PD-1	7-AAD
Stain 4	CD8	-	AH1	CD226	TIGIT	7-AAD
Stain 5	GITR	CD8	-	CD4	FoxP3	Zombie red

Table B.5.: Design of the 5-color panel for the analysis of tumor infiltrating lymphocytes and tumor-draining lymph nodes by flow cytometry

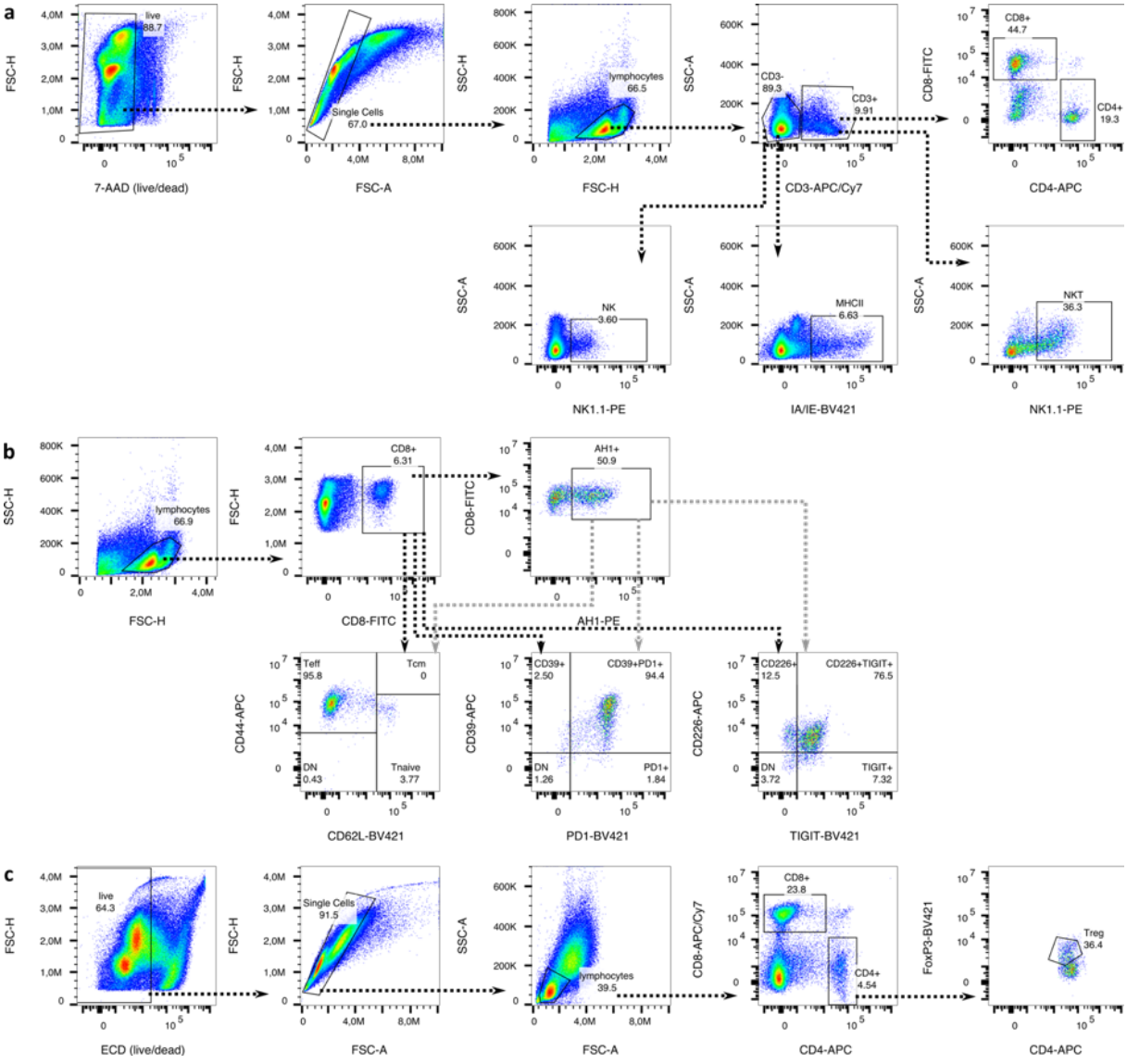

Figure B.7.: Gating strategy for the analysis of tumor-infiltrating lymphocytes and TDLN **(a)** samples were first gated for live cells followed by a singlet gating and gating for lymphocytes by scattering. To quantify the cell subsets, cells were divided by the expression of CD3 and then further analyzed for expression of CD4, CD8, NK1.1 and MHC-II (IA/IE) **(b)** To analyze the phenotype of CD8+ T cells, the cells were gated for lymphocytes as shown in part a and then the same gates were applied to bulk CD8+ T cells and AH1-specific T cells. **(c)** Fixed samples were also first gated for live cells, singlets and lymphocytes before they were analyzed for the expression of CD8, CD4 and FoxP3. The gating strategy is shown for 1 representative tumor sample, but the same gates were applied to all samples.

C. Supplementary material "An engineered 4-1BBL fusion protein"

This chapter contains the supplementary data accompanying the publication "An engineered 4-1BBL fusion protein with "activity-on-demand"".

Supplementary Methods

Immunofluorescence on tissue microarray Immunofluorescence was performed onto Frozen Tumor and Normal Tissue Array (Biochain, #T6235700). The array was fixed by ice-cold acetone for 5 minutes. After fixation, sections were let dry at room temperature for 10 minutes and then blocked for 45 min with 20% fetal bovine serum in PBS. FITC labeled IgG(F8) was added at 5 µg/ml in 2% BSA/PBS solution for 1h at room temperature. The tissue array was then washed twice with PBS and secondary rabbit anti-FITC antibody (Biorad, #4510-7804) was added to a final 1:1000 dilution in 2% BSA/PBS at room temperature for 1h. After washing the array twice with PBS, Goat Anti-Rabbit Alexa-488 (ThermoFisher, #A11032) was added to a final 1:500 dilution in 2% BSA/PBS. Dapi was used to counterstain nuclei. Slides were analyzed with Axioskop2 plus microscope (Zeiss).

***Ex vivo* detection of fluorescently labelled immunocytokines and serial scanning of the tumor section** The tumor section was prepared and stained as described in the main text. Serial images of the tumor sections were acquired and electronically assembled using a Leica DMI6000B microscope equipped with a HC PL APO 20x/ 0.70 DRY objective (#11506166), a Leica K5-14400781 camera and a fast filter wheel. The acquisition settings were 100 ms exposure, 12.5 % intensity for the green channel (λ_{ex} = 490 nm, λ_{em} = 525 nm), 150 ms exposure, 25% intensity for the red channel (λ_{ex} = 552 nm, λ_{em} = 600 nm) and 50 ms, 6.25% intensity for the blue channel (λ_{ex} = 450 nm, λ_{em} = 422 nm). For image processing the LAS X and ImageJ software v1.52k were used. The thresholds for the red and green channels were set to 300 – 506 and for the blue channel to 250 – 6000.

F8(scDb)-(4-1BBL)$_3$: $F8_{VH}$-linker-$F8_{VL}$-linker- $F8_{VH}$-linker-$F8_{VL}$-linker-4-1BBL-linker-4-1BBL-linker-4-1BBL (Format **1**)

EVQLLESGGGLVQPGGSLRLSCAASGFTFSLFTMSWVRQAPGKGLEWVSAISGSGGSTYYADSVKGRFTISRDNSK
NTLYLQMNSLRAEDTAVYYCAKSTHLYLFDYWGQGTLVTVSS-GGSGG- EIVLTQSPGTLSLSPGERATLSCRASQS
VSMPFLAWYQQKPGQAPRLLIYGASSRATGIPDRFSGSGSGTDFTLTISRLEPEDFAVYYCQQMRGRPPTFGQGT
KVEIK-GGGGSGGGGSGGGGS-EVQLLESGGGLVQPGGSLRLSCAASGFTFSLFTMSWVRQAPGKGLEWVSAISGS
GGSTYYADSVKGRFTISRDNSKNTLYLQMNSLRAEDTAVYYCAKSTHLYLFDYWGQGTLVTVSS-GGSGG- EIVLT
QSPGTLSLSPGERATLSCRASQSVSMPFLAWYQQKPGQAPRLLIYGASSRATGIPDRFSGSGSGTDFTLTISRLEPED
FAVYYCQQMRGRPPTFGQGTKVEIK-SSSSGSSSSGSSSSG-ATTQQGSPVFAKLLAKNQASLCNTTLNWHSQDGAG
SSYLSQGLRYEEDKKELVVDSPGLYYVFLELKLSPTFTNTGHKVQGWVSLVLQAKPQVDDFDNLALTVELFPCSM
ENKLVDRSWSQLLLLKAGHRLSVGLRAYLHGAQDAYRDWELSYPNTTSFGLFLVKPDNPWE-G-ATTQQGSPVFA
KLLAKNQASLCNTTLNWHSQDGAGSSYLSQGLRYEEDKKELVVDSPGLYYVFLELKLSPTFTNTGHKVQGWVSLV
LQAKPQVDDFDNLALTVELFPCSMENKLVDRSWSQLLLLKAGHRLSVGLRAYLHGAQDAYRDWELSYPNTTSFGL
FLVKPDNPWE-G-ATTQQGSPVFAKLLAKNQASLCNTTLNWHSQDGAGSSYLSQGLRYEEDKKELVVDSPGLYYV
FLELKLSPTFTNTGHKVQGWVSLVLQAKPQVDDFDNLALTVELFPCSMENKLVDRSWSQLLLLKAGHRLSVGLRA
YLHGAQDAYRDWELSYPNTTSFGLFLVKPDNPWE

F8(dDb)-(4-1BBL)$_3$: $F8_{VH}$-linker-$F8_{VL}$-linker-4-1BBL-linker-4-1BBL-linker-4-1BBL (Format **2**)

EVQLLESGGGLVQPGGSLRLSCAASGFTFSLFTMSWVRQAPGKGLEWVSAISGSGGSTYYADSVKGRFTISRDNSK
NTLYLQMNSLRAEDTAVYYCAKSTHLYLFDYWGQGTLVTVSS-GGSGG- EIVLTQSPGTLSLSPGERATLSCRASQS
VSMPFLAWYQQKPGQAPRLLIYGASSRATGIPDRFSGSGSGTDFTLTISRLEPEDFAVYYCQQMRGRPPTFGQGT
KVEIK-SSSSGSSSSGSSSSG-ATTQQGSPVFAKLLAKNQASLCNTTLNWHSQDGAGSSYLSQGLRYEEDKKELVVDS
PGLYYVFLELKLSPTFTNTGHKVQGWVSLVLQAKPQVDDFDNLALTVELFPCSMENKLVDRSWSQLLLLKAGHRL
SVGLRAYLHGAQDAYRDWELSYPNTTSFGLFLVKPDNPWE-G-ATTQQGSPVFAKLLAKNQASLCNTTLNWHSQD
GAGSSYLSQGLRYEEDKKELVVDSPGLYYVFLELKLSPTFTNTGHKVQGWVSLVLQAKPQVDDFDNLALTVELFP
CSMENKLVDRSWSQLLLLKAGHRLSVGLRAYLHGAQDAYRDWELSYPNTTSFGLFLVKPDNPWE-G-ATTQQGSP
VFAKLLAKNQASLCNTTLNWHSQDGAGSSYLSQGLRYEEDKKELVVDSPGLYYVFLELKLSPTFTNTGHKVQGW
VSLVLQAKPQVDDFDNLALTVELFPCSMENKLVDRSWSQLLLLKAGHRLSVGLRAYLHGAQDAYRDWELSYPNT
TSFGLFLVKPDNPWE

F8(IgG)-(4-1BBL)$_3$_HC: $F8_{VL}$-$F8_{CL}$**$F8_{VH}$-$F8_{CH}$-linker-4-1BBL-linker-4-1BBL-linker-4-1BBL (Format **3**)

EIVLTQSPGTLSLSPGERATLSCRASQSVSMPFLAWYQQKPGQAPRLLIYGASSRATGIPDRFSGSGSGTDFTLTISR
LEPEDFAVYYCQQMRGRPPTFGQGTKVEIKRTVAAPSVFIFPPSDEQLKSGTASVVCLLNNFYPREAKVQWKVDN
ALQSGNSQESVTEQDSKDSTYSLSSTLTLSKADYEKHKVYACEVTHQGLSSPVTKSFNRGEC** EVQLLESGGGLV
QPGGSLRLSCAASGFTFSLFTMSWVRQAPGKGLEWVSAISGSGGSTYYADSVKGRFTISRDNSKNTLYLQMNSLRA
EDTAVYYCAKSTHLYLFDYWGQGTLVTVSSASTKGPSVFPLAPSSKSTSGGTAALGCLVKDYFPEPVTVSWNSGA
LTSGVHTFPAVLQSSGLYSLSSVVTVPSSSLGTQTYICNVNHKPSNTKVDKKVEPKSCDKTHTCPPCPAPELLGGPS
VFLFPPKPKDTLMISRTPEVTCVVVDVSHEDPEVKFNWYVDGVEVHNAKTKPREEQYNSTYRVVSVLTVLHQDW
LNGKEYKCKVSNKALPAPIEKTISKAKGQPREPQVYTLPPSRDELTKNQVSLTCLVKGFYPSDIAVEWESNGQPEN
NYKTTPPVLDSDGSFFLYSKLTVDKSRWQQGNVFSCSVMHEALHNHYTQKSLSLSPGK-SSSSGSSSSGSSSSG-ATT
QQGSPVFAKLLAKNQASLCNTTLNWHSQDGAGSSYLSQGLRYEEDKKELVVDSPGLYYVFLELKLSPTFTNTGHK
VQGWVSLVLQAKPQVDDFDNLALTVELFPCSMENKLVDRSWSQLLLLKAGHRLSVGLRAYLHGAQDAYRDWELS
YPNTTSFGLFLVKPDNPWE-G-ATTQQGSPVFAKLLAKNQASLCNTTLNWHSQDGAGSSYLSQGLRYEEDKKELV
VDSPGLYYVFLELKLSPTFTNTGHKVQGWVSLVLQAKPQVDDFDNLALTVELFPCSMENKLVDRSWSQLLLLKAG
HRLSVGLRAYLHGAQDAYRDWELSYPNTTSFGLFLVKPDNPWE-G-ATTQQGSPVFAKLLAKNQASLCNTTLNWH
SQDGAGSSYLSQGLRYEEDKKELVVDSPGLYYVFLELKLSPTFTNTGHKVQGWVSLVLQAKPQVDDFDNLALTVE
LFPCSMENKLVDRSWSQLLLLKAGHRLSVGLRAYLHGAQDAYRDWELSYPNTTSFGLFLVKPDNPWE

F8(IgG)-(4-1BBL)$_3$_LC: $F8_{VL}$-$F8_{CL}$-linker-4-1BBL-linker-4-1BBL-linker-4-1BBL **$F8_{VH}$-$F8_{CH}$ (Format **4**)

EIVLTQSPGTLSLSPGERATLSCRASQSVSMPFLAWYQQKPGQAPRLLIYGASSRATGIPDRFSGSGSGTDFTLTISR
LEPEDFAVYYCQQMRGRPPTFGQGTKVEIKRTVAAPSVFIFPPSDEQLKSGTASVVCLLNNFYPREAKVQWKVD
NALQSGNSQESVTEQDSKDSTYSLSSTLTLSKADYEKHKVYACEVTHQGLSSPVTKSFNRGEC-SSSSGSSSSGSSSS
G-ATTQQGSPVFAKLLAKNQASLCNTTLNWHSQDGAGSSYLSQGLRYEEDKKELVVDSPGLYYVFLELKLSPTFTN
TGHKVQGWVSLVLQAKPQVDDFDNLALTVELFPCSMENKLVDRSWSQLLLLKAGHRLSVGLRAYLHGAQDAYRD
WELSYPNTTSFGLFLVKPDNPWE-G-ATTQQGSPVFAKLLAKNQASLCNTTLNWHSQDGAGSSYLSQGLRYEEDK
KELVVDSPGLYYVFLELKLSPTFTNTGHKVQGWVSLVLQAKPQVDDFDNLALTVELFPCSMENKLVDRSWSQLLL
LKAGHRLSVGLRAYLHGAQDAYRDWELSYPNTTSFGLFLVKPDNPWE-G-ATTQQGSPVFAKLLAKNQASLCNTT
LNWHSQDGAGSSYLSQGLRYEEDKKELVVDSPGLYYVFLELKLSPTFTNTGHKVQGWVSLVLQAKPQVDDFDNL
ALTVELFPCSMENKLVDRSWSQLLLLKAGHRLSVGLRAYLHGAQDAYRDWELSYPNTTSFGLFLVKPDNPWE** E
VQLLESGGGLVQPGGSLRLSCAASGFTFSLFTMSWVRQAPGKGLEWVSAISGSGGSTYYADSVKGRFTISRDNSKN
TLYLQMNSLRAEDTAVYYCAKSTHLYLFDYWGQGTLVTVSSASTKGPSVFPLAPSSKSTSGGTAALGCLVKDYFP
EPVTVSWNSGALTSGVHTFPAVLQSSGLYSLSSVVTVPSSSLGTQTYICNVNHKPSNTKVDKKVEPKSCDKTHTCP
PCPAPELLGGPSVFLFPPKPKDTLMISRTPEVTCVVVDVSHEDPEVKFNWYVDGVEVHNAKTKPREEQYNSTYR
VVSVLTVLHQDWLNGKEYKCKVSNKALPAPIEKTISKAKGQPREPQVYTLPPSRDELTKNQVSLTCLVKGFYPSDI
AVEWESNGQPENNYKTTPPVLDSDGSFFLYSKLTVDKSRWQQGNVFSCSVMHEALHNHYTQKSLSLSPGK

F8(scFv)-4-1BBL: $F8_{VH}$-linker-$F8_{VL}$-linker-4-1BBL (Format **5**)

EVQLLESGGGLVQPGGSLRLSCAASGFTFSLFTMSWVRQAPGKGLEWVSAISGSGGSTYYADSVKGRFTISRDNSK
NTLYLQMNSLRAEDTAVYYCAKSTHLYLFDYWGQGTLVTVSS-GGGGSGGGGSGGGG- EIVLTQSPGTLSLSPGE
RATLSCRASQSVSMPFLAWYQQKPGQAPRLLIYGASSRATGIPDRFSGSGSGTDFTLTISRLEPEDFAVYYCQQMR
GRPPTFGQGTKVEIK-SSSSGSSSSGSSSSG-ATTQQGSPVFAKLLAKNQASLCNTTLNWHSQDGAGSSYLSQGLRYE
EDKKELVVDSPGLYYVFLELKLSPTFTNTGHKVQGWVSLVLQAKPQVDDFDNLALTVELFPCSMENKLVDRSWS
QLLLLKAGHRLSVGLRAYLHGAQDAYRDWELSYPNTTSFGLFLVKPDNPWE

F8(scDb)-4-1BBL: $F8_{VH}$-linker-$F8_{VL}$-linker- $F8_{VH}$-linker-$F8_{VL}$-linker-4-1BBL (Format **6**)

EVQLLESGGGLVQPGGSLRLSCAASGFTFSLFTMSWVRQAPGKGLEWVSAISGSGGSTYYADSVKGRFTISRDNSK
NTLYLQMNSLRAEDTAVYYCAKSTHLYLFDYWGQGTLVTVSS-GGSGG- EIVLTQSPGTLSLSPGERATLSCRASQS
VSMPFLAWYQQKPGQAPRLLIYGASSRATGIPDRFSGSGSGTDFTLTISRLEPEDFAVYYCQQMRGRPPTFGQGT
KVEIK-GGGGSGGGGSGGGGS-EVQLLESGGGLVQPGGSLRLSCAASGFTFSLFTMSWVRQAPGKGLEWVSAISGS
GGSTYYADSVKGRFTISRDNSKNTLYLQMNSLRAEDTAVYYCAKSTHLYLFDYWGQGTLVTVSS-GGSGG- EIVLT
QSPGTLSLSPGERATLSCRASQSVSMPFLAWYQQKPGQAPRLLIYGASSRATGIPDRFSGSGSGTDFTLTISRLEPED
FAVYYCQQMRGRPPTFGQGTKVEIK-SSSSGSSSSGSSSSG-ATTQQGSPVFAKLLAKNQASLCNTTLNWHSQDGAG
SSYLSQGLRYEEDKKELVVDSPGLYYVFLELKLSPTFTNTGHKVQGWVSLVLQAKPQVDDFDNLALTVELFPCSM
ENKLVDRSWSQLLLLKAGHRLSVGLRAYLHGAQDAYRDWELSYPNTTSFGLFLVKPDNPWE

F8(dDb)-4-1BBL: $F8_{VH}$-linker-$F8_{VL}$-linker-4-1BBL (Format **7**)

EVQLLESGGGLVQPGGSLRLSCAASGFTFSLFTMSWVRQAPGKGLEWVSAISGSGGSTYYADSVKGRFTISRDNSK
NTLYLQMNSLRAEDTAVYYCAKSTHLYLFDYWGQGTLVTVSS-GGSGG- EIVLTQSPGTLSLSPGERATLSCRASQS
VSMPFLAWYQQKPGQAPRLLIYGASSRATGIPDRFSGSGSGTDFTLTISRLEPEDFAVYYCQQMRGRPPTFGQGT
KVEIK-SSSSGSSSSGSSSSG-ATTQQGSPVFAKLLAKNQASLCNTTLNWHSQDGAGSSYLSQGLRYEEDKKELVVDS
PGLYYVFLELKLSPTFTNTGHKVQGWVSLVLQAKPQVDDFDNLALTVELFPCSMENKLVDRSWSQLLLLKAGHRL
SVGLRAYLHGAQDAYRDWELSYPNTTSFGLFLVKPDNPWE

F8(IgG)-4-1BBL_HC: $F8_{VL}$-$F8_{CL}$**$F8_{VH}$-$F8_{CH}$-linker-4-1BBL (Format **8**)

EIVLTQSPGTLSLSPGERATLSCRASQSVSMPFLAWYQQKPGQAPRLLIYGASSRATGIPDRFSGSGSGTDFTLTISR
LEPEDFAVYYCQQMRGRPPTFGQGTKVEIKRTVAAPSVFIFPPSDEQLKSGTASVVCLLNNFYPREAKVQWKVDN
ALQSGNSQESVTEQDSKDSTYSLSSTLTLSKADYEKHKVYACEVTHQGLSSPVTKSFNRGEC** EVQLLESGGGLV
QPGGSLRLSCAASGFTFSLFTMSWVRQAPGKGLEWVSAISGSGGSTYYADSVKGRFTISRDNSKNTLYLQMNSLRA
EDTAVYYCAKSTHLYLFDYWGQGTLVTVSSASTKGPSVFPLAPSSKSTSGGTAALGCLVKDYFPEPVTVSWNSGA
LTSGVHTFPAVLQSSGLYSLSSVVTVPSSSLGTQTYICNVNHKPSNTKVDKKVEPKSCDKTHTCPPCPAPELLGGPS
VFLFPPKPKDTLMISRTPEVTCVVVDVSHEDPEVKFNWYVDGVEVHNAKTKPREEQYNSTYRVVSVLTVLHQDW
LNGKEYKCKVSNKALPAPIEKTISKAKGQPREPQVYTLPPSRDELTKNQVSLTCLVKGFYPSDIAVEWESNGQPEN
NYKTTPPVLDSDGSFFLYSKLTVDKSRWQQGNVFSCSVMHEALHNHYTQKSLSLSPGK-SSSSGSSSSGSSSSG-ATT
QQGSPVFAKLLAKNQASLCNTTLNWHSQDGAGSSYLSQGLRYEEDKKELVVDSPGLYYVFLELKLSPTFTNTGHK
VQGWVSLVLQAKPQVDDFDNLALTVELFPCSMENKLVDRSWSQLLLLKAGHRLSVGLRAYLHGAQDAYRDWELS
YPNTTSFGLFLVKPDNPWE

F8(IgG)-4-1BBL_LC: $F8_{VL}$-$F8_{CL}$-linker-4-1BBL**$F8_{VH}$-$F8_{CH}$ (Format **9**)

EIVLTQSPGTLSLSPGERATLSCRASQSVSMPFLAWYQQKPGQAPRLLIYGASSRATGIPDRFSGSGSGTDFTLTISR
LEPEDFAVYYCQQMRGRPPTFGQGTKVEIKRTVAAPSVFIFPPSDEQLKSGTASVVCLLNNFYPREAKVQWKVD
NALQSGNSQESVTEQDSKDSTYSLSSTLTLSKADYEKHKVYACEVTHQGLSSPVTKSFNRGEC-SSSSGSSSSGSSSS
G-ATTQQGSPVFAKLLAKNQASLCNTTLNWHSQDGAGSSYLSQGLRYEEDKKELVVDSPGLYYVFLELKLSPTFTN
TGHKVQGWVSLVLQAKPQVDDFDNLALTVELFPCSMENKLVDRSWSQLLLLKAGHRLSVGLRAYLHGAQDAYRD
WELSYPNTTSFGLFLVKPDNPWE** EVQLLESGGGLVQPGGSLRLSCAASGFTFSLFTMSWVRQAPGKGLEWVSA
ISGSGGSTYYADSVKGRFTISRDNSKNTLYLQMNSLRAEDTAVYYCAKSTHLYLFDYWGQGTLVTVSSASTKGPSV
FPLAPSSKSTSGGTAALGCLVKDYFPEPVTVSWNSGALTSGVHTFPAVLQSSGLYSLSSVVTVPSSSLGTQTYICNV
NHKPSNTKVDKKVEPKSCDKTHTCPPCPAPELLGGPSVFLFPPKPKDTLMISRTPEVTCVVVDVSHEDPEVKFNW
YVDGVEVHNAKTKPREEQYNSTYRVVSVLTVLHQDWLNGKEYKCKVSNKALPAPIEKTISKAKGQPREPQVYTL
PPSRDELTKNQVSLTCLVKGFYPSDIAVEWESNGQPENNYKTTPPVLDSDGSFFLYSKLTVDKSRWQQGNVFSCS
VMHEALHNHYTQKSLSLSPGK

KSF(IgG)-4-1BBL_HC: KSF_{VL}-KSF_{CL}**KSF_{VH}-KSF_{CH}-linker-4-1BBL (Format **8**)

SELTQDPAVSVALGQTVRITCQGDSLRSYYASWYQQKPGQAPVLVIYGKNNRPSGIPDRFSGSSSGNTASLTITGAQ
AEDEADYYCNSSPLNRLAVVFGGGTKLTVLGCNSSPLNRLAVVFGGGTKLTVLGQPKAAPSVTLFPPSSEELQAN
KATLVCLISDFYPGAVTVAWKADSSPVKAGVETTTPSKQSNNKYAASSYLSLTPEQWKSHKSYSCQVTHEGSTVE
KTVAPTECS** EVQLLESGGGLVQPGGSLRLSCAASGFTFSSYAMSWVRQAPGKGLEWVSAISGSGGSTYYADSVK
GRFTISRDNSKNTLYLQMNSLRAEDTAVYYCAKSPKVSLFDYWGQGTLVTVSSASTKGPSVFPLAPSSKSTSGGTA
ALGCLVKDYFPEPVTVSWNSGALTSGVHTFPAVLQSSGLYSLSSVVTVPSSSLGTQTYICNVNHKPSNTKVDKKVE
PKSCDKTHTCPPCPAPELLGGPSVFLFPPKPKDTLMISRTPEVTCVVVDVSHEDPEVKFNWYVDGVEVHNAKTK
PREEQYNSTYRVVSVLTVLHQDWLNGKEYKCKVSNKALPAPIEKTISKAKGQPREPQVYTLPPSRDELTKNQVSL
TCLVKGFYPSDIAVEWESNGQPENNYKTTPPVLDSDGSFFLYSKLTVDKSRWQQGNVFSCSVMHEALHNHYTQKS
LSLSPGK-SSSSGSSSSGSSSSG-ATTQQGSPVFAKLLAKNQASLCNTTLNWHSQDGAGSSYLSQGLRYEEDKKELVV
DSPGLYYVFLELKLSPTFTNTGHKVQGWVSLVLQAKPQVDDFDNLALTVELFPCSMENKLVDRSWSQLLLLKAGH
RLSVGLRAYLHGAQDAYRDWELSYPNTTSFGLFLVKPDNPWE

KSF(scFv)-4-1BBL: KSF_{VH}-linker-KSF_{VL}-linker-4-1BBL (Format **5**)

EVQLLESGGGLVQPGGSLRLSCAASGFTFSSYAMSWVRQAPGKGLEWVSAISGSGGSTYYADSVKGRFTISRDNSK
NTLYLQMNSLRAEDTAVYYCAKSPKVSLFDYWGQGTLVTVSS-GGGGSGGGGSGGGG- SELTQDPAVSVALGQT
VRITCQGDSLRSYYASWYQQKPGQAPVLVIYGKNNRPSGIPDRFSGSSSGNTASLTITGAQAEDEADYYCNSSPLNR
LAVVFGGGTKLTVLG-SSSSGSSSSGSSSSG-ATTQQGSPVFAKLLAKNQASLCNTTLNWHSQDGAGSSYLSQGLRYE
EDKKELVVDSPGLYYVFLELKLSPTFTNTGHKVQGWVSLVLQAKPQVDDFDNLALTVELFPCSMENKLVDRSWS
QLLLLKAGHRLSVGLRAYLHGAQDAYRDWELSYPNTTSFGLFLVKPDNPWE

Figure C.1.: Sequences of the 4-1BBL fusion proteins developed in this study

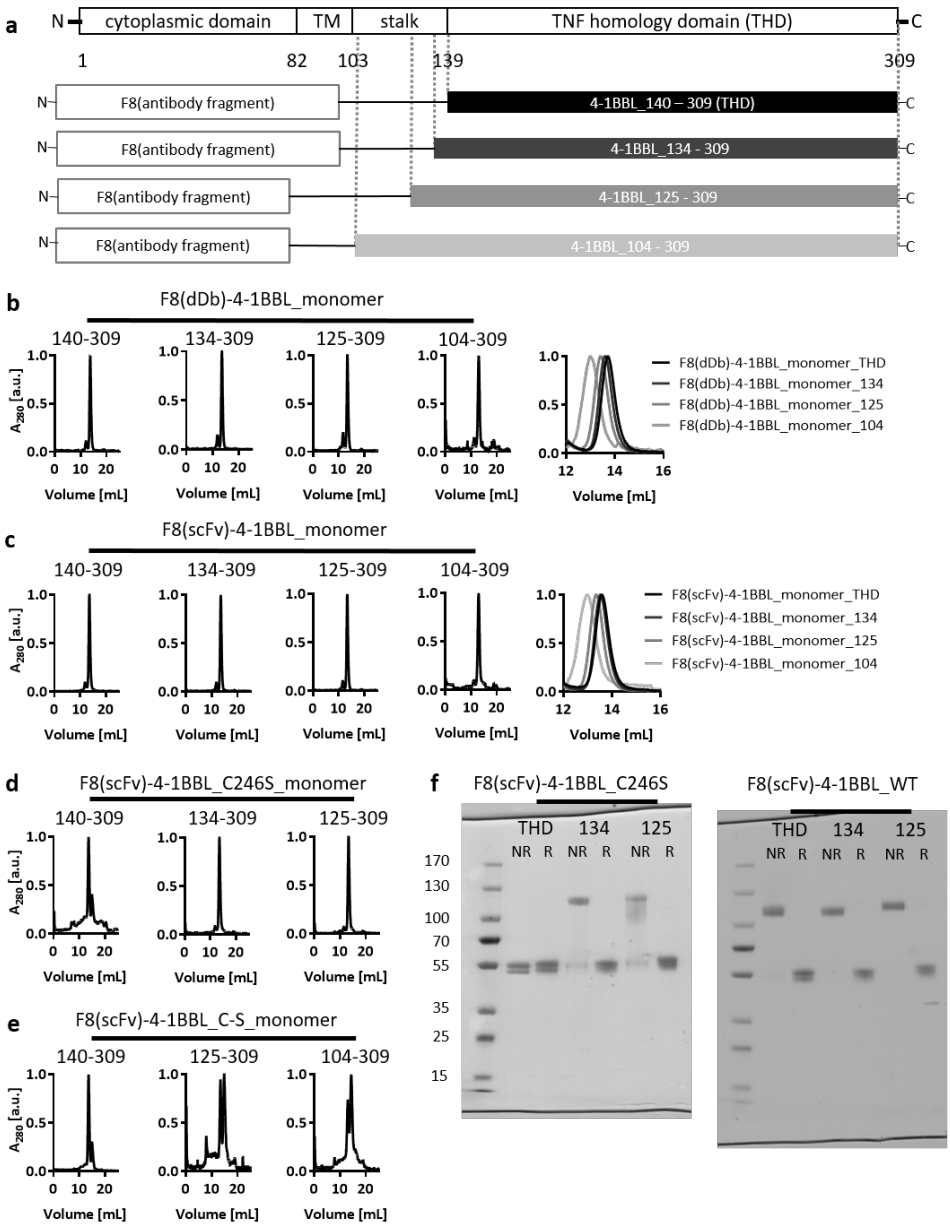

Figure C.2.: Screening of the extracellular domain and C-S mutants of murine 4-1BBL to determine the optimal design of the 4-1BBL moiety in F8-4-1BBL **(a)** schematic depiction of the domain architecture of 4-1BBL and of the constructs that were screened containing different parts of the stalk region in addition to the TNF-homology domain (THD). The numbers correspond to the amino acid number in murine 4-1BBL. **(b)** Size exclusion profiles of F8 in the diabody (dDb) format linked to a single 4-1BBL subunit including different parts of the extracellular domain of 4-1BBL. Longer fragments of 4-1BBL were more prone to aggregation and also gave lower expression yields (data not shown) **(c)** size exclusion profiles F8 in the scFv format linked to a single 4-1BBL subunit **(d)** Size exclusion profiles of different F8-4-1BBL variants featuring an C246S mutation in the 4-1BBL subunit preventing the formation of the disulfide bond that links two THD of 4-1BBL **(e)** Size exclusion profiles of different variants of F8-4-1BBL where all cysteines in the 4-1BBL domain were mutated to serines demonstrating the role of the disulfide bond for the stability of the fusion protein **(f)** SDS PAGE of the different C246S mutants revealing the presence of a second disulfide-forming cysteine outside the THD (NR: non-reducing, R: reducing)

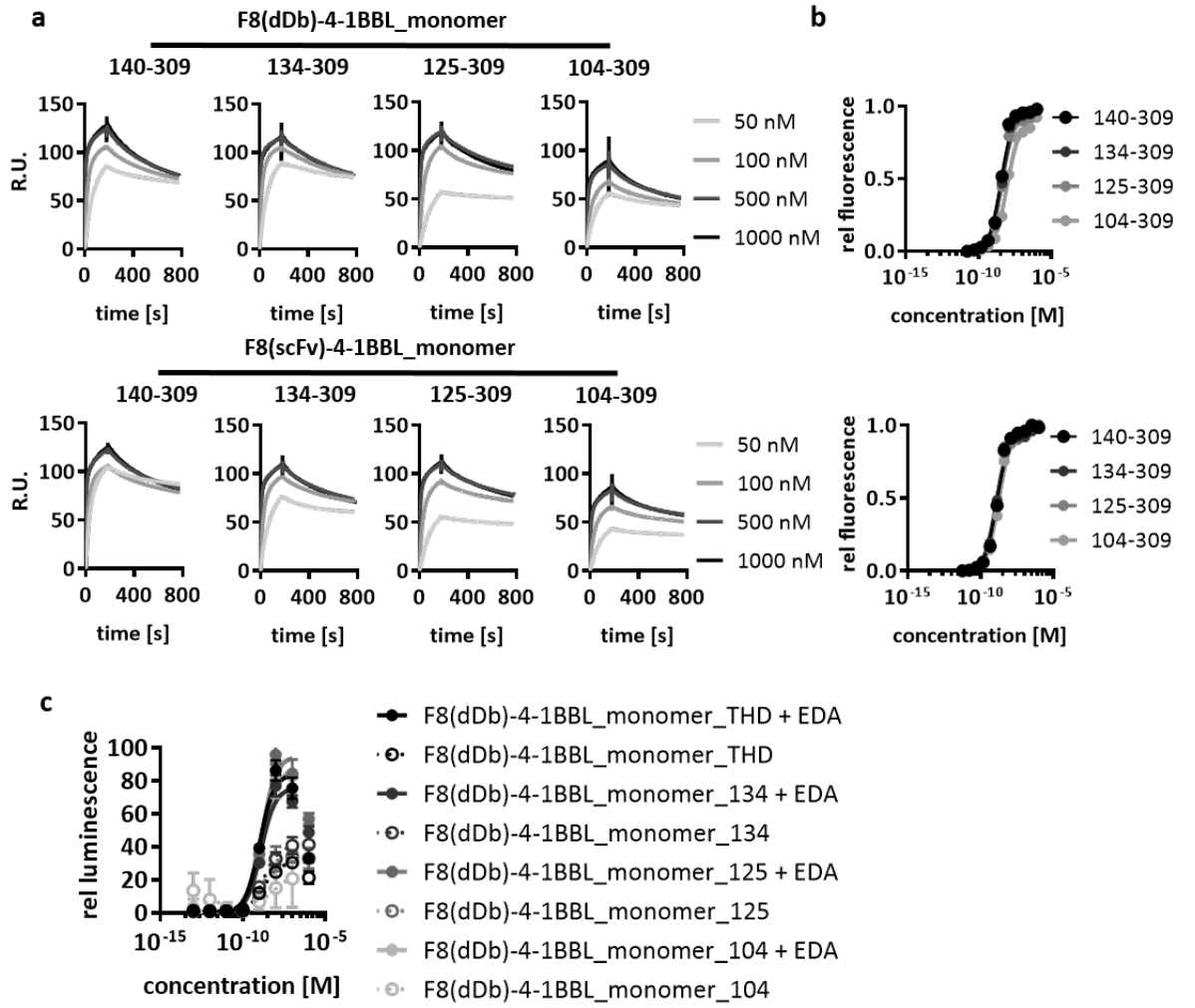

Figure C.3.: The different F8-4-1BBL variants all retained binding to EDA and to 4-1BB as evidenced by **(a)** the Surface Plasmon Resonance measurements of binding to EDA and **(b)** the flow cytometry experiments with the 4-1BB expressing CTLL-2 cells (top: antibody in the diabody format, bottom: antibody in the scFv format) and **(c)** comparative bioactivity assays using the CTLL-2 NF-κB cell line revealed that the TNF homology domain is sufficient to achieve full signaling activity. The numbers refer to the amino acid numbers of murine 4-1BBL that were included in the F8-4-1BBL construct.

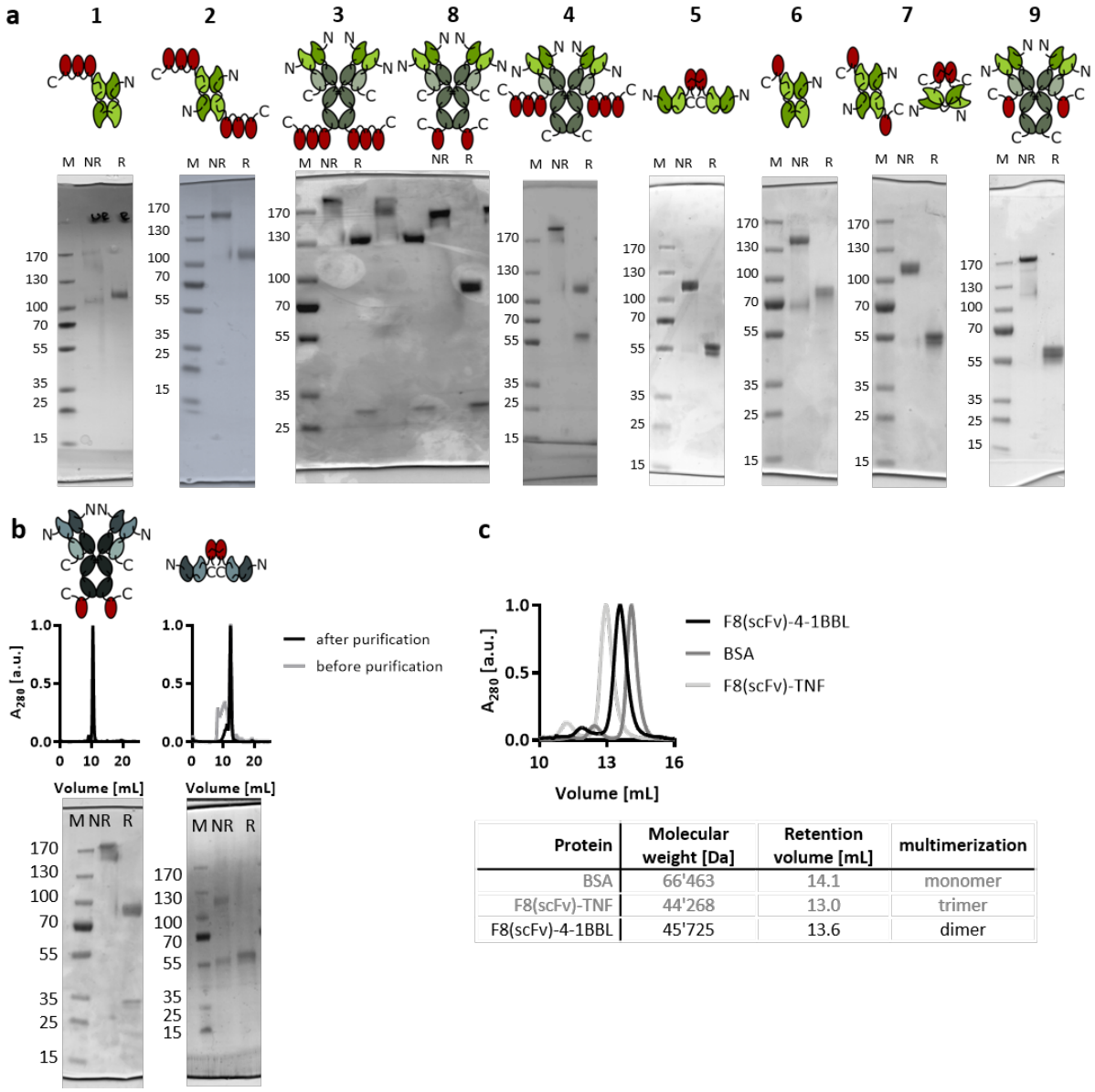

Protein	Molecular weight [Da]	Retention volume [mL]	multimerization
BSA	66'463	14.1	monomer
F8(scFv)-TNF	44'268	13.0	trimer
F8(scFv)-4-1BBL	45'725	13.6	dimer

Figure C.4.: (a) SDS PAGE analysis of the nine F8-4-1BBL formats that were produced in this study (M: marker, NR: non-reducing sample buffer, R: reducing sample buffer) **(b)** Size exclusion chromatography profiles and SDS PAGE gels of the KSF constructs that were used for the biodistribution. The aggregates of the KSF(scFv)-4-1BBL could be efficiently removed by preparative size exclusion chromatography **(c)** comparative size exclusion chromatography showed that F8(scFv)-4-1BBL forms a dimer in solution since the retention volume was higher than for F8(scFv)-TNF that forms a non-covalent homotrimer

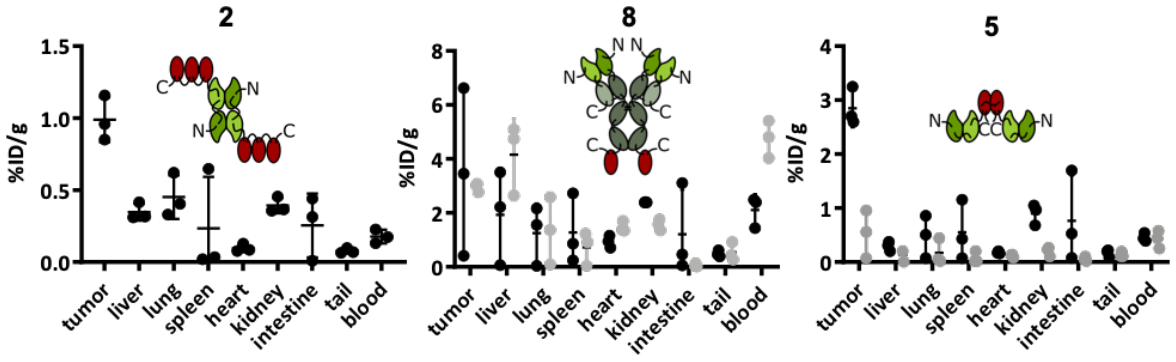

Figure C.5.: *In vivo* biodistribution studies of three F8-4-1BBL formats. The mice were sacrificed 24 h after the injection of the radio-iodinated proteins and the radioactivity of excised organs was measured and expressed as percent injected dose per gram of tissue (%ID/g). The KSF antibody targeting hen egg lysozyme was used as untargeted control. Shown are individual measurements and mean ± SD.

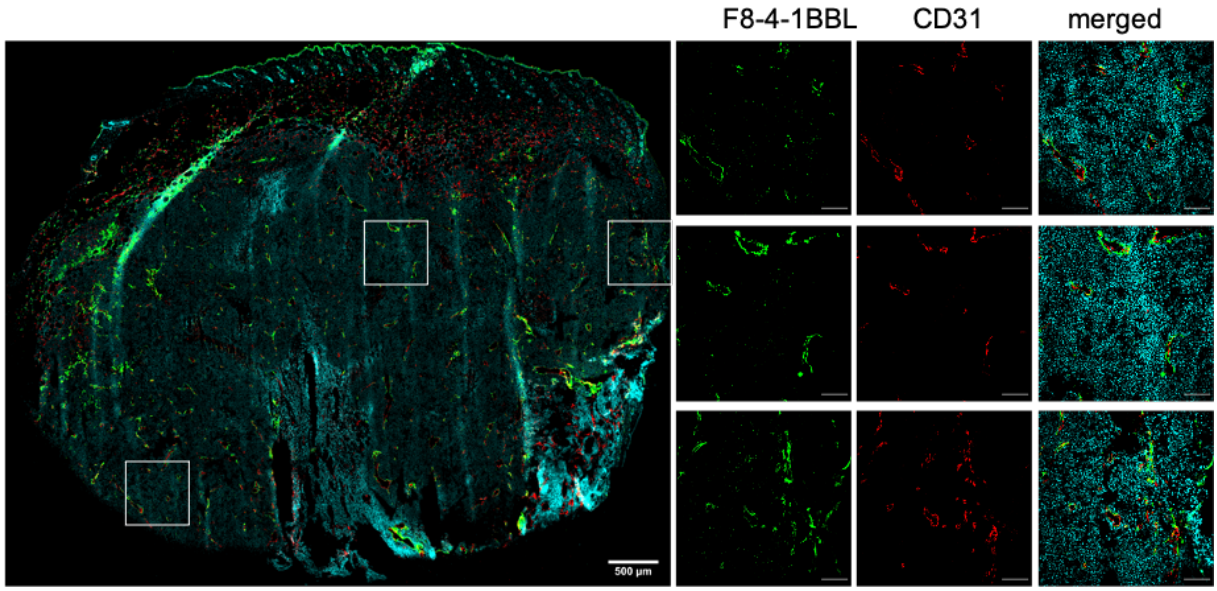

Figure C.6.: Serial images were taken of the tumor sections after ex vivo detection of FITC-labelled F8-4-1BBL and assembled to provide an overview of the entire tumor section. The channels showing CD31 and F8-4-1BBL are shown separately as well as the composite for relevant portions of the tumor sections (indicated by white squares) to show the colocalization of EDA-targeted antibody-cytokine conjugates and the tumor vasculature (green: αFITC, red: αCD31, cyan: nuclei; the scale bars in the single images represents 100 µm).

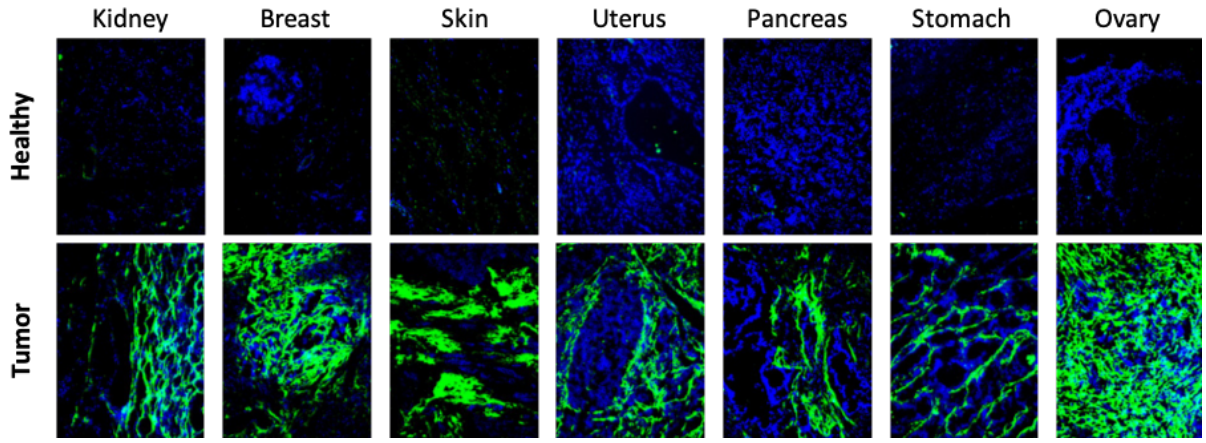

Figure C.7.: The expression of EDA was assessed on human tissue microarrays using FITC-labelled F8 in the IgG format. (green: EDA, blue: nuclei).

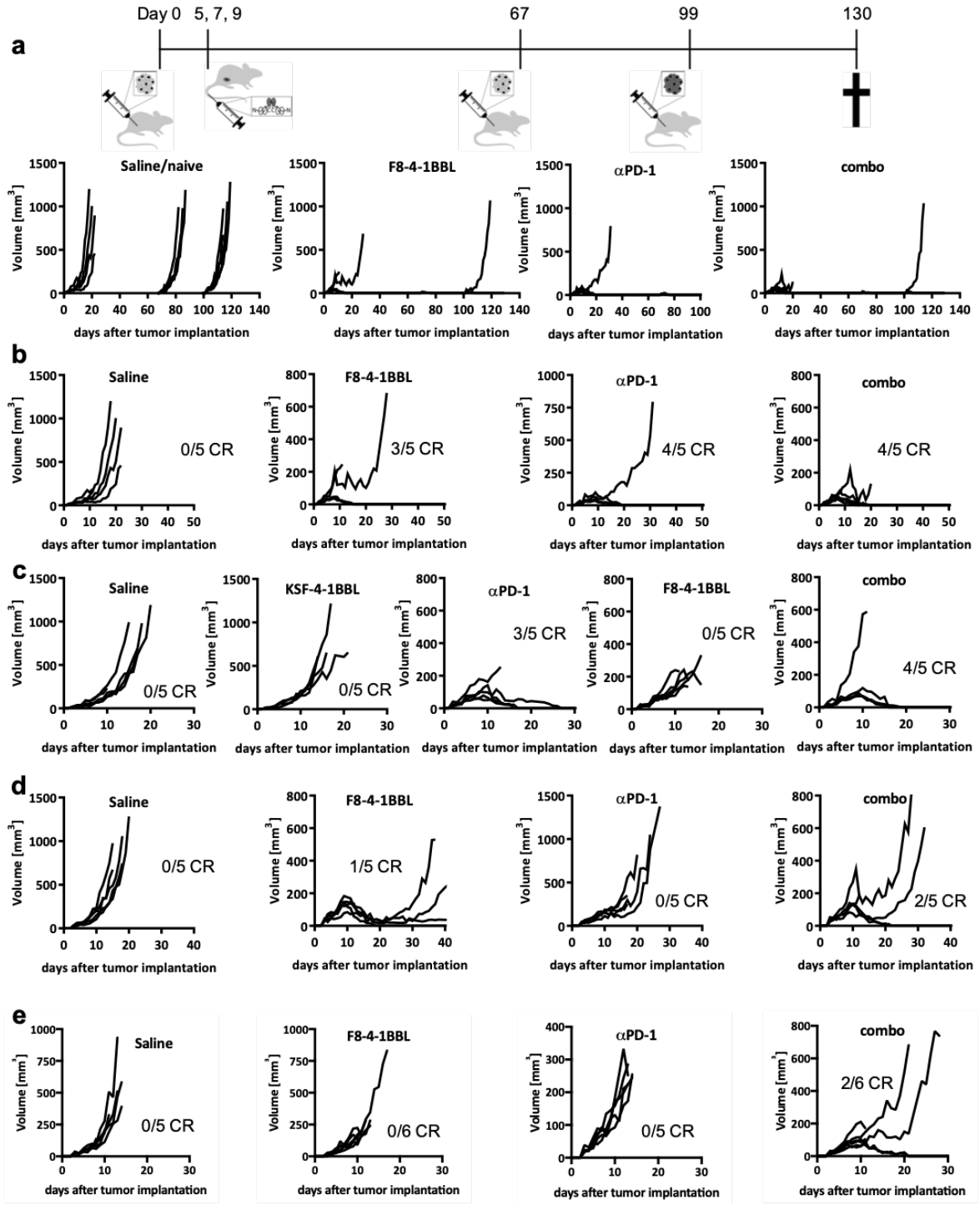

Figure C.8.: Individual growth curves of the therapies **(a)** mice cured from WEHI-164 fibrosarcoma in the preventive setting were challenged with WEHI-164 fibrosarcoma cells on day 67 and mice from the F8-4-1BBL and the combo group also received a challenge with CT26 colon carcinoma cells on day 99. All the naïve mice developed tumors while the cured mice rejected subsequent challenges with WEHI-164 fibrosarcoma cells and most were also immune against CT26 colon carcinoma. **(b)** the individual growth curves of WEHI-164 fibrosarcoma bearing mice that received the treatment starting on day 5 after tumor implantation when the tumor volume was > 40 mm^3 **(c)** the individual growth curves of WEHI-164 fibrosarcoma-bearing mice that received the treatment starting on day 7 after tumor implantation when the tumor volume was > 80 mm^3

Figure C.8.: (continued) **(d)** individual growth curves of the CT26 colon-carcinoma-bearing mice that received the treatment starting on day 7 when the tumor volume was > 80 mm^3 **(e)** individual growth curves of the MC38 colon-carcinoma-bearing mice that received the treatment starting on day 7 when the tumor volume was > 75 mm^3 (CR: complete response)

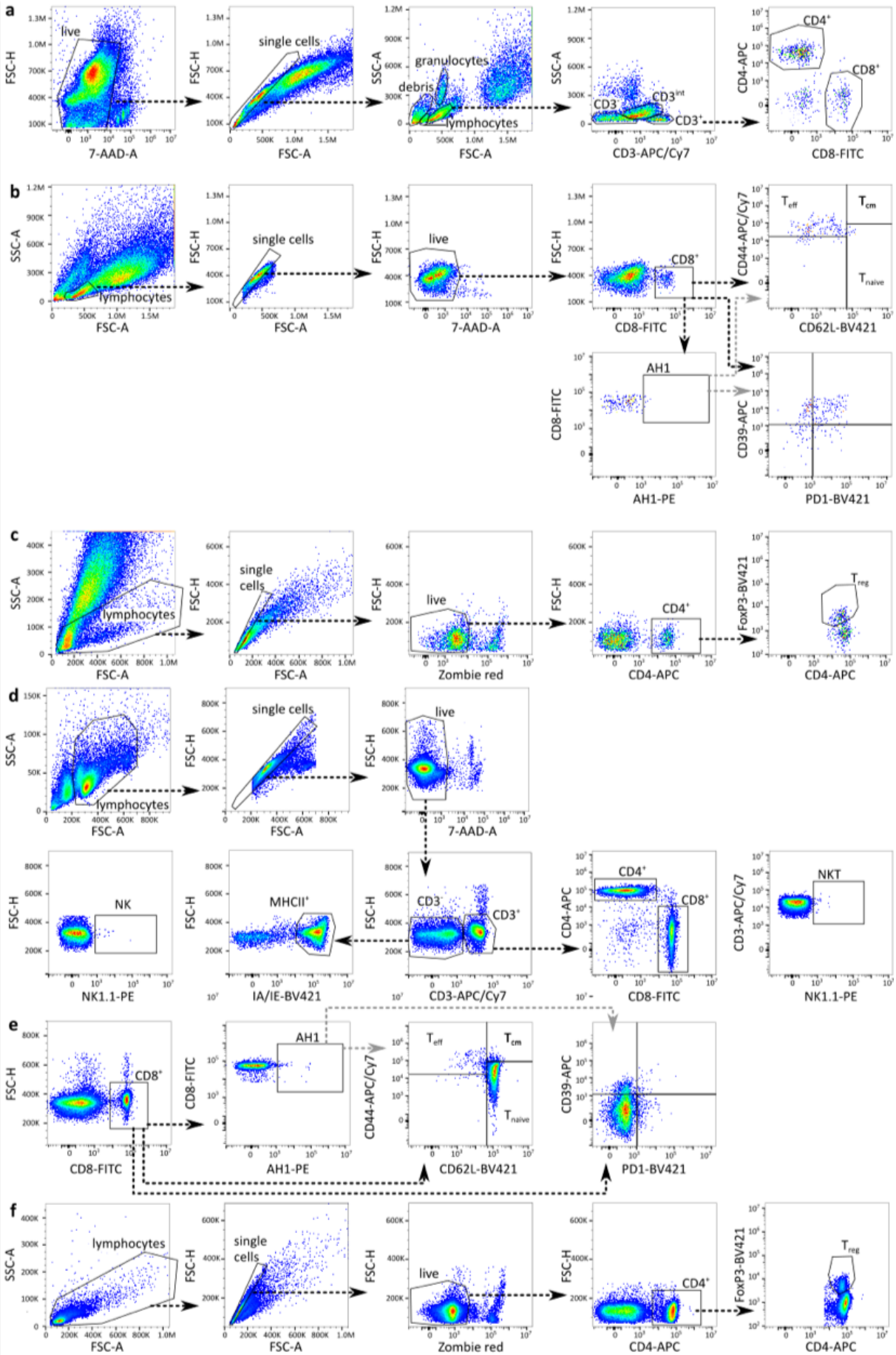
a
live
FSC-H
7-AAD-A
single cells
FSC-A
granulocytes
debris
lymphocytes
SSC-A
CD3
CD3int
CD3+
CD3-APC/Cy7
CD4+
CD8+
CD4-APC
CD8-FITC
b
lymphocytes
CD8+
CD44-APC/Cy7
Teff
Tcm
Tnaive
CD62L-BV421
AH1
AH1-PE
CD39-APC
PD1-BV421
c
Zombie red
CD4+
FoxP3-BV421
Treg
CD4-APC
d
NK
NK1.1-PE
MHCII+
IA/IE-BV421
CD3-
CD3+
NKT
e
CD8+
CD8-FITC
AH1
AH1-PE
CD62L-BV421
PD1-BV421
f

Figure C.9.: Gating strategy for the flow cytometry analysis of the tumor-infiltrating lymphocytes (TILs) and the tumor-draining lymph nodes (TDLN) **(a)** in order to quantify the tumor infiltrates, dead cells were excluded first by live/dead stain and then by scattering. Total living cells were calculated by subtracting dead cells and debris from the total number of events. Lymphocytes were further divided into the different subgroups (NKT, NK and MHCII+) as shown for the lymph nodes. **(b)** To assess the phenotype of tumor-infiltrating CD8+ cells, the events were gated by scattering and then live/dead, followed by CD8+ and AH1+. The same gates were applied to CD8+ and AH1+ cells for assessing the phenotypes. **(c)** To gate fixed tumor samples stained for intracellular FoxP3 the events were first gated by scattering and live/dead before the CD4+ cells were assessed for FoxP3 (Treg). **(d)** To quantify the immune subsets in the tumor-draining lymph node (TDLN), the events were first gated by scattering and live/dead before the subsets were divided by CD3 expression and further markers. **(e)** The phenotype of CD8+ in the TDLN was assessed as described for the tumor. **(f)** Regulatory T cells in the TDLN were also assessed with the same gating strategy as described for the tumor (FSC: forward scattering, SSC: side scattering)

D. List of vectors

The following pages contain a list of vectors that were produced during this PhD project. Most sequences were introduced by into pcDNA3.1(+) vectors by Gibson Isothermal Assembly. The cloning strategy is described in the respective chapters as part of the Methods section.

Project	Name	Insert	Backbone	Resistance	Description
4-1BBL	pJM008	F8(scDb)-(m4-1BBL_aa139-309)$_3$	pcDNA3.1(+)	Amp	F8 in single-chain diabody format fused to single-chain trimeric m4-1BBL (amino acids 139 - 309)
4-1BBL	pJM012	F8(dDb)-(m4-1BBL_aa139-309)$_3$	pcDNA3.1(+)	Amp	F8 in dimeric diabody format fused to single-chain trimeric m4-1BBL (amino acids 139 - 309)
CD40L	pJM013	F8(scDb)-(CD40L)$_3$	pcDNA3.1(+)	Amp	F8 in single-chain diabody format fused to single-chain trimeric CD40L
CD40L	pJM020	F8(dDb)-(CD40L)$_3$	pcDNA3.1(+)	Amp	F8 in dimeric diabody format fused to single-chain trimeric CD40L
4-1BBL	pJM022	KSF(dDb)-(m4-1BBL_aa139-309)$_3$	pcDNA3.1(+)	Amp	KSF in dimeric diabody format fused to single-chain trimeric m4-1BBL (amino acids 139 - 309)
CD40L	pJM023	F8(scDb)-(CD40L_N239Q)$_3$	pcDNA3.1(+)	Amp	same constructas pJM013 but featuring the N239Q mutation in the CD40L domain
CD40L	pJM024	F8(dDb)-(CD40L_N239Q)$_3$	pcDNA3.1(+)	Amp	same constructas pJM020 but featuring the N239Q mutation in the CD40L domain
4-1BBL	pJM025	F8(dDb)-(m4-1BBL_C->S)$_3$	pcDNA3.1(+)	Amp	same construct as pJM028 but with all cysteine residues in the m4-1BBL domain mutated to serines
4-1BBL	pJM026	F8(scDb)-m4-1BBL_aa139-309	pcDNA3.1(+)	Amp	F8 in single-chain diabody format fused to a single unit of m4-1BBL (amino acids 139 - 309)
4-1BBL	pJM027	F8(dDb)-m4-1BBL_aa139-309	pcDNA3.1(+)	Amp	F8 in dimeric diabody format fused to a single unit of m4-1BBL (amino acids 139 - 309)
4-1BBL	pJM028	F8(scFv)-m4-1BBL_aa139-309	pcDNA3.1(+)	Amp	F8 in scFv format fused to a single unit of m4-1BBL (amino acids 139 - 309)
GITRL	pJM029	F8(dDb)-(mGITRL)$_3$	pcDNA3.1(+)	Amp	F8 in dimeric diabody format fused to single-chain trimeric mGITRL (amino acids 46 - 170)

4-1BBL	pJM030	F8(scFv)-m4-1BBL_C->S	pcDNA3.1(+)	Amp	same construct as pJM012 but with all cysteine residues in the m4-1BBL domain mutated to serines
4-1BBL	pJM031	F8(dDb)-m4-1BBL_aa134-309	pcDNA3.1(+)	Amp	F8 in dimeric diabody format fused to a single unit of m4-1BBL (amino acids 134 - 309)
4-1BBL	pJM032	F8(scFv)-m4-1BBL_aa134-309	pcDNA3.1(+)	Amp	F8 in scFv format fused to a single unit of m4-1BBL (amino acids 134 - 309)
GITRL	pJM033	F8(scFv)-mGITRL	pcDNA3.1(+)	Amp	F8 in scFv format fused to a single unit of mGITRL (amino acids 46 - 170)
4-1BBL	pJM034	F8(dDb)-m4-1BBL_aa125-309	pcDNA3.1(+)	Amp	F8 in dimeric diabody format fused to a single unit of m4-1BBL (amino acids 125 - 309)
4-1BBL	pJM035	F8(scFv)-m4-1BBL_aa125-309	pcDNA3.1(+)	Amp	F8 in scFv format fused to a single unit of m4-1BBL (amino acids 125 - 309)
4-1BBL	pJM036	F8(scFv)-m4-1BBL_aa104-309	pcDNA3.1(+)	Amp	F8 in scFv format fused to a single unit of m4-1BBL (amino acids 104 - 309)
4-1BBL	pJM037	F8(dDb)-m4-1BBL_aa104-309	pcDNA3.1(+)	Amp	F8 in dimeric diabody format fused to a single unit of m4-1BBL (amino acids 104 - 309)
4-1BBL	pJM038	F8(scFv)-m4-1BBL_C->S_aa125-309	pcDNA3.1(+)	Amp	same construct as pJM035 but with all cysteine residues in the m4-1BBL domain mutated to serines
4-1BBL	pJM039	F8(scFv)-m4-1BBL_C->S_aa104-309	pcDNA3.1(+)	Amp	same construct as pJM036 but with all cysteine residues in the m4-1BBL domain mutated to serines
4-1BBL	pJM040	F8(scFv)-4-1BBL_C246S_aa139-309	pcDNA3.1(+)	Amp	same construct as pJM028 but with C246 in the m4-1BBL domain mutated to serine
4-1BBL	pJM041	F8(scFv)-4-1BBL_C246S_aa134-309	pcDNA3.1(+)	Amp	same construct as pJM032 but with C246 in the m4-1BBL domain mutated to serine
4-1BBL	pJM042	F8(scFv)-4-1BBL_C246S_aa125-309	pcDNA3.1(+)	Amp	same construct as pJM035 but with C246 in the m4-1BBL domain mutated to serine
CellLine	pJM046	NF-kB_secNluc-T2A-mCherry	pCDH	Amp	viral vector for NF-$\varkappa$B reporter cell line
GITRL	pJM047	KSF(dDb)-$(mGITRL)_3$	pcDNA3.1(+)	Amp	KSF in dimeric diabody format fused to single-chain trimeric mGITRL (amino acids 46 - 170)

4-1BBL	pJM048	KSF(scFv)-4-1BBL_139-309	pcDNA3.1(+)	Amp	KSF in scFv format fused to a single unit of m4-1BBL (amino acids 139 - 309)
GITRL	pJM051	F8(dDb)-(mGITRL_N74Q)$_3$	pcDNA3.1(+)	Amp	same construct as pJM029 but with N74 mutated to glutamine in the GITRL domain
GITRL	pJM052	F8(dDb)-(mGITRL_N74A)$_3$	pcDNA3.1(+)	Amp	same construct as pJM029 but with N74 mutated to alanine in the GITRL domain
4-1BBL	pJM054	F8(IgG)-(4-1BBL_aa139-309)$_3$_HC	pMM137	Amp	single-chain trimeric m4-1BBL fused to the heavy chain of F8 in the human IgG1 format
4-1BBL	pJM055	F8(IgG)-4-1BBL_aa139-309_HC	pMM137	Amp	a single unit of m4-1BBL fused to the heavy chain of F8 in the human IgG1 format
GITRL	pJM057	F8(IgG)-(mGITRL)$_3$_HC	pMM137	Amp	single-chain trimeric mGITRL fused to the heavy chain of F8 in the human IgG1 format
GITRL	pJM058	F8(IgG)-mGITRL_HC	pMM137	Amp	a single unit of mGITRL fused to the heavy chain of F8 in the human IgG1 format
GITRL	pJM062	F8(dDb)-(mGITRL_N74Q_N157T)$_3$	pcDNA3.1(+)	Amp	same construct as pJM029 but with N74 mutated to glutamine and N157 mutated to threonine in the GITRL domain
GITRL	pJM063	F8(dDb)-(mGITRL_N74S_N157T)$_3$	pcDNA3.1(+)	Amp	same construct as pJM029 but with N74 mutated to serine and N157 mutated to threonine in the GITRL domain
GITRL	pJM064	F8(dDb)-(mGITRL_N74A_N157T)$_3$	pcDNA3.1(+)	Amp	same construct as pJM029 but with N74 mutated to alanine and N157 mutated to threonine in the GITRL domain
GITRL	pJM066	F8(dDb)-(mGITRL_N157T)$_3$	pcDNA3.1(+)	Amp	same construct as pJM029 but with N157 mutated to threonine in the GITRL domain
4-1BBL	pJM070	KSF(IgG)-4-1BBL_aa139-309_HC	pcDNA3.1(+)	Amp	a single unit of m4-1BBL fused to the heavy chain of KSF in the human IgG1 format
4-1BBL	pJM071	F8(IgG)-(4-1BBL_aa139-309)$_3$_LC	pcDNA3.1(+)	Amp	single-chain trimeric m4-1BBL fused to the light chain of F8 in the human IgG1 format
4-1BBL	pJM072	F8(IgG)-4-1BBL_aa139-309_LC	pcDNA3.1(+)	Amp	a single unit of m4-1BBL fused to the light chain of F8 in the human IgG1 format

GITRL	pJM075	F8(IgG)-mGITRL_LC	pcDNA3.1(+)	Amp	a single unit of mGITRL fused to the light chain of F8 in the human IgG1 format
GITRL	pJM078	F8(IgG)-(mGITRL_N74S_N157T)$_3$_HC	pcDNA3.1(+)	Amp	single-chain trimeric mGITRL with the N74S N157T double mutation fused to the heavy chain of F8 in the human IgG1 format
GITRL	pJM081	KSF(dDb)-(mGITRL_N74S_N157T)$_3$	pcDNA3.1(+)	Amp	same construct as pJM047 but with N74 mutated to serine and N157 mutated to threonine in the GITRL domain
GITRL	pJM084	F8(IgG)-(mGITRL_N74S_N157T)$_3$_LC	pcDNA3.1(+)	Amp	single-chain trimeric mGITRL with the N74S N157T double mutation fused to the light chain of F8 in the human IgG1 format
GITRL	pJM085	KSF(IgG)-(mGITRL_N74S_N157T)$_3$_LC	pcDNA3.1(+)	Amp	single-chain trimeric mGITRL with the N74S N157T double mutation fused to the light chain of KSF in the human IgG1 format
4-1BBL	pJM089	F8(scFv)-h4-1BBL_93-254	pcDNA3.1(+)	Amp	F8 in scFv format fused to a single unit of human 4-1BBL (amino acids 93 - 254)
4-1BBL	pJM090	F8(scFv)-h4-1BBL_93-254_Y142C	pcDNA3.1(+)	Amp	same construct as pJM089 but with a Y142C mutation in the h4-1BBL domain
4-1BBL	pJM091	h4-1BB_lentivirus	pCDH	Amp	lentivirus encoding human 4-1BB
4-1BBL	pJM092	F8(scFv)-h4-1BBL_93-254_A188C	pcDNA3.1(+)	Amp	same construct as pJM089 but with a A18C mutation in the h4-1BBL domain

Table D.1.: List of vectors that were cloned in the course of this PhD thesis project

E. List of primers

The following pages contain a list of primers that were used during this PhD project.

Project		Overhang	Sequence	binds to	used for
general	P22		CTAACTAGAGAACCCACTGCTTACTG	CMV promoter on pcDNA3.1+	sequencing, colony PCR
general	P47		CATGAAGAATCTGCTTAGGGTTAG	pCDNA3.1+ before CMV promoter	sequencing of CMV promoter
general	P48		CTTCTGAGGCGGAAAGAAC	pCDNA3.1+ before f1 origin	sequencing of f1 origin
general	P6		TAGAAGGCACAGTCGAGGC	pCDNA3.1+ end of MCS	sequencing, colony PCR, amplification of inserts in pcDNA3.1+
general	P7		GCCTCGACTGTGCCTTCTA	pCDNA3.1+ end of MCS	amplification of pcDNA3.1+ backbone for Gibson assembly
general	P18		CGAgtgcacACCTGTAGCC	signal peptide	sequencing, amplification for Gibson assembly
general	P75		CGAGTGCACACCTGTAGCC	signal sequence of KSF	sequencing, amplification for Gibson assembly
general	P76		CTCGTCGCTGTGGCTACAG	signal sequence of KSF	sequencing, amplification for Gibson assembly
general	P29		Ttcatcctcggggagct	SSSSG-linker	sequencing, amplification of inserts for Gibson assembly
general	P30		agctccccgaggatgaA	SSSSG-linker	sequencing, amplification of inserts for Gibson assembly
general	P58		gccgctggacgatgag	SSSSG-linker	sequencing, amplification of inserts for Gibson assembly
general	P74		cggctcatcgtccagc	SSSSG-linker	sequencing, amplification of inserts for Gibson assembly
general	P100		TTTGATTTCCACCTTGGTCC	F8 VL	cloning scFv
general	P5		GGGACCAAGGTGGAAATC	F8 VL	sequencing, amplification of inserts for Gibson assembly
general	P51		CAGTGTATTACTGTCAGCAGATGC	F8 VL	clone dimeric diabody format
general	P52		CAAAATCTTCAGGCTCCAGTC	F8 VL	clone dimeric diabody format
general	P8		cccgaggatgaACTTTTG	F8-F8-scLIGHT	amplification of backbone for Gibson assembly
general	P9		GTGGAAATCAAAAGTTCATCC	F8 VL linker	sequencing
general	P146		TCCAGACTAGTCCACCATGGG	F8 IgG VL	clone IgG light chain fusion
general	P147	agctccccgaggatgaACT	ACACTCTCCCCTGTTGAAGC	F8 IgG VL	clone IgG light chain fusion
general	P148		CTCCACAGGTGTCCAGAAGC	F8 IgG VH	clone IgG heavy chain fusion
general	P149	agctccccgaggatgaACT	TTTACCCGGAGACAGGGAGAG	F8 IgG VH	clone IgG heavy chain fusion
general	P162		CAGCACCTGAACTCCTGGG	F8 IgG VH	sequencing of heavy chain fusions
general	P77		GAGGTGCAGCTGTTGGAGTC	KSF VH	sequencing, amplification of inserts for Gibson assembly
general	P78		GCTGTACCAAGCCTCCCC	KSF VH	sequencing, amplification of inserts for Gibson assembly
general	P79	CTACAGGTGTGCACTCG	GAGGTGCAGCTGTTGGAGTC	KSF VH	sequencing, amplification of inserts for Gibson assembly

Project		Overhang	Sequence	binds to	used for
cell line	P107	ggagaaggcaactggaccgaaggcgcttgtggagaaggagtt	catggtggctttaccaacag	nanolucplasmid	add secretion tag
cell line	P108	ctgggcctgctcctggtgttgcctgctgccttccctgcccca	GTCTTCACACTCGAAGATTTCG	Nluc	add secretion tag
cell line	P109	gaacgcattctggcg	GAGGGCAGAGGAAGTCTTC	T2A	
cell line	P110	gagtcgcggcc	TTACTTGTACAGCTCGTCCATG	mCherry	
cell line	P120		TCCCTGCTGTTCCGAGTAAC	Nluc	colony PCR, sequencing
cell line	P121		gcccaatacgcaaacggatc	pNluc3.2	colony PCR
cell line	P122		GCTTGGATACACGCCGC	murine virus	colony PCR
cell line	P123	TAAgagtcgcggcc	AATTCTCACGGCTTTCCG	PEST	insert T2A
cell line	P124	gaaatgttctggcacctgc	gatcgcagatccactagtatcg	virus vector	insert Nluc
CD40L	P82	CTCCGTATTTGTA**CAG**	GTCACGGAAGCAAGCC	CD154, 3rd unit	QC to remove glycosite
CD40L	P83	TGCTTCCGTGAC**CTG**	TACAAATACGGAGGCTCCC	CD154, 3rd unit	QC to remove glycosite
CD40L	P84	GTGTCTTCGTA**CAA**	GTAACTGAGGCATCCCAAG	CD154, 2nd unit	QC to remove glycosite
CD40L	P85	GCCTCAGTTAC**TTG**	TACGAAGACACTTGCTCCTG	CD154, 2nd unit	QC to remove glycosite
CD40L	P86	CTGTGTTTGTC**CAG**	GTGACTGAAGCAAGCCAAG	CD154, 1st unit	QC to remove glycosite
CD40L	P87	GCTTCAGTCAC**CTG**	GACAAACACAGAAGCACCAG	CD154, 1st unit	QC to remove glycosite
GITRL	P184	agctccccgaggatgaACT	TGAACATTCTGTAGGGGCCAC	KSF IgG VL	clone IgG light chain fusion
GITRL	P176	GACTGTGCCTTCTA	CGCATTGTCTGAGTAGGTGTC	pMM137 upstream of light chain	GITRL light chain fusion
GITRL	P163	CATATTCAGAAAA**C**	TAACACATACTGGGGGATCATC	GITRL (1st module)	N157T
GITRL	P164	CAGTATGTGTTA**G**	TTTTCTGAATATGGTCTTTAGAGTTGAAC	GITRL (1st module)	N157T
GITRL	P165	CACATACAAAAGA**C**	CAATACCTATTGGGGAATTATATTGATGC	GITRL (2nd module)	N157T
GITRL	P166	CAATAGGTATTG**G**	TCTTTTGTATGTGATCCTTACTATTAAATTTC	GITRL (2nd module)	N157T
GITRL	P167	CACATCCAAAAAA**C**	CAACACTTATTGGGGCATAATCC	GITRL (3rd module)	N157T
GITRL	P168	CAATAAGTGTTG**G**	TTTTTTGGATGTGGTCTTTGGAATTG	GITRL (3rd module)	N157T
GITRL	P136	CCTCACTGTGTG**GC**	TACGACATCTGATGGGAAGCTG	GITRL (1st module)	N74A
GITRL	P137	CCTCATTGTGTT**GC**	TACCACTTCTGATGGCAAACTC	GITRL (2nd module)	N74A
GITRL	P138	CCCCACTGCGTA**GC**	CACTACATCCGATGGTAAACTGAAAATTC	GITRL (3rd module)	N74A
GITRL	P139	ATCGGATGTAGT**GGC**	TACGCAGTGGGGTTTTGGTG	GITRL (3rd module)	N74A
GITRL	P140	ATCAGAAGTGGT**AGC**	AACACAATGAGGCTTAGGACTAG	GITRL (2nd module)	N74A
GITRL	P141	ATCAGATGTCGT**AGC**	CACACAGTGAGGTTTGGGAG	GITRL (1st module)	N74A
GITRL	P130	CCTCACTGTGTG**CAA**	ACGACATCTGATGGGAAGCTG	GITRL (1st module)	N74Q
GITRL	P131	CCTCATTGTGTT**CAA**	ACCACTTCTGATGGCAAACTC	GITRL (2nd module)	N74Q
GITRL	P132	CCCCACTGCGTA**CAA**	ACTACATCCGATGGTAAACTGAAAATTC	GITRL (3rd module)	N74Q
GITRL	P133	ATCGGATGTAGT**TTG**	TACGCAGTGGGGTTTTGGTG	GITRL (3rd module)	N74Q
GITRL	P134	ATCAGAAGTGGT**TTG**	AACACAATGAGGCTTAGGACTAG	GITRL (2nd module)	N74Q
GITRL	P135	ATCAGATGTCGT**TTG**	CACACAGTGAGGTTTGGGAG	GITRL (1st module)	N74Q
GITRL	P152	CTCACTGTGTGA**G**	TACGACATCTGATGGGAAGCTG	GITRL (1st module)	N74S
GITRL	P153	CTCATTGTGTTA**G**	TACCACTTCTGATGGCAAACTC	GITRL (2nd module)	N74S
GITRL	P154	CCCACTGCGTAA**G**	CACTACATCCGATGGTAAACTGAAAATTC	GITRL (3rd module)	N74S
GITRL	P155	TCGGATGTAGTG**C**	TTACGCAGTGGGGTTTTGG	GITRL (3rd module)	N74S
GITRL	P156	TCAGAAGTGGTA**C**	TAACACAATGAGGCTTAGGACTAG	GITRL (2nd module)	N74S
GITRL	P157	CAGATGTCGTA**C**	TCACACAGTGAGGTTTGGGAG	GITRL (1st module)	N74S
GITRL	P177	AGTGGCATATGAC**C**	AGTCCTAAGCCTCATTGTGTTAG	GITRL (2nd module)	QC remove SpeI cutting site
GITRL	P178	GAGGCTTAGGACT**G**	GTCATATGCCACTTGCTGCTAC	GITRL (2nd module)	QC remove SpeI cutting site

Project		Overhang	Sequence	binds to	used for
4-1BBL	P102	AATGCAGACCAGGTCACCCCTGTTTCC	CACATAGGATGTCCTGCAAC	4-1BBL ECD (3rd module)	add more aa to 4-1BBL
4-1BBL	P103	CACCTCGCCCAACCTGGGTACCCGAGAGAAT	AATGCAGACCAGGTCACCCCTGTTTCC	4-1BBL ECD (3rd module)	add more aa to 4-1BBL
4-1BBL	P104	GTGATTGTGAGCGCTGGCCGAGGCTCGGTGCG	gccgctggacgatgag	linker	add more aa to 4-1BBL
4-1BBL	P59	GGGGCAGCCAATGTG	gccgctggacgatgag	(SSSSG)3-linker	add more aa to 4-1BBL
4-1BBL	P60	CACATTGGCTGCCCC	GCCACTACACAACAGGGC	4-1BBL (1st module)	add more aa to 4-1BBL
4-1BBL	P61	TGGGCACCCGATATG	ACTCCCTCCACCTTCC	linker (1st module)	add more aa to 4-1BBL
4-1BBL	P62	CATATCGGGTGCCCA	GCTACTACTCAACAGGGAAGC	4-1BBL (2nd module)	add more aa to 4-1BBL
4-1BBL	P63	AGGACATCCTATGTG	AGATCCACCGCCTTCC	4-1BBL (2nd module)	add more aa to 4-1BBL
4-1BBL	P64	CACATAGGATGTCCT	GCAACAACGCAGCAAG	4-1BBL (3rd module)	add more aa to 4-1BBL
4-1BBL	P105	TCCCACATAGGAT**C**	TCCTGCAACAACGCAGC	4-1BBL ECD	C->S
4-1BBL	P106	GTTGTTGCAGGA**G**	ATCCTATGTGGGAAACAGGG	4-1BBL ECD	C->S
4-1BBL	P88	GCATCGTTGT**C**	CAATACAACTCTGAACTGGCAC	4-1BBL (1st module)	C->S
4-1BBL	P89	GAACTGTTCCCTT**C**	CTCCATGGAGAACAAGTTAGTG	4-1BBL (1st module)	C->S
4-1BBL	P90	CAGGCATCTCTTT**C**	TAACACAACATTGAACTGGCATAG	4-1BBL (2nd module)	C->S
4-1BBL	P91	GAACTCTTTCCCT**C**	TTCAATGGAAAATAAGCTCGTC	4-1BBL (2nd module)	C->S
4-1BBL	P92	GGCATCCCTTT**C**	CAACACCACACTCAATTGG	4-1BBL (3rd module)	C->S
4-1BBL	P93	GAACTTTTTCCTT**C**	TAGTATGGAGAATAAACTCGTTGAC	4-1BBL (3rd module)	C->S
4-1BBL	P94	GAGTTGTATTG**G**	ACAACGATGCTTGGTTTTTAG	4-1BBL (1st module)	C->S
4-1BBL	P95	GTTCTCCATGGAG**G**	AAGGGAACAGTTCCACTGTC	4-1BBL (1st module)	C->S
4-1BBL	P96	CAATGTTGTGTTA**G**	AAAGAGATGCCTGGTTCTTTG	4-1BBL (2nd module)	C->S
4-1BBL	P97	TATTTTCCATTGAA**G**	AGGGAAAGAGTTCGACTGTAAG	4-1BBL (2nd module)	C->S
4-1BBL	P98	GTGTGGTGTTG**G**	AAAGGGATGCCTGATTTTTG	4-1BBL (3rd module)	C->S
4-1BBL	P99	ATTCTCCATACTA**G**	AAGGAAAAAGTTCTACCGTGAG	4-1BBL (3rd module)	C->S
4-1BBL	P160	GGCATCCCTTT**C**	CCAAACCACACTCAATTGGC	4-1BBL_N161Q (3rd module)	C160S, N161Q
4-1BBL	P161	GTGTGGTTTGG**G**	AAAGGGATGCCTGATTTTTGG	4-1BBL_N161Q (3rd module)	C160S, N161Q
4-1BBL	P158	GGCATCCCTTT**C**	CAGCACCACACTCAATTGGC	4-1BBL_N161S (3rd module)	C160S, N161S
4-1BBL	P159	GTGTGGTGCTG**G**	AAAGGGATGCCTGATTTTTGG	4-1BBL_N161S (3rd module)	C160S, N161S
4-1BBL	P12		GCTACTACTCAACAGGGAAGC	4-1BBL (2nd module)	fw, linker engineering
4-1BBL	P14		GCAACAACGCAGCAAG	4-1BBL (3rd module)	fw, linker engineering
4-1BBL	P144	GCATCCCTTTGC**GC**	CACCACACTCAATTGGCACTC	4-1BBL (3rd module)	N161A
4-1BBL	P145	ATTGAGTGTGGT**GGC**	GCAAAGGGATGCCTGATTTTTG	4-1BBL (3rd module)	N161A
4-1BBL	P142	GCATCCCTTTGC**CAA**	ACCACACTCAATTGGCACTC	4-1BBL (3rd module)	N161Q
4-1BBL	P143	ATTGAGTGTGGT**TTG**	GCAAAGGGATGCCTGATTTTTG	4-1BBL (3rd module)	N161Q
4-1BBL	P150	GCATCCCTTTGCA**G**	CACCACACTCAATTGGCACTC	4-1BBL (3rd module)	N161S
4-1BBL	P151	TTGAGTGTGGTG**C**	TGCAAAGGGATGCCTGATTTTTG	4-1BBL (3rd module)	N161S

Table E.1.: List of primers that were designed and used in the course of this PhD thesis project (underlined: overhang; bold: mutations

F. Bibliography

[1] Kristian M. Hargadon, Coleman E. Johnson, and Corey J. Williams. "Immune checkpoint blockade therapy for cancer: An overview of FDA-approved immune checkpoint inhibitors". In: *International Immunopharmacology* 62 (2018), pp. 29 –39. ISSN: 1567-5769. DOI: https://doi.org/10.1016/j.intimp.2018.06.001. URL: http://www.sciencedirect.com/science/article/pii/S1567576918302522.

[2] Aleksandra Popovic, Elizabeth M. Jaffee, and Neeha Zaidi. "Emerging strategies for combination checkpoint modulators in cancer immunotherapy". In: *Journal of Clinical Investigation* 128.8 (2018), pp. 3209–3218. ISSN: 1558-8238. DOI: 10.1172/jci120775. URL: http://dx.doi.org/10.1172/JCI120775.

[3] Roberta Zappasodi, Taha Merghoub, and Jedd D. Wolchok. "Emerging Concepts for Immune Checkpoint Blockade-Based Combination Therapies". In: *Cancer Cell* 34.4 (2018), p. 690. ISSN: 1535-6108. DOI: 10.1016/j.ccell.2018.09.008. URL: http://dx.doi.org/10.1016/j.ccell.2018.09.008.

[4] Ignacio Melero et al. "Evolving synergistic combinations of targeted immunotherapies to combat cancer". In: *Nature Reviews Cancer* 15.8 (2015), pp. 457–472.

[5] Jeremy D Waight, Randi B Gombos, and Nicholas S Wilson. "Harnessing co-stimulatory TNF receptors for cancer immunotherapy: current approaches and future opportunities". In: *Human antibodies* 25.3-4 (2017), pp. 87–109.

[6] Amani Makkouk, Cariad Chester, and Holbrook E. Kohrt. "Rationale for anti-CD137 cancer immunotherapy". In: *European Journal of Cancer* 54 (2016), pp. 112–119. ISSN: 0959-8049. DOI: 10.1016/j.ejca.2015.09.026. URL: http://dx.doi.org/10.1016/j.ejca.2015.09.026.

[7] Deborah A Knee, Becker Hewes, and Jennifer L Brogdon. "Rationale for anti-GITR cancer immunotherapy". In: *European journal of cancer* 67 (2016), pp. 1–10.

[8] Robert H Vonderheide. "The immune revolution: a case for priming, not checkpoint". In: *Cancer cell* 33.4 (2018), pp. 563–569.

[9] Patrizia Murer and Dario Neri. "Antibody-cytokine fusion proteins: A novel class of biopharmaceuticals for the therapy of cancer and of chronic inflammation". In: *New Biotechnology* 52 (2019), pp. 42–53. ISSN: 1871-6784. DOI: 10.1016/j.nbt.2019.04.002. URL: http://dx.doi.org/10.1016/j.nbt.2019.04.002.

[10] Cornelia Hutmacher and Dario Neri. "Antibody-cytokine fusion proteins: Biopharmaceuticals with immunomodulatory properties for cancer therapy". In: *Advanced Drug Delivery Reviews* 141 (2019), pp. 67–91. ISSN: 0169-409X. DOI: 10.1016/j.addr.2018.09.002. URL: http://dx.doi.org/10.1016/j.addr.2018.09.002.

[11] Alessandra Villa et al. "A high-affinity human monoclonal antibody specific to the alternatively spliced EDA domain of fibronectin efficiently targets tumor neovasculaturein vivo". In: *International Journal of Cancer* 122.11 (2008), pp. 2405–2413. ISSN: 1097-0215. DOI: 10.1002/ijc.23408. URL: http://dx.doi.org/10.1002/ijc.23408.

[12] Jascha-N. Rybak et al. "The Extra-domain A of Fibronectin Is a Vascular Marker of Solid Tumors and Metastases". In: *Cancer Research* 67.22 (2007), pp. 10948–10957. ISSN: 1538-7445. DOI: 10.1158/0008-5472.can-07-1436. URL: http://dx.doi.org/10.1158/0008-5472.CAN-07-1436.

[13] Kathrin Schwager et al. "Preclinical characterization of DEKAVIL (F8-IL10), a novel clinical-stage immunocytokine which inhibits the progression of collagen-induced arthritis". In: *Arthritis Research & Therapy* 11.5 (2009), R142. ISSN: 1478-6354. DOI: 10.1186/ar2814. URL: http://dx.doi.org/10.1186/ar2814.

[14] World Health Organization. *Cancer*. 2020. URL: https://www.who.int/news-room/fact-sheets/detail/cancer.

[15] Bundesamt für Statistik. *Bundesamt für Statistik - Krebs*. 2020. URL: https://www.bfs.admin.ch/bfs/de/home/statistiken/gesundheit/gesundheitszustand/krankheiten/krebs.html.

[16] Rebecca L Siegel, Kimberly D Miller, and Ahmedin Jemal. "Cancer statistics, 2020". In: *CA: A Cancer Journal for Clinicians* 70.1 (2020), pp. 7–30.

[17] Stephen B Edge et al. *AJCC cancer staging manual*. Vol. 7. Springer New York, 2010.

[18] Kimberly D Miller et al. "Cancer treatment and survivorship statistics, 2019". In: *CA: a cancer journal for clinicians* 69.5 (2019), pp. 363–385.

[19] Douglas Hanahan and Robert A Weinberg. "Hallmarks of cancer: the next generation". In: *cell* 144.5 (2011), pp. 646–674.

[20] Judah Folkman. "Tumor angiogenesis: therapeutic implications". In: *New england journal of medicine* 285.21 (1971), pp. 1182–1186.

[21] Zachary R Chalmers et al. "Analysis of 100,000 human cancer genomes reveals the landscape of tumor mutational burden". In: *Genome medicine* 9.1 (2017), p. 34.

[22] John Christopher Castle et al. "Mutation-derived neoantigens for cancer immunotherapy". In: *Frontiers in immunology* 10 (2019), p. 1856.

[23] Jayne C Boyer et al. "Microsatellite instability, mismatch repair deficiency, and genetic defects in human cancer cell lines". In: *Cancer research* 55.24 (1995), pp. 6063–6070.

[24] Mariam Jamal-Hanjani et al. "Translational implications of tumor heterogeneity". In: *Clinical cancer research* 21.6 (2015), pp. 1258–1266.

[25] Nicholas McGranahan et al. "Clonal neoantigens elicit T cell immunoreactivity and sensitivity to immune checkpoint blockade". In: *Science* 351.6280 (2016), pp. 1463–1469.

[26] Choy-Pik Chiu and Calvin B Harley. "Replicative senescence and cell immortality: the role of telomeres and telomerase". In: *Proceedings of the Society for Experimental Biology and Medicine* 214.2 (1997), pp. 99–106.

[27] William C Hahn et al. "Inhibition of telomerase limits the growth of human cancer cells". In: *Nature medicine* 5.10 (1999), pp. 1164–1170.

[28] Paul TC Wan et al. "Mechanism of activation of the RAF-ERK signaling pathway by oncogenic mutations of B-RAF". In: *Cell* 116.6 (2004), pp. 855–867.

[29] A Petitjean et al. "TP53 mutations in human cancers: functional selection and impact on cancer prognosis and outcomes". In: *Oncogene* 26.15 (2007), pp. 2157–2165.

[30] Bert Vogelstein, David Lane, and Arnold J Levine. "Surfing the p53 network". In: *Nature* 408.6810 (2000), pp. 307–310.

[31] Ton N Schumacher and Nir Hacohen. "Neoantigens encoded in the cancer genome". In: *Current opinion in immunology* 41 (2016), pp. 98–103.

[32] Céline M Laumont et al. "Noncoding regions are the main source of targetable tumor-specific antigens". In: *Science translational medicine* 10.470 (2018), eaau5516.

[33] Carsten Linnemann et al. "High-throughput epitope discovery reveals frequent recognition of neo-antigens by CD4+ T cells in human melanoma". In: *Nature medicine* 21.1 (2015), p. 81.

[34] Katherine Woods et al. "Mismatch in epitope specificities between IFNγ inflamed and uninflamed conditions leads to escape from T lymphocyte killing in melanoma". In: *Journal for immunotherapy of cancer* 4.1 (2016), p. 10.

[35] Vijay Shankaran et al. "IFNγ and lymphocytes prevent primary tumour development and shape tumour immunogenicity". In: *Nature* 410.6832 (2001), pp. 1107–1111.

[36] Jason John Luke et al. *Correlation of WNT/β-catenin pathway activation with immune exclusion across most human cancers.* 2016.

[37] Sope Omowale Olugbile et al. *Molecular characterization of immune exclusion in small-cell lung cancer.* 2016.

[38] Johanna A Joyce and Douglas T Fearon. "T cell exclusion, immune privilege, and the tumor microenvironment". In: *Science* 348.6230 (2015), pp. 74–80.

[39] Daniela F Quail and Johanna A Joyce. "Microenvironmental regulation of tumor progression and metastasis". In: *Nature medicine* 19.11 (2013), p. 1423.

[40] FM Burnet. "The concept of immunological surveillance". In: *Immunological Aspects of Neoplasia.* Vol. 13. Karger Publishers, 1970, pp. 1–27.

[41] Anand S Dighe et al. "Enhanced in vivo growth and resistance to rejection of tumor cells expressing dominant negative IFNγ receptors". In: *Immunity* 1.6 (1994), pp. 447–456.

[42] Daniel H Kaplan et al. "Demonstration of an interferon γ-dependent tumor surveillance system in immunocompetent mice". In: *Proceedings of the national academy of sciences* 95.13 (1998), pp. 7556–7561.

[43] Maries E van den Broek et al. "Decreased tumor surveillance in perforin-deficient mice." In: *The Journal of experimental medicine* 184.5 (1996), pp. 1781–1790.

[44] Mark J Smyth et al. "Differential tumor surveillance by natural killer (NK) and NKT cells". In: *The Journal of experimental medicine* 191.4 (2000), pp. 661–668.

[45] Mark J Smyth et al. "Perforin-mediated cytotoxicity is critical for surveillance of spontaneous lymphoma". In: *The Journal of experimental medicine* 192.5 (2000), pp. 755–760.

[46] Gavin P Dunn et al. "Cancer immunoediting: from immunosurveillance to tumor escape". In: *Nature immunology* 3.11 (2002), pp. 991–998.

[47] Robert D Schreiber, Lloyd J Old, and Mark J Smyth. "Cancer immunoediting: integrating immunity's roles in cancer suppression and promotion". In: *Science* 331.6024 (2011), pp. 1565–1570.

[48] Michele WL Teng, Michael H Kershaw, and Mark J Smyth. "Cancer Immunoediting: From Surveillance to Escape". In: *Cancer Immunotherapy.* Elsevier, 2013, pp. 85–99.

[49] Lewis L Lanier. "NKG2D receptor and its ligands in host defense". In: *Cancer immunology research* 3.6 (2015), pp. 575–582.

[50] Kenneth Murphy and Casey Weaver. *Janeway's immunobiology.* Garland science, 2016.

[51] Els ME Verdegaal et al. "Neoantigen landscape dynamics during human melanoma–T cell interactions". In: *Nature* 536.7614 (2016), pp. 91–95.

[52] Y Jiang, Y Li, and B Zhu. "T-cell exhaustion in the tumor microenvironment". In: *Cell death & disease* 6.6 (2015), e1792.

[53] James W Behan et al. "Adipocytes impair leukemia treatment in mice". In: *Cancer research* 69.19 (2009), pp. 7867–7874.

[54] Kristin M Nieman et al. "Adipocytes promote ovarian cancer metastasis and provide energy for rapid tumor growth". In: *Nature medicine* 17.11 (2011), p. 1498.

[55] Yan Zhang et al. "Stromal progenitor cells from endogenous adipose tissue contribute to pericytes and adipocytes that populate the tumor microenvironment". In: *Cancer research* 72.20 (2012), pp. 5198–5208.

[56] Raghu Kalluri. "The biology and function of fibroblasts in cancer". In: *Nature Reviews Cancer* 16.9 (2016), p. 582.

[57] Christine Feig et al. "Targeting CXCL12 from FAP-expressing carcinoma-associated fibroblasts synergizes with anti–PD-L1 immunotherapy in pancreatic cancer". In: *Proceedings of the National Academy of Sciences* 110.50 (2013), pp. 20212–20217.

[58] Mark C Poznansky et al. "Active movement of T cells away from a chemokine". In: *Nature medicine* 6.5 (2000), pp. 543–548.

[59] Claire Lewis and Craig Murdoch. "Macrophage responses to hypoxia: implications for tumor progression and anti-cancer therapies". In: *The American journal of pathology* 167.3 (2005), pp. 627–635.

[60] María M Escribese, Mateo Casas, and Ángel L Corbí. "Influence of low oxygen tensions on macrophage polarization". In: *Immunobiology* 217.12 (2012), pp. 1233–1240.

[61] Johanna A Joyce et al. "Cathepsin cysteine proteases are effectors of invasive growth and angiogenesis during multistage tumorigenesis". In: *Cancer cell* 5.5 (2004), pp. 443–453.

[62] Vasilena Gocheva et al. "IL-4 induces cathepsin protease activity in tumor-associated macrophages to promote cancer growth and invasion". In: *Genes & development* 24.3 (2010), pp. 241–255.

[63] Sumanta Goswami et al. "Macrophages promote the invasion of breast carcinoma cells via a colony-stimulating factor-1/epidermal growth factor paracrine loop". In: *Cancer research* 65.12 (2005), pp. 5278–5283.

[64] Salvatore J Coniglio et al. "Microglial stimulation of glioblastoma invasion involves epidermal growth factor receptor (EGFR) and colony stimulating factor 1 receptor (CSF-1R) signaling". In: *Molecular medicine* 18.3 (2012), pp. 519–527.

[65] Bond Almand et al. "Clinical significance of defective dendritic cell differentiation in cancer". In: *Clinical Cancer Research* 6.5 (2000), pp. 1755–1766.

[66] Bond Almand et al. “Increased production of immature myeloid cells in cancer patients: a mechanism of immunosuppression in cancer”. In: *The Journal of Immunology* 166.1 (2001), pp. 678–689.

[67] Cunren Liu et al. “Expansion of spleen myeloid suppressor cells represses NK cell cytotoxicity in tumor-bearing host”. In: *Blood* 109.10 (2007), pp. 4336–4342.

[68] Pratima Sinha, Virginia K Clements, and Suzanne Ostrand-Rosenberg. “Reduction of myeloid-derived suppressor cells and induction of M1 macrophages facilitate the rejection of established metastatic disease”. In: *The Journal of Immunology* 174.2 (2005), pp. 636–645.

[69] Alessandra Mazzoni et al. “Myeloid suppressor lines inhibit T cell responses by an NO-dependent mechanism”. In: *The Journal of Immunology* 168.2 (2002), pp. 689–695.

[70] Weiping Zou. “Regulatory T cells, tumour immunity and immunotherapy”. In: *Nature Reviews Immunology* 6.4 (2006), pp. 295–307.

[71] Maurus De La Rosa et al. “Interleukin-2 is essential for CD4+ CD25+ regulatory T cell function”. In: *European journal of immunology* 34.9 (2004), pp. 2480–2488.

[72] Giovanna Borsellino et al. “Expression of ectonucleotidase CD39 by Foxp3+ Treg cells: hydrolysis of extracellular ATP and immune suppression”. In: *Blood, The Journal of the American Society of Hematology* 110.4 (2007), pp. 1225–1232.

[73] Silvia Deaglio et al. “Adenosine generation catalyzed by CD39 and CD73 expressed on regulatory T cells mediates immune suppression”. In: *The Journal of experimental medicine* 204.6 (2007), pp. 1257–1265.

[74] Kajsa Wing et al. “CTLA-4 control over Foxp3+ regulatory T cell function”. In: *Science* 322.5899 (2008), pp. 271–275.

[75] Francesca Fallarino et al. “Modulation of tryptophan catabolism by regulatory T cells”. In: *Nature immunology* 4.12 (2003), pp. 1206–1212.

[76] Dario AA Vignali, Lauren W Collison, and Creg J Workman. “How regulatory T cells work”. In: *Nature Reviews Immunology* 8.7 (2008), pp. 523–532.

[77] Guang L Wang and Gregg L Semenza. “Purification and characterization of hypoxia-inducible factor 1”. In: *Journal of biological chemistry* 270.3 (1995), pp. 1230–1237.

[78] Keiji Tanimoto et al. “Mechanism of regulation of the hypoxia-inducible factor-1α by the von Hippel-Lindau tumor suppressor protein”. In: *The EMBO journal* 19.16 (2000), pp. 4298–4309.

[79] Susana Salceda and Jaime Caro. "Hypoxia-inducible factor 1α (HIF-1α) protein is rapidly degraded by the ubiquitin-proteasome system under normoxic conditions Its stabilization by hypoxia depends on redox-induced changes". In: *Journal of Biological Chemistry* 272.36 (1997), pp. 22642–22647.

[80] Pekka J Kallio et al. "Regulation of the hypoxia-inducible transcription factor 1α by the ubiquitin-proteasome pathway". In: *Journal of Biological Chemistry* 274.10 (1999), pp. 6519–6525.

[81] Panu Jaakkola et al. "Targeting of HIF-α to the von Hippel-Lindau ubiquitylation complex by O2-regulated prolyl hydroxylation". In: *Science* 292.5516 (2001), pp. 468–472.

[82] Lvan Mircea et al. "HIFalpha targeted for VHL-mediated destruction by proline hydroxylation: implications for O 2 sensing". In: *Science* 292.5516 (2001), pp. 464–468.

[83] Jo A Forsythe et al. "Activation of vascular endothelial growth factor gene transcription by hypoxia-inducible factor 1." In: *Molecular and cellular biology* 16.9 (1996), pp. 4604–4613.

[84] Gabriele Bergers et al. "Matrix metalloproteinase-9 triggers the angiogenic switch during carcinogenesis". In: *Nature cell biology* 2.10 (2000), pp. 737–744.

[85] Napoleone Ferrara, Hans-Peter Gerber, and Jennifer LeCouter. "The biology of VEGF and its receptors". In: *Nature medicine* 9.6 (2003), pp. 669–676.

[86] Rakesh K Jain. "Molecular regulation of vessel maturation". In: *Nature medicine* 9.6 (2003), pp. 685–693.

[87] Gabriele Bergers and Laura E Benjamin. "Tumorigenesis and the angiogenic switch". In: *Nature reviews cancer* 3.6 (2003), pp. 401–410.

[88] Peter Carmeliet. "VEGF as a key mediator of angiogenesis in cancer". In: *Oncology* 69.Suppl. 3 (2005), pp. 4–10.

[89] Robert S Kerbel. "Inhibition of tumor angiogenesis as a strategy to circumvent acquired resistance to anti-cancer therapeutic agents". In: *Bioessays* 13.1 (1991), pp. 31–36.

[90] Katharina Frey et al. "Antibody-based targeting of interferon-alpha to the tumor neovasculature: a critical evaluation". In: *Integrative Biology* 3.4 (2011), pp. 468–478.

[91] Laura Borsi et al. "Selective targeting of tumoral vasculature: comparison of different formats of an antibody (L19) to the ED-B domain of fibronectin". In: *International journal of cancer* 102.1 (2002), pp. 75–85.

[92] Simon S Brack et al. "Tumor-targeting properties of novel antibodies specific to the large isoform of tenascin-C". In: *Clinical Cancer Research* 12.10 (2006), pp. 3200–3208.

[93] W Carey Hanly, James E Artwohl, and B Taylor Bennett. "Review of polyclonal antibody production procedures in mammals and poultry". In: *ILAR journal* 37.3 (1995), pp. 93–118.

[94] Georges Köhler and Cesar Milstein. "Continuous cultures of fused cells secreting antibody of predefined specificity". In: *nature* 256.5517 (1975), pp. 495–497.

[95] Greg Winter et al. "Making antibodies by phage display technology". In: *Annual review of immunology* 12.1 (1994), pp. 433–455.

[96] Jozef Hanes and Andreas Plückthun. "In vitro selection and evolution of functional proteins by using ribosome display". In: *Proceedings of the National Academy of Sciences* 94.10 (1997), pp. 4937–4942.

[97] Barrett R Harvey et al. "Anchored periplasmic expression, a versatile technology for the isolation of high-affinity antibodies from Escherichia coli-expressed libraries". In: *Proceedings of the National Academy of Sciences* 101.25 (2004), pp. 9193–9198.

[98] Ginger Chao et al. "Isolating and engineering human antibodies using yeast surface display". In: *Nature protocols* 1.2 (2006), p. 755.

[99] Roger R Beerli et al. "Isolation of human monoclonal antibodies by mammalian cell display". In: *Proceedings of the National Academy of Sciences* 105.38 (2008), pp. 14336–14341.

[100] Nachiket Shembekar et al. "Single-cell droplet microfluidic screening for antibodies specifically binding to target cells". In: *Cell reports* 22.8 (2018), pp. 2206–2215.

[101] JD Isaacs. "The antiglobulin response to therapeutic antibodies." In: *Seminars in immunology*. Vol. 2. 6. 1990, pp. 449–456.

[102] K Kuus-Reichel et al. "Will immunogenicity limit the use, efficacy, and future development of therapeutic monoclonal antibodies?" In: *Clin. Diagn. Lab. Immunol.* 1.4 (1994), pp. 365–372.

[103] Gabrielle L Boulianne, Nobumichi Hozumi, and Marc J Shulman. "Production of functional chimaeric mouse/human antibody". In: *Nature* 312.5995 (1984), pp. 643–646.

[104] MS Neuberger et al. "A hapten-specific chimaeric IgE antibody with human physiological effector function". In: *Nature* 314.6008 (1985), pp. 268–270.

[105] Gregory P Winter. *Recombinant altered antibodies and methods of making altered antibodies*. US Patent 5,225,539. 1993.

[106] Greg Winter and William J Harris. “Humanized antibodies”. In: *Trends in pharmacological sciences* 14.5 (1993), pp. 139–143.

[107] Greg Winter and Cesar Milstein. “Man-made antibodies”. In: *Nature* 349.6307 (1991), pp. 293–299.

[108] John McCafferty et al. “Phage antibodies: filamentous phage displaying antibody variable domains”. In: *nature* 348.6301 (1990), pp. 552–554.

[109] Lisa J Garrard et al. *Monovalent phage display*. US Patent 5,821,047. 1998.

[110] Julia Thompson et al. “Affinity maturation of a high-affinity human monoclonal antibody against the third hypervariable loop of human immunodeficiency virus: use of phage display to improve affinity and broaden strain reactivity”. In: *Journal of molecular biology* 256.1 (1996), pp. 77–88.

[111] Robert A Irving, Alexander A Kortt, and Peter J Hudson. “Affinity maturation of recombinant antibodies using E. coli mutator cells”. In: *Immunotechnology* 2.2 (1996), pp. 127–143.

[112] Derry C Roopenian and Shreeram Akilesh. “FcRn: the neonatal Fc receptor comes of age”. In: *Nature reviews immunology* 7.9 (2007), pp. 715–725.

[113] Victor Ghetie and E Sally Ward. “Transcytosis and catabolism of antibody”. In: *Immunologic research* 25.2 (2002), pp. 97–113.

[114] Stephen A Beers, Martin J Glennie, and Ann L White. “Influence of immunoglobulin isotype on therapeutic antibody function”. In: *Blood, The Journal of the American Society of Hematology* 127.9 (2016), pp. 1097–1101.

[115] Xin Chen et al. “FcγR-binding is an important functional attribute for immune checkpoint antibodies in cancer immunotherapy”. In: *Frontiers in immunology* 10 (2019).

[116] PH Schur. “IgG subclasses. A historical perspective.” In: *Monographs in allergy* 23 (1988), p. 1.

[117] William R Strohl and Lila M Strohl. *Therapeutic antibody engineering: current and future advances driving the strongest growth area in the pharmaceutical industry*. Elsevier, 2012.

[118] Gestur Vidarsson, Gillian Dekkers, and Theo Rispens. “IgG subclasses and allotypes: from structure to effector functions”. In: *Frontiers in immunology* 5 (2014), p. 520.

[119] TERJE E Michaelsen, BLAS Frangione, and EDWARD C Franklin. “Primary structure of the" hinge" region of human IgG3. Probable quadruplication of a 15-amino acid residue basic unit.” In: *Journal of Biological Chemistry* 252.3 (1977), pp. 883–889.

[120] Nigel M Stapleton et al. "Competition for FcRn-mediated transport gives rise to short half-life of human IgG3 and offers therapeutic potential". In: *Nature communications* 2.1 (2011), pp. 1–9.

[121] Y Diana Liu et al. "Human IgG2 antibody disulfide rearrangement in vivo". In: *Journal of Biological Chemistry* 283.43 (2008), pp. 29266–29272.

[122] Ann L White et al. "Conformation of the human immunoglobulin G2 hinge imparts superagonistic properties to immunostimulatory anticancer antibodies". In: *Cancer cell* 27.1 (2015), pp. 138–148.

[123] Aran F Labrijn et al. "Therapeutic IgG4 antibodies engage in Fab-arm exchange with endogenous human IgG4 in vivo". In: *Nature biotechnology* 27.8 (2009), p. 767.

[124] John-Paul Silva et al. "The S228P mutation prevents in vivo and in vitro IgG4 Fab-arm exchange as demonstrated using a combination of novel quantitative immunoassays and physiological matrix preparation". In: *Journal of Biological Chemistry* 290.9 (2015), pp. 5462–5469.

[125] Pierre Bruhns et al. "Specificity and affinity of human Fcγ receptors and their polymorphic variants for human IgG subclasses". In: *Blood, The Journal of the American Society of Hematology* 113.16 (2009), pp. 3716–3725.

[126] NM Van Sorge, W-L Van Der Pol, and JGJ Van de Winkel. "FcγR polymorphisms: implications for function, disease susceptibility and immunotherapy". In: *Tissue antigens* 61.3 (2003), pp. 189–202.

[127] Bruce D Wines et al. "The IgG Fc contains distinct Fc receptor (FcR) binding sites: the leukocyte receptors FcγRI and FcγRIIa bind to a region in the Fc distinct from that recognized by neonatal FcR and protein A". In: *The Journal of Immunology* 164.10 (2000), pp. 5313–5318.

[128] Tilman Schlothauer et al. "Novel human IgG1 and IgG4 Fc-engineered antibodies with completely abolished immune effector functions". In: *Protein Engineering, Design and Selection* 29.10 (2016), pp. 457–466.

[129] Peter Sondermann et al. "The 3.2-Å crystal structure of the human IgG1 Fc fragment–FcγRIII complex". In: *Nature* 406.6793 (2000), pp. 267–273.

[130] Roland Newman et al. "Modification of the Fc region of a primatized IgG antibody to human CD4 retains its ability to modulate CD4 receptors but does not deplete CD4+ T cells in chimpanzees". In: *Clinical Immunology* 98.2 (2001), pp. 164–174.

[131] Omid Vafa et al. "An engineered Fc variant of an IgG eliminates all immune effector functions via structural perturbations". In: *Methods* 65.1 (2014), pp. 114–126.

[132] Michael M Schmidt and K Dane Wittrup. “A modeling analysis of the effects of molecular size and binding affinity on tumor targeting”. In: *Molecular cancer therapeutics* 8.10 (2009), pp. 2861–2871.

[133] Robert E Bird et al. “Single-chain antigen-binding proteins”. In: *Science* 242.4877 (1988), pp. 423–426.

[134] James S Huston et al. “Protein engineering of antibody binding sites: recovery of specific activity in an anti-digoxin single-chain Fv analogue produced in Escherichia coli”. In: *Proceedings of the National Academy of Sciences* 85.16 (1988), pp. 5879–5883.

[135] Philipp Holliger, Terence Prospero, and Greg Winter. “" Diabodies": small bivalent and bispecific antibody fragments”. In: *Proceedings of the National Academy of Sciences* 90.14 (1993), pp. 6444–6448.

[136] Erqiu Li et al. “Mammalian cell expression of dimeric small immune proteins (SIP).” In: *Protein engineering* 10.6 (1997), pp. 731–736.

[137] David B Powers et al. “Expression of single-chain Fv-Fc fusions in Pichia pastoris”. In: *Journal of immunological methods* 251.1-2 (2001), pp. 123–135.

[138] Astrid AM Van Der Veldt et al. “Biodistribution and radiation dosimetry of 11 C-labelled docetaxel in cancer patients”. In: *European journal of nuclear medicine and molecular imaging* 37.10 (2010), pp. 1950–1958.

[139] Astrid Van Der Veldt, Egbert Smit, and Adriaan Anthonius Lammertsma. “Positron emission tomography as a method for measuring drug delivery to tumors in vivo: the example of [11C] docetaxel”. In: *Frontiers in oncology* 3 (2013), p. 208.

[140] Nikolaus Krall, Joerg Scheuermann, and Dario Neri. “Small targeted cytotoxics: current state and promises from DNA-encoded chemical libraries”. In: *Angewandte Chemie International Edition* 52.5 (2013), pp. 1384–1402.

[141] Samuele Cazzamalli et al. “Chemically defined antibody–and small molecule–drug conjugates for in vivo tumor targeting applications: a comparative analysis”. In: *Journal of the American Chemical Society* 140.5 (2018), pp. 1617–1621.

[142] Samuele Cazzamalli et al. “In Vivo Antitumor Activity of a Novel Acetazolamide–Cryptophycin Conjugate for the Treatment of Renal Cell Carcinomas”. In: *ACS omega* 3.11 (2018), pp. 14726–14731.

[143] Patrick J Kennedy et al. “Antibodies and associates: partners in targeted drug delivery”. In: *Pharmacology & therapeutics* 177 (2017), pp. 129–145.

[144] Michaela Gebauer and Arne Skerra. “Engineered Protein Scaffolds as Next-Generation Therapeutics”. In: *Annual Review of Pharmacology and Toxicology* 60 (2020), pp. 391–415.

[145] Takashi Yokota et al. “Rapid tumor penetration of a single-chain Fv and comparison with other immunoglobulin forms”. In: *Cancer research* 52.12 (1992), pp. 3402–3408.

[146] Chaitanya R Divgi et al. “Positron emission tomography/computed tomography identification of clear cell renal cell carcinoma: results from the REDECT trial”. In: *Journal of clinical oncology* 31.2 (2013), p. 187.

[147] Martin Benej, Silvia Pastorekova, and Jaromir Pastorek. “Carbonic anhydrase IX: regulation and role in cancer”. In: *Carbonic anhydrase: mechanism, regulation, links to disease, and industrial applications*. Springer, 2014, pp. 199–219.

[148] Gustavo Reynoso et al. “Carcinoembryonic antigen in patients with different cancers”. In: *Jama* 220.3 (1972), pp. 361–365.

[149] David A Silver et al. “Prostate-specific membrane antigen expression in normal and malignant human tissues.” In: *Clinical cancer research* 3.1 (1997), pp. 81–85.

[150] PILAR GarinChesa et al. “Organ-specific expression of the colon cancer antigen A33, a cell surface target for antibody-based therapy”. In: *International journal of oncology* 9.3 (1996), pp. 465–471.

[151] Rui Liu et al. “Fibroblast activation protein: A potential therapeutic target in cancer”. In: *Cancer biology & therapy* 13.3 (2012), pp. 123–129.

[152] Gian Luca Poli et al. “Radretumab radioimmunotherapy in patients with brain metastasis: a 124I-L19SIP dosimetric PET study”. In: *Cancer immunology research* 1.2 (2013), pp. 134–143.

[153] Paola A Erba et al. “Radioimmunotherapy with radretumab in patients with relapsed hematologic malignancies”. In: *Journal of nuclear medicine* 53.6 (2012), pp. 922–927.

[154] Dario Neri and Roy Bicknell. “Tumour vascular targeting”. In: *Nature Reviews Cancer* 5.6 (2005), pp. 436–446.

[155] Anthony W Tolcher. “The Evolution of Antibody-Drug Conjugates: A Positive Inflexion Point”. In: *American Society of Clinical Oncology Educational Book* 40 (2020), pp. 1–8.

[156] Giulio Casi and Dario Neri. “Noninternalizing targeted cytotoxics for cancer therapy”. In: *Molecular pharmaceutics* 12.6 (2015), pp. 1880–1884.

[157] Michael Ritchie, Lioudmila Tchistiakova, and Nathan Scott. “Implications of receptor-mediated endocytosis and intracellular trafficking dynamics in the development of antibody drug conjugates”. In: *MAbs*. Vol. 5. 1. Taylor & Francis. 2013, pp. 13–21.

[158] Rémy Gébleux et al. "Antibody format and drug release rate determine the therapeutic activity of noninternalizing antibody–drug conjugates". In: *Molecular cancer therapeutics* 14.11 (2015), pp. 2606–2612.

[159] Alberto Dal Corso et al. "Protease-cleavable linkers modulate the anticancer activity of noninternalizing antibody–drug conjugates". In: *Bioconjugate chemistry* 28.7 (2017), pp. 1826–1833.

[160] Elena Perrino et al. "Curative properties of noninternalizing antibody–drug conjugates based on maytansinoids". In: *Cancer research* 74.9 (2014), pp. 2569–2578.

[161] Gonçalo JL Bernardes et al. "A traceless vascular-targeting antibody–drug conjugate for cancer therapy". In: *Angewandte Chemie International Edition* 51.4 (2012), pp. 941–944.

[162] Cornelius Cilliers et al. "Improved tumor penetration and single-cell targeting of antibody–drug conjugates increases anticancer efficacy and host survival". In: *Cancer research* 78.3 (2018), pp. 758–768.

[163] Ian Nessler et al. "Increased Tumor Penetration of Single-Domain Antibody–Drug Conjugates Improves In Vivo Efficacy in Prostate Cancer Models". In: *Cancer Research* 80.6 (2020), pp. 1268–1278.

[164] FDA. *FDA grants accelerated approval of Trodelvy™*. 2020. URL: https://www.fda.gov/drugs/drug-approvals-and-databases/fda-grants-accelerated-approval-sacituzumab-govitecan-hziy-metastatic-triple-negative-breast-cancer.

[165] Antibodysociety. *FDA grants first approval to Belantamab mafodotin*. 2020. URL: https://www.antibodysociety.org/food-and-drug-administration/fda-grants-first-approval-to-belantamab-mafodotin-blmf/.

[166] Rajamanickam Baskar et al. "Cancer and radiation therapy: current advances and future directions". In: *International journal of medical sciences* 9.3 (2012), p. 193.

[167] John F Ward. "DNA damage produced by ionizing radiation in mammalian cells: identities, mechanisms of formation, and reparability". In: *Progress in nucleic acid research and molecular biology*. Vol. 35. Elsevier, 1988, pp. 95–125.

[168] Martin R Gill et al. "Targeted radionuclide therapy in combined-modality regimens". In: *The Lancet Oncology* 18.7 (2017), e414–e423.

[169] Robert Marcus. "Use of 90Y-ibritumomab tiuxetan in non-Hodgkin's lymphoma". In: *Seminars in oncology*. Vol. 32. Elsevier. 2005, pp. 36–43.

[170] Luigi Aloj et al. “Radioimmunotherapy with Tenarad, a 131 I-labelled antibody fragment targeting the extra-domain A1 of tenascin-C, in patients with refractory Hodgkin’s lymphoma”. In: *European journal of nuclear medicine and molecular imaging* 41.5 (2014), pp. 867–877.

[171] Shankar Vallabhajosula et al. “Radioimmunotherapy of metastatic prostate cancer with; 177Lu-DOTAhuJ591 anti prostate specific membrane antigen specific monoclonal antibody”. In: *Current radiopharmaceuticals* 9.1 (2016), pp. 44–53.

[172] Chaitanya R Divgi et al. “Preoperative characterisation of clear-cell renal carcinoma using iodine-124-labelled antibody chimeric G250 (124I-cG250) and PET in patients with renal masses: a phase I trial”. In: *The lancet oncology* 8.4 (2007), pp. 304–310.

[173] Stefanie Sauer et al. “Expression of the oncofetal ED-B–containing fibronectin isoform in hematologic tumors enables ED-B–targeted 131I-L19SIP radioimmunotherapy in Hodgkin lymphoma patients”. In: *Blood, The Journal of the American Society of Hematology* 113.10 (2009), pp. 2265–2274.

[174] Martin J Glennie et al. “Mechanisms of killing by anti-CD20 monoclonal antibodies”. In: *Molecular immunology* 44.16 (2007), pp. 3823–3837.

[175] Mitchell E Reff et al. “Depletion of B cells in vivo by a chimeric mouse human monoclonal antibody to CD20”. In: (1994).

[176] Guillaume Cartron et al. “From the bench to the bedside: ways to improve rituximab efficacy”. In: *Blood* 104.9 (2004), pp. 2635–2642.

[177] Marcin Okroj, Anders Österborg, and Anna M Blom. “Effector mechanisms of anti-CD20 monoclonal antibodies in B cell malignancies”. In: *Cancer treatment reviews* 39.6 (2013), pp. 632–639.

[178] Ann Wright and Sherie L Morrison. “Effect of glycosylation on antibody function: implications for genetic engineering”. In: *Trends in biotechnology* 15.1 (1997), pp. 26–32.

[179] Claudia Ferrara et al. “Unique carbohydrate–carbohydrate interactions are required for high affinity binding between FcγRIII and antibodies lacking core fucose”. In: *Proceedings of the National Academy of Sciences* 108.31 (2011), pp. 12669–12674.

[180] Pablo Umaña et al. “Engineered glycoforms of an antineuroblastoma IgG1 with optimized antibody-dependent cellular cytotoxic activity”. In: *Nature biotechnology* 17.2 (1999), pp. 176–180.

[181] Christian Klein et al. “Discovery and Development of Obinutuzumab (GAZYVA, GAZYVARO), a Glycoengineered Type II Anti-CD20 Antibody for the Treatment of Non-Hodgkin Lymphoma and Chronic Lymphocytic Leukemia”. In: *Successful Drug Discovery* 3 (2018), pp. 245–289.

[182] Christian Klein et al. “Epitope interactions of monoclonal antibodies targeting CD20 and their relationship to functional properties”. In: *MAbs*. Vol. 5. 1. Taylor & Francis. 2013, pp. 22–33.

[183] Michel De Weers et al. “Daratumumab, a novel therapeutic human CD38 monoclonal antibody, induces killing of multiple myeloma and other hematological tumors”. In: *The Journal of Immunology* 186.3 (2011), pp. 1840–1848.

[184] Balaji Balasa et al. “Elotuzumab enhances natural killer cell activation and myeloma cell killing through interleukin-2 and TNF-α pathways”. In: *Cancer immunology, immunotherapy* 64.1 (2015), pp. 61–73.

[185] Antonio Palumbo et al. “Daratumumab, bortezomib, and dexamethasone for multiple myeloma”. In: *New England Journal of Medicine* 375.8 (2016), pp. 754–766.

[186] Meletios A Dimopoulos et al. “Daratumumab, lenalidomide, and dexamethasone for multiple myeloma”. In: *New England Journal of Medicine* 375.14 (2016), pp. 1319–1331.

[187] Meletios A Dimopoulos et al. “Elotuzumab plus pomalidomide and dexamethasone for multiple myeloma”. In: *New England Journal of Medicine* 379.19 (2018), pp. 1811–1822.

[188] Arafat Ali Farooqui et al. *Efficacy of Elotuzumab Based Combinations in Patients with Multiple Myeloma-a Systematic Review*. 2019.

[189] Patrizia Murer et al. “Targeted delivery of TNF potentiates the antibody-dependent cell-mediated cytotoxicity of an anti-melanoma immunoglobulin”. In: *Journal of Investigative Dermatology* 139.6 (2019), pp. 1339–1348.

[190] Leonard G Presta et al. “Humanization of an anti-vascular endothelial growth factor monoclonal antibody for the therapy of solid tumors and other disorders”. In: *Cancer research* 57.20 (1997), pp. 4593–4599.

[191] Stephanie KA Blick and Lesley J Scott. “Cetuximab”. In: *Drugs* 67.17 (2007), pp. 2585–2607.

[192] Jose Baselga et al. “Recombinant humanized anti-HER2 antibody (Herceptin™) enhances the antitumor activity of paclitaxel and doxorubicin against HER2/neu overexpressing human breast cancer xenografts”. In: *Cancer research* 58.13 (1998), pp. 2825–2831.

[193] David Cunningham et al. “Cetuximab monotherapy and cetuximab plus irinotecan in irinotecan-refractory metastatic colorectal cancer”. In: *New England journal of medicine* 351.4 (2004), pp. 337–345.

[194] Derek J Jonker et al. “Cetuximab for the treatment of colorectal cancer”. In: *New England Journal of Medicine* 357.20 (2007), pp. 2040–2048.

[195] Eric Van Cutsem et al. “Cetuximab and chemotherapy as initial treatment for metastatic colorectal cancer”. In: *New England Journal of Medicine* 360.14 (2009), pp. 1408–1417.

[196] J Douillard et al. “Final results from PRIME: Randomized phase III study of panitumumab (pmab) with FOLFOX4 for first line metastatic colorectal cancer (mCRC).” In: *Journal of Clinical Oncology* 29.15_suppl (2011), pp. 3510–3510.

[197] Kelly S Oliner et al. *Analysis of KRAS/NRAS and BRAF mutations in the phase III PRIME study of panitumumab (pmab) plus FOLFOX versus FOLFOX as first-line treatment (tx) for metastatic colorectal cancer (mCRC).* 2013.

[198] Miguel A Molina et al. “Trastuzumab (herceptin), a humanized anti-Her2 receptor monoclonal antibody, inhibits basal and activated Her2 ectodomain cleavage in breast cancer cells”. In: *Cancer research* 61.12 (2001), pp. 4744–4749.

[199] Gail D Lewis Phillips et al. “Targeting HER2-positive breast cancer with trastuzumab-DM1, an antibody–cytotoxic drug conjugate”. In: *Cancer research* 68.22 (2008), pp. 9280–9290.

[200] Ian E Krop et al. “Phase I study of trastuzumab-DM1, an HER2 antibody-drug conjugate, given every 3 weeks to patients with HER2-positive metastatic breast cancer”. In: *J Clin Oncol* 28.16 (2010), pp. 2698–2704.

[201] Shanu Modi et al. “Trastuzumab deruxtecan in previously treated HER2-positive breast cancer”. In: *New England Journal of Medicine* 382.7 (2020), pp. 610–621.

[202] Dennis J Slamon et al. “Use of chemotherapy plus a monoclonal antibody against HER2 for metastatic breast cancer that overexpresses HER2”. In: *New England journal of medicine* 344.11 (2001), pp. 783–792.

[203] Sunil Verma et al. “Trastuzumab emtansine for HER2-positive advanced breast cancer”. In: *New England Journal of Medicine* 367.19 (2012), pp. 1783–1791.

[204] Thomas Boehm et al. “Antiangiogenic therapy of experimental cancer does not induce acquired drug resistance”. In: *Nature* 390.6658 (1997), pp. 404–407.

[205] Robert S Warren et al. “Regulation by vascular endothelial growth factor of human colon cancer tumorigenesis in a mouse model of experimental liver metastasis.” In: *The Journal of clinical investigation* 95.4 (1995), pp. 1789–1797.

[206] P Borgstrom et al. "Complete inhibition of angiogenesis and growth of microtumors by anti-VEGF neutralizing antibody: Novel concepts of angiostatic therapy from intravital videomicroscopy". In: *Cancer Res* 56.17 (1996), pp. 4032–4039.

[207] P Borgström et al. "Importance of VEGF for breast cancer angiogenesis in vivo: implications from intravital microscopy of combination treatments with an anti-VEGF neutralizing monoclonal antibody and doxorubicin." In: *Anticancer research* 19.5B (1999), pp. 4203–4214.

[208] Per Borgström et al. "Neutralizing anti-vascular endothelial growth factor antibody completely inhibits angiogenesis and growth of human prostate carcinoma micro tumors in vivo". In: *The Prostate* 35.1 (1998), pp. 1–10.

[209] Hans-Peter Gerber et al. "Complete inhibition of rhabdomyosarcoma xenograft growth and neovascularization requires blockade of both tumor and host vascular endothelial growth factor". In: *Cancer research* 60.22 (2000), pp. 6253–6258.

[210] Napoleone Ferrara et al. "Discovery and development of bevacizumab, an anti-VEGF antibody for treating cancer". In: *Nature reviews Drug discovery* 3.5 (2004), pp. 391–400.

[211] Jocelyn Holash et al. "VEGF-Trap: a VEGF blocker with potent antitumor effects". In: *Proceedings of the National Academy of Sciences* 99.17 (2002), pp. 11393–11398.

[212] Napoleone Ferrara. "The role of the vegf signaling pathway in tumor angiogenesis". In: *Tumor Angiogenesis: A Key Target for Cancer Therapy* (2019), pp. 211–226.

[213] Rajendra S Apte, Daniel S Chen, and Napoleone Ferrara. "VEGF in signaling and disease: beyond discovery and development". In: *Cell* 176.6 (2019), pp. 1248–1264.

[214] Sophie J Bakri et al. "Safety and efficacy of anti-vascular endothelial growth factor therapies for neovascular age-related macular degeneration: a report by the american academy of ophthalmology". In: *Ophthalmology* 126.1 (2019), pp. 55–63.

[215] Dana R Leach, Matthew F Krummel, and James P Allison. "Enhancement of antitumor immunity by CTLA-4 blockade". In: *Science* 271.5256 (1996), pp. 1734–1736.

[216] Tyler R Simpson et al. "Fc-dependent depletion of tumor-infiltrating regulatory T cells co-defines the efficacy of anti–CTLA-4 therapy against melanoma". In: *Journal of Experimental Medicine* 210.9 (2013), pp. 1695–1710.

[217] Anu Sharma et al. "Anti-CTLA-4 immunotherapy does not deplete FOXP3+ regulatory T cells (Tregs) in human cancers". In: *Clinical Cancer Research* 25.4 (2019), pp. 1233–1238.

[218] Vernon K Sondak et al. *Ipilimumab*. 2011.

[219] Yasumasa Ishida et al. “Induced expression of PD-1, a novel member of the immunoglobulin gene superfamily, upon programmed cell death.” In: *The EMBO journal* 11.11 (1992), pp. 3887–3895.

[220] Yasutoshi Agata et al. “Expression of the PD-1 antigen on the surface of stimulated mouse T and B lymphocytes”. In: *International immunology* 8.5 (1996), pp. 765–772.

[221] Rajeev Vibhakar et al. “Activation-induced expression of human programmed death-1 gene in T-lymphocytes”. In: *Experimental cell research* 232.1 (1997), pp. 25–28.

[222] Gordon J Freeman et al. “Engagement of the PD-1 immunoinhibitory receptor by a novel B7 family member leads to negative regulation of lymphocyte activation”. In: *The Journal of experimental medicine* 192.7 (2000), pp. 1027–1034.

[223] Yvette Latchman et al. “PD-L2 is a second ligand for PD-1 and inhibits T cell activation”. In: *Nature immunology* 2.3 (2001), pp. 261–268.

[224] R Houston Thompson et al. “Costimulatory B7-H1 in renal cell carcinoma patients: Indicator of tumor aggressiveness and potential therapeutic target”. In: *Proceedings of the National Academy of Sciences* 101.49 (2004), pp. 17174–17179.

[225] Takashi Shinohara et al. “Structure and chromosomal localization of the human PD-1 gene (PDCD1)”. In: *Genomics* 23.3 (1994), pp. 704–706.

[226] Jens M Chemnitz et al. “SHP-1 and SHP-2 associate with immunoreceptor tyrosine-based switch motif of programmed death 1 upon primary human T cell stimulation, but only receptor ligation prevents T cell activation”. In: *The Journal of Immunology* 173.2 (2004), pp. 945–954.

[227] Taku Okazaki et al. “PD-1 immunoreceptor inhibits B cell receptor-mediated signaling by recruiting src homology 2-domain-containing tyrosine phosphatase 2 to phosphotyrosine”. In: *Proceedings of the National Academy of Sciences* 98.24 (2001), pp. 13866–13871.

[228] Tadashi Yokosuka et al. “Programmed cell death 1 forms negative costimulatory microclusters that directly inhibit T cell receptor signaling by recruiting phosphatase SHP2”. In: *Journal of Experimental Medicine* 209.6 (2012), pp. 1201–1217.

[229] Taku Okazaki et al. “A rheostat for immune responses: the unique properties of PD-1 and their advantages for clinical application”. In: *Nature immunology* 14.12 (2013), pp. 1212–1218.

[230] Fumiya Hirano et al. “Blockade of B7-H1 and PD-1 by monoclonal antibodies potentiates cancer therapeutic immunity”. In: *Cancer research* 65.3 (2005), pp. 1089–1096.

[231] Tyler J Curiel et al. “Blockade of B7-H1 improves myeloid dendritic cell–mediated antitumor immunity”. In: *Nature medicine* 9.5 (2003), pp. 562–567.

[232] Jedd D Wolchok et al. “Nivolumab plus ipilimumab in advanced melanoma”. In: *N Engl J Med* 369 (2013), pp. 122–133.

[233] Michael A Postow et al. “Nivolumab and ipilimumab versus ipilimumab in untreated melanoma”. In: *New England Journal of Medicine* 372.21 (2015), pp. 2006–2017.

[234] Matthew D Hellmann et al. “Nivolumab plus ipilimumab in lung cancer with a high tumor mutational burden”. In: *New England Journal of Medicine* 378.22 (2018), pp. 2093–2104.

[235] Georgina V Long et al. “Standard-dose pembrolizumab in combination with reduced-dose ipilimumab for patients with advanced melanoma (KEYNOTE-029): an open-label, phase 1b trial”. In: *The Lancet Oncology* 18.9 (2017), pp. 1202–1210.

[236] Michael C Kirchberger et al. “Combined low-dose ipilimumab and pembrolizumab after sequential ipilimumab and pembrolizumab failure in advanced melanoma”. In: *European Journal of Cancer* 65 (2016), pp. 182–184.

[237] Lavinia Spain, Stefan Diem, and James Larkin. “Management of toxicities of immune checkpoint inhibitors”. In: *Cancer treatment reviews* 44 (2016), pp. 51–60.

[238] Jeryl Villadolid and Asim Amin. “Immune checkpoint inhibitors in clinical practice: update on management of immune-related toxicities”. In: *Translational lung cancer research* 4.5 (2015), p. 560.

[239] Weijie Ma et al. “Current status and perspectives in translational biomarker research for PD-1/PD-L1 immune checkpoint blockade therapy”. In: *Journal of hematology & oncology* 9.1 (2016), p. 47.

[240] Mizuki Nishino et al. “Monitoring immune-checkpoint blockade: response evaluation and biomarker development”. In: *Nature reviews Clinical oncology* 14.11 (2017), p. 655.

[241] Lawrence P Andrews et al. “LAG 3 (CD 223) as a cancer immunotherapy target”. In: *Immunological reviews* 276.1 (2017), pp. 80–96.

[242] Yayi He et al. “TIM-3, a promising target for cancer immunotherapy”. In: *OncoTargets and therapy* 11 (2018), p. 7005.

[243] Sandrine Aspeslagh et al. “Rationale for anti-OX40 cancer immunotherapy”. In: *European Journal of Cancer* 52 (2016), pp. 50–66.

[244] Sufia Butt Hassan et al. “Anti-CD40-mediated cancer immunotherapy: an update of recent and ongoing clinical trials”. In: *Immunopharmacology and immunotoxicology* 36.2 (2014), pp. 96–104.

[245] Raymond A Kempf et al. "Recombinant interferon alpha-2 (INTRON A) in a phase II study of renal cell carcinoma." In: *Journal of biological response modifiers* 5.1 (1986), pp. 27–35.

[246] Paul A Volberding et al. "Treatment of Kaposi's sarcoma with interferon alfa-2b (Intron® A)". In: *Cancer* 59.S3 (1987), pp. 620–625.

[247] Tetsuo Taguchi. "Clinical studies of recombinant interferon alfa-2a (Roferon®-A) in cancer patients". In: *Cancer* 57.S8 (1986), pp. 1705–1708.

[248] Gary J Jones and Loretta M Itri. "Safety and tolerance of recombinant interferon alfa-2a (roferon®-A) in Cancer Patients". In: *Cancer* 57.S8 (1986), pp. 1709–1715.

[249] Michael B Atkins et al. "High-dose recombinant interleukin 2 therapy for patients with metastatic melanoma: analysis of 270 patients treated between 1985 and 1993". In: *Journal of clinical oncology* 17.7 (1999), pp. 2105–2105.

[250] Kimberly R Lindsey, Steven A Rosenberg, Richard M Sherry, et al. "Impact of the number of treatment courses on the clinical response of patients who receive high-dose bolus interleukin-2". In: *Journal of clinical oncology* 18.9 (2000), pp. 1954–1959.

[251] John Geigert et al. "Development and shelf-life determination of recombinant interleukin-2 (Proleukin)". In: *Stability and Characterization of Protein and Peptide Drugs*. Springer, 1993, pp. 249–262.

[252] XN Sheng et al. "Clinical study on recombinant human interleukin-2 (Proleukin) in the treatment of metastatic renal cell carcinoma". In: *Zhonghua zhong liu za zhi [Chinese journal of oncology]* 30.2 (2008), pp. 129–133.

[253] HG Smith et al. "Isolated limb perfusion with melphalan and tumour necrosis factor α for in-transit melanoma and soft tissue sarcoma". In: *Annals of surgical oncology* 22.3 (2015), pp. 356–361.

[254] Brian A Baldo. "Side effects of cytokines approved for therapy". In: *Drug safety* 37.11 (2014), pp. 921–943.

[255] Connie Jackaman et al. "IL-2 intratumoral immunotherapy enhances CD8+ T cells that mediate destruction of tumor cells and tumor-associated vasculature: a novel mechanism for IL-2". In: *The Journal of Immunology* 171.10 (2003), pp. 5051–5063.

[256] Katrin L Gutbrodt, Giulio Casi, and Dario Neri. "Antibody-based delivery of IL2 and cytotoxics eradicates tumors in immunocompetent mice". In: *Molecular cancer therapeutics* 13.7 (2014), pp. 1772–1776.

[257] N. Pasche et al. "The Antibody-Based Delivery of Interleukin-12 to the Tumor Neovasculature Eradicates Murine Models of Cancer in Combination with Paclitaxel". In: *Clinical Cancer Research* 18.15 (2012), pp. 4092–4103. ISSN: 1557-3265. DOI: 10.1158/1078-0432.ccr-12-0282. URL: http://dx.doi.org/10.1158/1078-0432.CCR-12-0282.

[258] T Hemmerle et al. "The antibody-based targeted delivery of TNF in combination with doxorubicin eradicates sarcomas in mice and confers protective immunity". In: *British Journal of Cancer* 109.5 (2013), pp. 1206–1213. ISSN: 1532-1827. DOI: 10.1038/bjc.2013.421. URL: http://dx.doi.org/10.1038/bjc.2013.421.

[259] Greg M Thurber, Michael M Schmidt, and K Dane Wittrup. "Factors determining antibody distribution in tumors". In: *Trends in pharmacological sciences* 29.2 (2008), pp. 57–61.

[260] Greg M Thurber and K Dane Wittrup. "A mechanistic compartmental model for total antibody uptake in tumors". In: *Journal of theoretical biology* 314 (2012), pp. 57–68.

[261] Christian Klein et al. "Cergutuzumab amunaleukin (CEA-IL2v), a CEA-targeted IL-2 variant-based immunocytokine for combination cancer immunotherapy: Overcoming limitations of aldesleukin and conventional IL-2-based immunocytokines". In: *Oncoimmunology* 6.3 (2017), e1277306.

[262] Benjamin Ribba et al. "Prediction of the optimal dosing regimen using a mathematical model of tumor uptake for immunocytokine-based cancer immunotherapy". In: *Clinical Cancer Research* 24.14 (2018), pp. 3325–3333.

[263] Anatol G Morell et al. "The role of sialic acid in determining the survival of glycoproteins in the circulation". In: *Journal of Biological Chemistry* 246.5 (1971), pp. 1461–1467.

[264] Sena J Lee et al. "Mannose receptor-mediated regulation of serum glycoprotein homeostasis". In: *Science* 295.5561 (2002), pp. 1898–1901.

[265] Franziska Bootz et al. "Different tissue distribution properties for glycosylation variants of fusion proteins containing the p40 subunit of murine interleukin-12". In: *Protein Engineering, Design and Selection* 29.10 (2016), pp. 445–455.

[266] Dario Venetz et al. "Glycosylation profiles determine extravasation and disease-targeting properties of armed antibodies". In: *Proceedings of the National Academy of Sciences* 112.7 (2015), pp. 2000–2005.

[267] Stephen D Gillies et al. "Antibody-targeted interleukin 2 stimulates T-cell killing of autologous tumor cells". In: *Proceedings of the National Academy of Sciences* 89.4 (1992), pp. 1428–1432.

[268] Jurgen C Becker et al. "T cell-mediated eradication of murine metastatic melanoma induced by targeted interleukin 2 therapy." In: *The Journal of experimental medicine* 183.5 (1996), pp. 2361–2366.

[269] Kari Kendra et al. "Pharmacokinetics and stability of the ch14. 18–interleukin-2 fusion protein in mice". In: *Cancer Immunology, Immunotherapy* 48.5 (1999), pp. 219–229.

[270] Yan Zeng et al. "Anti-neuroblastoma effect of ch14. 18 antibody produced in CHO cells is mediated by NK-cells in mice". In: *Molecular immunology* 42.11 (2005), pp. 1311–1319.

[271] Jennifer AA Gubbels et al. "Ab-IL2 fusion proteins mediate NK cell immune synapse formation by polarizing CD25 to the target cell-effector cell interface". In: *Cancer Immunology, Immunotherapy* 60.12 (2011), pp. 1789–1800.

[272] Kaci L Osenga et al. "A phase I clinical trial of the hu14. 18-IL2 (EMD 273063) as a treatment for children with refractory or recurrent neuroblastoma and melanoma: a study of the Children's Oncology Group". In: *Clinical cancer research* 12.6 (2006), pp. 1750–1759.

[273] Brett H Yamane et al. "The development of antibody-IL-2 based immunotherapy with hu14. 18-IL2 (EMD-273063) in melanoma and neuroblastoma". In: *Expert opinion on investigational drugs* 18.7 (2009), pp. 991–1000.

[274] Mark R Albertini et al. "Phase II trial of hu14. 18-IL2 for patients with metastatic melanoma". In: *Cancer Immunology, Immunotherapy* 61.12 (2012), pp. 2261–2271.

[275] Suzanne Shusterman et al. "Antitumor activity of hu14. 18-IL2 in patients with relapsed/refractory neuroblastoma: a Children's Oncology Group (COG) phase II study". In: *Journal of Clinical Oncology* 28.33 (2010), p. 4969.

[276] Jacquelyn A Hank et al. "Immunogenicity of the hu14. 18-IL2 immunocytokine molecule in adults with melanoma and children with neuroblastoma". In: *Clinical Cancer Research* 15.18 (2009), pp. 5923–5930.

[277] Katharina Frey et al. "The immunocytokine F8-IL2 improves the therapeutic performance of sunitinib in a mouse model of renal cell carcinoma". In: *The Journal of urology* 184.6 (2010), pp. 2540–2548.

[278] Barbara Carnemolla et al. "Enhancement of the antitumor properties of interleukin-2 by its targeted delivery to the tumor blood vessel extracellular matrix". In: *Blood, The Journal of the American Society of Hematology* 99.5 (2002), pp. 1659–1665.

[279] Jessica Mårlind et al. "Antibody-mediated delivery of interleukin-2 to the stroma of breast cancer strongly enhances the potency of chemotherapy". In: *Clinical Cancer Research* 14.20 (2008), pp. 6515–6524.

[280] Francesca Pretto et al. "Preclinical evaluation of IL2-based immunocytokines supports their use in combination with dacarbazine, paclitaxel and TNF-based immunotherapy". In: *Cancer Immunology, Immunotherapy* 63.9 (2014), pp. 901–910.

[281] Thomas K Eigentler et al. "A dose-escalation and signal-generating study of the immunocytokine L19-IL2 in combination with dacarbazine for the therapy of patients with metastatic melanoma". In: *Clinical cancer research* 17.24 (2011), pp. 7732–7742.

[282] Manfred Johannsen et al. "The tumour-targeting human L19-IL2 immunocytokine: preclinical safety studies, phase I clinical trial in patients with solid tumours and expansion into patients with advanced renal cell carcinoma". In: *European journal of cancer* 46.16 (2010), pp. 2926–2935.

[283] Riccardo Danielli et al. "Intralesional administration of L19-IL2/L19-TNF in stage III or stage IVM1a melanoma patients: results of a phase II study". In: *Cancer immunology, immunotherapy* 64.8 (2015), pp. 999–1009.

[284] Onur Boyman et al. "Selective stimulation of T cell subsets with antibody-cytokine immune complexes". In: *Science* 311.5769 (2006), pp. 1924–1927.

[285] Carsten Krieg et al. "Improved IL-2 immunotherapy by selective stimulation of IL-2 receptors on lymphocytes and endothelial cells". In: *Proceedings of the National Academy of Sciences* 107.26 (2010), pp. 11906–11911.

[286] Natalia Arenas-Ramirez et al. "Improved cancer immunotherapy by a CD25-mimobody conferring selectivity to human interleukin-2". In: *Science translational medicine* 8.367 (2016), 367ra166–367ra166.

[287] Michiko Kobayashi et al. "Identification and purification of natural killer cell stimulatory factor (NKSF), a cytokine with multiple biologic effects on human lymphocytes." In: *The Journal of experimental medicine* 170.3 (1989), pp. 827–845.

[288] Chris E Lawrence et al. "What's new in IL-12? Combination!" In: *Journal for immunotherapy of cancer* 3.S2 (2015), P363.

[289] Michael J Brunda et al. "Antitumor and antimetastatic activity of interleukin 12 against murine tumors." In: *The Journal of experimental medicine* 178.4 (1993), pp. 1223–1230.

[290] Chet L Nastala et al. "Recombinant IL-12 administration induces tumor regression in association with IFN-gamma production." In: *The Journal of Immunology* 153.4 (1994), pp. 1697–1706.

[291] Johanna EA Portielje et al. "Phase I study of subcutaneously administered recombinant human interleukin 12 in patients with advanced renal cell cancer". In: *Clinical cancer research* 5.12 (1999), pp. 3983–3989.

[292] C Halin et al. “Enhancement of the antitumor activity of interleukin-12 by targeted delivery to neovasculature”. In: *Nature biotechnology* 20.3 (2002), pp. 264–269.

[293] Tiziano Ongaro et al. “A novel anti-cancer L19-interleukin-12 fusion protein with an optimized peptide linker efficiently localizes in vivo at the site of tumors”. In: *Journal of biotechnology* 291 (2019), pp. 17–25.

[294] Kin-Ming Lo et al. “huBC1-IL12, an immunocytokine which targets EDB-containing oncofetal fibronectin in tumors and tumor vasculature, shows potent anti-tumor activity in human tumor models”. In: *Cancer Immunology, Immunotherapy* 56.4 (2007), pp. 447–457.

[295] Barbara Carnemolla et al. “A tumor-associated fibronectin isoform generated by alternative splicing of messenger RNA precursors.” In: *The Journal of cell biology* 108.3 (1989), pp. 1139–1148.

[296] Giuliano Mariani et al. “Tumor targeting potential of the monoclonal antibody BC-1 against oncofetal fibronectin in nude mice bearing human tumor implants”. In: *Cancer: Interdisciplinary International Journal of the American Cancer Society* 80.S12 (1997), pp. 2378–2384.

[297] Giuliano Mariani et al. “A pilot pharmacokinetic and immunoscintigraphic study with the technetium-99m-labeled monoclonal antibody BC-1 directed against oncofetal fibronectin in patients with brain tumors”. In: *Cancer: Interdisciplinary International Journal of the American Cancer Society* 80.S12 (1997), pp. 2484–2489.

[298] Sarah M Rudman et al. “A phase 1 study of AS1409, a novel antibody-cytokine fusion protein, in patients with malignant melanoma or renal cell carcinoma”. In: *Clinical Cancer Research* 17.7 (2011), pp. 1998–2005.

[299] Jonathan Fallon et al. “The immunocytokine NHS-IL12 as a potential cancer therapeutic”. In: *Oncotarget* 5.7 (2014), p. 1869.

[300] Julius Strauss et al. “First-in-human phase I trial of a tumor-targeted cytokine (NHS-IL12) in subjects with metastatic solid tumors”. In: *Clinical Cancer Research* 25.1 (2019), pp. 99–109.

[301] Heinold Gamm et al. “Phase I trial of recombinant human tumour necrosis factor α in patients with advanced malignancy”. In: *European Journal of Cancer and Clinical Oncology* 27.7 (1991), pp. 856–863.

[302] Philipp Probst et al. “Sarcoma eradication by doxorubicin and targeted TNF relies upon CD8+ T-cell recognition of a retroviral antigen”. In: *Cancer research* 77.13 (2017), pp. 3644–3654.

[303] Kathrin Schwager et al. “The immunocytokine L19–IL2 eradicates cancer when used in combination with CTLA-4 blockade or with L19-TNF”. In: *Journal of Investigative Dermatology* 133.3 (2013), pp. 751–758.

[304] Tobias Weiss et al. “Immunocytokines are a promising immunotherapeutic approach against glioblastoma”. In: *Science Translational Medicine* 12.564 (2020).

[305] Sheila Dakhel et al. “Targeted enhancement of the therapeutic window of L19-TNF by transient and selective inhibition of RIPK1-signaling cascade”. In: *Oncotarget* 10.62 (2019), p. 6678.

[306] Hans D Menssen et al. “Antibody-based delivery of tumor necrosis factor (L19-TNFα) and interleukin-2 (L19-IL2) to tumor-associated blood vessels has potent immunological and anticancer activity in the syngeneic J558L BALB/c myeloma model”. In: *Journal of cancer research and clinical oncology* 144.3 (2018), pp. 499–507.

[307] Roberto De Luca et al. “Potency-matched Dual Cytokine–Antibody Fusion Proteins for Cancer Therapy”. In: *Molecular cancer therapeutics* 16.11 (2017), pp. 2442–2451.

[308] Roberto De Luca et al. “A novel fully-human potency-matched dual cytokine-antibody fusion protein targets carbonic anhydrase IX in renal cell carcinomas”. In: *Frontiers in Oncology* 9 (2019), p. 1228.

[309] Teresa Hemmerle et al. “Tumor targeting properties of antibody fusion proteins based on different members of the murine tumor necrosis superfamily”. In: *Journal of biotechnology* 172 (2014), pp. 73–76.

[310] Martin Siegemund et al. “An optimized antibody-single-chain TRAIL fusion protein for cancer therapy”. In: *MAbs*. Vol. 8. 5. Taylor & Francis. 2016, pp. 879–891.

[311] Christina Claus et al. “Tumor-targeted 4-1BB agonists for combination with T cell bispecific antibodies as off-the-shelf therapy”. In: *Science translational medicine* 11.496 (2019), eaav5989.

[312] Martin Felices et al. *CD16-IL15-CD33 Trispecific Killer Engager (TriKE) induces NK cell expansion, persistence, and myeloid blast antigen specific killing.* 2016.

[313] Dhifaf Sarhan et al. “161533 TriKE stimulates NK-cell function to overcome myeloid-derived suppressor cells in MDS”. In: *Blood advances* 2.12 (2018), pp. 1459–1469.

[314] Vanessa Kermer et al. “An antibody fusion protein for cancer immunotherapy mimicking IL-15 trans-presentation at the tumor site”. In: *Molecular cancer therapeutics* 11.6 (2012), pp. 1279–1288.

[315] Vanessa Kermer et al. “Combining antibody-directed presentation of IL-15 and 4-1BBL in a trifunctional fusion protein for cancer immunotherapy”. In: *Molecular cancer therapeutics* 13.1 (2014), pp. 112–121.

[316] Nadine Beha et al. “IL15-Based Trifunctional Antibody-Fusion Proteins with Costimulatory TNF-Superfamily Ligands in the Single-Chain Format for Cancer Immunotherapy”. In: *Molecular cancer therapeutics* 18.7 (2019), pp. 1278–1288.

[317] Ryotaro Nakamura et al. *Immunologic and Clinical Responses To a CD20-Targeted Immunocytokine, DI-Leu16-IL2, In Relapsed Non-Hodgkin Lymphoma*. 2013.

[318] Erika Vacchelli et al. “Trial watch—immunostimulation with cytokines in cancer therapy”. In: *Oncoimmunology* 5.2 (2016), e1115942.

[319] Veronika Bachanova et al. *Remission induction in a phase I/II study of an anti-CD20-interleukin-2 immunocytokine DI-Leu16-IL2 in patients with relapsed B-cell lymphoma*. 2015.

[320] Frederick Lansigan et al. *Phase I/II study of an anti-CD20-interleukin-2 immunocytokine DI-Leu16-IL2 in patients with relapsed b-cell lymphoma (NHL).* 2016.

[321] Frederick Lansigan et al. *DI-Leu16-IL2, an anti-CD20-interleukin-2 immunocytokine, is safe and active in patients with relapsed and refractory B-cell lymphoma: a report of maximum tolerated dose, optimal biologic dose, and recommended phase 2 dose*. 2016.

[322] Christian Klein et al. *A novel PD1-IL2v immunocytokine for preferential cis-activation of IL-2R signaling on PD-1 expressing T cell subsets strongly potentiates anti-tumor T cell activity of PD-1 checkpoint inhibition and IL-2R-beta-gamma agonism*. 2019.

[323] Valeria Nicolini et al. *Combining CEA-IL2v and FAP-IL2v immunocytokines with PD-L1 checkpoint blockade*. 2016.

[324] Morten Mau Soerensen et al. *Safety, PK/PD, and anti-tumor activity of RO6874281, an engineered variant of interleukin-2 (IL-2v) targeted to tumor-associated fibroblasts via binding to fibroblast activation protein (FAP).* 2018.

[325] Benjamin Weide et al. “Intralesional treatment of stage III metastatic melanoma patients with L19–IL2 results in sustained clinical and systemic immunologic responses”. In: *Cancer immunology research* 2.7 (2014), pp. 668–678.

[326] Chiara Catania et al. “The tumor-targeting immunocytokine F16-IL2 in combination with doxorubicin: dose escalation in patients with advanced solid tumors and expansion into patients with metastatic breast cancer”. In: *Cell adhesion & migration* 9.1-2 (2015), pp. 14–21.

[327] FG De Braud et al. “Combinations of the immunocytokine F16-IL2 with doxorubicin or with paclitaxel investigated in phase Ib studies in patients with advanced solid tumors.” In: *Journal of Clinical Oncology* 28.15_suppl (2010), e13017–e13017.

[328] FG De Braud et al. “Combination of the immunocytokine F16-IL2 with doxorubicin or paclitaxel in patients with solid tumors: Results from two phase Ib trials.” In: *Journal of Clinical Oncology* 29.15_suppl (2011), pp. 2595–2595.

[329] Christoph Schliemann et al. *Targeting Interleukin-2 to the Bone Marrow Stroma for Therapy of Acute Myeloid Leukemia Relapsing after Allogeneic Hematopoietic Stem Cell Transplantation*. 2014.

[330] Michel M van den Heuvel et al. “NHS-IL2 combined with radiotherapy: preclinical rationale and phase Ib trial results in metastatic non-small cell lung cancer following first-line chemotherapy”. In: *Journal of translational medicine* 13.1 (2015), p. 32.

[331] Silke Gillessen et al. “A phase I dose-escalation study of the immunocytokine EMD 521873 (Selectikine) in patients with advanced solid tumours”. In: *European journal of cancer* 49.1 (2013), pp. 35–44.

[332] Yanlan Wang, Ziyan Zhu, and Meng Zhang. *Abstract LB-A21: Decouple the toxicity and efficacy of BJ-001, an integrin targeting IL-15*. 2019.

[333] Yoo-Joung Ko et al. “Safety, pharmacokinetics, and biological pharmacodynamics of the immunocytokine EMD 273066 (huKS-IL2): results of a phase I trial in patients with prostate cancer”. In: *Journal of immunotherapy* 27.3 (2004), pp. 232–239.

[334] JP Connor et al. “Phase IB trial of EMD 273066 (huKS-IL2) with cyclophosphamide in patients with EpCAM-positive advanced solid tumors.” In: *Journal of Clinical Oncology* 29.15_suppl (2011), pp. 2556–2556.

[335] Oleg Gladkov et al. “Cyclophosphamide and tucotuzumab (huKS-IL2) following first-line chemotherapy in responding patients with extensive-disease small-cell lung cancer”. In: *Anti-cancer drugs* 26.10 (2015), pp. 1061–1068.

[336] JF Spicer et al. “A phase I study of AS1409, a novel antibody-cytokine fusion protein, in patients with malignant melanoma (MM) or renal cell carcinoma (RCC)”. In: *Journal of Clinical Oncology* 27.15S (2009), pp. 3024–3024.

[337] Gianluca Spitaleri et al. “Phase I/II study of the tumour-targeting human monoclonal antibody–cytokine fusion protein L19-TNF in patients with advanced solid tumours”. In: *Journal of cancer research and clinical oncology* 139.3 (2013), pp. 447–455.

[338] Francesco Papadia et al. “Isolated limb perfusion with the tumor-targeting human monoclonal antibody–cytokine fusion protein L19-TNF plus melphalan and mild hyperthermia in patients with locally advanced extremity melanoma”. In: *Journal of surgical oncology* 107.2 (2013), pp. 173–179.

[339] Michael Croft and Richard M Siegel. “Beyond TNF: TNF superfamily cytokines as targets for the treatment of rheumatic diseases”. In: *Nature Reviews Rheumatology* 13.4 (2017), p. 217.

[340] Jean-Luc Bodmer, Pascal Schneider, and Jürg Tschopp. “The molecular architecture of the TNF superfamily”. In: *Trends in biochemical sciences* 27.1 (2002), pp. 19–26.

[341] Helmut R Salih et al. “Soluble CD137 (4-1BB) ligand is released following leukocyte activation and is found in sera of patients with hematological malignancies”. In: *The Journal of Immunology* 167.7 (2001), pp. 4059–4066.

[342] Michael Croft, Chris A Benedict, and Carl F Ware. “Clinical targeting of the TNF and TNFR superfamilies”. In: *Nature Reviews Drug Discovery* 12.2 (2013), pp. 147–168.

[343] Éva S Vanamee and Denise L Faustman. “Structural principles of tumor necrosis factor superfamily signaling”. In: *Sci. Signal.* 11.511 (2018), eaao4910.

[344] Christos Karathanasis et al. “Single-molecule imaging reveals the oligomeric state of functional TNFα-induced plasma membrane TNFR1 clusters in cells”. In: *Science Signaling* 13.614 (2020).

[345] Kausik Chattopadhyay et al. “Evolution of GITRL immune function: murine GITRL exhibits unique structural and biochemical properties within the TNF superfamily”. In: *Proceedings of the National Academy of Sciences* 105.2 (2008), pp. 635–640.

[346] Aruna Bitra et al. “Crystal structure of the m4-1BB/4-1BBL complex reveals an unusual dimeric ligand that undergoes structural changes upon 4-1BB receptor binding”. In: *Journal of Biological Chemistry* 294.6 (2018), pp. 1831–1845. ISSN: 1083-351X. DOI: 10.1074/jbc.ra118.006297. URL: http://dx.doi.org/10.1074/jbc.RA118.006297.

[347] Jawahar Sudhamsu et al. “Dimerization of LTβR by LTα1β2 is necessary and sufficient for signal transduction”. In: *Proceedings of the National Academy of Sciences* 110.49 (2013), pp. 19896–19901.

[348] J Silke and R Brink. “Regulation of TNFRSF and innate immune signalling complexes by TRAFs and cIAPs”. In: *Cell death and differentiation* 17.1 (2010), p. 35.

[349] Antonio Lanzavecchia. "Licence to kill". In: *Nature* 393.6684 (1998), pp. 413–414. ISSN: 1476-4687. DOI: 10.1038/30845. URL: http://dx.doi.org/10.1038/30845.

[350] Ramsay Fuleihan, Narayanaswamy Ramesh, and Raif S Geha. "Role of CD40-CD40-ligand interaction in Ig-isotype switching". In: *Current opinion in immunology* 5.6 (1993), pp. 963–967.

[351] Cees van Kooten and Jacques Banchereau. "CD40-CD40 ligand". In: *Journal of Leukocyte Biology* 67.1 (2000), pp. 2–17. ISSN: 0741-5400. DOI: 10.1002/jlb.67.1.2. URL: http://dx.doi.org/10.1002/jlb.67.1.2.

[352] Karin Karmann et al. "Activation and homologous desensitization of human endothelial cells by CD40 ligand, tumor necrosis factor, and interleukin 1." In: *The Journal of experimental medicine* 184.1 (1996), pp. 173–182.

[353] Randolph J Noelle et al. "A 39-kDa protein on activated helper T cells binds CD40 and transduces the signal for cognate activation of B cells". In: *Proceedings of the National Academy of Sciences* 89.14 (1992), pp. 6550–6554.

[354] Richard J Armitage et al. "Molecular and biological characterization of a murine ligand for CD40". In: *Nature* 357.6373 (1992), pp. 80–82.

[355] Michael Karpusas et al. "2 Å crystal structure of an extracellular fragment of human CD40 ligand". In: *Structure* 3.10 (1995), pp. 1031–1039.

[356] Gonzalo J Mazzei et al. "Recombinant soluble trimeric CD40 ligand is biologically active". In: *Journal of Biological Chemistry* 270.13 (1995), pp. 7025–7028.

[357] RP Gladue et al. "In vivo efficacy of the CD40 agonist antibody CP-870,893 against a broad range of tumor types: impact of tumor CD40 expression, dendritic cells, and chemotherapy". In: *Journal of Clinical Oncology* 24.18_suppl (2006), pp. 2514–2514.

[358] Robert H Vonderheide et al. "Clinical activity and immune modulation in cancer patients treated with CP-870,893, a novel CD40 agonist monoclonal antibody". In: *Journal of Clinical Oncology* 25.7 (2007), pp. 876–883.

[359] Peter W Johnson et al. *Abstract LB-142: A trial of agonistic anti-CD40 antibody: Biological effects in a Cancer Research UK phase I study.* 2013.

[360] Gregory L Beatty et al. "A phase I study of an agonist CD40 monoclonal antibody (CP-870,893) in combination with gemcitabine in patients with advanced pancreatic ductal adenocarcinoma". In: *Clinical cancer research* 19.22 (2013), pp. 6286–6295.

[361] Robert H Vonderheide et al. "Phase I study of the CD40 agonist antibody CP-870,893 combined with carboplatin and paclitaxel in patients with advanced solid tumors". In: *Oncoimmunology* 2.1 (2013), e23033.

[362] Fabrice Barlesi et al. *291 Phase Ib study of selicrelumab (CD40 agonist) in combination with atezolizumab (anti-PD-L1) in patients with advanced solid tumors*. 2020.

[363] David L Bajor et al. *Abstract CT137: Combination of agonistic CD40 monoclonal antibody CP-870,893 and anti-CTLA-4 antibody tremelimumab in patients with metastatic melanoma*. 2015.

[364] John C Byrd et al. "Phase I study of the anti-CD40 humanized monoclonal antibody lucatumumab (HCD122) in relapsed chronic lymphocytic leukemia". In: *Leukemia & lymphoma* 53.11 (2012), pp. 2136–2142.

[365] William Bensinger et al. "A phase 1 study of lucatumumab, a fully human anti-CD 40 antagonist monoclonal antibody administered intravenously to patients with relapsed or refractory multiple myeloma". In: *British journal of haematology* 159.1 (2012), pp. 58–66.

[366] Arnold S Freedman et al. *Clinical activity of lucatumumab (HCD122) in patients (pts) with relapsed/refractory Hodgkin or non-Hodgkin lymphoma treated in a phase Ia/II clinical trial (NCT00670592)*. 2010.

[367] Michelle Fanale et al. "Phase IA/II, multicentre, open-label study of the CD 40 antagonistic monoclonal antibody lucatumumab in adult patients with advanced non-H odgkin or H odgkin lymphoma". In: *British journal of haematology* 164.2 (2014), pp. 258–265.

[368] TS Lewis et al. "Proapoptotic signaling activity of the anti-CD40 monoclonal antibody dacetuzumab circumvents multiple oncogenic transformation events and chemosensitizes NHL cells". In: *Leukemia* 25.6 (2011), pp. 1007–1016.

[369] Luis Fayad et al. "Dacetuzumab plus rituximab, ifosfamide, carboplatin and etoposide as salvage therapy for patients with diffuse large B-cell lymphoma relapsing after rituximab, cyclophosphamide, doxorubicin, vincristine and prednisolone: a randomized, double-blind, placebo-controlled phase 2b trial". In: *Leukemia & lymphoma* 56.9 (2015), pp. 2569–2578.

[370] Mohamad Hussein et al. "A phase I multidose study of dacetuzumab (SGN-40; humanized anti-CD40 monoclonal antibody) in patients with multiple myeloma". In: *haematologica* 95.5 (2010), pp. 845–848.

[371] Richard R Furman et al. "A phase I study of dacetuzumab (SGN-40, a humanized anti-CD40 monoclonal antibody) in patients with chronic lymphocytic leukemia". In: *Leukemia & lymphoma* 51.2 (2010), pp. 228–235.

[372] Ranjana Advani et al. "Phase I study of the humanized anti-CD40 monoclonal antibody dacetuzumab in refractory or recurrent non-Hodgkin's lymphoma". In: *Journal of Clinical Oncology* 27.26 (2009), pp. 4371–4377.

[373] Andres Forero-Torres et al. "Pilot study of dacetuzumab in combination with rituximab and gemcitabine for relapsed or refractory diffuse large B-cell lymphoma". In: *Leukemia & Lymphoma* 54.2 (2013), pp. 277–283.

[374] Shyra J Gardai et al. *SEA-CD40, a sugar engineered non-fucosylated anti-CD40 antibody with improved immune activating capabilities*. 2015.

[375] Juneko E Grilley-Olson et al. *SEA-CD40, a non-fucosylated CD40 agonist: Interim results from a phase 1 study in advanced solid tumors.* 2018.

[376] Haley Neff-LaFord et al. *SEA-CD40 is a non-fucosylated anti-CD40 antibody with potent pharmacodynamic activity in preclinical models and patients with advanced solid tumors*. 2020.

[377] Andrew L Coveler et al. *Phase I study of SEA-CD40, gemcitabine, nab-paclitaxel, and pembrolizumab in patients with metastatic pancreatic ductal adenocarcinoma (PDAC).* 2020.

[378] Erin L Filbert et al. *The CD40 agonistic antibody APX005M 'licenses' antigen presenting cells to promote tumor-specific T-cell responses*. 2016.

[379] Mark H O'Hara et al. *Abstract CT004: A Phase Ib study of CD40 agonistic monoclonal antibody APX005M together with gemcitabine (Gem) and nab-paclitaxel (NP) with or without nivolumab (Nivo) in untreated metastatic ductal pancreatic adenocarcinoma (PDAC) patients*. 2019.

[380] Harriet Kluger et al. *Abstract CT089: Phase Ib/II of CD40 agonistic antibody APX005M in combination with nivolumab (nivo) in subjects with metastatic melanoma (M) or non-small cell lung cancer (NSCLC)*. 2019.

[381] Emiliano Calvo et al. *A phase I study to assess safety, pharmacokinetics (PK), and pharmacodynamics (PD) of JNJ-64457107, a CD40 agonistic monoclonal antibody, in patients (pts) with advanced solid tumors.* 2019.

[382] David A Knorr, Rony Dahan, and Jeffrey V Ravetch. "Toxicity of an Fc-engineered anti-CD40 antibody is abrogated by intratumoral injection and results in durable antitumor immunity". In: *Proceedings of the National Academy of Sciences* 115.43 (2018), pp. 11048–11053.

[383] Sara M Mangsbo et al. "The human agonistic CD40 antibody ADC-1013 eradicates bladder tumors and generates T-cell–dependent tumor immunity". In: *Clinical Cancer Research* 21.5 (2015), pp. 1115–1126.

[384] Sandra MM Irenaeus et al. "First-in-human study with intratumoral administration of a CD40 agonistic antibody, ADC-1013, in advanced solid malignancies". In: *International journal of cancer* 145.5 (2019), pp. 1189–1199.

[385] Daniel H Johnson et al. *Phase I/II dose escalation and expansion cohort safety and efficacy study of image guided intratumoral CD40 agonistic monoclonal antibody APX005M in combination with systemic pembrolizumab for treatment naive metastatic melanoma.* 2018.

[386] Laura A Vitale et al. "Development of CDX-1140, an agonist CD40 antibody for cancer immunotherapy". In: *Cancer Immunology, Immunotherapy* 68.2 (2019), pp. 233–245.

[387] Rachel E Sanborn et al. *Abstract LB-194: First-in-human Phase I study of the CD40 agonist mAb CDX-1140 and in combination with CDX-301 (rhFLT3L) in patients with advanced cancers: Interim results.* 2019.

[388] Shiming Ye et al. "A bispecific molecule targeting CD40 and tumor antigen mesothelin enhances tumor-specific immunity". In: *Cancer Immunology Research* 7.11 (2019), pp. 1864–1875.

[389] JJ Luke et al. "Phase I study evaluating safety, pharmacokinetics (PK), pharmacodynamics, and preliminary efficacy of ABBV-428, first-in-class mesothelin (MSLN)-CD40 bispecific, in patients (pts) with advanced solid tumours". In: *Annals of Oncology* 30 (2019), pp. v498–v499.

[390] Ravindra Majeti et al. "CD47 is an adverse prognostic factor and therapeutic antibody target on human acute myeloid leukemia stem cells". In: *Cell* 138.2 (2009), pp. 286–299.

[391] Stephen B Willingham et al. "The CD47-signal regulatory protein alpha (SIRPa) interaction is a therapeutic target for human solid tumors". In: *Proceedings of the National Academy of Sciences* 109.17 (2012), pp. 6662–6667.

[392] Richard K Tsai and Dennis E Discher. "Inhibition of "self" engulfment through deactivation of myosin-II at the phagocytic synapse between human cells". In: *The Journal of cell biology* 180.5 (2008), pp. 989–1003.

[393] Diane Tseng et al. "Anti-CD47 antibody–mediated phagocytosis of cancer by macrophages primes an effective antitumor T-cell response". In: *Proceedings of the National Academy of Sciences* 110.27 (2013), pp. 11103–11108.

[394] George Fromm et al. *Agonist redirected checkpoint (ARC), SIRPα-Fc-CD40L, for cancer immunotherapy.* 2018.

[395] Matthew Ingham et al. *A phase II trial with safety lead-in to evaluate the addition of APX005M, a CD40 agonistic monoclonal antibody, to standard-of-care doxorubicin chemotherapy for the treatment of advanced soft tissue sarcoma.* 2020.

[396] Sven De Vos et al. "A phase II study of dacetuzumab (SGN-40) in patients with relapsed diffuse large B-cell lymphoma (DLBCL) and correlative analyses of patient-specific factors". In: *Journal of hematology & oncology* 7.1 (2014), p. 44.

[397] Edward Agura et al. *Dacetuzumab (SGN-40), Lenalidomide, and Weekly Dexamethasone in Relapsed or Refractory Multiple Myeloma: Multiple Responses Observed in a Phase 1b Study.* 2009.

[398] Jean-Pascal Machiels et al. "Phase Ib study of anti-CSF-1R antibody emactuzumab in combination with CD40 agonist selicrelumab in advanced solid tumor patients". In: *Journal for ImmunoTherapy of Cancer* 8.2 (2020), e001153.

[399] Christian Merz et al. *The hexavalent CD40 agonist HERA-CD40L augments multilevel crosstalk between T cells and antigen-presenting cells.* 2018.

[400] Meinolf Thiemann et al. *Novel bispecific molecules combining HERA-CD40L with anti-CEA or with anti-PD-L1 for targeting.* 2020.

[401] Sina Fellermeier-Kopf et al. "Duokines: a novel class of dual-acting co-stimulatory molecules acting in cis or trans". In: *Oncoimmunology* 7.9 (2018), e1471442.

[402] Nicolo Rigamonti et al. *A tumor-targeted CD40 agonistic DARPin® molecule leading to antitumor activity with limited systemic toxicity.* 2020.

[403] Bernardo Martinez-Miguel et al. *The trimeric engineered fusion protein with CD40L peptide mimetic (OmpC-CD154p), induced apoptotic signaling on B-NHL cell lines: Higher effect than the recombinant CD40L or anti-CD40 mAb.* 2008.

[404] Jürgen Bajorath and Alejandro Aruffo. "Construction and analysis of a detailed three-dimensional model of the ligand binding domain of the human B cell receptor CD40". In: *Proteins: Structure, Function, and Bioinformatics* 27.1 (1997), pp. 59–70.

[405] Mario I Vega et al. "A Salmonella typhi OmpC fusion protein expressing the CD154 Trp140–Ser149 amino acid strand binds CD40 and activates a lymphoma B-cell line". In: *Immunology* 110.2 (2003), pp. 206–216.

[406] Giuseppe Nocentini et al. "A new member of the tumor necrosis factor/nerve growth factor receptor family inhibits T cell receptor-induced apoptosis". In: *Proceedings of the National Academy of Sciences* 94.12 (1997), pp. 6216–6221.

[407] Simona Ronchetti et al. "Glucocorticoid-induced TNFR-related protein lowers the threshold of CD28 costimulation in CD8+ T cells". In: *The Journal of Immunology* 179.9 (2007), pp. 5916–5926.

[408] Jun Shimizu et al. "Stimulation of CD25+ CD4+ regulatory T cells through GITR breaks immunological self-tolerance". In: *Nature immunology* 3.2 (2002), pp. 135–142.

[409] Geoffrey L Stephens et al. "Engagement of glucocorticoid-induced TNFR family-related receptor on effector T cells by its ligand mediates resistance to suppression by CD4+ CD25+ T cells". In: *The Journal of Immunology* 173.8 (2004), pp. 5008–5020.

[410] Kausik Chattopadhyay et al. "Assembly and structural properties of glucocorticoid-induced TNF receptor ligand: Implications for function". In: *Proceedings of the National Academy of Sciences* 104.49 (2007), pp. 19452–19457.

[411] Z. Zhou et al. "Structural basis for ligand-mediated mouse GITR activation". In: *Proceedings of the National Academy of Sciences* 105.2 (2008), pp. 641–645. ISSN: 1091-6490. DOI: 10.1073/pnas.0711206105. URL: http://dx.doi.org/10.1073/pnas.0711206105.

[412] Kimberley M Heinhuis et al. "Safety, Tolerability, and Potential Clinical Activity of a Glucocorticoid-Induced TNF Receptor–Related Protein Agonist Alone or in Combination With Nivolumab for Patients With Advanced Solid Tumors: A Phase 1/2a Dose-Escalation and Cohort-Expansion Clinical Trial". In: *JAMA oncology* 6.1 (2020), pp. 100–107.

[413] Ana Maria Gonzalez et al. *A novel agonist antibody (INCAGN01876) that targets the costimulatory receptor GITR.* 2016.

[414] Ravit Geva et al. *First-in-human phase 1 study of MK-1248, an anti-human glucocorticoid-induced tumor necrosis factor receptor (GITR) monoclonal antibody, as monotherapy or in combination with pembrolizumab in patients with advanced solid tumors.* 2018.

[415] Ravit Geva et al. "First-in-human phase 1 study of MK-1248, an anti–glucocorticoid-induced tumor necrosis factor receptor agonist monoclonal antibody, as monotherapy or with pembrolizumab in patients with advanced solid tumors". In: *Cancer* ().

[416] Kyriakos P Papadopoulos et al. *Phase 1 study of MK-4166, an anti-human glucocorticoid-induced tumor necrosis factor receptor (GITR) antibody, as monotherapy or with pembrolizumab (pembro) in patients (pts) with advanced solid tumors.* 2019.

[417] M Rosenzweig et al. "Development of TRX518, an aglycosyl humanized monoclonal antibody (Mab) agonist of huGITR." In: *Journal of Clinical Oncology* 28.15_suppl (2010), e13028–e13028.

[418] Henry B Koon et al. *First-in-human phase 1 single-dose study of TRX-518, an anti-human glucocorticoid-induced tumor necrosis factor receptor (GITR) monoclonal antibody in adults with advanced solid tumors.* 2016.

[419] CS Denlinger et al. "A phase I study of MEDI1873, a novel GITR agonist, in advanced solid tumors". In: *Annals of Oncology* 29 (2018), p. viii411.

[420] Ivan H Chan et al. "A In vitro functional activity of OMP-336B11, a GITRL-Fc fusion protein, on primary human immune cells". In: *Cancer Res* 78 (2018), p. 2726.

[421] Selvakumar Sukumar et al. "Characterization of MK-4166, a clinical agonistic antibody that targets human GITR and inhibits the generation and suppressive effects of T regulatory cells". In: *Cancer research* 77.16 (2017), pp. 4378–4388.

[422] ClinicalTrials.gov. *Termination of the study NCT03295942*. 2019. URL: `https://clinicaltrials.gov/ct2/show/NCT03295942`.

[423] Natalie J Tigue et al. "MEDI1873, a potent, stabilized hexameric agonist of human GITR with regulatory T-cell targeting potential". In: *Oncoimmunology* 6.3 (2017), e1280645.

[424] Jacop Plieth. *12 years on, Astra draws a line under Medimmune*. 2019. URL: `https://www.evaluate.com/vantage/articles/news/corporate-strategy/12-years-astra-draws-line-under-medimmune`.

[425] Peisheng Hu et al. "Construction and preclinical characterization of Fc-mGITRL for the immunotherapy of cancer". In: *Clinical Cancer Research* 14.2 (2008), pp. 579–588.

[426] David M Richards et al. "HERA-GITRL activates T cells and promotes anti-tumor efficacy independent of FcγR-binding functionality". In: *Journal for immunotherapy of cancer* 7.1 (2019), p. 191.

[427] Cariad Chester, Siddhant Ambulkar, and Holbrook E Kohrt. "4-1BB agonism: adding the accelerator to cancer immunotherapy". In: *Cancer Immunology, Immunotherapy* 65.10 (2016), pp. 1243–1248.

[428] Chikara Takahashi, Robert S Mittler, and Anthony T Vella. "Cutting edge: 4-1BB is a bona fide CD8 T cell survival signal". In: *The Journal of Immunology* 162.9 (1999), pp. 5037–5040.

[429] Karen E Pollok et al. "Inducible T cell antigen 4-1BB. Analysis of expression and function." In: *The Journal of Immunology* 150.3 (1993), pp. 771–781.

[430] Ignacio Melero et al. "NK1. 1 cells express 4-1BB (CDw137) costimulatory molecule and are required for tumor immunity elicited by anti-4-1BB monoclonal antibodies". In: *Cellular immunology* 190.2 (1998), pp. 167–172.

[431] Hyeon-Woo Lee et al. "4-1BB promotes the survival of CD8+ T lymphocytes by increasing expression of Bcl-xL and Bfl-1". In: *The Journal of Immunology* 169.9 (2002), pp. 4882–4888.

[432] Ryan A Wilcox et al. "Ligation of CD137 receptor prevents and reverses established anergy of CD8+ cytolytic T lymphocytes in vivo". In: *Blood* 103.1 (2004), pp. 177–184.

[433] Ashley V Menk et al. “4-1BB costimulation induces T cell mitochondrial function and biogenesis enabling cancer immunotherapeutic responses”. In: *Journal of Experimental Medicine* 215.4 (2018), pp. 1091–1100.

[434] Toshiro Futagawa et al. “Expression and function of 4-1BB and 4-1BB ligand on murine dendritic cells”. In: *International immunology* 14.3 (2002), pp. 275–286.

[435] Beom K Choi et al. “4-1BB functions as a survival factor in dendritic cells”. In: *The Journal of Immunology* 182.7 (2009), pp. 4107–4115.

[436] Beom K Choi et al. “4-1BB-based Isolation and Expansion of CD8+ T Cells Specific for Self-Tumor and Non–Self-Tumor Antigens for Adoptive T-cell Therapy”. In: *Journal of Immunotherapy* 37.4 (2014), pp. 225–236.

[437] Asís Palazón et al. “The HIF-1α hypoxia response in tumor-infiltrating T lymphocytes induces functional CD137 (4-1BB) for immunotherapy”. In: *Cancer discovery* 2.7 (2012), pp. 608–623.

[438] Asís Palazón et al. “Agonist anti-CD137 mAb act on tumor endothelial cells to enhance recruitment of activated T lymphocytes”. In: *Cancer research* 71.3 (2011), pp. 801–811.

[439] Karin Broll et al. “CD137 expression in tumor vessel walls: high correlation with malignant tumors”. In: *American journal of clinical pathology* 115.4 (2001), pp. 543–549.

[440] Álvaro Teijeira et al. “CD137 on inflamed lymphatic endothelial cells enhances CCL21-guided migration of dendritic cells”. In: *The FASEB Journal* 26.8 (2012), pp. 3380–3392.

[441] Sara Labiano et al. “Hypoxia-induced soluble CD137 in malignant cells blocks CD137L-costimulation as an immune escape mechanism”. In: *Oncoimmunology* 5.1 (2016), e1062967.

[442] Zachary T Freeman et al. “A conserved intratumoral regulatory T cell signature identifies 4-1BB as a pan-cancer target”. In: *The Journal of Clinical Investigation* 130.3 (2020).

[443] Sarah L Buchan et al. “Antibodies to costimulatory receptor 4-1BB enhance anti-tumor immunity via T regulatory cell depletion and promotion of CD8 T cell effector function”. In: *Immunity* 49.5 (2018), pp. 958–970.

[444] Martina Lubrano Di Ricco et al. “Tumor necrosis factor receptor family co-stimulation increases regulatory T cell activation and function via NF-κB”. In: *European Journal of Immunology* (2020).

[445] Cariad Chester et al. “Immunotherapy targeting 4-1BB: mechanistic rationale, clinical results, and future strategies”. In: *Blood, The Journal of the American Society of Hematology* 131.1 (2018), pp. 49–57.

[446] Dass S Vinay and Byoung S Kwon. “Immunotherapy of cancer with 4-1BB”. In: *Molecular cancer therapeutics* 11.5 (2012), pp. 1062–1070.

[447] Aruna Bitra et al. “Crystal structures of the human 4-1BB receptor bound to its ligand 4-1BBL reveal covalent receptor dimerization as a potential signaling amplifier”. In: *Journal of Biological Chemistry* 293.26 (2018), pp. 9958–9969.

[448] Aruna Bitra et al. “Crystal structure of murine 4-1BB and its interaction with 4-1BBL support a role for galectin-9 in 4-1BB signaling”. In: *Journal of Biological Chemistry* 293.4 (2017), pp. 1317–1329. ISSN: 1083-351X. DOI: 10.1074/jbc.m117.814905. URL: http://dx.doi.org/10.1074/jbc.M117.814905.

[449] MFSH Sznol et al. “Phase I study of BMS-663513, a fully human anti-CD137 agonist monoclonal antibody, in patients (pts) with advanced cancer (CA)”. In: *Journal of Clinical Oncology* 26.15_suppl (2008), pp. 3007–3007.

[450] Neil Howard Segal et al. *A phase 1 study of PF-05082566 (anti-4-1BB) in patients with advanced cancer.* 2014.

[451] Xinyue Qi et al. “Optimization of 4-1BB antibody for cancer immunotherapy by balancing agonistic strength with FcγR affinity”. In: *Nature communications* 10.1 (2019), pp. 1–11.

[452] Sun K Ho et al. “Epitope and Fc-Mediated Cross-linking, but Not High Affinity, Are Critical for Antitumor Activity of CD137 Agonist Antibody with Reduced Liver Toxicity”. In: *Molecular Cancer Therapeutics* 19.4 (2020), pp. 1040–1051.

[453] Aran F Labrijn et al. “Bispecific antibodies: a mechanistic review of the pipeline”. In: *Nature Reviews Drug Discovery* 18.8 (2019), pp. 585–608.

[454] Elena Garralda et al. *412 First-in-human phase I/IIa trial to evaluate the safety and initial clinical activity of DuoBody®-PD-L1× 4–1BB (GEN1046) in patients with advanced solid tumors.* 2020.

[455] Paul Tacken et al. *820 MCLA-145 is a bispecific IgG1 antibody that inhibits PD-1/PD-L1 signaling while simultaneously activating CD137 signaling on T cells.* 2020.

[456] Cecile A Geuijen et al. *An unbiased screen identifies a CD137xPD-L1 bispecific IgG1 antibody with unique T cell activation and binding properties.* 2019.

[457] Tea Gunde et al. “A novel, monovalent tri-specific antibody-based molecule that simultaneously modulates PD-L1 and 4-1BB exhibits potent anti-tumoral activity in vivo”. In: *SEA* 2.109 (2019), p. 40000.

[458] Marlon J Hinner et al. "Tumor-Localized Costimulatory T-Cell Engagement by the 4-1BB/HER2 Bispecific Antibody-Anticalin Fusion PRS-343". In: *Clinical Cancer Research* 25.19 (2019), pp. 5878–5889.

[459] G Ku et al. "A phase I dose escalation study of PRS-343, a HER2/4-1BB bispecific molecule, in patients with HER2-positive malignancies". In: *Annals of Oncology* 31 (2020), S462–S463.

[460] I Melero et al. "1025MO First-in-human (FIH) phase I study of RO7122290 (RO), a novel FAP-targeted 4-1BB agonist, administered as single agent and in combination with atezolizumab (ATZ) to patients with advanced solid tumours". In: *Annals of Oncology* 31 (2020), S707.

[461] Anthony Tolcher et al. *Abstract A082: A phase 1, first-in-human, dose-escalation study of ADG106, a fully human anti-CD137 agonistic antibody, in subjects with advanced or metastatic solid tumors and/or relapsed/refractory non-Hodgkin lymphoma*. 2019.

[462] Li Zhang et al. *A phase I, dose-escalation study of ADG106, a fully human anti-CD137 agonistic antibody, in subjects with advanced solid tumors or relapsed/refractory non-Hodgkin lymphoma.* 2020.

[463] Claire Galand et al. "AGEN2373 is a conditionally-active agonist antibody targeting the co-stimulatory receptor CD137 for the treatment of human malignancies". In: *Journal of Clinical Oncology*. Vol. 37. 15. AMER SOC CLINICAL ONCOLOGY. 2019.

[464] Doreen Werchau et al. "ATOR-1017, a 4-1BB Antibody Developed for Tumor-Directed Immunotherapy of Cancer". In: *Journal for immunotherapy of cancer*. Vol. 7. BMC. 2019.

[465] Eva Dahlén et al. *Abstract A183: ATOR-1017: A 4-1BB antibody designed for superior safety/efficacy profile in cancer immunotherapy*. 2019.

[466] Neil H Segal et al. "Phase I study of single-agent utomilumab (PF-05082566), a 4-1BB/CD137 agonist, in patients with advanced cancer". In: *Clinical Cancer Research* 24.8 (2018), pp. 1816–1823.

[467] Ajay K Gopal et al. "First-in-Human Study of Utomilumab, a 4-1BB/CD137 Agonist, in Combination with Rituximab in Patients with Follicular and Other CD20+ Non-Hodgkin Lymphomas". In: *Clinical Cancer Research* 26.11 (2020), pp. 2524–2534.

[468] Anthony W Tolcher et al. "Phase Ib study of utomilumab (PF-05082566), a 4-1BB/CD137 agonist, in combination with pembrolizumab (MK-3475) in patients with advanced solid tumors". In: *Clinical Cancer Research* 23.18 (2017), pp. 5349–5357.

[469] Alberto Chiappori et al. *P860 Results from a combination of OX40 (PF-04518600) and 4–1BB (utomilumab) agonistic antibodies in melanoma and non-small cell lung cancer in a phase 1 dose expansion cohort*. 2020.

[470] Marta Compte et al. "A tumor-targeted trimeric 4-1BB-agonistic antibody induces potent anti-tumor immunity without systemic toxicity". In: *Nature Communications* 9.1 (2018). ISSN: 2041-1723. DOI: 10.1038/s41467-018-07195-w. URL: http://dx.doi.org/10.1038/s41467-018-07195-w.

[471] Luis Alvarez-Vallina et al. "Carcinoembryonic antigen (CEA)-specific 4-1BB-costimulation induced by CEA-targeted 4-1BB-agonistic trimerbodies". In: *Frontiers in immunology* 10 (2019), p. 1791.

[472] Punit Upadhyaya et al. *706 BT7480, a fully synthetic tumor-targeted immune cell agonist (TICA™) induces tumor localized CD137 agonism and modulation of tumor immune microenvironment*. 2020.

[473] Kristen Hurov et al. *700 EphA2/CD137 Bicycle tumor-targeted immune cell agonists (TICAs™) induce tumor regressions, immunogenic memory, and reprogramming of the tumor immune microenvironment*. 2020.

[474] Molecular Partners. *Preclinical pharmacology of MP0310: a 4-1BB/FAP bispecific DARPin drug candidate promoting tumor-restricted T cell co-stimulation*. 2019. URL: https://investors.molecularpartners.com/~/media/Files/M/Molecular-Partners/documents/201804-mp0310-pharmacology-poster-3752.pdf.

[475] Liqin Liu et al. "Tumor-antigen expression-dependent activation of the CD137 costimulatory pathway by bispecific DART® proteins". In: *The American Association for Cancer Research annual meeting, AACR*. Vol. 17. 2017, pp. 1–5.

[476] Brett Schrand et al. "Reducing toxicity of 4–1BB costimulation: targeting 4–1BB ligands to the tumor stroma with bi-specific aptamer conjugates". In: *Oncoimmunology* 4.3 (2015), e970918.

[477] C Arndt et al. "Costimulation improves the killing capability of T cells redirected to tumor cells expressing low levels of CD33: description of a novel modular targeting system". In: *Leukemia* 28.1 (2014), pp. 59–69.

[478] Emanuele Puca et al. "Comparative evaluation of bolus and fractionated administration modalities for two antibody-cytokine fusions in immunocompetent tumor-bearing mice". In: *Journal of Controlled Release* 317 (2020), pp. 282–290.

[479] Teresa Hemmerle and Dario Neri. "The Dose-Dependent Tumor Targeting of Antibody–IFNγ Fusion Proteins Reveals an Unexpected Receptor-Trapping Mechanism In Vivo". In: *Cancer immunology research* 2.6 (2014), pp. 559–567.

[480] DAVID J Peace and MARTIN A Cheever. "Toxicity and therapeutic efficacy of high-dose interleukin 2. In vivo infusion of antibody to NK-1.1 attenuates toxicity without compromising efficacy against murine leukemia." In: *The Journal of experimental medicine* 169.1 (1989), pp. 161–173.

[481] Terry P Maddatu et al. "Mouse phenome database (MPD)". In: *Nucleic acids research* 40.D1 (2012), pp. D887–D894.

[482] Seung-Hwan Lee, Maria F Fragoso, and Christine A Biron. "Cutting edge: a novel mechanism bridging innate and adaptive immunity: IL-12 induction of CD25 to form high-affinity IL-2 receptors on NK cells". In: *The Journal of Immunology* 189.6 (2012), pp. 2712–2716.

[483] Stephen D Gillies et al. "A low-toxicity IL-2–based immunocytokine retains antitumor activity despite its high degree of IL-2 receptor selectivity". In: *Clinical Cancer Research* 17.11 (2011), pp. 3673–3685.

[484] Aron M Levin et al. "Exploiting a natural conformational switch to engineer an interleukin-2 'superkine'". In: *Nature* 484.7395 (2012), pp. 529–533.

[485] S. D. Gillies. "A new platform for constructing antibody-cytokine fusion proteins (immunocytokines) with improved biological properties and adaptable cytokine activity". In: *Protein Engineering Design and Selection* 26.10 (2013), pp. 561–569. ISSN: 1741-0134. DOI: 10.1093/protein/gzt045. URL: http://dx.doi.org/10.1093/protein/gzt045.

[486] Geneviève Garcin et al. "High efficiency cell-specific targeting of cytokine activity". In: *Nature communications* 5 (2014), p. 3016.

[487] Sarah L Pogue et al. "Targeting attenuated interferon-α to myeloma cells with a CD38 antibody induces potent tumor regression with reduced off-target activity". In: *PLoS One* 11.9 (2016).

[488] Anje Cauwels et al. "A safe and highly efficient tumor-targeted type I interferon immunotherapy depends on the tumor microenvironment". In: *Oncoimmunology* 7.3 (2018), e1398876.

[489] Leander Huyghe et al. "Safe eradication of large established tumors using neovasculature-targeted tumor necrosis factor-based therapies". In: *EMBO Molecular Medicine* (2020).

[490] Anje Cauwels et al. "Delivering type I interferon to dendritic cells empowers tumor eradication and immune combination treatments". In: *Cancer research* 78.2 (2018), pp. 463–474.

[491] Juliane Medler et al. "TNFRSF receptor-specific antibody fusion proteins with targeting controlled FcγR-independent agonistic activity". In: *Cell death & disease* 10.3 (2019), p. 224.

[492] Sina Fellermeier et al. "Advancing targeted co-stimulation with antibody-fusion proteins by introducing TNF superfamily members in a single-chain format". In: *OncoImmunology* 5.11 (2016), e1238540. ISSN: 2162-402X. DOI: 10.1080/2162402x.2016.1238540. URL: http://dx.doi.org/10.1080/2162402X.2016.1238540.

[493] Dario Venetz et al. "Targeted Reconstitution of Cytokine Activity upon Antigen Binding using Split Cytokine Antibody Fusion Proteins". In: *Journal of Biological Chemistry* 291.35 (2016), pp. 18139–18147. ISSN: 1083-351X. DOI: 10.1074/jbc.m116.737734. URL: http://dx.doi.org/10.1074/jbc.M116.737734.

[494] Mikala Egeblad and Zena Werb. "New functions for the matrix metalloproteinases in cancer progression". In: *Nature Reviews Cancer* 2.3 (2002), pp. 161–174.

[495] Elin Hadler-Olsen, Jan-Olof Winberg, and Lars Uhlin-Hansen. "Matrix metalloproteinases in cancer: their value as diagnostic and prognostic markers and therapeutic targets". In: *Tumor Biology* 34.4 (2013), pp. 2041–2051.

[496] Luc R Desnoyers et al. "Tumor-specific activation of an EGFR-targeting probody enhances therapeutic index". In: *Science translational medicine* 5.207 (2013), 207ra144–207ra144.

[497] Krishna R Polu and Henry B Lowman. *Probody therapeutics for targeting antibodies to diseased tissue*. 2014.

[498] Karen A Autio et al. "Probody therapeutics: an emerging class of therapies designed to enhance on-target effects with reduced off-tumor toxicity for use in immuno-oncology". In: *Clinical Cancer Research* 26.5 (2020), pp. 984–989.

[499] Thomas Wüest et al. "TNF-Selectokine: a novel prodrug generated for tumor targeting and site-specific activation of tumor necrosis factor". In: *Oncogene* 21.27 (2002), pp. 4257–4265.

[500] Jeannette Gerspach et al. "Target-selective activation of a TNF prodrug by urokinase-type plasminogen activator (uPA) mediated proteolytic processing at the cell surface". In: *Cancer Immunology, Immunotherapy* 55.12 (2006), pp. 1590–1600.

[501] J Gerspach et al. "Restoration of membrane TNF-like activity by cell surface targeting and matrix metalloproteinase-mediated processing of a TNF prodrug". In: *Cell Death & Differentiation* 13.2 (2006), pp. 273–284.

[502] I Watermann et al. "Activation of CD95L fusion protein prodrugs by tumor-associated proteases". In: *Cell Death & Differentiation* 14.4 (2007), pp. 765–774.

[503] Eric Hsu et al. “A cytokine receptor-masked IL2 prodrug selectively activates tumor-infiltrating lymphocytes for potent antitumor therapy”. In: (2020).

[504] Kenta Narumi et al. “Local administration of GITR agonistic antibody induces a stronger antitumor immunity than systemic delivery”. In: *Scientific reports* 9.1 (2019), pp. 1–11.

[505] Jixi Li, Qian Yin, and Hao Wu. “Structural basis of signal transduction in the TNF receptor superfamily”. In: *Advances in immunology*. Vol. 119. Elsevier, 2013, pp. 135–153.

[506] Dario Neri. “Antibody–Cytokine Fusions: Versatile Products for the Modulation of Anticancer Immunity”. In: *Cancer Immunology Research* 7.3 (2019), pp. 348–354. ISSN: 2326-6074. DOI: 10.1158/2326-6066.cir-18-0622. URL: http://dx.doi.org/10.1158/2326-6066.CIR-18-0622.

[507] Teresa Hemmerle et al. “Tumor targeting properties of antibody fusion proteins based on different members of the murine tumor necrosis superfamily”. In: *Journal of Biotechnology* 172 (2014), pp. 73–76. ISSN: 0168-1656. DOI: 10.1016/j.jbiotec.2013.12.010. URL: http://dx.doi.org/10.1016/j.jbiotec.2013.12.010.

[508] C Giuliani et al. “Nf-kB transcription factor: role in the pathogenesis of inflammatory, autoimmune, and neoplastic diseases and therapy implications”. In: *La Clinica Terapeutica* 152.4 (2001), pp. 249–253.

[509] Dario Neri and Paul M Sondel. “Immunocytokines for cancer treatment: past, present and future”. In: *Current Opinion in Immunology* 40 (2016), pp. 96–102. ISSN: 0952-7915. DOI: 10.1016/j.coi.2016.03.006. URL: http://dx.doi.org/10.1016/j.coi.2016.03.006.

[510] Salah-Eddine Bentebibel et al. “A First-in-Human Study and Biomarker Analysis of NKTR-214, a Novel IL2R$\beta\gamma$-Biased Cytokine, in Patients with Advanced or Metastatic Solid Tumors”. In: *Cancer Discovery* 9.6 (2019), pp. 711–721. ISSN: 2159-8290. DOI: 10.1158/2159-8290.cd-18-1495. URL: http://dx.doi.org/10.1158/2159-8290.CD-18-1495.

[511] Karen Autio and Martin Oft. “Pegylated Interleukin-10: Clinical Development of an Immunoregulatory Cytokine for Use in Cancer Therapeutics”. In: *Current Oncology Reports* 21.2 (2019). ISSN: 1534-6269. DOI: 10.1007/s11912-019-0760-z. URL: http://dx.doi.org/10.1007/s11912-019-0760-z.

[512] Nathan Karin. “Chemokines and cancer: new immune checkpoints for cancer therapy”. In: *Current Opinion in Immunology* 51 (2018), pp. 140–145. ISSN: 0952-7915. DOI: 10.1016/j.coi.2018.03.004. URL: http://dx.doi.org/10.1016/j.coi.2018.03.004.

[513] Ming Shi et al. "Application potential of toll-like receptors in cancer immunotherapy". In: *Medicine* 95.25 (2016), e3951. ISSN: 0025-7974. DOI: 10.1097/md.0000000000003951. URL: http://dx.doi.org/10.1097/MD.0000000000003951.

[514] A MEAGER. "Measurement of cytokines by bioassays: Theory and application". In: *Methods* 38.4 (2006), pp. 237–252. ISSN: 1046-2023. DOI: 10.1016/j.ymeth.2005.11.005. URL: http://dx.doi.org/10.1016/j.ymeth.2005.11.005.

[515] Lyanne Weston, Andrew Geczy, and Caroline Farrell. "A convenient and reliable IL-2 bioassay using frozen CTLL-2 to improve the detection of helper T lymphocyte precursors". In: *Immunology and Cell Biology* 76.2 (1998), pp. 190–192. ISSN: 0818-9641. DOI: 10.1046/j.1440-1711.1998.00733.x. URL: http://dx.doi.org/10.1046/j.1440-1711.1998.00733.x.

[516] JIANG-HONG Gong, G Maki, and HG Klingemann. "Characterization of a human cell line (NK-92) with phenotypical and functional characteristics of activated natural killer cells." In: *Leukemia* 8.4 (1994), pp. 652–658.

[517] Ralph Patrick BraunGiuseppe Palladino. *Methods and compositions for assessing il-12 or the neutralization of il-12 in a sample*. Patent. 2008.

[518] Angelo Corti et al. "Tumor necrosis factor (TNF) α quantification by ELISA and bioassay: effects of TNFα-soluble TNF receptor (p55) complex dissociation during assay incubations". In: *Journal of immunological methods* 177.1-2 (1994), pp. 191–198.

[519] N. Zhang et al. "Targeted and Untargeted CD137L Fusion Proteins for the Immunotherapy of Experimental Solid Tumors". In: *Clinical Cancer Research* 13.9 (2007), pp. 2758–2767. ISSN: 1557-3265. DOI: 10.1158/1078-0432.ccr-06-2343. URL: http://dx.doi.org/10.1158/1078-0432.CCR-06-2343.

[520] Xiaojie Yu et al. "Complex Interplay between Epitope Specificity and Isotype Dictates the Biological Activity of Anti-human CD40 Antibodies". In: *Cancer Cell* 33.4 (2018), 664–675.e4. ISSN: 1535-6108. DOI: 10.1016/j.ccell.2018.02.009. URL: http://dx.doi.org/10.1016/j.ccell.2018.02.009.

[521] Linsey E Haswell, Martin J Glennie, and Aymen Al-Shamkhani. "Analysis of the oligomeric requirement for signaling by CD40 using soluble multimeric forms of its ligand, CD154". In: *European journal of immunology* 31.10 (2001), pp. 3094–3100.

[522] Soumen Basak and Alexander Hoffmann. "Crosstalk via the NF-κB signaling system". In: *Cytokine & Growth Factor Reviews* 19.3-4 (2008), pp. 187–197. ISSN: 1359-6101. DOI: 10.1016/j.cytogfr.2008.04.005. URL: http://dx.doi.org/10.1016/j.cytogfr.2008.04.005.

[523] Michael J Lenardo and David Baltimore. "NF-κB: a pleiotropic mediator of inducible and tissue-specific gene control". In: *Cell* 58.2 (1989), pp. 227–229.

[524] Maria Carmen Mulero et al. "DNA-binding affinity and transcriptional activity of the RelA homodimer of nuclear factor κB are not correlated". In: *Journal of Biological Chemistry* 292.46 (2017), pp. 18821–18830. ISSN: 1083-351X. DOI: 10.1074/jbc.m117.813980. URL: http://dx.doi.org/10.1074/jbc.M117.813980.

[525] Giuseppina Bonizzi and Michael Karin. "The two NF-κB activation pathways and their role in innate and adaptive immunity". In: *Trends in Immunology* 25.6 (2004), pp. 280–288. ISSN: 1471-4906. DOI: 10.1016/j.it.2004.03.008. URL: http://dx.doi.org/10.1016/j.it.2004.03.008.

[526] Christian AJ Voßhenrich and James P Di Santo. "Interleukin signaling". In: *Current Biology* 12.22 (2002), R760–R763.

[527] Ji-Young Jang and Choong-Eun Lee. "IL-4-induced upregulation of adenine nucleotide translocase 3 and its role in Th cell survival from apoptosis". In: *Cellular Immunology* 241.1 (2006), pp. 14–25. ISSN: 0008-8749. DOI: 10.1016/j.cellimm.2006.07.006. URL: http://dx.doi.org/10.1016/j.cellimm.2006.07.006.

[528] Soo Ok Lee et al. "Requirement for NF-κB in interleukin-4-induced androgen receptor activation in prostate cancer cells". In: *The Prostate* 64.2 (2005), pp. 160–167. ISSN: 1097-0045. DOI: 10.1002/pros.20218. URL: http://dx.doi.org/10.1002/pros.20218.

[529] Ursula Grohmann et al. "IL-12 acts directly on DC to promote nuclear localization of NF-κB and primes DC for IL-12 production". In: *Immunity* 9.3 (1998), pp. 315–323.

[530] F Paliogianni et al. "Novel mechanism for inhibition of human T cells by glucocorticoids. Glucocorticoids inhibit signal transduction through IL-2 receptor." In: *The Journal of Immunology* 151.8 (1993), pp. 4081–4089.

[531] James Muller, Audrey Baeyens, and Michael L. Dustin. "Tumor Necrosis Factor Receptor Superfamily in T Cell Priming and Effector Function". In: *Advances in Immunology* (2018), pp. 21–57. ISSN: 0065-2776. DOI: 10.1016/bs.ai.2018.08.001. URL: http://dx.doi.org/10.1016/bs.ai.2018.08.001.

[532] Ajithkumar Vasanthakumar et al. "The TNF Receptor Superfamily-NF-κB Axis Is Critical to Maintain Effector Regulatory T Cells in Lymphoid and Non-lymphoid Tissues". In: *Cell Reports* 20.12 (2017), pp. 2906–2920. ISSN: 2211-1247. DOI: 10.1016/j.celrep.2017.08.068. URL: http://dx.doi.org/10.1016/j.celrep.2017.08.068.

[533] Ruslan Medzhitov et al. "MyD88 is an adaptor protein in the hToll/IL-1 receptor family signaling pathways". In: *Molecular cell* 2.2 (1998), pp. 253–258.

[534] Ann Richmond. "NF-κB, chemokine gene transcription and tumour growth". In: *Nature Reviews Immunology* 2.9 (2002), pp. 664–674. ISSN: 1474-1741. DOI: 10.1038/nri887. URL: http://dx.doi.org/10.1038/nri887.

[535] Alessandro Pini et al. "Design and Use of a Phage Display Library". In: *Journal of Biological Chemistry* 273.34 (1998), pp. 21769–21776. ISSN: 1083-351X. DOI: 10.1074/jbc.273.34.21769. URL: http://dx.doi.org/10.1074/jbc.273.34.21769.

[536] Bei Wang et al. "Combination cancer immunotherapy targeting PD-1 and GITR can rescue CD8+T cell dysfunction and maintain memory phenotype". In: *Science Immunology* 3.29 (2018), eaat7061. ISSN: 2470-9468. DOI: 10.1126/sciimmunol.aat7061. URL: http://dx.doi.org/10.1126/sciimmunol.aat7061.

[537] David A Schaer, Daniel Hirschhorn-Cymerman, and Jedd D Wolchok. "Targeting tumor-necrosis factor receptor pathways for tumor immunotherapy". In: *Journal for ImmunoTherapy of Cancer* 2.1 (2014), p. 7. ISSN: 2051-1426. DOI: 10.1186/2051-1426-2-7. URL: http://dx.doi.org/10.1186/2051-1426-2-7.

[538] Roberto De Luca et al. "A novel dual-cytokine–antibody fusion protein for the treatment of CD38-positive malignancies". In: *Protein Engineering, Design and Selection* 31.5 (2018), pp. 173–179. ISSN: 1741-0134. DOI: 10.1093/protein/gzy015. URL: http://dx.doi.org/10.1093/protein/gzy015.

[539] Philipp Holliger and Peter J Hudson. "Engineered antibody fragments and the rise of single domains". In: *Nature Biotechnology* 23.9 (2005), pp. 1126–1136. ISSN: 1546-1696. DOI: 10.1038/nbt1142. URL: http://dx.doi.org/10.1038/nbt1142.

[540] Anja S. Schmid and Dario Neri. "Advances in antibody engineering for rheumatic diseases". In: *Nature Reviews Rheumatology* 15.4 (2019), pp. 197–207. ISSN: 1759-4804. DOI: 10.1038/s41584-019-0188-8. URL: http://dx.doi.org/10.1038/s41584-019-0188-8.

[541] Franziska Bootz and Dario Neri. "Immunocytokines: a novel class of products for the treatment of chronic inflammation and autoimmune conditions". In: *Drug Discovery Today* 21.1 (2016), pp. 180–189. ISSN: 1359-6446. DOI: 10.1016/j.drudis.2015.10.012. URL: http://dx.doi.org/10.1016/j.drudis.2015.10.012.

[542] Laura Borsi et al. "Selective targeted delivery of TNFα to tumor blood vessels". In: *Blood* 102.13 (2003), pp. 4384–4392. ISSN: 1528-0020. DOI: 10.1182/blood-2003-04-1039. URL: http://dx.doi.org/10.1182/blood-2003-04-1039.

[543] Nora Hornig et al. "Combination of a Bispecific Antibody and Costimulatory Antibody-Ligand Fusion Proteins for Targeted Cancer Immunotherapy". In: *Journal of Immunotherapy* 35.5 (2012), pp. 418–429. ISSN: 1524-9557. DOI: 10.1097/cji.0b013e3182594387. URL: http://dx.doi.org/10.1097/CJI.0b013e3182594387.

[544] Nora Hornig et al. "Evaluating combinations of costimulatory antibody–ligand fusion proteins for targeted cancer immunotherapy". In: *Cancer Immunology, Immunotherapy* 62.8 (2013), pp. 1369–1380. ISSN: 1432-0851. DOI: 10.1007/s00262-013-1441-7. URL: http://dx.doi.org/10.1007/s00262-013-1441-7.

[545] Sarah L. Pogue et al. "Targeting Attenuated Interferon-α to Myeloma Cells with a CD38 Antibody Induces Potent Tumor Regression with Reduced Off-Target Activity". In: *PLOS ONE* 11.9 (2016). Ed. by Claire M.Editor Edwards, e0162472. ISSN: 1932-6203. DOI: 10.1371/journal.pone.0162472. URL: http://dx.doi.org/10.1371/journal.pone.0162472.

[546] Erika M. Cook et al. "Antibodies That Efficiently Form Hexamers upon Antigen Binding Can Induce Complement-Dependent Cytotoxicity under Complement-Limiting Conditions". In: *The Journal of Immunology* 197.5 (2016), pp. 1762–1775. ISSN: 1550-6606. DOI: 10.4049/jimmunol.1600648. URL: http://dx.doi.org/10.4049/jimmunol.1600648.

[547] Rob N. de Jong et al. "A Novel Platform for the Potentiation of Therapeutic Antibodies Based on Antigen-Dependent Formation of IgG Hexamers at the Cell Surface". In: *PLOS Biology* 14.1 (2016). Ed. by DavidEditor Nemazee, e1002344. ISSN: 1545-7885. DOI: 10.1371/journal.pbio.1002344. URL: http://dx.doi.org/10.1371/journal.pbio.1002344.

[548] Roy A. Black et al. "A metalloproteinase disintegrin that releases tumour-necrosis factor-α from cells". In: *Nature* 385.6618 (1997), pp. 729–733. ISSN: 1476-4687. DOI: 10.1038/385729a0. URL: http://dx.doi.org/10.1038/385729a0.

[549] Fabienne Pietravalle et al. "Human Native Soluble CD40L Is a Biologically Active Trimer, Processed Inside Microsomes". In: *Journal of Biological Chemistry* 271.11 (1996), pp. 5965–5967. ISSN: 1083-351X. DOI: 10.1074/jbc.271.11.5965. URL: http://dx.doi.org/10.1074/jbc.271.11.5965.

[550] Sampsa Matikainen et al. "IFN-α and IL-18 synergistically enhance IFN-γ production in human NK cells: differential regulation of Stat4 activation and IFN-γ gene expression by IFN-α and IL-12". In: *European journal of immunology* 31.7 (2001), pp. 2236–2245.

[551] Paola Bonaventura et al. "Cold tumors: a therapeutic challenge for immunotherapy". In: *Frontiers in immunology* 10 (2019), p. 168.

[552] Gregory L Beatty et al. "CD40 agonists alter tumor stroma and show efficacy against pancreatic carcinoma in mice and humans". In: *Science* 331.6024 (2011), pp. 1612–1616.

[553] Katelyn T Byrne and Robert H Vonderheide. "CD40 stimulation obviates innate sensors and drives T cell immunity in cancer". In: *Cell reports* 15.12 (2016), pp. 2719–2732.

[554] Leslie A Mitchell et al. "Multichange isothermal mutagenesis: a new strategy for multiple site-directed mutations in plasmid DNA". In: *ACS synthetic biology* 2.8 (2013), pp. 473–477.

[555] Kristian M. Hargadon, Coleman E. Johnson, and Corey J. Williams. "Immune checkpoint blockade therapy for cancer: An overview of FDA-approved immune checkpoint inhibitors". In: *International Immunopharmacology* 62 (2018), pp. 29–39. ISSN: 1567-5769. DOI: 10.1016/j.intimp.2018.06.001. URL: http://dx.doi.org/10.1016/j.intimp.2018.06.001.

[556] Christina Pfirschke et al. "Immunogenic chemotherapy sensitizes tumors to checkpoint blockade therapy". In: *Immunity* 44.2 (2016), pp. 343–354.

[557] F Stephen Hodi et al. "Improved survival with ipilimumab in patients with metastatic melanoma". In: *New England Journal of Medicine* 363.8 (2010), pp. 711–723.

[558] Alice Tzeng et al. "Antigen specificity can be irrelevant to immunocytokine efficacy and biodistribution". In: *Proceedings of the National Academy of Sciences* 112.11 (2015), pp. 3320–3325.

[559] Dana C Andersen and Charles F Goochee. "The effect of cell-culture conditions on the oligosaccharide structures of secreted glycoproteins". In: *Current Opinion in Biotechnology* 5.5 (1994), pp. 546–549.

[560] Patrick Hossler, Sarwat F Khattak, and Zheng Jian Li. "Optimal and consistent protein glycosylation in mammalian cell culture". In: *Glycobiology* 19.9 (2009), pp. 936–949.

[561] Alex Y Huang et al. "The immunodominant major histocompatibility complex class I-restricted antigen of a murine colon tumor derives from an endogenous retroviral gene product". In: *Proceedings of the National Academy of Sciences* 93.18 (1996), pp. 9730–9735.

[562] Bei Wang et al. "Combination cancer immunotherapy targeting PD-1 and GITR can rescue CD8+ T cell dysfunction and maintain memory phenotype". In: *Science immunology* 3.29 (2018), eaat7061.

[563] Roberta Zappasodi et al. "Rational design of anti-GITR-based combination immunotherapy". In: *Nature medicine* 25.5 (2019), pp. 759–766.

[564] Ari Helenius and Markus Aebi. "Roles of N-linked glycans in the endoplasmic reticulum". In: *Annual review of biochemistry* 73.1 (2004), pp. 1019–1049.

[565] Marco Stringhini, Philipp Probst, and Dario Neri. "Immunotherapy of CT26 murine tumors is characterized by an oligoclonal response of tissue-resident memory T cells against the AH1 rejection antigen". In: *European Journal of Immunology* (2020).

[566] Philipp Probst et al. "Antibody-based delivery of TNF to the tumor neovasculature potentiates the therapeutic activity of a peptide anticancer vaccine". In: *Clinical Cancer Research* 25.2 (2019), pp. 698–709.

[567] Rebecca Leyland et al. "A novel murine GITR ligand fusion protein induces anti-tumor activity as a monotherapy that is further enhanced in combination with an OX40 agonist". In: *Clinical Cancer Research* 23.13 (2017), pp. 3416–3427.

[568] Ben Tran et al. "Dose escalation results from a first-in-human, phase 1 study of glucocorticoid-induced TNF receptor–related protein agonist AMG 228 in patients with advanced solid tumors". In: *Journal for immunotherapy of cancer* 6.1 (2018), pp. 1–9.

[569] Jacqueline Mock, Christian Pellegrino, and Dario Neri. "A universal reporter cell line for bioactivity evaluation of engineered cytokine products". In: *Scientific Reports* 10.1 (2020). ISSN: 2045-2322. DOI: 10.1038/s41598-020-60182-4. URL: http://dx.doi.org/10.1038/s41598-020-60182-4.

[570] Sylvia Lee and Kim Margolin. "Cytokines in cancer immunotherapy". In: *Cancers* 3.4 (2011), pp. 3856–3893.

[571] Glenn Dranoff. "Cytokines in cancer pathogenesis and cancer therapy". In: *Nature Reviews Cancer* 4.1 (2004), pp. 11–22.

[572] Giorgio Parmiani et al. "Cytokines in cancer therapy". In: *Immunology letters* 74.1 (2000), pp. 41–44.

[573] Cornelia Hutmacher et al. "Targeted delivery of IL2 to the tumor stroma potentiates the action of immune checkpoint inhibitors by preferential activation of NK and CD8+ T cells". In: *Cancer immunology research* 7.4 (2019), pp. 572–583.

[574] Steven A Rosenberg. "IL-2: the first effective immunotherapy for human cancer". In: *The Journal of Immunology* 192.12 (2014), pp. 5451–5458.

[575] Michelle I Wilde and Diana Faulds. "Oprelvekin". In: *BioDrugs* 10.2 (1998), pp. 159–171.

[576] Val R Adams and Timothy L Brenner. "Oprelvekin (Neumega®)". In: *Journal of Oncology Pharmacy Practice* 5.3 (1999), pp. 117–124.

[577] Paul B Chapman et al. "Clinical pharmacology of recombinant human tumor necrosis factor in patients with advanced cancer." In: *Journal of Clinical Oncology* 5.12 (1987), pp. 1942–1951.

[578] Robert J Spiegel. "Intron A (interferon alfa-2b): clinical overview and future directions." In: *Seminars in oncology*. Vol. 13. 3 Suppl 2. 1986, pp. 89–101.

[579] Volker Limmroth, Norman Putzki, and Norman J Kachuck. "The interferon beta therapies for treatment of relapsing–remitting multiple sclerosis: are they equally efficacious? A comparative review of open-label studies evaluating the efficacy, safety, or dosing of different interferon beta formulations alone or in combination". In: *Therapeutic Advances in Neurological Disorders* 4.5 (2011), pp. 281–296.

[580] Claus Madsen. "The innovative development in interferon beta treatments of relapsing-remitting multiple sclerosis". In: *Brain and behavior* 7.6 (2017), e00696.

[581] Catriona HT Miller, Stephen G Maher, and Howard A Young. "Clinical use of interferon-γ". In: *Annals of the New York Academy of Sciences* 1182 (2009), p. 69.

[582] Alan C Herman, Thomas C Boone, and Hsieng S Lu. "Characterization, formulation, and stability of Neupogen®(Filgrastim), a recombinant human granulocyte-colony stimulating factor". In: *Formulation, characterization, and stability of protein drugs: case histories*. Springer, 2002, pp. 303–328.

[583] John Geigert and Barbara FD Ghrist. "Development and shelf-life determination of recombinant human granulocyte-macrophage colony-stimulating factor (Leukine®, GM-CSF)". In: *Formulation, Characterization, and Stability of Protein Drugs: Case Histories*. Springer, 2002, pp. 329–342.

[584] E Vazquez. "Leukine studies move forward." In: *Positively aware: the monthly journal of the Test Positive Aware Network* 10.4 (1999), p. 29.

[585] F Lejeune et al. "Administration of high-dose tumor necrosis factor alpha by isolation perfusion of the limbs. Rationale and results." In: *The Journal of infusional chemotherapy* 5.2 (1995), pp. 73–81.

[586] John P Leonard et al. "Effects of single-dose interleukin-12 exposure on interleukin-12–associated toxicity and interferon-γ production". In: *Blood, The Journal of the American Society of Hematology* 90.7 (1997), pp. 2541–2548.

[587] PF Geertsen et al. "Safety and efficacy of subcutaneous and continuous intravenous infusion rIL-2 in patients with metastatic renal cell carcinoma". In: *British journal of cancer* 90.6 (2004), pp. 1156–1162.

[588] James F Eliason. "Pegylated cytokines". In: *BioDrugs* 15.11 (2001), pp. 705–711.

[589] Jalal A Jazayeri and Graeme J Carroll. "Fc-based cytokines". In: *BioDrugs* 22.1 (2008), pp. 11–26.

[590] Deborah H Charych et al. "NKTR-214, an engineered cytokine with biased IL2 receptor binding, increased tumor exposure, and marked efficacy in mouse tumor models". In: *Clinical Cancer Research* 22.3 (2016), pp. 680–690.

[591] Eric T Harvill and Sherie L Morrison. "An IgG3-IL2 fusion protein activates complement, binds FcγRI, generates LAK activity and shows enhanced binding to the high affinity IL-2R". In: *Immunotechnology* 1.2 (1995), pp. 95–105.

[592] Holger N Lode et al. "Immunocytokines: a promising approach to cancer immunotherapy". In: *Pharmacology & therapeutics* 80.3 (1998), pp. 277–292.

[593] Peisheng Hu et al. "A chimeric Lym-1/interleukin 2 fusion protein for increasing tumor vascular permeability and enhancing antibody uptake". In: *Cancer research* 56.21 (1996), pp. 4998–5004.

[594] Jahangir Sharifi et al. "Generation of human interferon gamma and tumor Necrosis factor alpha chimeric TNT-3 fusion proteins". In: *Hybridoma and hybridomics* 21.6 (2002), pp. 421–432.

[595] Manuel L Penichet and Sherie L Morrison. "Antibody–cytokine fusion proteins for the therapy of cancer". In: *Journal of immunological methods* 248.1-2 (2001), pp. 91–101.

[596] Patricia A Young, Sherie L Morrison, and John M Timmerman. "Antibody-cytokine fusion proteins for treatment of cancer: engineering cytokines for improved efficacy and safety". In: *Seminars in oncology*. Vol. 41. 5. Elsevier. 2014, pp. 623–636.

[597] Melissa G Lechner et al. "Chemokines, costimulatory molecules and fusion proteins for the immunotherapy of solid tumors". In: *Immunotherapy* 3.11 (2011), pp. 1317–1340.

[598] Paul M Sondel and Stephen D Gillies. "Current and potential uses of immunocytokines as cancer immunotherapy". In: *Antibodies* 1.2 (2012), pp. 149–171.

[599] Roland E Kontermann. "Antibody–cytokine fusion proteins". In: *Archives of Biochemistry and Biophysics* 526.2 (2012), pp. 194–205.

[600] Gwendolyn Fyfe et al. "Results of treatment of 255 patients with metastatic renal cell carcinoma who received high-dose recombinant interleukin-2 therapy." In: *Journal of clinical oncology* 13.3 (1995), pp. 688–696.

[601] Eric S White, Francisco E Baralle, and Andrés F Muro. "New insights into form and function of fibronectin splice variants". In: *The Journal of Pathology: A Journal of the Pathological Society of Great Britain and Ireland* 216.1 (2008), pp. 1–14.

[602] Kathrin Schwager et al. "A comparative immunofluorescence analysis of three clinical-stage antibodies in head and neck cancer". In: *Head & neck oncology* 3.1 (2011), p. 25.

[603] Raymond G Goodwin et al. "Molecular cloning of a ligand for the inducible T cell gene 4-1BB: a member of an emerging family of cytokines with homology to tumor necrosis factor". In: *European journal of immunology* 23.10 (1993), pp. 2631–2641.

[604] Karen E Pollok et al. "4-1BB T-cell antigen binds to mature B cells and macrophages, and costimulates anti-μ-primed splenic B cells". In: *European journal of immunology* 24.2 (1994), pp. 367–374.

[605] Mark A DeBenedette et al. "Analysis of 4-1BB ligand (4-1BBL)-deficient mice and of mice lacking both 4-1BBL and CD28 reveals a role for 4-1BBL in skin allograft rejection and in the cytotoxic T cell response to influenza virus". In: *The Journal of Immunology* 163.9 (1999), pp. 4833–4841.

[606] RS MacHugh et al. "CD4CD25 immunoregulatory T cells: gene expression analysis reveals a functional role for the glucocorticoid-induced TNF receptor". In: *Immunity* 16 (2002), pp. 311–323.

[607] Suzanne IS Mosely et al. "Rational selection of syngeneic preclinical tumor models for immunotherapeutic drug discovery". In: *Cancer immunology research* 5.1 (2017), pp. 29–41.

[608] Jong W Yu et al. "Tumor-immune profiling of murine syngeneic tumor models as a framework to guide mechanistic studies and predict therapy response in distinct tumor microenvironments". In: *PLoS One* 13.11 (2018), e0206223.

[609] Mark J Selby et al. "Preclinical development of ipilimumab and nivolumab combination immunotherapy: mouse tumor models, in vitro functional studies, and cynomolgus macaque toxicology". In: *PLoS One* 11.9 (2016), e0161779.

[610] Emanuele Puca et al. "The antibody-based delivery of interleukin-12 to solid tumors boosts NK and CD8+ T cell activity and synergizes with immune checkpoint inhibitors". In: *International journal of cancer* 146.9 (2020), pp. 2518–2530.

[611] Andrew C Scott et al. "TOX is a critical regulator of tumour-specific T cell differentiation". In: *Nature* 571.7764 (2019), pp. 270–274.

[612] Fernando P Canale et al. "CD39 expression defines cell exhaustion in tumor-infiltrating CD8+ T cells". In: *Cancer research* 78.1 (2018), pp. 115–128.

[613] Juan Dubrot et al. "Treatment with anti-CD137 mAbs causes intense accumulations of liver T cells without selective antitumor immunotherapeutic effects in this organ". In: *Cancer immunology, immunotherapy* 59.8 (2010), pp. 1223–1233.

[614] Todd Bartkowiak et al. "Activation of 4-1BB on Liver Myeloid Cells Triggers Hepatitis via an Interleukin-27–Dependent Pathway". In: *Clinical Cancer Research* 24.5 (2018), pp. 1138–1151.

[615] Eva Dahlén, Niina Veitonmäki, and Per Norlén. "Bispecific antibodies in cancer immunotherapy". In: *Therapeutic advances in vaccines and immunotherapy* 6.1 (2018), pp. 3–17.

[616] Christian Reichen et al. *FAP-mediated tumor accumulation of a T-cell agonistic FAP/4-1BB DARPin drug candidate analyzed by SPECT/CT and quantitative biodistribution*. 2018.

[617] Kristen Hurov et al. "A novel fully synthetic dual targeted Nectin-4/4-1BB Bicycle (R) peptide induces tumor localized 4-1BB agonism". In: *Journal for Immunotherapy of Cancer* 7 (2019).

[618] Tobias Weiss et al. "NKG2D-dependent antitumor effects of chemotherapy and radiotherapy against glioblastoma". In: *Clinical Cancer Research* 24.4 (2018), pp. 882–895.

[619] Tobias Weiss et al. "NKG2D-based CAR T cells and radiotherapy exert synergistic efficacy in glioblastoma". In: *Cancer research* 78.4 (2018), pp. 1031–1043.

[620] Bicycle Therapeutics. *A novel fully synthetic dual targeted EphA2/4-1BB Bicycle® peptide induces tumor localized 4-1BB agonism*. 2019. URL: https://www.bicycletherapeutics.com/wp-content/uploads/2019_SITC_EphA2-CD137-poster-P794_final.pdf.

[621] Daniel-Adriano Silva et al. "De novo design of potent and selective mimics of IL-2 and IL-15". In: *Nature* 565.7738 (2019), pp. 186–191.

[622] Teresa Hemmerle and Dario Neri. "The antibody-based targeted delivery of interleukin-4 and 12 to the tumor neovasculature eradicates tumors in three mouse models of cancer". In: *International journal of cancer* 134.2 (2014), pp. 467–477.